

Spring 1-1-2011

Transition Regime Heat Conduction of Argon/ Hydrogen and Xenon/Hydrogen Mixtures in a Parabolic Trough Receiver

Frank Burkholder

University of Colorado at Boulder, Frank.Burkholder@gmail.com

Follow this and additional works at: https://scholar.colorado.edu/cven_gradetds



Part of the [Energy Systems Commons](#)

Recommended Citation

Burkholder, Frank, "Transition Regime Heat Conduction of Argon/Hydrogen and Xenon/Hydrogen Mixtures in a Parabolic Trough Receiver" (2011). *Civil Engineering Graduate Theses & Dissertations*. 330.
https://scholar.colorado.edu/cven_gradetds/330

This Dissertation is brought to you for free and open access by Civil, Environmental, and Architectural Engineering at CU Scholar. It has been accepted for inclusion in Civil Engineering Graduate Theses & Dissertations by an authorized administrator of CU Scholar. For more information, please contact cuscholaradmin@colorado.edu.

TRANSITION REGIME HEAT CONDUCTION OF ARGON/HYDROGEN AND XENON/HYDROGEN
MIXTURES IN A PARABOLIC TROUGH RECEIVER

by

FRANK W. BURKHOLDER

B.S., Stanford University, 1995

M.S., University of Wisconsin, Madison, 2004

A thesis submitted to the
Faculty of the Graduate School of the
University of Colorado in partial fulfillment
of the requirement for the degree of
Doctor of Philosophy
Department of Civil, Environmental, and Architectural Engineering

2011

*TRANSITION REGIME HEAT CONDUCTION OF ARGON/HYDROGEN AND XENON/HYDROGEN
MIXTURES IN A PARABOLIC TROUGH RECEIVER*

This thesis entitled:
Transition Regime Heat Conduction of Argon/Hydrogen and Xenon/Hydrogen Mixtures in a Parabolic
Trough Receiver by Frank W. Burkholder
has been approved for the Department of Civil, Environmental, and Architectural Engineering

Dr. Michael Brandemuehl

Dr. Chuck Kutscher

Dr. Moncef Krarti

Dr. Harihar Rajaram

Dr. Ed Wolfrum

Date _____

The final copy of this thesis has been examined by the signatories, and we
Find that both the content and the form meet acceptable presentation standards
Of scholarly work in the above mentioned discipline.

Burkholder, Frank W. (Ph.D., Civil, Environmental, and Architectural Engineering)

Transition Regime Heat Conduction of Argon/Hydrogen and Xenon/Hydrogen Mixtures in a Parabolic Trough Receiver

Thesis directed by Professor Michael Brandemuehl

ABSTRACT

The annulus of a parabolic trough receiver is normally evacuated to prevent heat conduction between the internal absorber pipe and the external glass envelope. In the past, this vacuum has been compromised by hydrogen permeation from the heat transfer fluid through the absorber pipe. Heat conduction is significantly increased by the presence of hydrogen in the annulus even though its final pressure – 10 to 100 Pa – is sufficiently low that the thermal conductivity and temperature difference alone cannot predict it. Heat conduction for the concentric cylinder receiver geometry at these pressures is in the transition regime, where neither free molecule nor continuum heat conduction solutions apply.

Most solutions to transition regime concentric cylinder heat conduction focus on single species, monatomic gases with small temperature difference boundary conditions. Further constraints limiting their applicability to this research include their typical wire-in-tube geometry and assumption of complete thermal accommodation on the outer cylinder surface. Much experimental data focuses on validating these solutions so is similarly constrained.

This study measures heat conduction across the annulus of a parabolic trough receiver in the free-molecular, transition, temperature jump, and continuum regimes for argon-hydrogen and xenon-hydrogen mixtures at an absorber temperature of 350°C. Experimental values are predicted successfully by Sherman's interpolation formula and the Direct Simulation Monte Carlo Method. Depending on pressure, heat conduction of hydrogen in the annulus of a receiver can be greater than 500 W/m receiver length and decrease the annual net electricity production of a parabolic trough power plant by more than 50% relative to a plant with evacuated receivers. However, heat conduction can be reduced to 50-100 W/m when hydrogen is mixed with an inert gas such that the molar fraction of the inert gas is 95% or greater.

This results in annual net electricity production penalty of 3-7% instead of more than 50%. Assuming 100 Pa of hydrogen in the annulus of a current receiver, the addition of 1900 Pa of xenon or 4900 Pa of argon will effect this reduction while avoiding natural convection in the annulus.

DEDICATION

To Mom and Dad. Thanks for being so supportive.

ACKNOWLEDGMENTS

I've received a lot of support along this long road. Thanks to the CSP team at NREL. They could have given up on me finishing a long time ago but they didn't. Thanks to my advisors at CU-Boulder for the same reason. Thanks to Judy Netter for always having time to help, and thanks to Mike Martinez for holding that receiver steady more times than I can count. The data acquisition system would be 4 times more complicated if not for Chuck Kutscher's timely advice. I've really enjoyed talking experimental uncertainty with Mark Mehos, and Reda Ibrahim's advice on calibration and uncertainty analysis were very valuable. I'm sorry if I didn't follow all of your advice here, Reda. But I was listening.

My sincere thanks to Schott for supplying the specially modified receiver. I wouldn't have had a dissertation topic without it.

I doubt my friends will ever read this, but if they do...THANK YOU. Thanks for sticking by a friend that owes you at least 4 or 5 dinner parties and countless invites to other exciting events. I'm relieved that this chapter of my life is ending, and I'm looking forward to seeing more of you soon.

CONTENTS

CHAPTER

I.	Introduction.....	1
	Motivation.....	3
	Scope.....	4
	Arrangement of the Dissertation	5
II.	Literature review.....	6
	Heat conduction regimes	7
	Free molecular regime	11
	Accommodation coefficients	12
	Temperature jump regime.....	15
	Continuum regime	18
	Transition regime.....	19
	Boltzmann transport equation	19
	Transition regime solution methods.....	23
	BGK collision model	23
	Lees moment method.....	23
	Sherman interpolation formula	26
	Direct Simulation Monte Carlo method (DSMC)	27
	Transition regime solution methods applied to gas heat conduction in solar collectors.....	28
	Selection of models for this study.....	33
	Transition regime experimental data in the literature	35
	Uncertainty analysis.....	36
	Differential analysis	38

	Monte Carlo analysis.....	39
	Latin Hypercube sampling.....	44
III.	Modeling.....	47
	Estimating accommodation coefficients	48
	Sherman Interpolation Formula	51
	Gas mixture thermal conductivity	52
	Sherman summary	53
	Direct Simulation Monte Carlo (DSMC) Method.....	56
	Molecule movement and collision with boundaries.....	57
	Collisions between molecules	58
	Collision dynamics.....	60
	Inelastic collisions.....	61
	DSMC gas inputs	62
	Convergence investigation	65
	DSMC convergence summary	72
IV.	Testing.....	74
	Heat conduction test overview.....	75
	Parabolic trough receiver specifications.....	83
	Temperature measurement.....	84
	Power measurement	91
	Pressure measurement.....	92
	Baking out and off-gassing.....	93
	The gases.....	94
	Safety	94
	Heat conduction test procedure.....	95
	Uncertainty calculation.....	97
	Equipment list	100
V.	Results	102

	Hydrogen accommodation coefficient on absorber	103
	Pure gas results	108
	Gas mixture results	121
VI.	Conclusions	126
	Limiting heat conduction using large molar fractions of inert gas.....	127
	Natural convection limits the total pressure in the annulus	129
	Effect of inert gases on plant performance	130
	BIBLIOGRAPHY	134
	APPENDIX	
A.	Experimental data in the transition regime	138
B.	EES listing of the Sherman interpolation formula	149
C.	DSMC1 Fortran code	156
D.	Safe Operating Procedure	195
E.	Experimental results in tabular form.....	226
F.	Matlab® front end for DSMC1 calculation with Latin hypercube sampling	228
G.	Solar Advisor Model reference parabolic trough plant inputs	233

TABLES

Table		
1.1	Dissertation scope	4
2.1	Metrics of the heat conduction problem of this research	35
3.1	DSMC1 gas inputs	62
4.1	Parabolic trough receiver specifications	83
6.1	SAM simulation cases and results	132

FIGURES

Figure

1.1	Kramer Junction solar field	1
1.2	Parabolic trough receiver schematic.....	2
2.1	Heat conduction regimes	8
2.2	Sample accommodation coefficients	13
2.3	Langmuir's temperature jump method	15
2.4	Maxwellian velocity distributions.....	22
2.5	Transition regime parallel plate gas mixture heat conduction results.....	26
2.6	Heat loss from a cylindrical solar receiver with air in the annulus	30
2.7	Sherman formula results for a tubular solar collector	32
2.8	DSMC results for a tubular solar collector	33
2.9	Normal probability density distribution predicted by differential analysis	39
2.10	Probability density distribution predicted by Monte Carlo analysis.....	40
2.11	Monte Carlo distribution from 10 simulations	41
2.12	Monte Carlo - 10 simulations repeated 1000 times	42
2.13	Monte Carlo confidence interval results from 1000 10 run simulation results.....	43
2.14	A Latin hypercube sample	44
2.15	LHS - 10 simulations repeated 1000 times	46
3.1	Accommodation coefficients predicts by Song's correlation	50
3.2	Expected continuum radial temperature distribution	55
3.3	DSMC1 program flow diagram	56
3.4	DSMC representation of a binary collision	60
3.5	Power law fits of hydrogen's viscosity	64
3.6	Convergence study results at 33 Pa – number of molecules	67

3.7	Convergence study results at 33 Pa – time step	68
3.8	Convergence study results at 5.5 Pa	69
3.9	Convergence study results at 0.7 Pa	70
3.10	Convergence study results – number of cells	71
3.11	Convergence study results – number of updates to steady flow	72
4.1	NREL heat loss test stand, front view	75
4.2	NREL heat loss test stand, side view	76
4.3	Vacuum and gas-delivery system	76
4.4	Calculating heat conduction from heat loss measurements	77
4.5	Cartridge heater and coil heaters	79
4.6	Heaters inside the copper pipe	80
4.7	Thermocouple locations	81
4.8	Close view of thermocouples used to measure absorber temperature	81
4.9	Connection between gas delivery system and glass port of receiver	82
4.10	End view of cartridge heat, copper pipe, and absorber diameter	85
4.11	Baffles used to prevent natural convection	85
4.12	Attempted thermocouple shielding and contact configurations	87
4.13	Insulation levels used in temperature investigation	88
4.14	Data gathered in absorber temperature study	89
4.15	Absorber temperature regression result	91
4.16	Heaters in uncertainty calculation	97
4.17	Uncertainty in heat loss measurement due to absorber temperature uncertainty	99
5.1	Free molecular hydrogen heat conduction	103
5.2	Plot of inverse heat loss versus inverse pressure	106
5.3	Accommodation coefficient of hydrogen on absorber based on TJ	107
5.4	Pure hydrogen results: Sherman, Foristall results and experimental data	108
5.5	Pure hydrogen results: DSMC results and experimental data	109
5.6	Pure gas experimental and Sherman results	111

5.7	Pure gas experimental and Sherman results, zoomed in.....	112
5.8	Sherman model hydrogen confidence interval contributors	113
5.9	Pure gas experimental and DSMC results	114
5.10	Pure gas experimental and DSMC results, zoomed in.....	115
5.11	Comparison of DSMC and Sherman confidence intervals	116
5.12	Distribution of DSMC1 results from 10 simulations	117
5.13	Distribution of DSMC1 results from 750 simulations	118
5.14	Confidence interval of pure gas DSMC results with no input uncertainty.....	119
5.15	Confidence interval of DSMC results with no input uncertainty.....	120
5.16	Hydrogen/Argon gas mixture results compared to Sherman results.....	121
5.17	Hydrogen/Argon gas mixture results compared to DSMC results.....	122
5.18	Hydrogen/Xenon gas mixture results compared to Sherman results.....	123
5.19	Hydrogen/Xenon gas mixture results compared to DSMC results.....	124
6.1	Heat conduction in a receiver depending on the molar fractions of H ₂ and Xe	128
6.2	Heat conduction in a receiver depending on the molar fractions of H ₂ and Ar.....	128
6.3	Onset of natural convection in the annulus	130

CHAPTER I

Introduction

A parabolic trough power plant generates electricity for utilities using sunlight as the heat source for its power cycle. Rows of single-axis-tracking, linear parabolic mirrors concentrate sunlight onto tubular receivers located along the focal line of each collector. The sun-heated receivers warm a mineral oil heat transfer fluid (HTF) pumped through them. After being sufficiently heated by the solar field, the HTF travels to a power block where it generates steam in a series of heat exchangers to run a Rankine steam turbine power cycle. Then the HTF returns to the solar field to be re-heated and continue the cycle. Figure 1.1 shows a portion of a 30 MW parabolic trough power plant near Kramer Junction, CA.

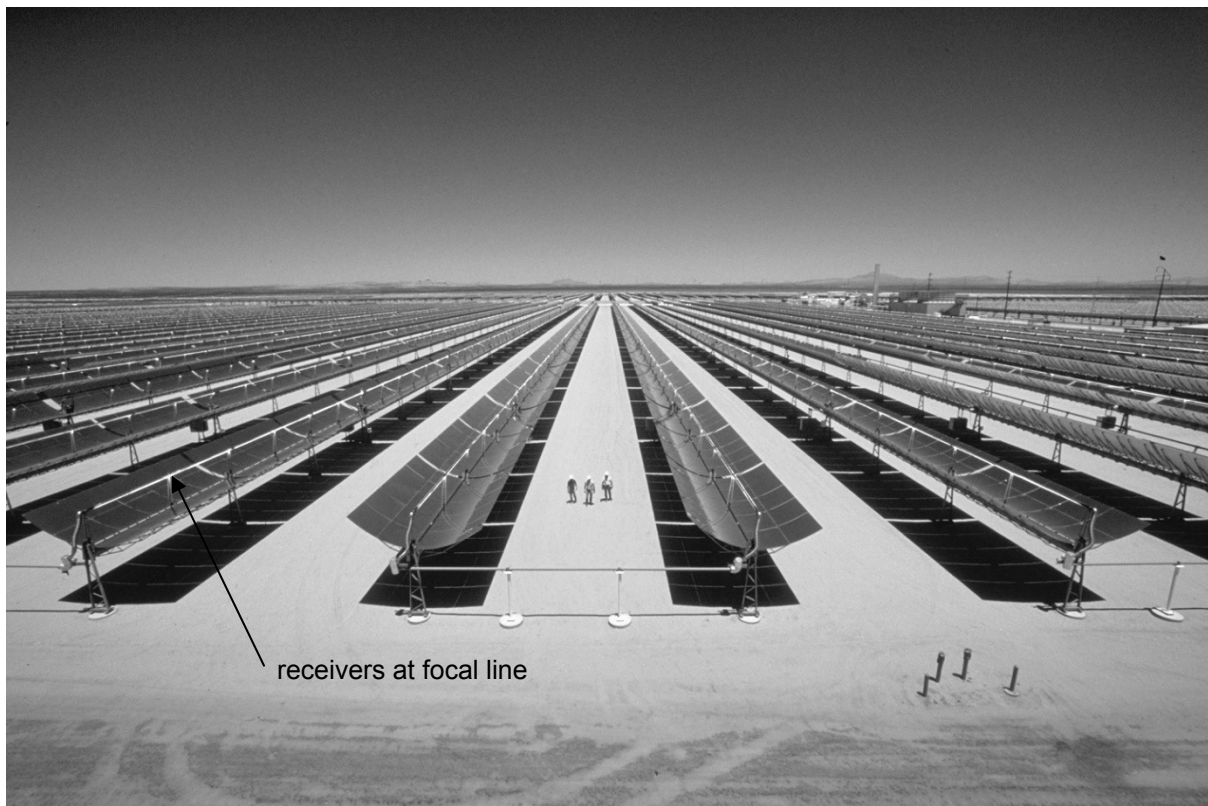


Figure 1.1 Parabolic trough receivers at a solar parabolic trough power plant.

Parabolic trough receivers are designed to absorb sunlight and transfer the energy to the HTF running inside their absorbers while minimizing heat loss to the environment. Several receiver design features, shown in Figure 1.2, make this possible.

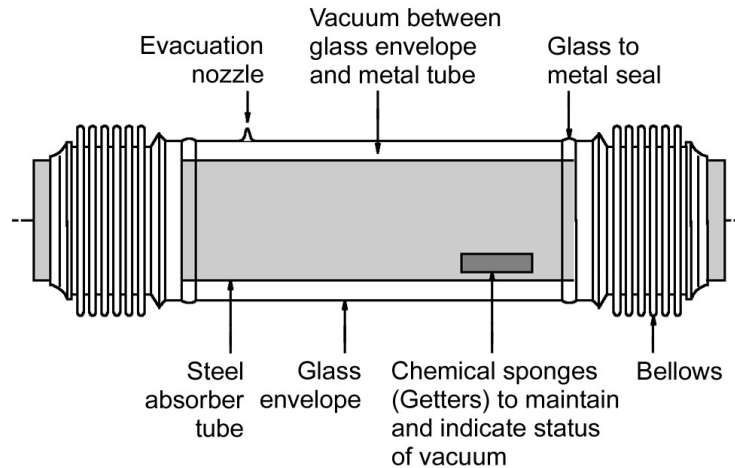


Figure 1.2 A shortened schematic of a parabolic trough receiver.
Source: Flabeg Solar International

A receiver is comprised of two concentric cylinders. The outer cylinder is a borosilicate, low-iron glass envelope with anti-reflective coatings on its inner and outer surfaces. The inner cylinder, the absorber, is a stainless steel pipe with a selective surface on its outer surface. The spectrally selective surface has high absorptance in the solar spectrum (>95%) and low thermal emittance (<10% at 400°C) to prevent radiation heat loss at high temperatures. The inside of the absorber contacts the HTF. The receiver used in this study is a little over 4 m long, with a 3 mm thick glass envelope that has an outer diameter of 12.5 cm. Its absorber is 2mm thick with an outer diameter of 7 cm.

The vacuum between the absorber and glass envelope eliminates heat conduction across the annulus. Getters in the annulus maintain the vacuum by adsorbing gas molecules that off-gas from the absorber and glass envelope during bake-out in the manufacturing process. They also bind hydrogen that permeates through the absorber during operation in the solar field. Their capacity is limited, however, and the build-up of hydrogen in the receiver annulus leads to the motivation for this dissertation.

MOTIVATION

Moens et al. [1] describe the thermal decomposition of the organic oil (Therminol VP1) that serves as HTF for present parabolic trough power plants. High temperatures and impurities in the HTF, comprised of a eutectic mixture of biphenyl and diphenyl oxide, cleave the carbon-carbon bond in the diphenyl oxide. This releases radicals that catalyze a series of reactions terminating in hydrogen formation. The hydrogen slowly permeates through the absorber into the annulus where its presence can increase the glass envelope temperature from 60-80°C to more than 150°C. Infrared images of glass envelope temperatures determine the presence of these receivers in the field [2]. Bingham et al. [3] estimated the amount of hydrogen gas present in the annuli of several old receivers taken from a solar field with spectral measurements. They found hydrogen pressures between 1 and 100 Pa. Burkholder et al. [4] compared the heat loss of a couple of these receivers with the heat loss of evacuated receivers. The receivers with hydrogen in their annuli lost 200-800 watts per meter length more than their evacuated counterparts, depending on the temperatures of the absorber and getters. These experiments and a parabolic trough receiver model [5] proved that significant amounts of heat can be lost by a receiver with small amounts of hydrogen in its annulus, and that the heat conduction is pressure dependent at lower pressures. Simulations with a validated parabolic trough power plant model [6,7] indicate that 50% less net electrical energy is generated per year by a solar field where all receivers compromised by hydrogen relative a plant with evacuated receivers. An infrared survey of glass temperatures in a commercial plant in the last five years found that more than half the receivers had glass temperatures consistent with hydrogen permeation [2]. Most of the receivers surveyed were more than 15 years old.

Reducing hydrogen-induced receiver heat loss is the motivation for this dissertation. This dissertation explores, through modeling and testing, the viability of using inert gases to reduce heat loss caused by hydrogen in the annulus. The addition of a small amount of inert gas at the time of manufacture or in the field will impede the ability of hydrogen molecules to move energy from the hot absorber surface to the cooler glass envelope. Modeling results suggest that 10 Pa of solely hydrogen in the annulus conducts about 270 W/m from a 350°C absorber to the glass envelope. This triples the total heat loss of a current receiver. However, if 90 Pa of argon is added to the annulus so that the gas mixture

is 10% hydrogen/90% argon, the 270 W/m drops to 130 W/m. If 90 Pa of xenon is added instead of argon, the heat loss due to conduction drops to 62 W/m. Larger molar fractions of the inert gases further decrease heat loss.

SCOPE

This study predicts and tests heat conduction of argon/hydrogen and xenon/hydrogen gas mixtures in a parabolic trough receiver at an absorber temperature typical of operating solar field temperatures. The heat conduction of the pure gases (hydrogen, argon, xenon) is investigated as well. As the permeation rate and equilibrium pressure of hydrogen in the annuli of receivers in the field are variable and unknown, heat conduction is studied over a wide range of pressures from the free molecular regime to the continuum regime. The study examines the ability of two models in the literature to predict the heat conduction in the free-molecule and transition regimes. Though transition regime heat transfer has been much studied, several aspects of this heat conduction problem restrict the applicability of most data and models. These aspects include the large temperature difference between the surfaces, the presence of a gas mixture where one component has internal degrees of freedom (hydrogen's rotational degrees of freedom), incomplete thermal accommodation (partial energy transfer) of all gases on both surfaces, a concentric cylinder geometry that is far-removed from the wire-in-tube geometry of most concentric cylinder studies, and the desire to predict heat conduction over a wide of range of pressures.

Table 1.1 summarizes the testing and modeling scope of this dissertation.

Table 1.1 Dissertation scope

Gases	Pure gases:	H ₂ , Ar, Xe		
	Mixtures:	H ₂ /Ar, H ₂ /Xe		
Gas molar fractions	Pure gases:	1.0 H ₂	1.0 Ar	1.0 Xe
	Mixtures:	0.50 H ₂ /0.50 Ar 0.525 H ₂ /0.475 Xe	0.25 H ₂ /0.75 Ar 0.272 H ₂ /0.728 Xe	0.10 H ₂ /0.90 Ar 0.118 H ₂ /0.882 Xe
Absorber temperature	350°C			
Glass temperature	60-150°C depending on gas composition and pressure			
Test pressure range	0.1 – 10,000 Pa			
Simulation models	Sherman interpolation formula Direct Simulation Monte Carlo method (DSMC)			

ARRANGEMENT OF DISSERTATION

Chapter II, the Literature Review, begins with background on heat conduction in the free molecular, transition, and continuum regimes. It summarizes transition regime solution methods and presents data and analysis most relevant to this work. Chapter II also discusses uncertainty analysis and describes the uncertainty estimation methods used in this dissertation.

Chapter III, Modeling, describes the two models selected to predict heat conduction in this research. The Sherman Interpolation Formula is discussed and the uncertainty of its inputs quantified. The remainder of the chapter is about the DSMC model. Its movement and collision algorithms are described. The uncertainties of its inputs are quantified. A convergence study is performed to determine simulation inputs that give reliable results.

Chapter IV, Testing, describes the tests. The hardware used to measure pressure, temperature, and power is described, and an overview is given of the test procedure. Experimental uncertainty is derived. Chapter IV concludes with an equipment list.

Chapter V, Results, presents heat conduction test and modeling results. Model results are compared to experimental data and their agreement is discussed.

Chapter VI, Conclusions, links heat conduction results to parabolic trough power plant performance and concludes with recommendations for the type and amount of inert gas that should be added to a parabolic trough receiver annulus to prevent hydrogen-induced heat loss.

CHAPTER II

Literature Review

This chapter serves dual purpose as background for rarefied heat transfer and a review of heat conduction between concentric cylinders. The chapter begins by discussing the heat conduction regimes – free molecule, transition, temperature jump, and continuum in order of decreasing rarefaction and increasing pressure – but it does them slightly out of sequence, leaving the most complicated regime, the transition regime, for last. Information relevant to each regime is discussed as it comes up; the discussion of accommodation coefficients in the free molecule regime being an example. Effort is made in each regime to show how a concentric cylinder heat conduction problem might be solved, and specifically if a solution is possible that will predict the heat conduction that is the subject of this dissertation. The method used to solve the heat conduction must:

- 1) be useful at a large temperature difference between the surfaces ($\Delta T \approx 250^\circ\text{C}$)
- 2) allow for a gas mixture
- 3) allow for incomplete accommodation (described later) of both gases of the mixture on each surface
- 4) account for energy carried by a hydrogen molecule's internal degrees of freedom (energy associated with molecular rotation perpendicular to the line between the two hydrogen atoms)
- 5) not be restricted to a wire-in-tube geometry

Once the heat conduction regimes are introduced, the solutions to the transition regime are discussed. Applications of the solution methods to heat conduction in solar collectors are highlighted.

Two of the methods – the Sherman interpolation formula and the Direct Simulation Monte Carlo method - are chosen for this study.

Next, a survey of experimental data in the transition regime is discussed in the context of temperature difference, gases studied, concentric cylinder geometry, and pressure regimes and compared to the data gathered in this research. It will be shown that the data gathered by this work are unique and serve as a fresh test for the simulation methods.

Finally, uncertainty is discussed. There is uncertainty associated with the experimental results because temperature, pressure, and electrical power can't be measured perfectly. There is uncertainty associated with modeled results because it's impossible to know the exact values of the model inputs, such as accommodation coefficients and thermal conductivity values. A central question of this dissertation is whether the Sherman and DSMC simulation models predict the experimental data accurately. This question will be answered largely by the extent to which the 95% confidence intervals in the simulated and experimental data overlap. Many experimental results in the literature are not presented with uncertainty bounds, and very few modeled results show uncertainty bounds either. This researcher does not want to repeat these mistakes. All examples of data from previous work excerpted in this dissertation will show uncertainty bounds if presented in the original work.

HEAT CONDUCTION REGIMES

In 1959 H.J. Bomelburg studied heat conduction from a heated fine wire surrounded by a cylindrical glass bell-jar with a wide range of pressures of air in the annulus between the wire and the jar [8]. He maintained a small temperature difference, about 30°C, between the wire and the bell-jar to limit radiation heat transfer. Figure 2.1 presents his results as well as the conduction regime they fall in depending on gas pressure, and relatedly, the Knudsen number.

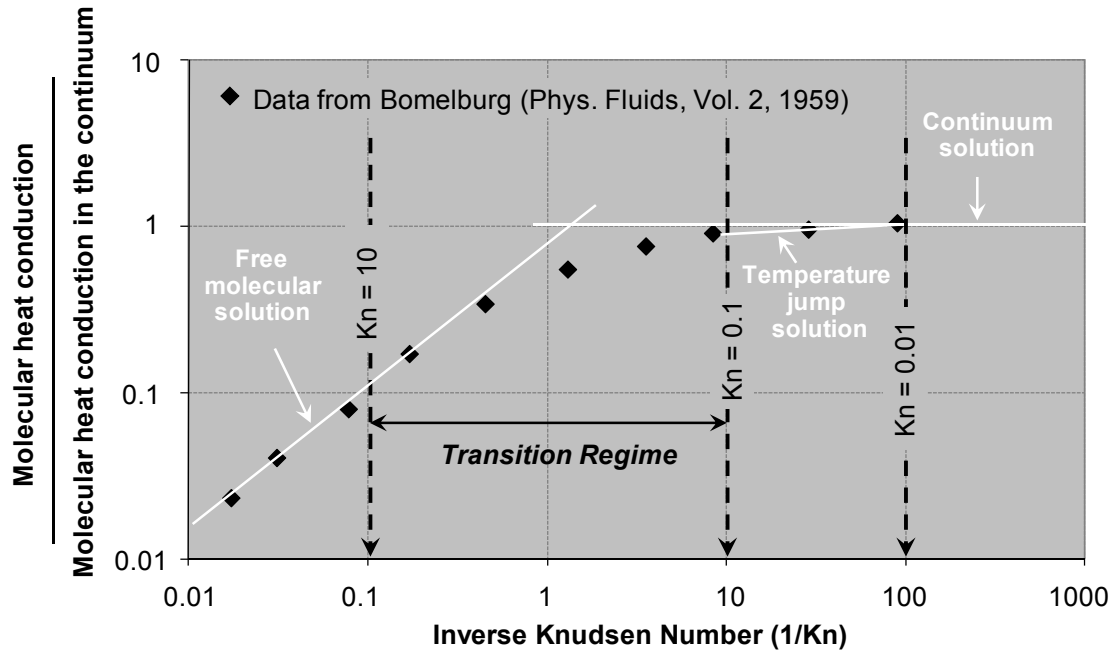


Figure 2.1 Concentric cylinder (wire in tube) molecular heat conduction results in all pressure regimes.

The inverse Knudsen number on the x-axis is a function of the mean free path of the molecules and a characteristic dimension of the flow. As the pressure increases, the inverse Knudsen number increases. The mean free path is the average distance traveled by gas molecules between intermolecular collisions. Numerous equations exist to estimate the mean free path, with some calculating the mean free path directly from thermophysical properties. Equation 2.1 calculates the mean free path from the molecule number density (a function of pressure and temperature) and a collision cross section based on the molecular diameter.

$$\lambda = \frac{1}{\sqrt{2} \pi d^2 n} \quad (2.1)$$

where:

d is the molecular diameter

n is the molecule number density, where $n = \rho/m$

ρ is the gas density

m is the mass of one molecule

The Knudsen number (Kn) is a measure of gas rarefaction. The Knudsen number is defined as

$$Kn = \frac{\lambda}{L} \quad (2.2)$$

where

λ = the mean free path of gas molecules between intermolecular collisions

L = characteristic length of interest, in Bommelburg's case the diameter of the wire

In his comprehensive review of heat transfer in rarified gases, Springer [9] classifies heat conduction regimes using the Knudsen number:

$Kn < 0.01$	continuum
$0.01 < Kn < 0.1$	temperature-jump
$0.1 < Kn < 10$	transition
$10 < Kn$	free molecular

Springer states:

When the Knudsen number is very small, then, in the vicinity of the body, the number of collisions between the molecules is large compared to the number of collisions between the molecules and the body. In this case the usual continuum concepts are applicable and the Navier-Stokes equations and Fourier heat conduction law are valid.

...

When the Knudsen number becomes sufficiently large, then the continuum concepts must be modified for calculating heat transfer. At very high Knudsen numbers (i.e., at the other end of the rarefaction scale from the continuum) where the number of collisions between the molecules and wall is much larger than the number of collisions between the molecules, the flow is termed "free molecule."

Springer clarifies that heat conduction regime classification by Knudsen number is a guideline only. Two practical reasons for this are that the choice of equation used to calculate the mean free path and the choice for the characteristic length are both subjective. For instance, in Bommelburg's case it is obvious that the characteristic length should be the diameter of the wire because the ratio of the wire radius to the bell jar radius is very small and heat conduction is being governed by the relatively

infrequent impact of molecules on the wire surface. In the case of heat conduction between flat plates the characteristic length is defined as the gap between the plates. But for a concentric cylinder heat conduction problem, at what inner radius/outer radius ratio does one begin to use the gap between the radii (r_o-r_i) instead of just the inner radius (r_i) as the characteristic length? Bird [10] suggests calculation of a local Knudsen number defined as the ratio of a local macroscopic quantity, density for instance, to its gradient. This is convenient if the gradient and local macroscopic quantities are known. However, these are often what one hopes to find from the solution of the problem.

One consequence of the Knudsen number definition is that increased gas rarefaction is indicated by larger Knudsen numbers, and decreased rarefaction (usually corresponding to increased pressure) is indicated by smaller Knudsen numbers. As shown by Figure 2.1, heat conduction increases with increasing pressure (to a point). In the desire to show heat conduction increasing as pressure increases from left to the right on the x-axis of figures in this dissertation, figures involving the Knudsen number on the x-axis will use the inverse Knudsen number as shown in Figure 2.1. Springer's classification of the heat transfer regimes using the inverse Knudsen number becomes:

$1/\text{Kn} > 100$	continuum
$100 > 1/\text{Kn} > 10$	temperature-jump
$10 > 1/\text{Kn} > 0.1$	transition
$0.1 > 1/\text{Kn}$	free molecular

Figure 2.1 illustrates that heat conduction varies depending on the rarefaction of the gas. The geometry of the experiment was maintained for all tests, so the increase or decrease in rarefaction was caused by a decrease or an increase in gas pressure, respectively. When the gas is highly rarified (free molecular), the heat conduction increases linearly with pressure. However, as the pressure increases into the transition regime, heat conduction continues to increase but at a slower rate than it did in the free molecular regime. The temperature-jump regime is the last regime where pressure affects the amount of heat conducted, but in this regime large rarefaction changes are required to cause small changes in heat

conduction. Finally, in the continuum regime heat conduction is unaffected by decreasing rarefaction until buoyancy forces cause convective flow in the annulus.

Predicting concentric cylinder gas mixture heat conduction in the continuum, temperature-jump, and free-molecular regimes is not difficult. Closed-form solutions for each of these regimes are presented below. However, few closed form solutions exist for transition regime heat conduction and this regime is discussed last.

THE FREE MOLECULAR REGIME

In the free-molecular regime energy is conducted from one surface to another by molecules that 1) collide with the hot surface and gain translational, vibrational, and rotational energy from it, then 2) travel across the space separating the surfaces without impacting other molecules, and finally 3) collide with the cooler surface and transfer some of their translational, vibrational, and rotational energy to it.

Knudsen [11] found that the heat conducted per unit time per unit area from a surface in this regime could be calculated from

$$q_{FM} = \frac{1}{\frac{1}{\alpha_1} + (R^*)^b \left(\frac{1}{\alpha_2} - 1 \right)} \times \frac{P \left(C_v + \frac{R_g}{2} \right)}{\left(2\pi M R_g T_{avg} \right)^{1/2}} \times (T_1 - T_2) \quad (2.3)$$

where

q_{FM} is the heat flux

P is the pressure of a Maxwellian gas (velocities follow a Maxwellian distribution) at the same density as the gas between the surfaces at temperature T_{avg}

R^* is the reduced radius = R_1/R_2

b is a geometry constant equal to 0 for parallel plates, 1 for concentric cylinders, and 2 for concentric spheres

M is the molecular mass of the gas

R_g is the gas constant

C_v is the heat capacity of the gas at constant volume

T_1 and T_2 are the surface temperatures

α_1 and α_2 are the accommodation coefficients at each surface

ACCOMMODATION COEFFICIENTS

Equation 2.3 shows that the free molecular heat conduction flux is directly proportional to the pressure, the heat capacity, and the temperature difference between the surfaces. The heat flux also depends on how well the gas molecules accommodate to the wall temperature after they collide with it. This is determined by empirical accommodation coefficients. The thermal accommodation coefficient was defined by Knudsen [12] and interpreted by Kennard [11] as

the fractional extent to which those molecules that fall on the surface and are reflected or re-emitted from it, have their mean energy adjusted or 'accommodated' toward what it would be if the returning molecules were issuing as a stream out of a mass of gas at the temperature of the wall. If E_i denotes the energy brought up to unit area per second by the incident stream, and E_r that carried away by these molecules as they leave the wall after reflection from it, and if E_w is the energy that this latter stream would carry away if it carried the same mean energy per molecule as does a stream issuing from a gas in equilibrium at the wall temperature T_w , then α is given by the equation:

$$\alpha = \frac{E_i - E_r}{E_i - E_w} \quad (2.4)$$

The thermal accommodation coefficient is the ratio of the energy difference between a molecule's incident and reflected energy to the energy difference between its incident and reflected energy if its reflected energy were determined by the wall temperature. An accommodation coefficient of 1 for a wall-molecule interaction means that, regardless of a molecule's incident energy, it will reflect with an energy determined by the wall temperature. Energy is exchanged between the molecule and wall completely in this case. An accommodation coefficient of 0 means that no net energy is exchanged between the molecule and the wall and the molecule's reflected energy is determined completely by its incident energy. An accommodation coefficient between 0 and 1 indicates that the reflected energy of a molecule after colliding with a wall is determined by both its incident energy and the wall temperature, with larger accommodation coefficients indicating more accommodation to the wall temperature and more energy exchange.

As part of their study of free molecular heat conduction of gases in all glass receivers, Harding et al. [13] determined accommodation coefficients in a tubular solar collector comprised of a glass borosilicate envelope and an inner glass absorber coated with a copper-sputtered selective surface. A subset of their results is presented in Figure 2.2.

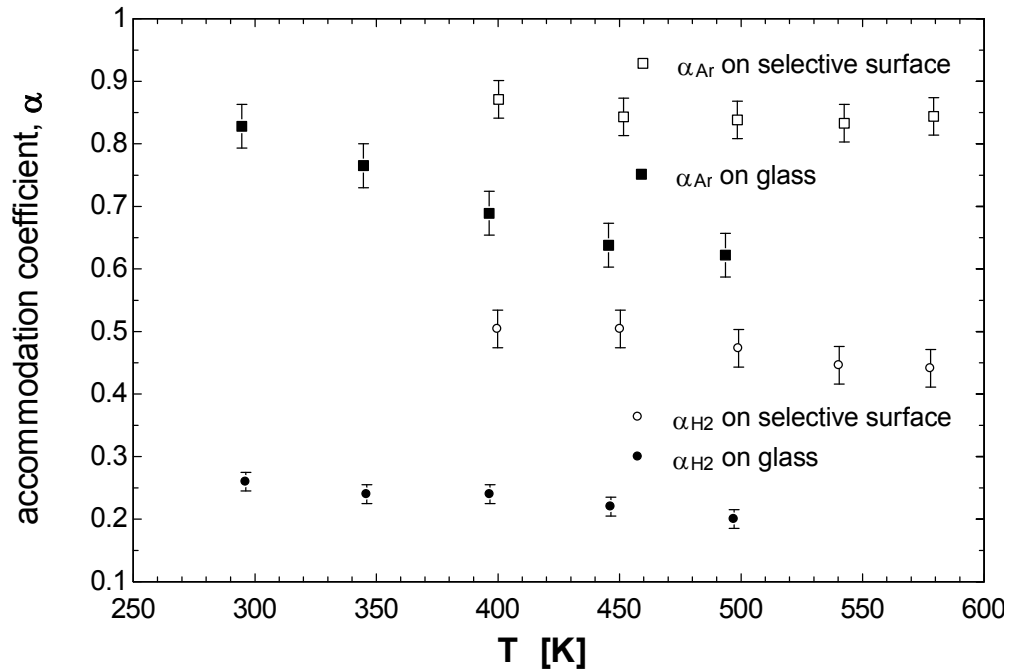


Figure 2.2. Accommodation coefficients of argon and hydrogen on borosilicate glass and a copper sputtered selective surface, from [13]

As seen in the figure, higher molecular weight gases have accommodation coefficients near unity on most surfaces, while smaller, faster molecules have accommodation coefficients less than 0.5. Accommodation coefficients also tend to decrease with increasing temperature and depend not only on the gas, but the structure, composition, and cleanliness of the surface the gas molecules collides with.

Testing in the free molecular regime can determine accommodation coefficients, especially if the two surfaces enclosing the gas are the same material and are close to the same temperature. In this case $\alpha_1 = \alpha_2$ in equation 2.3 and α is determined directly from the free molecular heat conduction measurement. The downside of this approach is that very low pressures are required to guarantee that the flow is free molecular, consequently very low amounts of heat are conducted, and so sensitive,

accurate instrumentation is required to measure both these small values with low uncertainty. An alternative is to determine accommodation coefficients from small differences in heat conducted in the temperature jump regime, and Thomas et al. [14] showed that the free molecular and temperature jump methods give the same accommodation coefficients. Dickens [15] describes the temperature jump method and it is later elaborated in the Testing chapter where the testing of the accommodation coefficient of hydrogen on the absorber of this research is determined by both the free molecular and temperature jump methods.

Whether the free molecular or temperature jump method is used, small heat conduction values or small differences in heat conduction values must be measured to determine accommodation coefficients experimentally. Hydrogen conducts a lot of heat relative to argon and xenon, so accommodation coefficients for hydrogen are more easily measured experimentally with low uncertainty than the heat conduction of the other two gases. For Ar and Xe it was necessary to turn to the literature for correlations to predict their accommodation coefficients on the Al_2O_3 coating of the selective surface and the SiO_2 silica anti-reflective coating on the borosilicate glass. Song et al. [16] found that experimental accommodation coefficient data can be matched to within $\pm 25\%$ by a correlation that weights “adsorbed surface” and “clean surface” accommodation coefficients with a weighting function that depends on surface temperature. This model matches most existing data for argon and xenon and is further described in the Modeling chapter.

The final detail of the free molecular heat conduction of a gas mixture, as opposed to a pure gas, needs to be addressed. In the free molecular regime gas molecules rarely collide with each other. Therefore heat conduction of a gas mixture in this regime is simply the sum of equation 2.3 evaluated for each species at that species’ pressure. Care must be taken to ensure that the Knudsen number evaluated for the gas mixture mean free path places it in the free molecule regime. Another check of free molecular heat conduction is that it should increase linearly with pressure. Heat conduction increasing with pressure, but linearly, is the harbinger of the transition regime.

THE TEMPERATURE JUMP REGIME

The temperature jump solution arose out of the desire to use a continuum solution in a slightly rarified gas regime, and so it modifies a continuum solution to account for rarefaction effects.

In 1914 and 1915 Irving Langmuir [17, 18] was studying dissociation of hydrogen molecules into hydrogen atoms at high temperature. His experimental apparatus was a fine tungsten wire in a cylindrical bulb, and to investigate convection and conduction in the annulus he applied pressures between 2 and 100,000 Pa. He was attempting to correlate the conduction heat loss with dissociation rates when he realized that the molecular conduction values, especially at lower pressures, were much smaller than he expected. For example, even though his tungsten wire was 1500 K, the heat conduction that he was measuring at a hydrogen pressure of 1333 Pa was consistent with only an 800 K wire temperature. He derived the following model to explain the discrepancy.

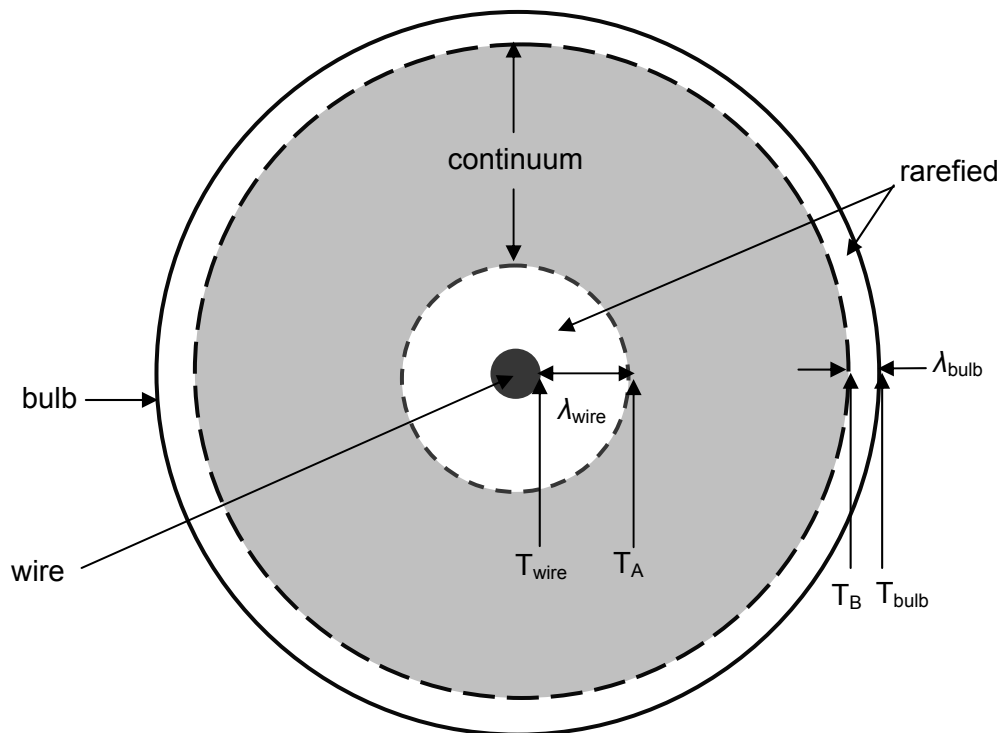


Figure 2.3. Depiction of Langmuir's temperature jump method between concentric cylinders

Langmuir reasoned that as the gas became more rarefied a distance of the order of the mean free path (λ) grew out from the wire. The definition of the mean free path means that over this distance there are few intermolecular collisions so it's inappropriate to consider this region a continuum. Because the wire, and the gas surrounding it, are hotter than the bulb and the gas adjacent to the bulb surface, the mean free path will be larger next to the wire than it is next to the bulb. This effect is so significant for a wire-in-tube geometry that it is possible to assume that $T_B = T_{bulb}$ and only investigate the temperature discrepancy between T_{wire} and T_A . T_A can be estimated from a modified Fourier equation for continuum steady-state heat conduction:

$$q_{TJ} = \frac{2\pi L k_{gas} (T_A - T_{bulb})}{\ln\left(\frac{r_{bulb}}{r_{wire} + \lambda_{wire}}\right)} \quad (2.5)$$

where

q_{TJ} = steady state heat conduction in the temperature jump regime

k_{gas} = thermal conductivity of the gas

L = the length of wire

T_A = the temperature one mean free path away from the wire

T_{bulb} = the temperature of the bulb

r_{bulb} = the inner radius of the bulb

r_{wire} = the radius of the wire

λ_{wire} = the gas mean free path adjacent to the wire

The fact that there is a temperature discontinuity between T_A and T_{wire} occurring over a distance the order of the mean free path lead to the definition of this phenomenon as a “temperature jump” or, analogous to the velocity slip effect in the viscosity of gases, a “temperature slip.” Smoluchowski [19]

shows the temperature jump being proportional to a coefficient of discontinuity and the temperature gradient normal to the surface:

$$\Delta T = \gamma \frac{dT}{dn} \quad (2.6)$$

where

ΔT = the temperature jump

γ = the temperature discontinuity coefficient

$\frac{dT}{dn}$ = the temperature gradient in the vicinity of, and normal to, the surface

Smoluchowski goes on to relate the discontinuity coefficient to the mean free path and the accommodation coefficient of the gas on the surface:

$$\gamma = \frac{15}{2\pi} \lambda \frac{2-\alpha}{2\alpha} \quad (2.7)$$

Dickens [15] uses this relation and a modified version of Fourier's steady state heat conduction equation between concentric cylinders to determine accommodation coefficients for hydrogen and a few other gases near room temperature in a wire-in-tube apparatus. He shows that the heat conducted in the temperature jump regime can be related to the temperature discontinuities at each surface:

$$q_{TJ} = \frac{2\pi L k_{gas} (T_{wire} - T_{tube})}{\ln\left(\frac{r_{tube}}{r_{wire}}\right) + \frac{\gamma_{wire}}{r_{wire}} + \frac{\gamma_{tube}}{r_{tube}}} \quad (2.8)$$

In his apparatus the radius of the tube is much greater than the radius of the wire so the third term in the denominator of equation 2.8 is assumed negligible, and by reasoning that the temperature discontinuity coefficient at the wire is a function of the mean free path, and the mean free path is a function of gas pressure, he alters the second term in the denominator to transform 2.8 into

$$q_{TJ} = \frac{2\pi L k_{gas} (T_{wire} - T_{tube})}{\ln\left(\frac{r_{tube}}{r_{wire}}\right) + \frac{X}{P}} \quad (2.9)$$

where

P is the gas pressure

X is a constant involving the accommodation coefficient of the gas on the wire surface and the mean free path at atmospheric pressure

X is determined from a series of experiments and its solution is described in the Testing chapter where this temperature jump procedure is used to determine the accommodation coefficient of hydrogen on the receiver absorber.

The temperature jump method successfully predicts heat conduction not far from the continuum regime [14, 15, 20, 21], though it hasn't been used to look at gas mixtures. In fact, such is its utility and ease of use that there have been frequent attempts, some recent [22], to extend its use from the temperature jump regime through the transition regime into the free molecule regime. Applications of the temperature jump method to heat conduction in solar collectors are described later in this chapter.

THE CONTINUUM REGIME

In the continuum regime the mean free path is so small and intermolecular and wall-molecule collisions are so frequent that no temperature jump exists and the accommodation coefficients are inconsequential. Heat conduction is independent of pressure.

Steady-state heat conduction is governed by Fourier's law:

$$q_{\infty} = \frac{2 \pi k_{gas} (T_1 - T_2)}{\ln\left(\frac{R_2}{R_1}\right)} \quad (2.10)$$

The thermal conductivity of a gas mixture can be determined by Wilke's procedure [23] which will be described later.

THE TRANSITION REGIME

Though the transition regime falls between the free molecular regime and the temperature jump regime, it was saved last for discussion. The transition regime is the most complex regime to analyze. Perusal of the literature cited in this work will find numerous PhD theses dedicated to finding solutions in this regime. Solutions are often geometry, gas, and temperature difference dependent.

In the transition regime the molecular mean free path is not very large or very small compared to a characteristic linear dimension in the flow. What this means physically is that both intermolecular and molecule-boundary interactions significantly affect the molecular velocity distribution. For diverse applications, such as diffuse solute transport, shock-waves, and high altitude skin-drag, the primary recourse for solution in this regime has been to the Boltzmann transport equation.

THE BOLTZMANN TRANSPORT EQUATION

The Boltzmann transport equation uses a probability distribution function f to describe the state of molecules in a 6 dimensional phase space – 3 dimensions in space ($\mathbf{x}_1, \mathbf{x}_2, \mathbf{x}_3$), and three dimensions in velocity ($\mathbf{v}_1, \mathbf{v}_2, \mathbf{v}_3$). The distribution function is also a function of time, so $f = f(t, \mathbf{x}, \mathbf{v})$. Different authors define this distribution function in different ways. Kogan [24] explains the probability distribution function as

the probable number of molecules in the element of physical volume $d\mathbf{x}$ near the point \mathbf{x} at time t , with velocities in the element $d\mathbf{v}$ near \mathbf{v} is equal to $f(t, \mathbf{x}, \mathbf{v})d\mathbf{x}d\mathbf{v}$

The distribution function f can be used to find the number of molecules per unit volume, n , from

$$n(t, \mathbf{x}) = \int f(t, \mathbf{x}, \mathbf{v}) d\mathbf{v} \quad (2.11)$$

and the mean energy of thermal motion of the molecules (the temperature) is defined by

$$\frac{3}{2}kT = \frac{1}{n} \int \frac{mc^2}{2} f(t, \mathbf{x}, \mathbf{v}) d\mathbf{v} \quad (2.12)$$

where

k is Boltzmann's constant

c is the thermal velocity defined by $\mathbf{v} - \mathbf{u}$

\mathbf{u} is the bulk velocity

Other quantities of interest, such as the gas mass, momentum, energy, and heat flux, can be similarly calculated from the probability distribution function.

As the molecules are followed over a period dt the distribution function will change due to intermolecular collisions, so

$$\frac{df}{dt} = \frac{\partial f}{\partial t} + \mathbf{v} \frac{\partial f}{\partial \mathbf{x}} + \mathbf{a} \frac{\partial f}{\partial \mathbf{v}} = \int (f' f_1' - f f_1) g b db d\varepsilon d\mathbf{v}_1 \quad (2.13)$$

where

' denotes a post collision value

f_1 is the distribution function of molecules with a velocity of interest, \mathbf{v}_1

f' is the distribution function after the molecular collisions occur

f_1' is the distribution function of molecules with \mathbf{v}_1'

and g , b , and ε are impact parameters associated with binary collisions

Equation 2.13 is Boltzmann's transport equation. The term on the right hand side is the collision integral. Difficulty solving the Boltzmann equation usually arises from the difficulty of determining

the distribution functions in this integral. If the gas is single species with translational energy and no internal degrees of freedom (such as a monatomic gas without rotational or vibrational energy), the collision integral appears as above. However, additional collision integrals are required for each additional gas and each additional degree of freedom. The additional distribution functions significantly complicate the collision integral, and the farthest extension of solution of the collision integral for transition regime heat transfer of a gas mixture involved two monatomic gases. This was the subject of Braun's PhD thesis (1976), published in German but with two summary papers in English [25, 26].

Boltzmann's transport equation can be solved once the distribution functions are known. Using the idea of a simple homogeneous gas composed of rigid spheres, James Clerk Maxwell [27] showed that the velocity distribution function for molecular speeds for a gas at equilibrium is

$$f(v) = 4\pi v^2 \left(\frac{m}{2\pi kT} \right)^{3/2} e^{-\frac{mv^2}{2kT}} \quad (2.14)$$

where

m is the mass of the sphere

k is Boltzmann's constant

T is the absolute temperature

v is the scalar magnitude of the total molecular velocity, $v = \sqrt{\mathbf{v}_1^2 + \mathbf{v}_2^2 + \mathbf{v}_3^2}$

Figure 2.4 shows the equilibrium probability distribution functions for hydrogen, argon, and xenon at 225°C, roughly the average temperature of the gases in the annulus in this research. The area under each of the probability distribution functions sums to 1. Hydrogen molecules are likely to move much faster than xenon or argon molecules.

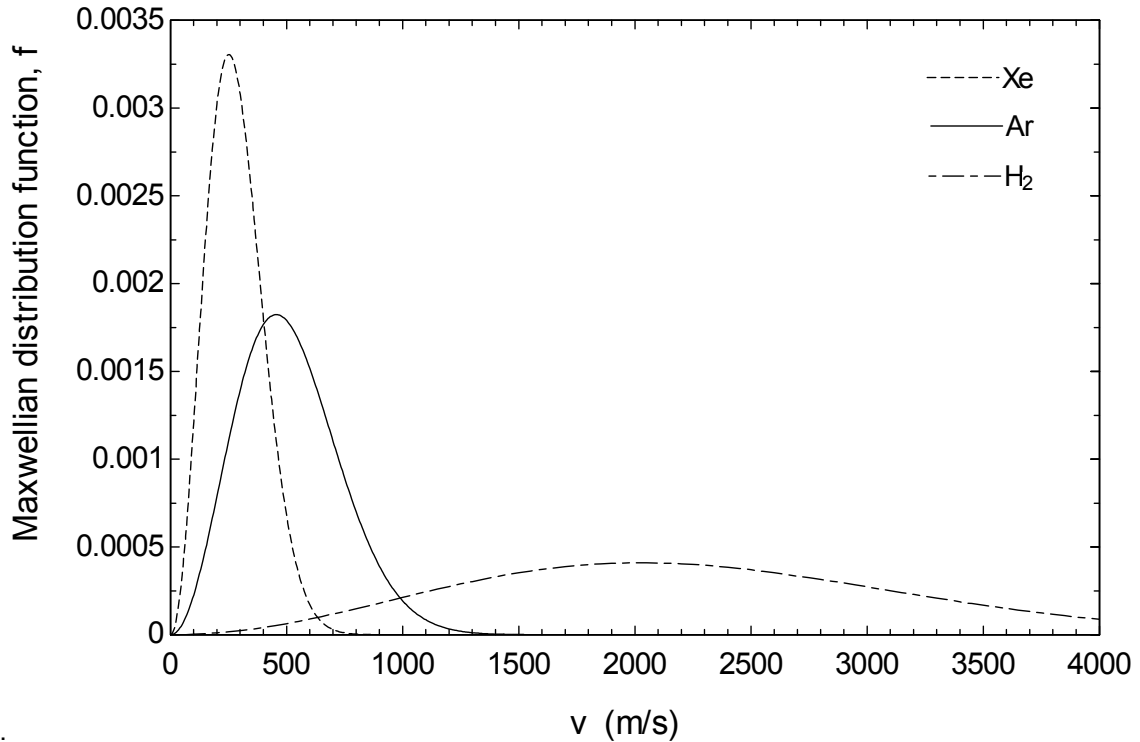


Figure 2.4 Maxwellian velocity distributions for Xe, Ar, and H₂ at 225°C

For transport phenomena, the equilibrium solution is not very interesting. However, such is the difficulty of solving Boltzmann's transport equation that solutions methods often focus on using Maxwell's equilibrium distribution perturbed by some value, where that value is very small [see Bird, Stewart, and Lightfoot (2002) Appendix D] .

There have been successful applications of the Boltzmann transport equation to transition regime heat transfer. They are included in the next section.

TRANSITION REGIME SOLUTION METHODS

Some transition regime solution methods, such as the BGK collision model and the moment method approaches, solve the Boltzmann transport equation directly. Others circumvent the difficulties associated with the Boltzmann equation by relating transition regime values to free molecular and continuum regimes values (Sherman formula) or simulating the physical system directly (the DSMC method). These methods are described briefly below.

THE BGK COLLISION MODEL

In 1954 Bhatnagar, Gross, and Krook (BGK) [28] proposed replacing the collision integral in the Boltzmann equation with

$$\frac{f_{Maxwellian} - f}{\tau} \quad (2.15)$$

where

$f_{Maxwellian}$ is the Maxwellian equilibrium distribution

τ is a velocity dependent collision time

In 1968 Bassanini et al. [29] used the BGK collision model to match experimental transition regime heat conduction data within 10% for single species, monatomic gases between parallel plates and concentric cylinders at small temperature differences (<10°C) with incomplete accommodation.

LEES MOMENT METHOD

In 1962 Lester Lees [30] wrote,

At present there is no general agreement concerning the connection between highly rarefied gas flows and gas dynamics as described by the Navier-Stokes equations. Some insight into the nature of the transition between these two regimes is provided by the work of Willis, who employed a simplified Krook model for the collision integral in the Maxwell-Boltzmann equation for the single-particle velocity distribution function. But the Krook model implies isotropic scattering, which is highly suspect when there are large mean velocity and mean temperature differences or surface curvature, especially in

rarefied gases. One would like to preserve the main features of the collision process, while retaining the ability to deal with nonlinear problems.

Lees proposed using Maxwell's moment method, where quantities of interest are solved for by equations similar to 2.11 and 2.12, and two discontinuous local Maxwellians in space to solve for quantities of interest in the transition regime. A "moment" means a quantity multiplied by and then integrated with the distribution function, so equation 2.11 is a moment equation that determines particle density, and equation 2.12 is a moment equation that determines temperature. Similar moment equations can be written for the mass, momentum, energy, and energy flux. Fortuitously mass, momentum, and energy are conserved in molecular collisions, so the collision integral in Boltzmann's transport equation for these quantities is zero. Lees assumes a Maxwellian for the distribution function to calculate heat flux, but the Maxwellian he chooses depends on the direction of the molecules at a point in space of interest.

As shown in the experimental literature summary of Appendix A, numerous experimenters have successfully compared their transition regime heat transfer data for parallel plates, concentric cylinders, and concentric spheres to that predicted by the Lees 4 moment (mass, momentum, energy, heat flux) method. For monatomic molecules between concentric cylinders at small temperature differences with incomplete accommodation on the inner surface [31], Lees' solution has the following closed form:

$$\frac{q}{q_{FM}} = \frac{1}{\frac{4}{15} \alpha_1 \frac{R_1}{\lambda_1} \ln\left(\frac{R_2}{R_1}\right) + 1} \quad (2.16)$$

where

q_{FM} is the conduction in the free molecule regime

R_1 is the inner radius

R_2 is the outer radius

α_1 is the accommodation coefficient on the inner cylinder

λ_1 is the mean free path evaluated at the inner cylinder

Lord [32] extended this solution to include incomplete accommodation on the outer cylinder, but the lack of concentric cylinder heat conduction results for concentric cylinder geometries other than wire-in-tube makes it difficult to evaluate his method.

The furthest that the Lees method has been extended in the direction of this research is for mixtures of monatomic gases between parallel plates at high temperature differences. Braun et al. [25, 26] used an 8 moment method and a numerical solution technique to model heat conduction results between flat plates from $1e-4 < Kn < 10$. They compared their modeled results to their experimental data. A subset of their results is presented in Figure 2.5. Model results agree with experimental results in all pressure regimes, except perhaps in the late transition/early temperature-jump regime. Lack of confidence intervals on either the experimental or model results limits the ability of one to conclude that modeled results match experimental results in this region.

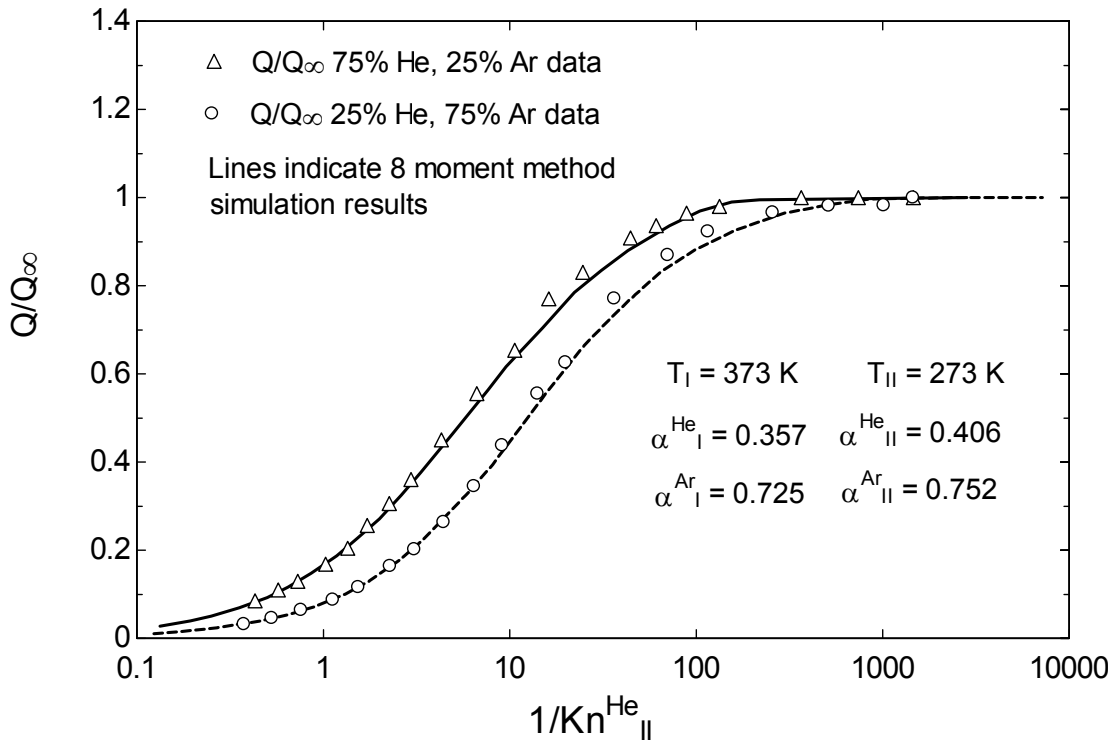


Figure 2.5 Gas mixture heat conduction results between parallel plates for large Kn number range, from Braun et al. [25]

Braun also compared linearized moment equation results to non-linearized results to quantify the error associated with linearization of the model at these large temperature differences. There is a 15 – 30% error associated with a linearized solution for the temperature difference investigated by this research.

SHERMAN INTERPOLATION MODEL

In 1963 Sherman published “A survey of experimental results and methods for the transition regime of rarefied gas dynamics” [33]. The purpose of the paper was to present the understanding of transition flow in gases composed of simple, non-reacting, electrically neutral molecules. The results of many transition flow experiments were reviewed, including heat conduction between stationary concentric cylinders, drag of insulated cylinders normal to subsonic and supersonic flow, drag of plates parallel to subsonic and supersonic flow, and pressure drop across an orifice. He found that a subsonic quantity of

interest in the transition regime, F , could often be determined from its free molecular (F_{FM}) and continuum counterparts (F_{oo}) according to the following weighting formula:

$$\frac{F}{F_{FM}} = \frac{1}{1 + \frac{F_{FM}}{F_{\infty}}} \quad (2.17)$$

This equation is easily arranged algebraically, and substituting q for F to signify transition regime heat transfer, and q_{FM} and q_{oo} for heat conduction in the free molecular and continuum regimes, respectively, the equation simplifies to

$$\frac{1}{q} = \frac{1}{q_{FM}} + \frac{1}{q_{\infty}} \quad (2.18)$$

Practically this means that any subsonic transition regime problem can be solved knowing its continuum and free molecular solutions. In the case of heat conduction the continuum solution is governed by the thermal conductivity which is unaffected by the pressure of the gas, so rarefaction's effect on transition regime heat conduction enters through the pressure dependence of the free molecular solution. An added convenience for the analysis of a gas mixture is that the gas mixture thermal conductivity takes into account all the internal energy modes (rotation, vibration) of the gases, and the free molecular solution (which is the sum of the solution for each gas separately) accounts for the accommodation coefficient of each gas on each surface as well all the energy modes of each gas through the gas's heat capacity at constant volume.

THE DIRECT SIMULATION MONTE CARLO METHOD (DSMC)

Bird [34] describes the DSMC method:

The direct simulation Monte Carlo method is a technique for the computer modeling of a real gas flow by several thousand simulated molecules. The velocity components and position coordinates of the simulated molecules are stored in the computer and these are modified with time as the molecules are concurrently followed through representative collisions and boundary interactions in the simulated physical space.

...

The simulated region is divided into a network of spatial cells with dimensions Δx such that the change in flow properties across each cell is small. Time is advanced by discrete

steps of magnitude Δt small compared with the mean free time per molecule. Both Δx and Δt may vary with time and position.

...

The molecular motion and the collision processes are uncoupled over the time interval Δt by the repeated application of the following procedure:

(i) All the molecules are moved through distances appropriate to their instantaneous velocity components and Δt .

(ii) A representative set of collisions, appropriate to Δt , is computed among the molecules, and the pre-collision velocity components of those molecules involved in the collisions are replaced by the post-collision values.

Bird wrote a book on this method [10] that comes with FORTRAN demonstration programs.

One of these programs, DSMC1, was modified and applied to this research. It's a one dimensional code useful for parallel plates, concentric cylinders, and concentric spheres that allows gas mixtures. DSMC1's only shortcoming was the assumption of complete thermal accommodation for all gases on all surfaces. The code was modified to allow incomplete thermal accommodation.

While Bird makes clear the applicability of DSMC to transition regime phenomena in general, many of the examples and studies in his book concern upper atmosphere flight and analysis of shockwaves. At CU-Boulder a class on DSMC was offered by the Aerospace department.

TRANSITION REGIME SOLUTION METHODS APPLIED TO GAS HEAT CONDUCTION IN SOLAR COLLECTORS

The Advanced Research Projects Agency (ARPA) was formed after the launch of Sputnik in 1957 to prevent the United States from being further surprised by technological advances of other countries. ARPA and the Ballistic Missile Defense funded much early transition regime heat conduction research, as shown in Appendix A. The application of the research is often not discussed, though the funding organizations and timeliness of research indicate that the rarefied regime of interest was the upper atmosphere for aerospace applications.

It wasn't until later that the application of interest turned to limiting heat loss of solar collectors. Ratzel et al. [35] performed the first in-depth investigation of annular gas heat conduction in concentric cylinder solar collectors. They presented the following set of equations to calculate parabolic trough receiver heat conduction in all pressure regimes.

$$q = 2\pi r_i LH(T_i - T_o) \quad (2.19)$$

$$H = \frac{k_{gas}}{r_i \ln\left(\frac{r_o}{r_i}\right) + \left(\frac{2 - \alpha_1}{\alpha_1}\right) \times \left(\frac{9\chi - 5}{2(\chi + 1)}\right) \times \lambda \times \left(\frac{r_i}{r_o} + 1\right)} \quad (2.20)$$

where

L is the length of the receiver

r_i, r_o are the inner and outer radii of the annulus

χ is the ratio of specific heats of the gas in the annulus (c_p/c_v)

α_1 is the accommodation coefficient on the selective surface (r_1)

λ is the mean free path of the gas

k_{gas} is the thermal conductivity of the gas

Ratzel et al. cite Dushman's text Scientific Foundations of Vacuum Technique (1962) [35] as the source for their molecular conduction model. Dushman does not cite a reference for the conduction model presented in his text, though it appears similar to the temperature jump model described by Dickens (1933) [15]. Thus equation 2.20 is a temperature-jump model that Ratzel et al. extended to all pressure regimes. Ratzel et al. compared modeled results to experimental results and both are presented in Figure 2.6. Within their stated ability to know the absorber's emittance (± 0.05), their model agrees with most of their experimental results.

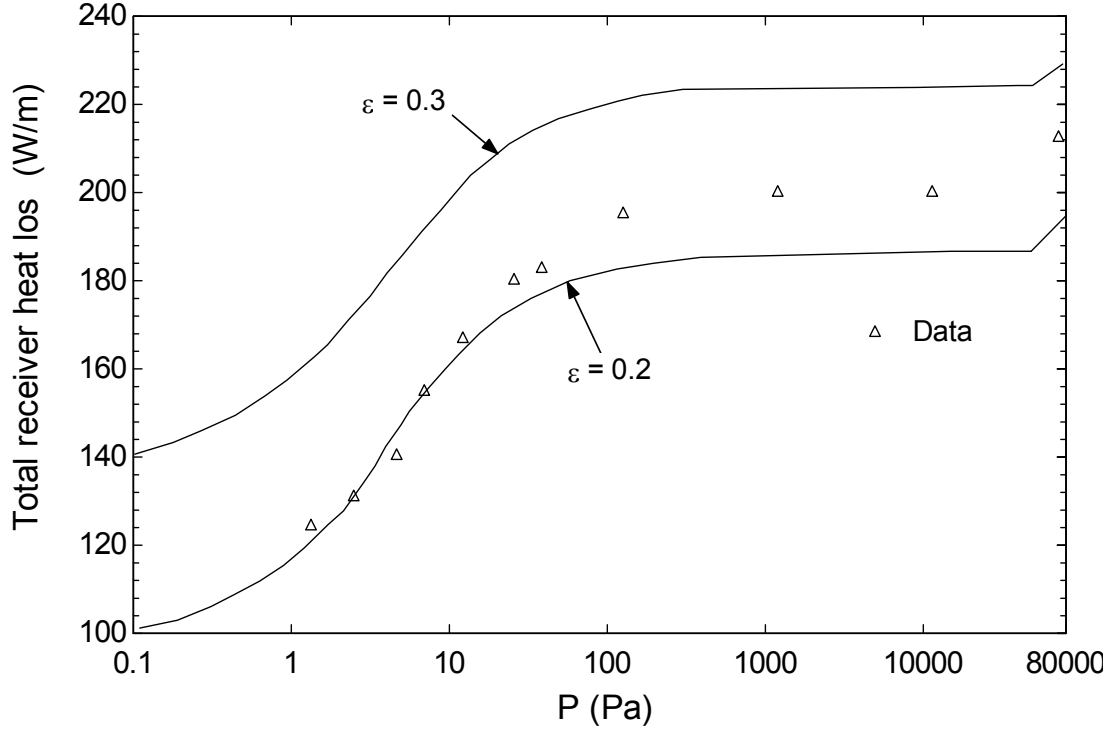


Figure 2.6 Total heat loss from a cylindrical solar receiver with varying levels of air in the annulus, from [35]

Ratzel et al.'s molecular conduction model has seen further use in parabolic trough receivers. The molecular heat conduction model of Russ Forristall's Engineering Equation Solver (EES) model of a parabolic trough receiver (2004) [5] is based on the performance model described in Dudley et al.'s "Test Results, SEGS LS-2 Solar Collector" of 1994 [37]. Dudley et al.'s performance model is a simplified version of Ratzel et al.'s model:

$$q = 2\pi r_i LH(T_i - T_o) \quad (2.21)$$

$$H = \frac{k_{gas}}{r_i \ln\left(\frac{r_o}{r_i}\right) + \left(\frac{9\chi - 5}{2(\chi + 1)}\right) \times \lambda \times \left(\frac{r_i}{r_o} + 1\right)} \quad (2.22)$$

Equation 2.22 assumes that the accommodation coefficient of the gas on the inner radius is equal to 1 (complete accommodation). Therefore this model assumes complete accommodation of the gas on each surface. Dudley et al.'s rationale for this assumption is:

The accommodation coefficient is not well characterized for glass-air surfaces and, not surprisingly, no data could be found for selective surfaces. However, several references noted that for normal surface-gas interactions " α " is near unity. One experimental study for several surfaces and gases determined that $\alpha = 1$ unless the surfaces were *extremely* well cleaned. This is what we assumed here.

They do not specify the references these conclusions were based on.

Ratzel's temperature jump method could work for a gas mixture. First the gas mixture's thermal conductivity is calculated using the procedure derived by Wilke [23]. This procedure is described and advocated by Bird, Stewart and Lightfoot [38] who compare the accuracy of its predictions to data in Mason et al. [39]. Bird, Stewart, and Lightfoot find that Wilke's equation's accuracy is $\pm 4\%$ for non-polar gases near room temperature. Mason et al. compare their more complex method to their data and find an absolute average deviation of about 4.4%, with the best results for monatomic gases. Larger deviations, around $\pm 10\%$, exist for both models when predicting the thermal conductivity of gas mixtures that include hydrogen.

More difficult for the application of the temperature jump methods to this research is that each gas, especially the gases of this research, will have different thermal accommodation coefficients on each surface so that some type of molar fraction averaging of these accommodation coefficients will be required before using the equations. A standard, prescribed method of doing this does not exist in the literature.

Sherman's interpolation formula has been applied to evacuated solar collectors. O'Shea et al. [40] investigated off-gassing as a way to decrease the stagnation temperature of an evacuated tubular solar collector. They picked gases, benzene and n-hexane, that would condense on to the selective surface near operating temperatures around 100°C, leaving the annulus evacuated and limiting heat conduction, but would desorb as the selective surface temperature increased due to lack of fluid flow in its absorber. The gases were not mixed; they were tried separately. They compare measured heat

conduction to heat conduction modeled by Sherman's interpolation formula in the figure below. They found that all their experimental data were fitted to within $\pm 7\%$ by Sherman's formula.

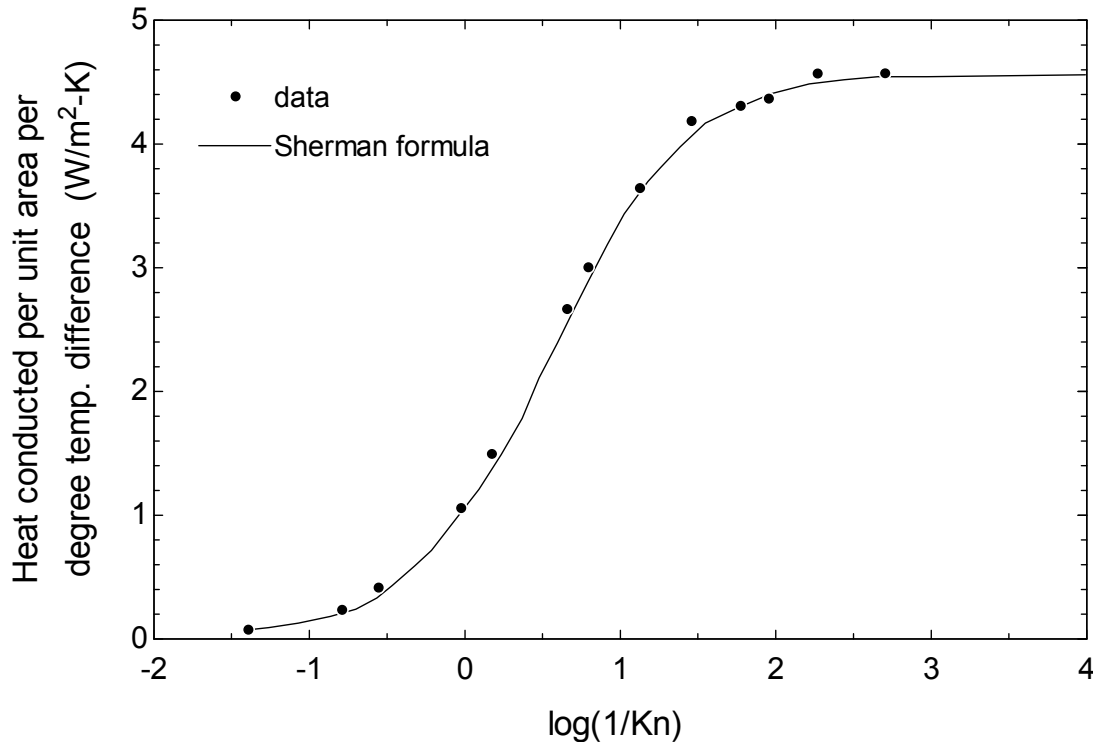


Figure 2.7 Heat conducted across approximately 75°C temperature difference in a cylindrical tubular collector, from [40]

Beikircher et al. [22, 41] investigated gas heat conduction over a wide Knudsen range in two types of evacuated solar collectors, the first being the typical concentric cylinder type and the second being a plate in tube. They use the four moment method to generalize the Boltzmann equation for pure polyatomic gases and then show that the solution for concentric cylinders is algebraically equivalent to Sherman's formula. For the plate-in-tube collector they found that Sherman's formula over-predicts the heat conduction through a large portion of the transition region, while their modified temperature jump method shows good agreement. In all cases they use pure gases (not gas mixtures) and the temperature difference between the surfaces was about 120°C.

In the case of solar collectors, O'Shea et al. [40] also compared their heat conduction data to DSMC results. Figure 2.8 shows experimental results, Sherman modeling results, and DSMC results.

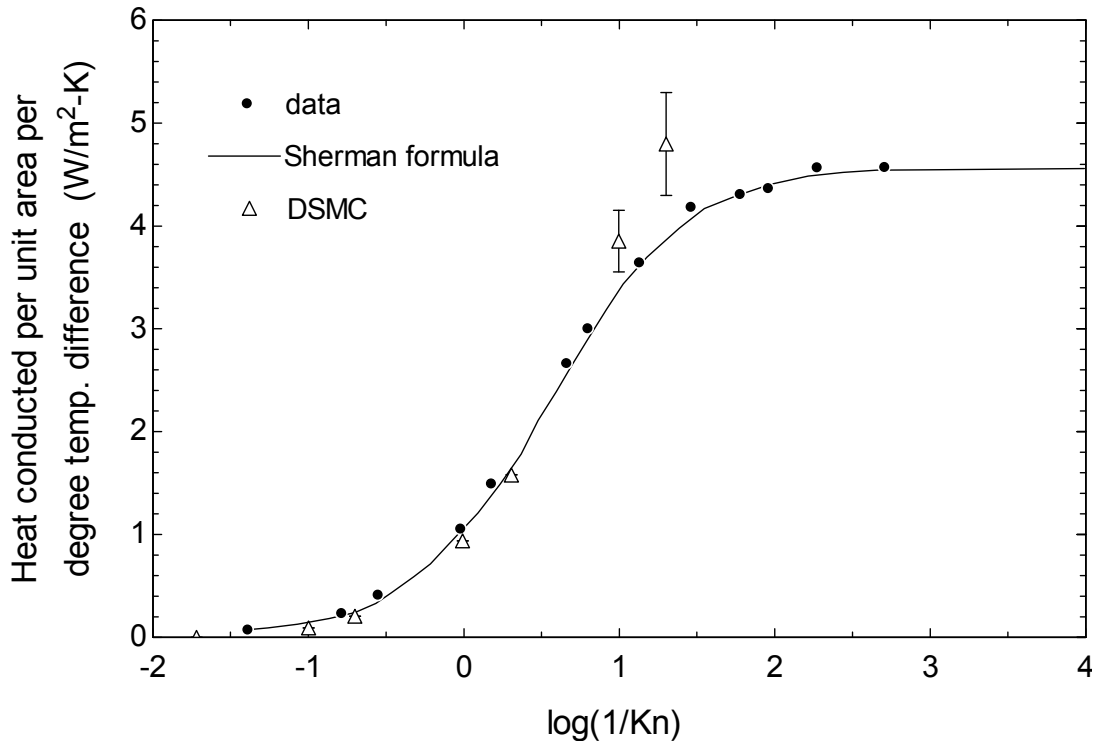


Figure 2.8. Heat conducted across approximately 75°C temperature difference in a cylindrical tubular collector, same as Figure 2.7 but with DSMC results [40]

O'Shea et al. state that the DSMC results appear to agree well for inverse Knudsen numbers less than 10, but attribute the over-prediction at larger inverse Knudsen numbers to the lack of good DSMC input parameters for these gases at these higher pressures. They do not explain the wider spread of the DSMC results at these pressures.

SELECTION OF MODELS FOR THIS STUDY

Though the concentric cylinder transition regime work is sizable, as evidenced by Appendix A, most closed-form models aren't applicable to this research. Most experiments and analyses focused on a wire-in-tube geometry, a small temperature difference, and a single monatomic gas in the annulus.

These constraints made the problem amenable to analysis by the Boltzmann transport equation, but they limit usefulness of the resulting solution.

It's possible to attempt a numerical solution to the Boltzmann equation for larger temperature differences and gas mixtures. The most promising approach would be to review the 8 moment method for a mixture of two monatomic gases described by Braun [25, 26] and build upon his work.

However, if the solution requires computer simulation, why not simulate the Boltzmann equation directly? That's what DSMC does. It's already been applied to transition regime heat conduction in concentric cylinder solar collectors with polyatomic gases and has yielded interesting results ([40] and Figure 2.9). It has shown limited promise to predict the results of this research.

Though a book exists on the DSMC method, and free FORTRAN demonstration codes are available with the book and on the internet, there's still more effort associated with running a computer simulation than a closed form algebraic equation. The Sherman model is a closed-form solution with the flexibility to calculate the heat conduction of this research. Its genesis from a wide survey of subsonic experimental results also recommends it, as do the promising results shown in Figure 2.8.

TRANSITION REGIME EXPERIMENTAL DATA IN THE LITERATURE

The most relevant data were already reviewed in this chapter. The purpose of this section is to better define the scope of the data gathered by this research and put it in context with previous work.

Table 2.1 specifies the geometry, the gases, the Knudsen number range, and the suspected accommodation coefficients of the data of this study.

Table 2.1 Metrics of the data gathered by this study

Geometry	Ratio of outer radius to inner radius (Ro/Ri)	Gases in annulus	Knudsen number range	Temperature difference, $T_{hot}/T_{cold} - 1$	Accommodation coefficient on the hot surface	Accommodation coefficient on the cold surface
Concentric Cylinder	1.7	pure species: Ar, Xe, H ₂ ----- mixtures: Ar-H ₂ , Xe-H ₂	2e-5 - 50	ΔT : 200 - 300°C ----- 0.5 – 0.9 (ratio from temperatures in Kelvin)	0.3 - 1	0.3 - 1

Appendix A summarizes experimental data from 1898 to present on transition regime heat transfer according to the metrics listed in the table above. **There are no data comparable to this research.** There are several reasons for this. As mentioned previously, the difficulties associated with the Boltzmann equation led researchers to investigate gases with the fewest distribution functions, i.e. monatomic gases. Gas mixtures with internal degrees of freedom have many distribution functions and are therefore difficult to analyze. The second constraint researchers faced was that they didn't want radiation heat transfer results to confound their molecular heat conduction results, so they limited the temperature difference between the surfaces. The selective coating on the absorber of our parabolic trough mitigates, but does not eliminate, radiation heat transfer. A third complication is that hydrogen especially does not accommodate well to the temperature of surfaces, and so the modeling method must be able to handle poor accommodation at each surface. Mathematical models were simpler using

complete accommodation at each surface – both the BGK and Lees solution methods had to be extended later for incomplete accommodation. Finally, almost all of the concentric cylinder heat conduction data are for a wire in tube geometry where complete accommodation on the outer cylinder can be assumed. The parabolic trough receiver's more modest R_o/R_i ratio and its low emittance selective coating are enablers of this research.

UNCERTAINTY ANALYSIS

Dieck [42] defines error and uncertainty:

It is important to note that every measurement ever made by every engineer or scientist has been in error and will be so in the future. There has never been and will never be a case when a person measured a variable and offered the *true* value. Error is the difference between the measurement and true value.

...

Uncertainty is not error, only an estimate of its limits.

...

There are random errors and random uncertainties. Random errors are values that affect test data in a random fashion from one reading to the next. Random error sources (random uncertainty sources) are those sources that cause scatter in the test results. This is always true.

Error sources (uncertainty sources) whose errors do not cause scatter in the test results are systematic sources and are estimated with systematic uncertainties. Systematic errors are constant for the duration of the test or experiment. Systematic uncertainty estimates the limits between which expect the systematic errors to lie with some confidence.

This research compares simulation and experimental results. There are errors associated with the measurements of experimental quantities that affect the uncertainty of the experimental results. There are uncertainties in the simulation inputs that propagate to uncertainty in the simulation results. The purpose of this section is to describe the uncertainty models used to propagate measurement and simulation input uncertainties to uncertainties in experimental and simulation results. Detailed uncertainty calculations for the experiments and the simulation models are presented in the Testing and Results chapters.

It is generally understood that when a result is presented with uncertainty limits after it, like $x = 5 \pm 0.2$, then x most likely lies between 4.8 and 5.2. A more rigorous understanding of this statement is the there is a 95% probability, or confidence, that x lies between 4.8 and 5.2. The exact mathematical model

of this statement is that x represents the mean (μ) of a population of x values that are represented by a normal distribution. The spread of the varying x values of the population is represented by the population's standard deviation, σ , and 95% of the x values of the population are no more than 2σ away from the population mean (1.96 approximated as 2 in this discussion). Thus the ± 0.2 represents 2σ , so the standard deviation of the population is 0.1.

When one receives an instrument from a manufacturer it is often provided with a calibration certification that states that under proper operating conditions the uncertainty of the instrument is \pm some value. The value could be a fixed number, a percentage of the full scale reading, or a percentage of reading. Unfortunately it is often left up to the user to determine what that number means. Convention is that it is the 2σ value, but sometimes it isn't. Discussions with manufacturers about whether the underlying distribution is normal, or uniform, or some other distribution, can be similarly frustrating. A researcher takes chances by simply taking these values at the word of the manufacturer and should have the instrument calibrations checked independently. This was done in this study.

UNCERTAINTY PROPOGATION

Helton et al. [43] describe several methods for propagating uncertainty. Three of these methods are used in this research: differential analysis, Monte Carlo analysis, and Monte Carlo analysis with Latin hypercube sampling. Each method is described below. To assist the explanations, each method is applied to propagating uncertainty in the following equation:

$$q_c = (q_T \pm \Delta q_T) - (q_R \pm \Delta q_R) \quad (2.23)$$

where

q_c is the heat conduction value whose uncertainty limits will be estimated

q_T is the total measured heat loss (conduction + radiation), assume 200 W/m

Δq_T is the 2σ uncertainty in the total measured heat loss, assume ± 8 W/m

q_R is the measured radiative heat loss (vacuum in annulus); assume 100 W/m

Δq_R is the 2σ uncertainty in the radiation heat loss; assume ± 6 W/m

DIFFERENTIAL ANALYSIS

Differential analysis involves approximating a model or an equation by a Taylor series expansion.

In the case of a first-order Taylor series expansion:

$$y(x) = f(x_0) + \sum_{i=1}^n \frac{\partial f(x_0)}{\partial x_i} [x_i - x_{i,0}] \quad (2.24)$$

where

y is a function of x_n values

x_0 is a vector, length n , of base case values for x_i given x 's distribution

Variance propagation formulas determine the uncertainty in y from the uncertainty in x . As long as the x_i values are uncorrelated:

$$V(y) = \sum_{i=1}^n \left(\frac{\partial f(x_0)}{\partial x_i} \right)^2 V(x_i) \quad (2.25)$$

where

$V(y)$ is the variance of y

$V(x_i)$ is the variance of x_i

In the case of equation 2.23, this procedure results in the following expression for the heat conduction uncertainty:

$$\Delta q_c = \sqrt{\Delta q_T^2 + \Delta q_R^2} \quad (2.26)$$

The heat conduction is $200-100 = 100$ W/m. This is the mean, μ , of the population. Its 95% confidence limits are indicated by the calculation of the 2σ spread, $(8^2+6^2)^{1/2} = \pm 10$ W/m. Figure 2.9 shows the normal distribution for the population of heat conduction values ($\mu = 100$, $\sigma = 5$).

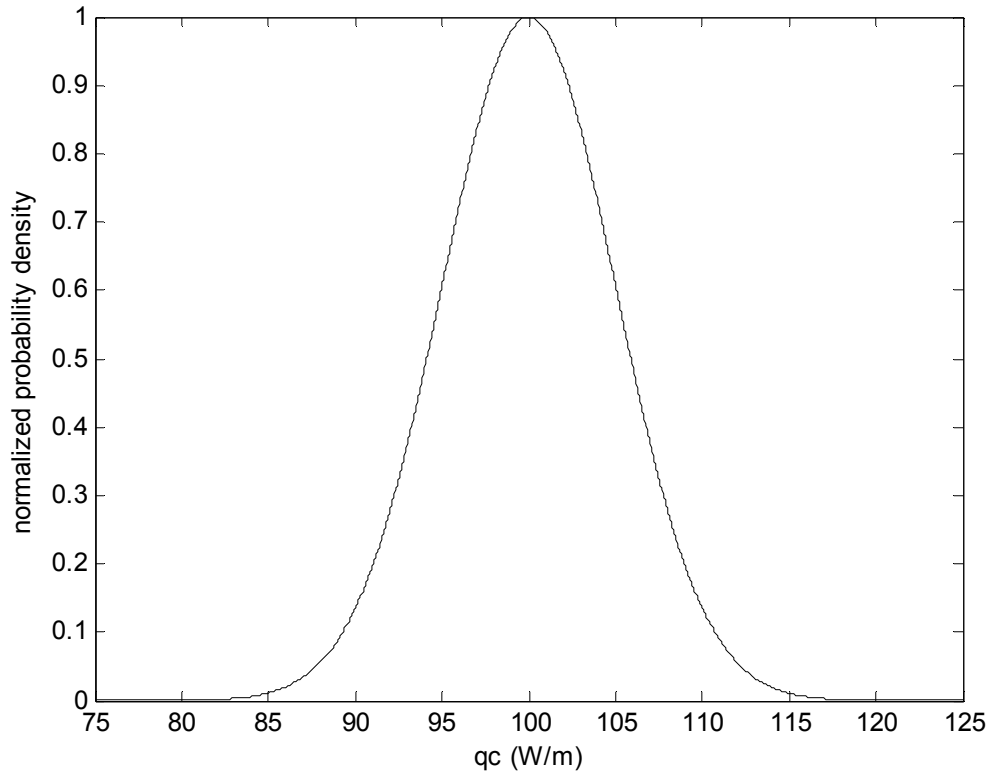


Figure 2.9 Heat conduction normalized probability density distribution for $\mu = 100$, $\sigma = 5$

MONTE CARLO ANALYSIS

Monte Carlo analysis seeks to recreate the distribution shown in Figure 2,9 using a methodology based on random sampling of the inputs and repeated evaluation of the model. $q_T \pm \Delta q_T$ and $q_R \pm \Delta q_R$ are the inputs for the heat conduction equation. One input set is created by generating one q_T value and one q_R value. q_T 's mean value is altered slightly by a value drawn at random from its uncertainty distribution, Δq_T . q_R 's value is modified similarly by a value drawn from its uncertainty distribution, Δq_R . Then q_c is calculated and recorded, and the process is repeated as many times as desired. A distribution of q_c results is created, and if the number of simulations is large enough the central limit theorem dictates that

a normal distribution is the likely result. The mean and standard deviation of the data yield the q_c value as well as its 2σ uncertainty limits. Figure 2.10 shows the results of one million simulations. It's a histogram of Monte Carlo results with the normal distribution plotted on top of it. The mean of the Monte Carlo results is 99.986, and the standard deviation is 4.997. Rounding to the first decimal place the result is $q_c = 100.0 \pm 5.0$ W/m. This is the same answer as that of the differential analysis.

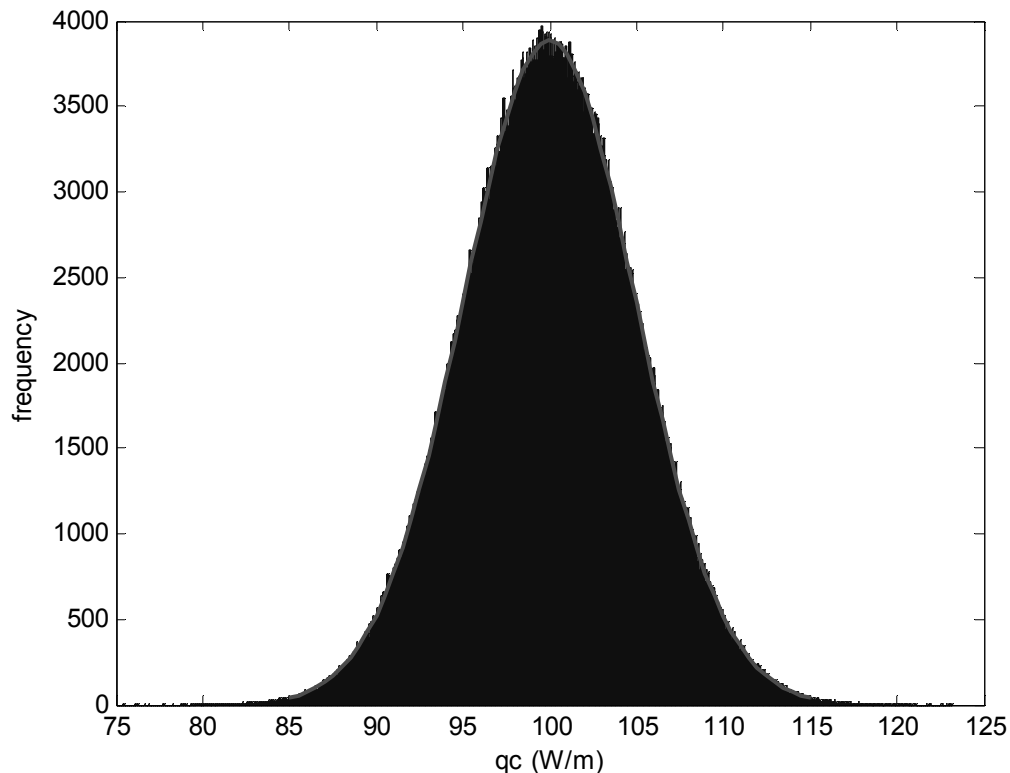


Figure 2.10 Comparison of Monte Carlo frequency distribution from one million simulations to a normal distribution with $\mu = 100$, $\sigma = 5$

Determining the mean and confidence of a distribution with Monte Carlo analysis is straightforward when many simulations are run to generate the population distribution, as above. However, when each simulation lasts from 2-5 minutes and 250 simulations are used to generate a curve representative of results (as in this research), fewer simulations are required. In this case, the distribution that is created from the Monte Carlo results is a sample of the population distribution. All values created

from that sample distribution are sample values: \bar{X} as sample mean, s the sample standard deviation.

Assuming that the sample comes from a Gaussian distribution, confidence intervals can be deduced from sample values using the student t distribution.

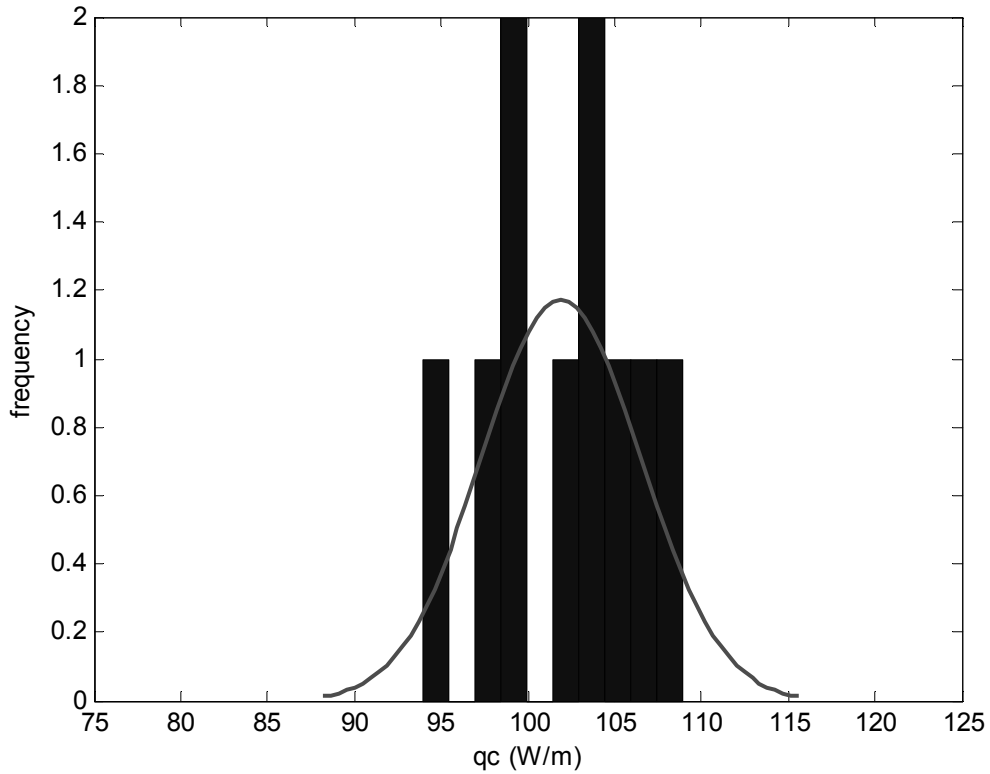


Figure 2.11 Comparison of Monte Carlo frequency distribution from 10 simulations to a normal distribution with $\mu = 100$, $\sigma = 5$

Figure 2.11 shows distribution results for $n = 10$ simulations. The mean of this sample is 101.9, and the standard deviation is 4.58. The confidence interval in the mean can be deduced from the sample standard error and the student t value for $(n-1) = 9$ degrees of freedom

$$t_{95} \frac{s}{\sqrt{n}} = 2.26 \frac{4.58}{\sqrt{10}} = \pm 3 \text{ W / m} \quad (2.27)$$

so that $\bar{X} = 102 \pm 3 \text{ W/m}$. The 95% confidence interval of the distribution, Δq_c , is $t_{95}s = 2.26 \cdot 4.58 = \pm 10.4 \text{ W/m}$. From these 10 simulations, one could conclude that the heat conduction was

102 ± 10 W/m. This is remarkably close to the one million run Monte Carlo result, with $1/100,000^{\text{th}}$ the computational cost.

Less precision is the disadvantage of using fewer simulations to determine the confidence intervals of the mean and the distribution. The precision of these metrics can be estimated through the process of statistical bootstrapping. For example, suppose that the 10 run simulation is repeated 1000 times. Each 10 run simulation will result in a sample mean, \bar{X} , and a distribution confidence interval, Δq_c . Figure 2.12 shows the spread of the heat conduction sample mean, \bar{X} , from 1000 simulations.

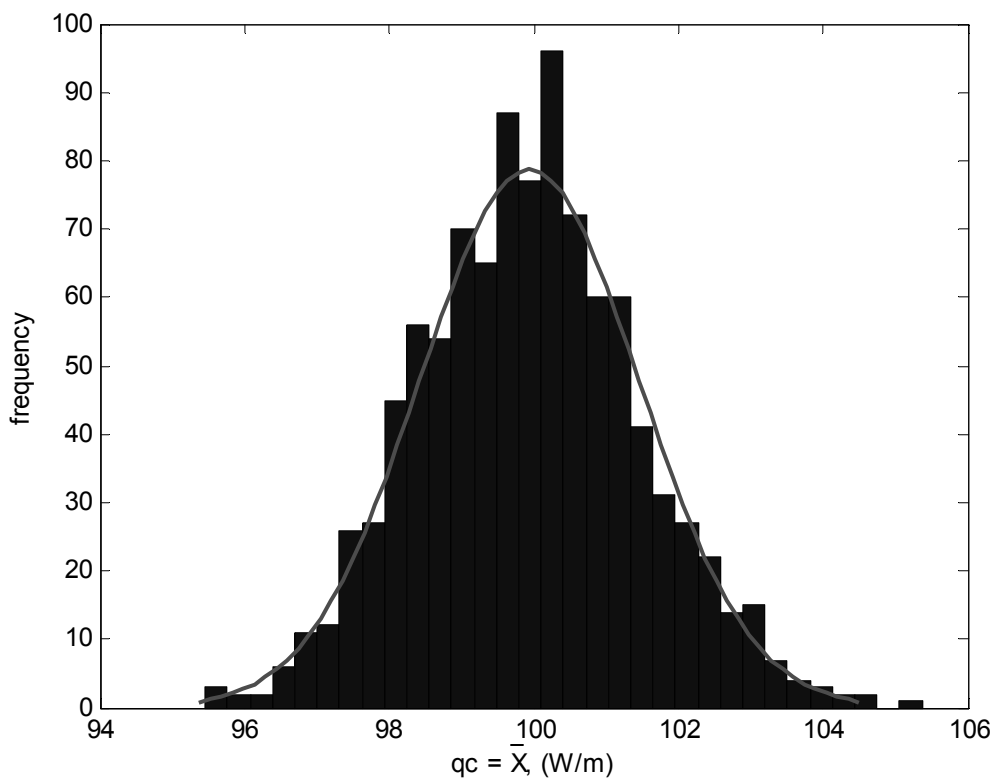


Figure 2.12 Sample mean results for 1000 simulations, where each simulation was based on 10 runs.

Based on the above distribution, the confidence interval on the sample mean is ± 3 W/m. This agrees well with the calculation of equation 2.27. Figure 2.13 shows the spread of the distribution confidence interval, Δq_c .

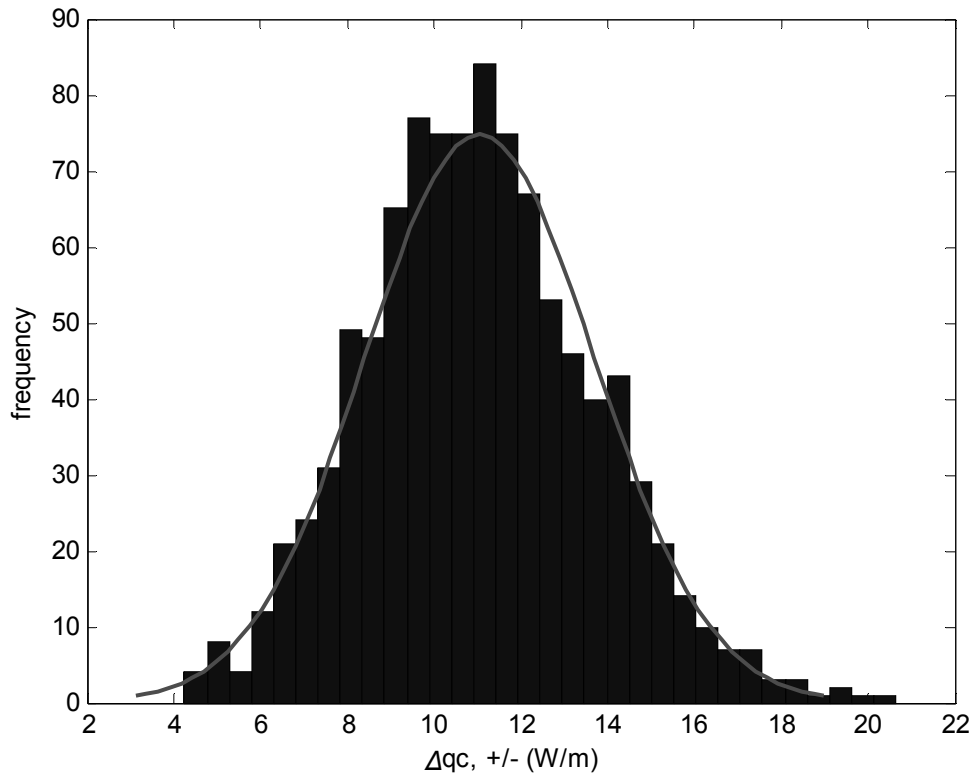


Figure 2.13 Sample confidence interval results for 1000 simulations, where each simulation was based on 10 runs.

The differential analysis and the one million run Monte Carlo analysis provide the correct answer of $\Delta q_c = \pm 10$ W/m. The 10 run Monte Carlo analysis also yielded ± 10 W/m, but that was lucky. Figure 2.13 shows that the average confidence interval is close to ± 10 W/m, but depending on the run it could be as little as ± 5 W/m or as large as ± 20 W/m.

It's understood that the use of small sample sizes leads to more uncertainty in calculated parameters. However, it's desirable to find a way to retain the reduction in computational cost for Monte Carlo analyses for fewer simulation runs while reducing the spread of the parameters calculated from the results. This is one of the goals of Latin hypercube sampling.

LATIN HYPERCUBE SAMPLING

Latin hypercube sampling (LHS) is a sampling method for Monte Carlo analyses [43]. It divides the probability distribution functions of the input parameters into equal probability bins. Say, as before, 10 simulation runs are desired. There are two input parameters, $q_T = 200 \text{ W/m}$ and $q_R = 100 \text{ W/m}$, with uncertainty distributions $\Delta q_T = \pm 8 \text{ W/m}$ and $\Delta q_R = \pm 6 \text{ W/m}$. Based on its cumulative distribution function, Δq_T is divided in 10 equal probability bins. The same thing is done with Δq_R . One value is selected from each bin. This value can either be the midpoint value in each bin, or it can be chosen randomly from within the bin. Then the bins from each parameter are placed in random order and matched up with bins from the other input parameters that were also arranged in random order. Figure 2.14 shows an example Latin hypercube sample for 10 simulations.

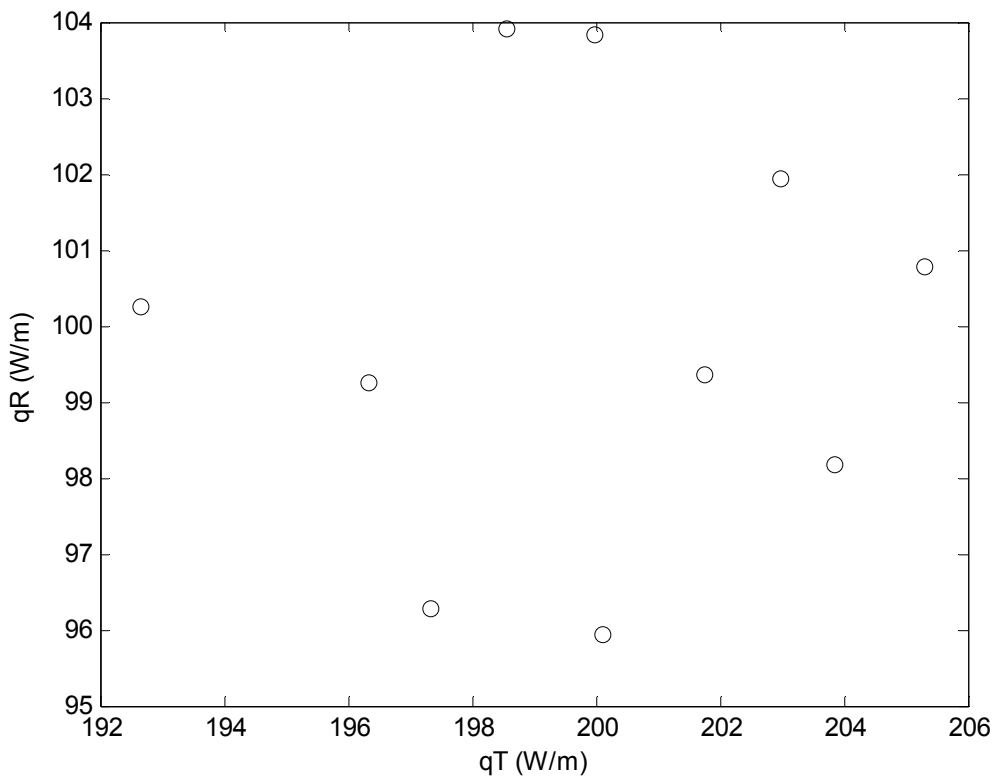


Figure 2.14 An example Latin hypercube input sample for 10 Monte Carlo simulations of $q_C = q_T - q_R$

There are 10 circles in Figure 2.14. Each circle indicates a q_T and q_R input pair for one Monte Carlo simulation. Once all inputs are used, the simulation is finished.

Besides viewing the input pairs, Figure 2.14 is useful in that it allows visualization of the correlation between the inputs. The algorithm used to generate this LHS is built into MATLAB® [45] as the command `lhsnorm`, based on Stein's algorithm [46]. The algorithm allows the user to select the degree of correlation between the variables. The algorithm iterates to deliver an input set with the desired level of correlation. Zero correlation was specified for this example, the resulting correlation in Figure 2.14 is -0.2 between q_R and q_T .

These 10 input sets are used in 10 simulations of the heat conduction problem to yield $q_C = 99.9 \pm 10.3$ W/m. Using bootstrapping (a 10 run simulation repeated 1000 times) to investigate the precision of the confidence intervals of the mean and distribution results in ± 1 W/m for the confidence interval of the mean (as compared to ± 3 W/m for random sampling) and a reduced spread of the distribution confidence interval, as shown in Figure 2.15.

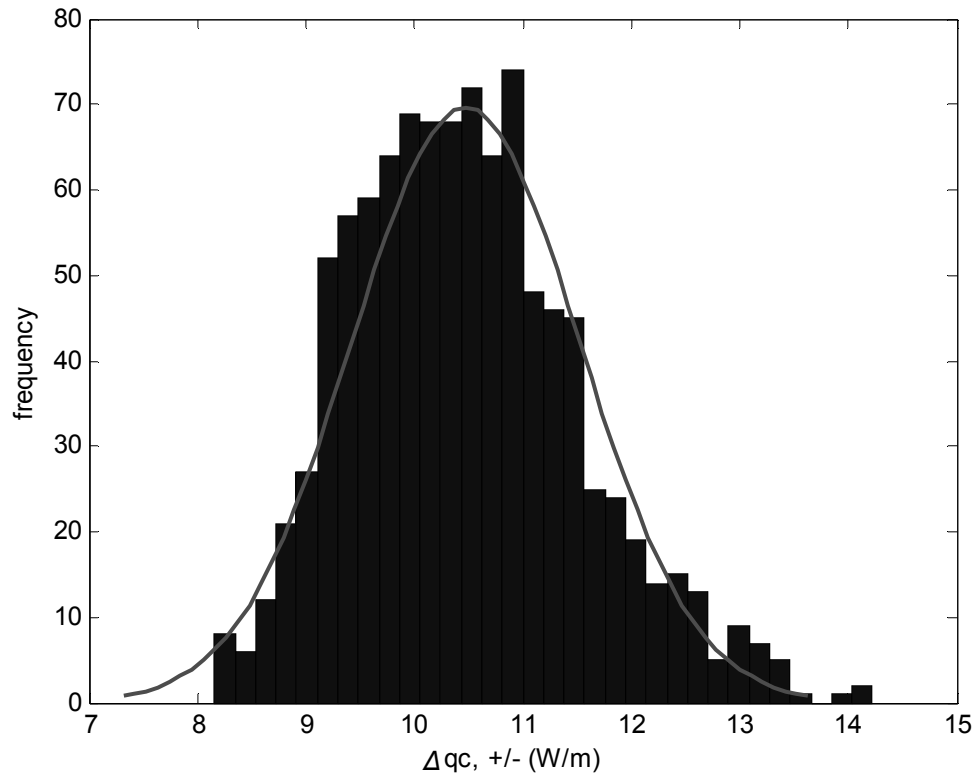


Figure 2.15 LHS confidence interval results for 1000 simulations, where each simulation was based on 10 runs.

Figure 2.13 shows that the confidence interval ranged from ± 4 to ± 20 W/m when random sampling was used, while LHS results in Figure 2.15 show a reduced range from ± 8 to ± 14 W/m. The increased precision in the confidence interval and decreased number of required simulations warrants LHS usage in the Monte Carlo simulations of this research. Specifically, Latin hypercube sampling is used in a Matlab® code to pre-process DSMC1 inputs to investigate uncertainty propagation in the DSMC method.

CHAPTER III

Modeling

This chapter describes the implementation of the Sherman interpolation formula and Direct Simulation Monte Carlo method to predict heat conduction of the pure gases (Ar, Xe, H₂) and gas mixtures (H₂/Ar, H₂/Xe) of this research in a parabolic trough receiver. Both methods use thermal accommodation coefficients so estimating them is discussed first. Then the implementation of Sherman's interpolation formula is described and an important detail of its implementation – determining a gas mixture's thermal conductivity – is elaborated.

The Direct Simulation Monte Carlo method is the subject for the remainder of the chapter. First an overview of the program flow is presented, then details of molecular movement and molecular collisions are described. Gas-related inputs to the model are presented and justified. As the Monte Carlo method is a probabilistic method based on evaluation of random numbers, the DSMC procedures that use random numbers are highlighted. Finally, how the model discretizes the gas, time, and space is discussed and a convergence study is performed to determine how many molecules, how many spatial cells, what time step, and what simulation time should be used in the DSMC simulations.

The uncertainty of both models is presented in the Results chapter. However, the uncertainties in each model's inputs are detailed here.

ESTIMATING ACCOMMODATION COEFFICIENTS

Equations 2.3 and 2.8 show that accommodation coefficients can be determined from heat conduction data in the free molecular or temperature jump regimes. However, in heat conduction tests the measured quantities are the temperatures of the surfaces and the total heat lost. Radiation heat loss is subtracted from the total heat loss to determine the heat conducted. The heat conducted becomes q_{FM} or q_{TJ} in equations 2.3 or 2.8, respectively. This presents an issue for determining the accommodation coefficients: there is one equation, and two unknowns (α_1 and α_2).

If surface 1 and surface 2 are the same material, and they are close to the same temperature (small ΔT), then the approximation that $\alpha_1 = \alpha_2 = \alpha$ is reasonable and the accommodation coefficient for both surfaces is determined. Similarly, if the experimental apparatus is concentric cylinders and the outer cylinder (surface 2) has a much larger radius than the inner cylinder (surface 1), then the assumption is made that $\alpha_2 = 1$ and α_1 is determined from testing.

Neither of these assumptions is possible in this research. Past solar collector heat conduction studies that calculated accommodation coefficients [13, 40] had one experimental set-up where borosilicate glass was both the glass envelope (surface 2) as well as the absorber (surface 1). Then they assumed that in their other test articles that the accommodation coefficient of the glass envelope didn't change (α_2) so that they could determine α_1 from their heat conduction tests.

The parabolic trough receiver of this research has a borosilicate glass envelope. One could assume that hydrogen and argon accommodate the same on this glass envelope as it did in Harding et al. [13]: $\alpha_{H_2} = 0.25 \pm 0.03$ and $\alpha_{Ar} = 0.72 \pm 0.04$ at 373 K. They didn't test xenon. However, the receiver glass of this research is covered with a silica (SiO_2) anti-reflective coating on its inside and outside surfaces (the inside surface being the relevant surface in this research). It's unclear whether Harding et al.'s receiver had this same coating. Borosilicate glass is about 70% silica, 30% boron and other materials.

Early sensitivity studies showed that simulation results were strongly dependent on hydrogen's accommodation coefficient on the absorber surface. Hydrogen conducts enough heat that getting an experimental result with acceptable uncertainty was possible. However, the experimental result relies on

a known accommodation coefficient of hydrogen on the silica surface, and for this reason a reliable method for estimating accommodation coefficients was sought in the literature.

In their paper “Correlation of thermal accommodation coefficient for ‘engineering’ surfaces”, Song and Yovanovich [16] found that experimental accommodation coefficient data can be matched to within $\pm 25\%$ by a correlation that weights “adsorbed surface” and “clean surface” accommodation coefficients while taking into account surface temperature. Their theory is that at lower temperatures gas molecules are sufficiently adsorbed on the solid surface so that impacting gas molecules interact with adsorbed gas molecules and not the solid surface, therefore the “adsorbed surface” accommodation coefficient is solely a function of the gas molecular weight and isn’t surface dependent. However, at higher temperatures the gas molecules won’t stick appreciably to the surface and so the “clean surface” accommodation coefficient is a function of the ratio of the molecular weight of the gas to the molecular weight of the molecules comprising the solid surface. Their correlation uses the molar mass of the gas and the surface it’s impacting, the temperature of the surface, and only a couple of fitting coefficients.

$$\alpha = \exp\left[C_0\left(\frac{T_s - T_0}{T_0}\right)\right]\left(\frac{M_g^*}{C_1 + M_g^*}\right) + \left\{1 - \exp\left[C_0\left(\frac{T_s - T_0}{T_0}\right)\right]\right\}\left\{\frac{2.4\mu}{(1 + \mu)^2}\right\} \quad (3.1)$$

where

M_g^* is the molar mass for monatomic gases, 1.4 times the molar mass for diatomic/polyatomic gases

C_0 is -0.57, dimensionless

C_1 is 6.8 (g/mole)

$\mu = \frac{M_g}{M_s}$ = ratio of molar mass of gas to the molar mass of the surface

$T_0 = 273$ K

The molar mass of SiO_2 is 60.09 g/mol, and the molar mass Al_2O_3 , the anti-reflective coating on the selective surface is, 102 g/mol. Figure 3.1 presents the accommodation coefficients predicted by equation 3.1 for H_2 , Ar, Xe on these two surfaces at representative temperatures.

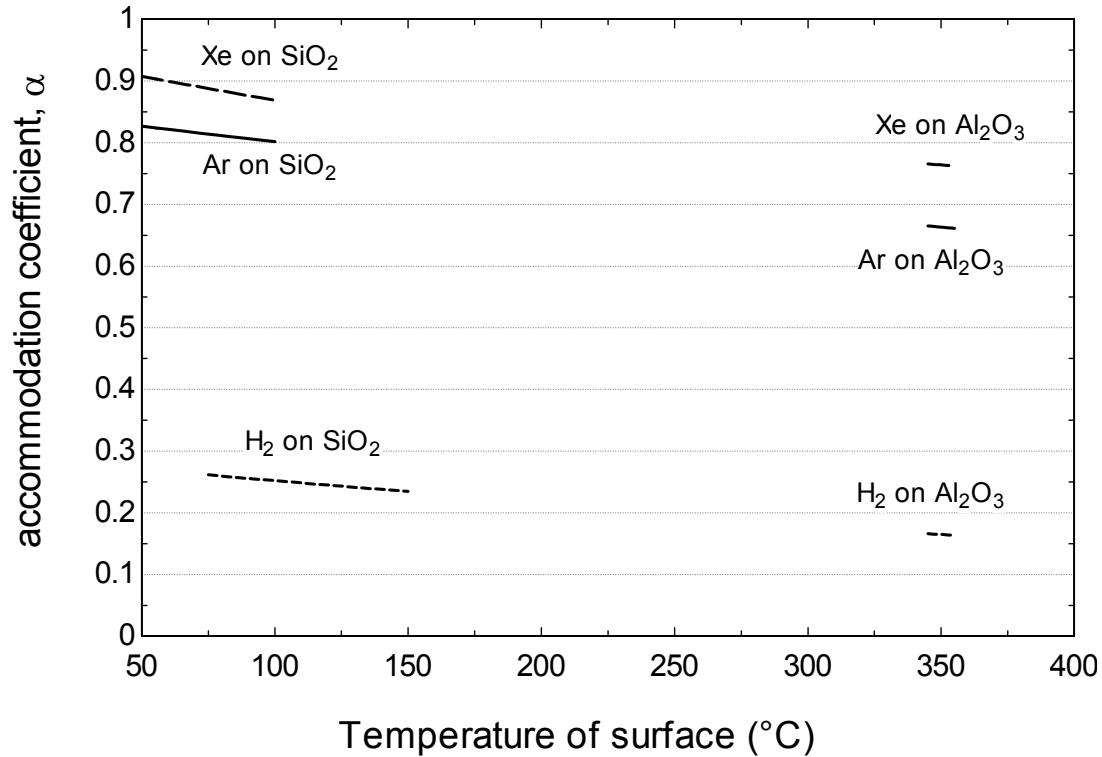


Figure 3.1 Accommodation coefficients predicted by [16] for gases and surfaces of this research

On the silica covered borosilicate glass, Song et al.'s equation predicts accommodation coefficients between 0.87 and 0.91 for xenon, 0.80 to 0.83 for argon, and 0.23 to 0.26 for hydrogen. Harding et al.'s experimental values [13], presented in Figure 2.2, for argon and hydrogen on borosilicate glass in this temperature range are 0.72 ± 0.04 for argon and 0.25 ± 0.03 for hydrogen. Song's uncertainty in each value is $\pm 25\%$, so taking average values this is 0.82 ± 0.2 for argon and 0.25 ± 0.06 for hydrogen. Harding's and Song's values agree between experiment and correlation uncertainty, though once again it's not clear whether they are for the same surface.

On the aluminum oxide covered absorber, Song et al.'s equation predicts accommodation coefficients between 0.76 and 0.77 for xenon, 0.66 to 0.67 for argon, and 0.16 to 0.17 for hydrogen. The

reason for the smaller spread of these values is that the absorber temperature is maintained at 350°C, while the glass envelope temperature is allowed to float and increases in temperature as more heat is conducted.

Hydrogen's predicted accommodation coefficient on the absorber, 0.16 ± 0.04 , is small with a small uncertainty band. Accommodation coefficients for light gases can be this small; Song et al. mention that accommodation coefficients for helium range from 0.07 to 0.38 depending on the temperature and the surface. But Harding et al. show a copper selective coating accommodation coefficient for hydrogen around 0.4 at this temperature. As this value was critical for simulated results it was determined experimentally and is discussed in the results section.

Song et al.'s correlation predicts the rest of the accommodation coefficients of this study with an assumed $\pm 25\%$ uncertainty.

SHERMAN INTERPOLATION FORMULA

This multi-regime heat conduction solution was introduced in Chapter II and its implementation is discussed here. To review, the Sherman interpolation formula uses estimates for the heat conduction in the continuum and free molecular regime to predict heat conduction in all regimes. It is remarkable that it allows for large temperature differences, gas mixtures involving polyatomic gases, and accommodation coefficients on all surfaces. Though derived as an empirical fit, it has been shown to be identical to a 4 moment solution of the Boltzmann equation by Beikircher et al. [41].

Implementation is straightforward. Accommodation coefficients are taken from literature or test data. Song et al.'s equation 3.1 is recommended. Next the thermal conductivity of the gas mixture is estimated using Wilke's procedure [23] described below. The equations are for a two-component gas mixture.

GAS MIXTURE THERMAL CONDUCTIVITY

$$k_{mixture} = \frac{X_1 k_1}{\Phi_1} + \frac{X_2 k_2}{\Phi_2} \quad (3.2)$$

where

$k_{mixture}$ is the thermal conductivity of the gas mixture

X_1, X_2 are the molar fractions of the two gases

k_1, k_2 are the thermal conductivities of the two gases

Φ_1, Φ_2 are dimensionless quantities calculated from:

$$\begin{aligned} \Phi_1 &= X_1 \Phi_{1,1} + X_2 \Phi_{1,2} \\ \Phi_2 &= X_1 \Phi_{2,1} + X_2 \Phi_{2,2} \end{aligned} \quad (3.3)$$

$\Phi_{1,1}, \Phi_{1,2}, \Phi_{2,1}, \Phi_{2,2}$ are dimensionless quantities calculated from

$$\begin{aligned} \Phi_{1,1} &= \frac{1}{\sqrt{8}} \cdot \frac{1}{\sqrt{1 + \frac{M_1}{M_1}}} \cdot \left[1 + \sqrt{\frac{\mu_1}{\mu_1}} \cdot \left(\frac{M_1}{M_1} \right)^{\frac{1}{4}} \right]^2 \\ \Phi_{1,2} &= \frac{1}{\sqrt{8}} \cdot \frac{1}{\sqrt{1 + \frac{M_1}{M_2}}} \cdot \left[1 + \sqrt{\frac{\mu_1}{\mu_2}} \cdot \left(\frac{M_2}{M_1} \right)^{\frac{1}{4}} \right]^2 \\ \Phi_{2,1} &= \frac{1}{\sqrt{8}} \cdot \frac{1}{\sqrt{1 + \frac{M_2}{M_1}}} \cdot \left[1 + \sqrt{\frac{\mu_2}{\mu_1}} \cdot \left(\frac{M_1}{M_2} \right)^{\frac{1}{4}} \right]^2 \\ \Phi_{2,2} &= \frac{1}{\sqrt{8}} \cdot \frac{1}{\sqrt{1 + \frac{M_2}{M_2}}} \cdot \left[1 + \sqrt{\frac{\mu_2}{\mu_2}} \cdot \left(\frac{M_2}{M_2} \right)^{\frac{1}{4}} \right]^2 \end{aligned} \quad (3.4)$$

where

M_1, M_2 are the molar masses of gas 1 and gas 2

μ_1, μ_2 are the viscosities of gas 1 and gas 2

Wilke [23] and Bird, Stewart and Lightfoot [38] cite an average agreement between this correlation and experimental data [39] of $\pm 4\%$. However, upon review of the papers there are several instances where the thermal conductivity of a gas mixture including hydrogen is $\pm 10-15\%$ different than that predicted by this correlation. Another reason to increase the uncertainty is that the thermal conductivities for this research are at elevated temperatures. Near room temperature, the uncertainty of pure gas thermal conductivities is 0.5% or less, but around 200-300°C this increases to 2% [46]. The uncertainty of gas mixtures will increase similarly [46]. Therefore the uncertainty of the pure gas thermal conductivities is $\pm 2\%$, while the uncertainty of the gas mixture thermal conductivity is $\pm 10\%$.

SHERMAN SUMMARY

With the accommodation coefficients (equation 3.1) and thermal conductivity (equation 3.2) determined, the following set of equations are solved to determine the heat conduction in any heat conduction regime.

$$q_{FM,1} = \frac{1}{\frac{1}{\alpha_{1,1}} + \frac{R_1}{R_2} \left(\frac{1}{\alpha_{1,2}} - 1 \right)} \cdot \frac{P_1 \left(C_{v,1} + \frac{R_g}{2} \right)}{\left(2\pi M_1 R_g T_{avg} \right)^{1/2}} \cdot (T_1 - T_2) \cdot 2\pi R_1$$

$$q_{FM,2} = \frac{1}{\frac{1}{\alpha_{2,1}} + \frac{R_1}{R_2} \left(\frac{1}{\alpha_{2,2}} - 1 \right)} \cdot \frac{P_2 \left(C_{v,2} + \frac{R_g}{2} \right)}{\left(2\pi M_2 R_g T_{avg} \right)^{1/2}} \cdot (T_1 - T_2) \cdot 2\pi R_1$$
(3.5)

where

$q_{FM,1}, q_{FM,2}$ are the free molecular heat conduction of gases 1 and 2 evaluated at surface 1 (W/m)

P_1, P_2 are the partial pressures of gas 1 and gas 2

R_1, R_2 are the inner and outer radii, respectively

$\alpha_{1,1}$ and $\alpha_{1,2}$ are the accommodation coefficients of gas 1 on the inner and outer surface, respectively

$\alpha_{2,1}$ and $\alpha_{2,2}$ are the accommodation coefficients of gas 2 on the inner and outer surface, respectively

M_1, M_2 are the molecular masses of gas 1 and gas 2

$C_{v,1}, C_{v,2}$ are heat capacities of gas 1 and gas 2 at T_{avg}

T_{avg} is the average gas temperature; its calculation is discussed below

R_g is the gas constant

T_1 and T_2 are the temperatures of surface 1 (the inner radius) and surface 2 (the outer radius)

The heat conduction of the gas mixture in the continuum is calculated from

$$q_{\infty} = \frac{2\pi k_{mixture}(T_1 - T_2)}{\ln\left(\frac{R_2}{R_1}\right)} \quad (3.6)$$

where

q_{∞} is the heat conducted in the continuum (W/m)

$k_{mixture}$ is the gas mixture thermal conductivity calculated by equation 3.2

Thermophysical properties are required in equations 3.2, 3.4, and 3.5. The temperature at which these properties are evaluated should be discussed. In the case of flat plates, it's common to calculate properties at the average temperature of the surfaces: $T_{avg} = (T_1 + T_2)/2$. This is less clear for concentric cylinders because the radial temperature distribution is expected to be non-linear. Figure 3.2 shows the

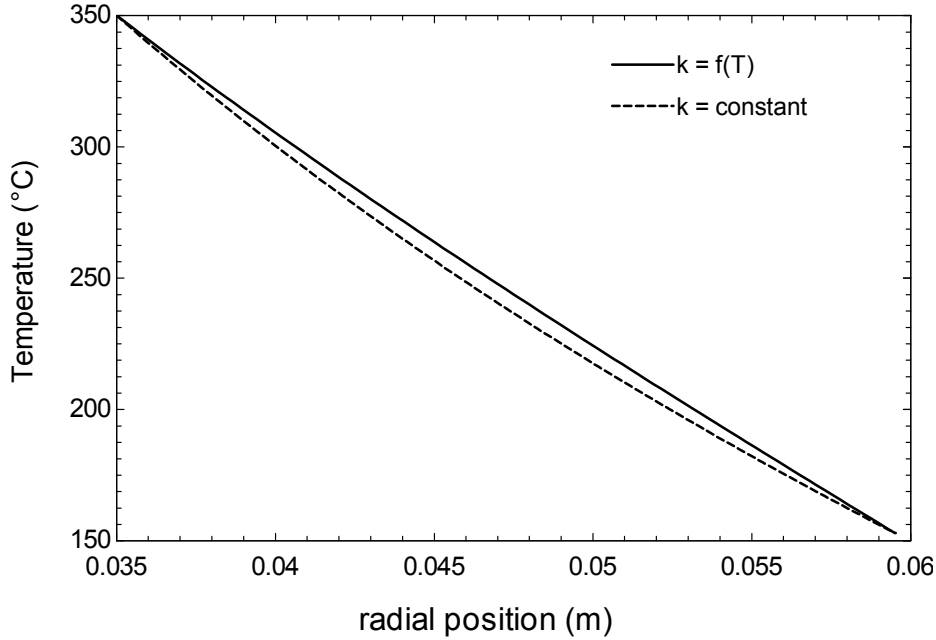


Figure 3.2 Continuum radial temperature distributions for hydrogen assuming constant thermal conductivity and conductivity that increases with temperature

radial temperature distribution expected in the continuum assuming a constant thermal conductivity and then using hydrogen's actual thermal conductivity that increases with temperature. The expected distribution is essentially linear due to the relatively small ratio of the outer cylinder radius to the inner cylinder radius and the variation of the thermal conductivity with temperature. This is true for xenon and argon as well. For these reasons thermophysical properties are calculated as the average of the surface temperatures, $T_{avg} = (T_1 + T_2)/2$.

Finally, the heat conduction, q , is calculated from

$$\frac{1}{q} = \frac{1}{q_{FM,1} + q_{FM,2}} + \frac{1}{q_{\infty}} \quad (3.7)$$

EES® [47] calculates the thermophysical properties with algorithms based on [48]. The Sherman model presented above is implemented in EES and presented in Appendix B.

DIRECT SIMULATION MONTE CARLO METHOD

G.A. Bird developed the Direct Simulation Monte Carlo (DSMC) method for the study of rarefied gas flows [34]. He later wrote a book on the method [10]. Initial criticism of the method claimed that its random sampling techniques distorted the unvarying solution of the Boltzmann equation that it attempted to model, but Bird shows [34] that it is an exact numerical solution to the Boltzmann equation.

DSMC takes a real gas that has between 10^{18} and 10^{22} molecules per m^3 and reduces its density by assigning the momentum, translational energy, and rotational energy of 10^{13} to 10^{18} molecules to one molecule. The trajectory of that molecule is traced in a discretized space over discrete time steps. In each time step the molecule is allowed to move, perhaps collide with a system boundary, and then given the opportunity to collide with other adjacent molecules. Figure 3.3 is a flow diagram of the DSMC1 code used in this research. The FORTRAN code that comprises the model is listed in Appendix C. A Matlab® pre-processor that prepares the DATA1 file for DSMC1 and implements the Latin hypercube sample is listed in Appendix F.

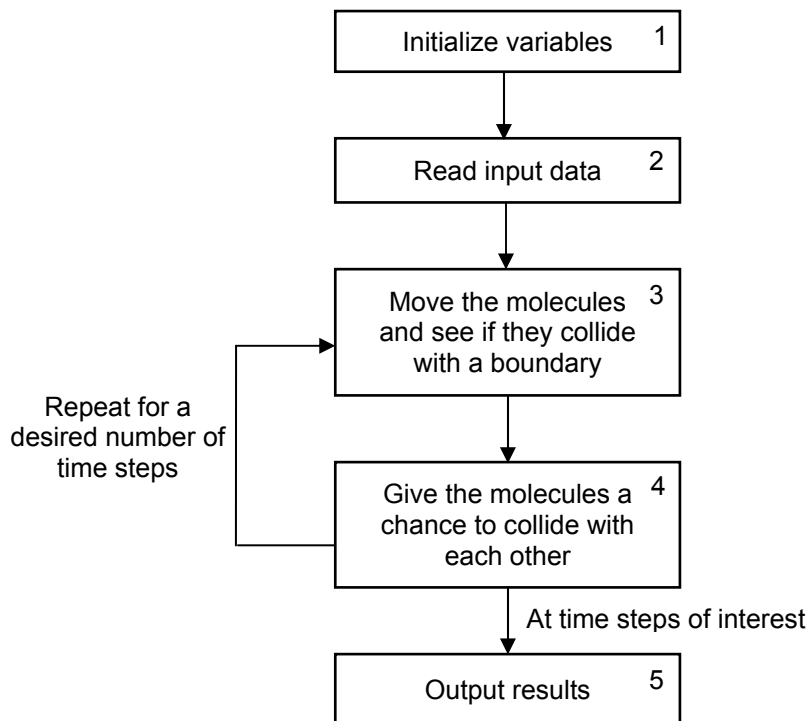


Figure 3.3 DSMC1 flow diagram

The most interesting and important sections of the program flow are 3) molecule movement and 4) molecule collisions. Each section is discussed below.

MOLECULE MOVEMENT AND COLLISIONS WITH BOUNDARIES

Molecule motion follows rules of particle kinematics with no acceleration (unless the user wishes gravity to be considered). In the case of a cylindrical geometry, a particle's velocity is broken down into a radial, tangential, and longitudinal (along the cylinder's long axis) components. The particle displacement along each of these axes is calculated based on the corresponding velocity and the Δt of the time step. At the conclusion of the time step, the new radial position is calculated and the radial and tangential velocities at the beginning of the time step are transformed through rotation into new radial and tangential velocities. Only the radial position of the molecule is stored in memory, but the three-dimensional molecular velocity is always stored.

Eventually a molecule will hit the inner or outer cylinder during a time step. When this happens the amount of time it took for the molecule to hit the boundary is calculated, and that time is subtracted from Δt leaving a remaining time interval over which the molecule will be moved after reflection from the surface. Then the molecule – surface interaction is determined.

When a molecule hits a surface, its incident translational energy, rotational energy (if any), and incident momentum are recorded. These values, when paired with reflected values, determine the pressure of the gas and the heat transferred to or from the surface. Then the molecule-surface interaction is determined. The only molecule-surface interaction in Bird's DSMC1 code is diffuse reflection with complete thermal accommodation. This means that reflected velocities are independent of incident velocities, with the reflected velocities based entirely on the temperature of the surface and random numbers that generate the three reflected components of the velocity.

Maxwell's accommodation coefficient model [49] was added to DSMC1. In this model one of two things happens during a molecule-surface interaction. Either the molecule is briefly adsorbed by the surface, thereby completely accommodating to its temperature and diffusely reflecting from it, or it doesn't

and it specularly reflects from the surface with no net energy exchange. In the Maxwell model an accommodation coefficient of 0.7 means that there is a 70% chance during a molecular collision with the surface the former occurs (complete accommodation), and a 30% chance that no accommodation occurs. This is a simple, classical model, but still used to define accommodation coefficients today [50].

COLLISIONS BETWEEN MOLECULES

The DSMC method is useful for modeling dilute gases. In a dilute gas, collisions predominantly involve only two molecules. This is one reason why the DSMC method is not applied to dense gases.

DSMC divides the physical space between two surfaces into cells, and within the cells, sub-cells. Macroscopic quantities for the cells are calculated using the averages of the quantities in the subcells. The primary function of the sub-cells is to provide molecules with nearby potential collision partners.

The probability of a collision between two simulated molecules over the time interval Δt is equal to the ratio of the volume swept out by their collision cross-section moving at the relative speed between the two molecules to the cell volume:

$$P = \frac{F_N \sigma_T c_r \Delta t}{V_C} \quad (3.8)$$

where

P is the probability of a collision

F_N is the number of real molecules that the simulated molecule represents

σ_T is the collision cross-section

c_r is the relative velocity defined by the scalar length of the vector difference of the molecules' 3 component velocities

Δt is the desired time step interval

V_C is the volume of the cell

Though DSMC once used equation 3.8 to determine the likelihood of two adjacent molecules colliding, it was discarded because it was computationally inefficient. P is usually a very small number. Additionally, it was computationally expensive to go through each simulated molecule in each cell and calculate possible collision with all its neighbors. A better solution was to select, through a random process, only a fraction of the molecules in each cell for possible collision, and to scale up the probability by the inverse of this fraction. The least calls to the random number generator result when the maximum probability (based on the maximum product of the relative velocity and collision cross-section) is scaled by this procedure to 1. In this case the number of collision pairs selected per cell per time step is

$$P_s = \frac{1/2 N \bar{N} F_N (\sigma_T c_r)_{\max} \Delta t}{V_C} \quad (3.9)$$

where

P_s is the number of collision pairs selected in the cell during one time step

N is the instantaneous number of simulated molecules in the cell

\bar{N} is the average number of simulated molecules in the cell calculated from the real number density, cell volume, and the number of real molecules represented by a simulated molecule

$\sigma_T c_r$ is the maximum product of the relative velocity and collision cross-section.

The probability of a collision is computed by generating a uniform random number R_f between 0 and 1 and comparing it to

$$P = \frac{(\sigma_T c_r)}{(\sigma_T c_r)_{\max}} \quad (3.10)$$

where

$(\sigma_T c_r)$ is the product of the relative velocity and collision cross-section of the collision pair in question

$(\sigma_T c_r)_{\max}$ is the maximum product of the relative velocity and collision cross-section in the cell

If $R_f < P$, a collision occurs.

COLLISIONS DYNAMICS

Through conservation of energy and the conservation of linear and angular momentum, Bird [10] shows that an elastic collision between two particles can be reduced to the motion of a reduced mass particle in the plane containing the two velocities with the center of mass as its origin. In this frame of reference three quantities, the pre-impact relative velocity vector \mathbf{c}_r , the distance of closest approach b , and the deflection angle χ , completely determine the post-collision relative velocity vector \mathbf{c}_r^* . From \mathbf{c}_r^* and the velocity of the center of mass, which doesn't change during the collision, the post collision velocities for the two molecules are determined. Figure 3.4 illustrates some of these quantities.

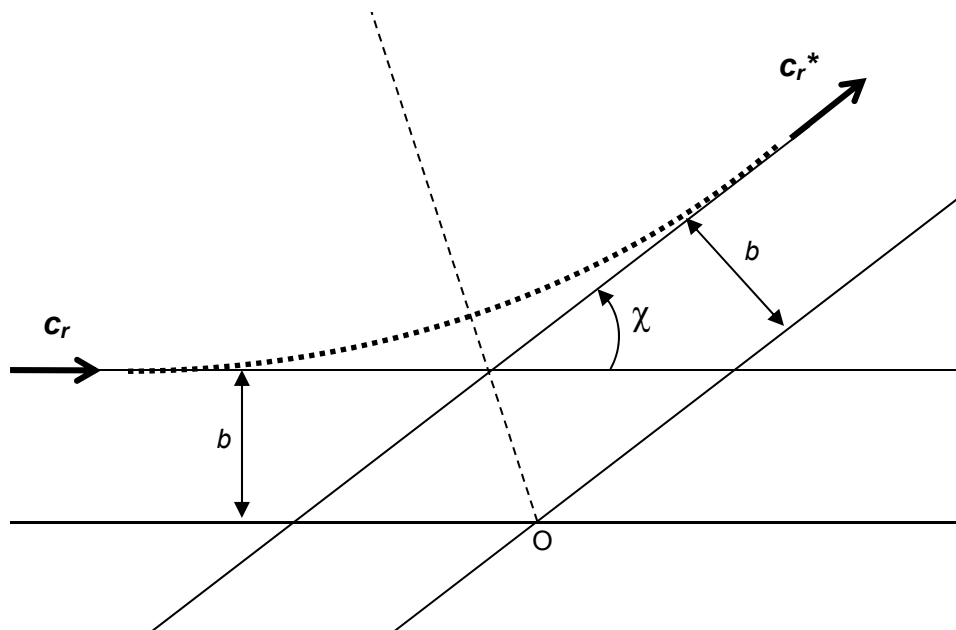


Figure 3.4 Impact parameters of a reduced mass particle with a fixed scattering center, O

The velocities of the center of mass, the pre-impact relative velocity \mathbf{c}_r , and the distance of closest approach b can be calculated before the collision. These quantities are known. What remains is to calculate the deflection angle χ .

The deflection angle is calculated from R_f , a uniformly distributed random number between 0 and 1, and a characteristic of the gas called the scattering coefficient, α_s , in the following equation.

$$\cos(\chi) = 2R_f^{1/\alpha_s} - 1 \quad (3.11)$$

The scattering coefficient is calculated from the self diffusion coefficient of the gas. This quantity is described further in the DSMC inputs section.

INELASTIC COLLISIONS

Molecules with internal degrees of freedom, such as a hydrogen molecule, have energy stored in internal energy modes. Translational and internal energies can be exchanged in a collision, and a purely elastic model of the collision won't allow this. DSMC accounts for inelastic collisions and this section describes the methodology.

DSMC uses the Larsen-Borgnakke calculation to determine the energy redistribution between the internal and translational energy modes. To start, the probability that this exchange will occur is determined from the comparison of a uniform random number R_f to the inverse of the relaxation collision number for the gas, Z . This number is a characteristic of the gas. For hydrogen at these temperatures, Z is roughly 5. This means that on average hydrogen requires 5 collisions before the energy stored in its internal (rotational) energy modes is in equilibrium with the energy in its translational energy modes. Next the total energy in the collision is calculated (translational and rotational). Based on the average temperature of the gas, probability distribution functions are created for the internal and translational energy modes. The post collision translational energy is selected using a random number, and is apportioned between the two molecules by another random number. Random numbers also split the internal energy between the two molecules if both have internal degrees of freedom.

This is a broad overview that neglects many details. The interested reader is referred to Chapter 5 and Chapter 11 in Bird's text [10]. The DSMC1 subroutine INELR in Appendix C presents the calculations in detail.

DSMC GAS INPUTS

The DSMC method simulates molecules as spheres whose diameter is used in collision cross-section calculations. The spheres are given mass but no moment of inertia. The energy associated with internal degrees of freedom (for a non-monatomic molecule) is stored for each molecule and allowed to participate in collisions. Other inputs relate macroscopic quantities to coefficients describing collision dynamics. Bird [10] provides recommended values for each input in Appendix A in his text and these inputs were used in the simulations. Though Bird does not present uncertainties for the inputs, he does show how they are calculated from thermophysical properties. Uncertainties in the inputs can be estimated from uncertainty in the thermophysical properties.

A table with all gas inputs used in this research is presented below.

Table 3.1 DSMC1 gas related inputs

DSMC input	Hydrogen	Argon	Xenon	Uncertainty estimate
Molecular diameter (m)	2.88e-10	4.11e-10	5.65e-10	±0.5%
Diameter reference temperature (K)	273	273	273	-
Viscosity temperature index (-)	0.67	0.81	0.85	±1%
Reciprocal of scattering coefficient (-)	0.7407	0.7143	0.6944	±3.5%
Mass of one molecule (kg)	3.44e-27	66.3e-27	218e-27	-
Rotational degrees of freedom (-)	2	0	0	-
Rotational relaxation number (-)	5	0	0	±40%
Accommodation on absorber	0.34 ^a	0.66 ^b	0.76 ^b	±25%
Accommodation on glass	0.25 ^b	0.82 ^b	0.90 ^b	±25%

a = calculated from experimental results in this research

b = from Song et al's correlation [16]

The reason for the diameter reference temperature is that realistic molecular diameters are not constant but depend on the relative translational energy in the collision. Bird [10] shows that the molecular diameter of a gas involved in a collision is

$$d = d_{ref} \left(\frac{c_{r,ref}}{c_r} \right)^{\omega - 1/2} \quad (3.12)$$

where

d = the molecular diameter due to the relative speed of the collision

d_{ref} = the reference diameter in the table above defined at the reference temperature

$c_{r,ref}$ = the relative speed of collisions at the reference temperature

c_r = the relative speed of the collision

ω = the viscosity temperature index

Bird [10] says the following about the viscosity temperature index:

While the coefficients of viscosity and heat conduction can be regarded as continuum gas properties, it will be found that an essential feature of a successful molecular model for rarefied gas flow studies is that it should reproduce the viscosity coefficient of the real gas...

Bird shows that the intermolecular force inverse power law and a molecular model that realistically modifies the molecular diameter by the translational energy in a collision lead to a power law temperature dependence of the coefficient of viscosity, i.e. $\mu \propto T^\omega$ where ω is the viscosity temperature index. Figure 3.5 shows two power law fits of hydrogen's viscosity. The coefficient that matches best is the value presented in table 3.1. The second fit is shown to make the case that there is a $\pm 1\%$ uncertainty in the viscosity temperature index value. A similar exercise was performed for argon and xenon and similar fits with the values of table 3.1 were observed. An interesting side note is that the molecular model would be that of simple, hard spheres (fixed collision diameter, isotropic scattering in center of mass frame of reference) for $\omega = 1/2$ and a scattering coefficient, $\alpha_s = 1$.

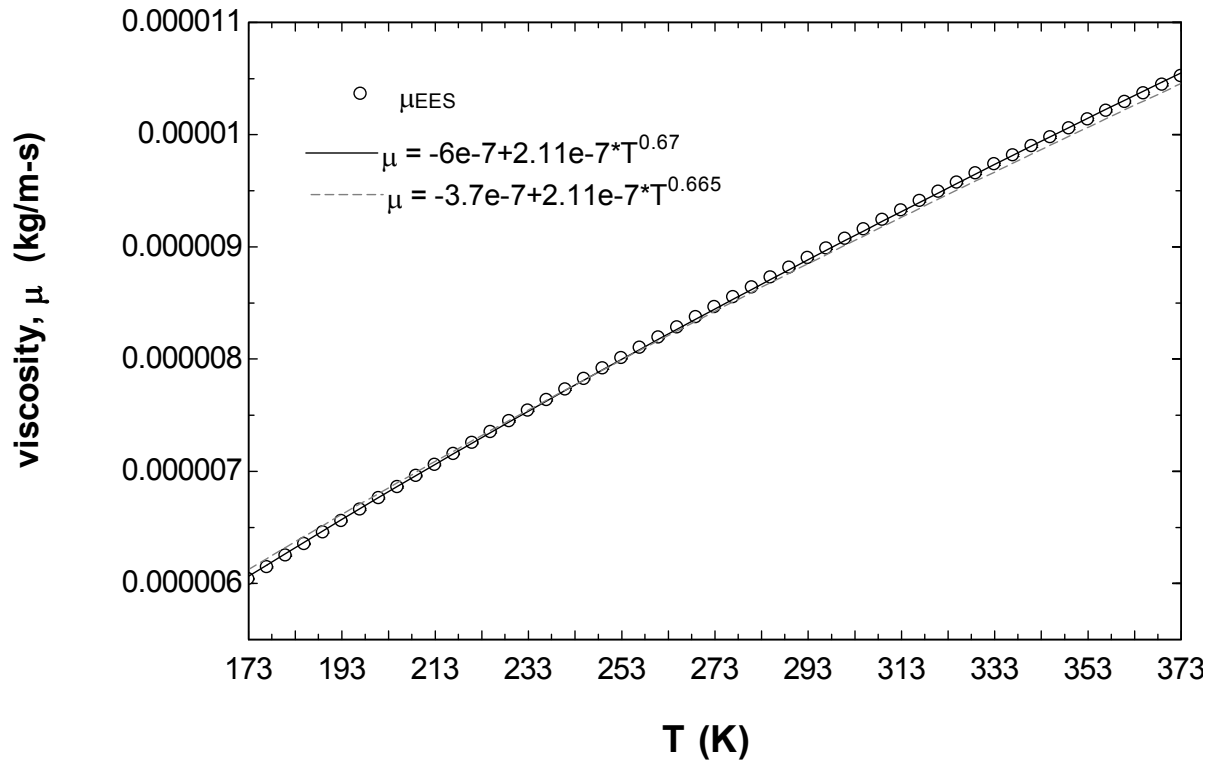


Figure 3.5 Power law fits of hydrogen's viscosity

The scattering coefficient, introduced in equation 3.11, affects the deflection angle of a molecule in an intermolecular collision. It can be related to the Schmidt number

$$\frac{2 + \alpha_s}{\frac{3}{5}(7 - 2\omega)\alpha_s} = \frac{\mu_{ref}}{\rho \cdot D_{ref}} \quad (3.13)$$

where

α_s is the scattering coefficient

ω is the viscosity temperature index

μ_{ref} = viscosity at the reference temperature

D_{ref} = self diffusivity coefficient

NIST [51, 52] states that uncertainties in gas viscosities, diffusivities, and densities are approximately 0.5%, 2%, and <0.02%, respectively. The uncertainty in the scattering coefficient is $\pm 3.5\%$ as a result.

Hydrogen is the only molecule in this study with internal degrees of freedom due to its diatomic structure and the ability of the molecule to rotate with significant rotational energy about axes orthogonal to the line between the two atoms comprising its structure. The rotational relaxation number is an estimate of the number of collisions the molecule requires for the energy in the internal energy modes and translational energy modes to come to equilibrium. Bird [10] presents a figure (Fig. A2, pg. 413) showing rotational relaxation number versus temperature, and the mean value is about 5 with about a ± 2 spread at the temperatures of this research. The uncertainty in this value is estimated at 40%.

The accommodation coefficients here are the same accommodation coefficients used in the Sherman formula. The uncertainty in each accommodation coefficient is 25%. The accommodation coefficient of hydrogen on the absorber is a tested value, while all the other accommodation coefficients come from Song et al. [16], equation 3.1.

CONVERGENCE INVESTIGATION

DSMC1 inputs besides gas inputs consist of defining the geometry, the time step, and the number of time steps until steady flow. In Chapter 11, Bird [10] analyzes a 6 Pa homogenous gas mixture using DSMC and compares DSMC collision rates and other properties favorably to theory. His DSMC study used 1000 molecules, 50 cells, and 8 subcells per cell (400 subcells total). One simulated molecule represented 10^{17} real molecules. The gas was placed between parallel plates 1 m apart. His cell width was the order of the mean free path, but more importantly the sub-cell width was much smaller than the mean free path. He chose a time step such that the mean value of one component of the molecular velocity would cause the molecule to travel $\frac{1}{4}$ of the cell width in one time step. The simulation was stopped at 500 updates, where each update was 160 time steps. Bird states that the accuracy of DSMC simulations should increase with more molecules, shorter time steps, and longer simulation times.

Bird's study was a homogenous gas mixture with no gradients, but it provides a good starting point for the convergence and discretization study of this research. The 24.5 mm gap between the glass envelope and absorber was divided into 20 cells with 20 subcells per cell (400 subcells total). The time step was based on the mean collision time, which is the mean free path divided by the mean thermal speed of the gas. One update was set equal to 100 time steps. The gas in the annulus was set to pure hydrogen. The absorber surface was set to 350°C, and the glass temperatures were set consistent with the pressures and mentioned below.

3 pressures were studied: 33 Pa, 5 Pa, and 0.7 Pa. 0.7 Pa corresponds to near free-molecular flow conditions. 5 Pa is in the middle of the transition regime, and 33 Pa is in the temperature jump regime for hydrogen. The purpose of the convergence study was to find the number of molecules, the number of cells, the size of the time step, and the number of time steps (measured in updates) needed to obtain consistent results at these three pressures. Based on prior experience, it was expected that the temperature jump case would be the most demanding.

The first investigation was the number of molecules to use in the simulation. Figure 3.6 shows the predicted heat conduction based on the number of molecules for the 33 Pa hydrogen case.

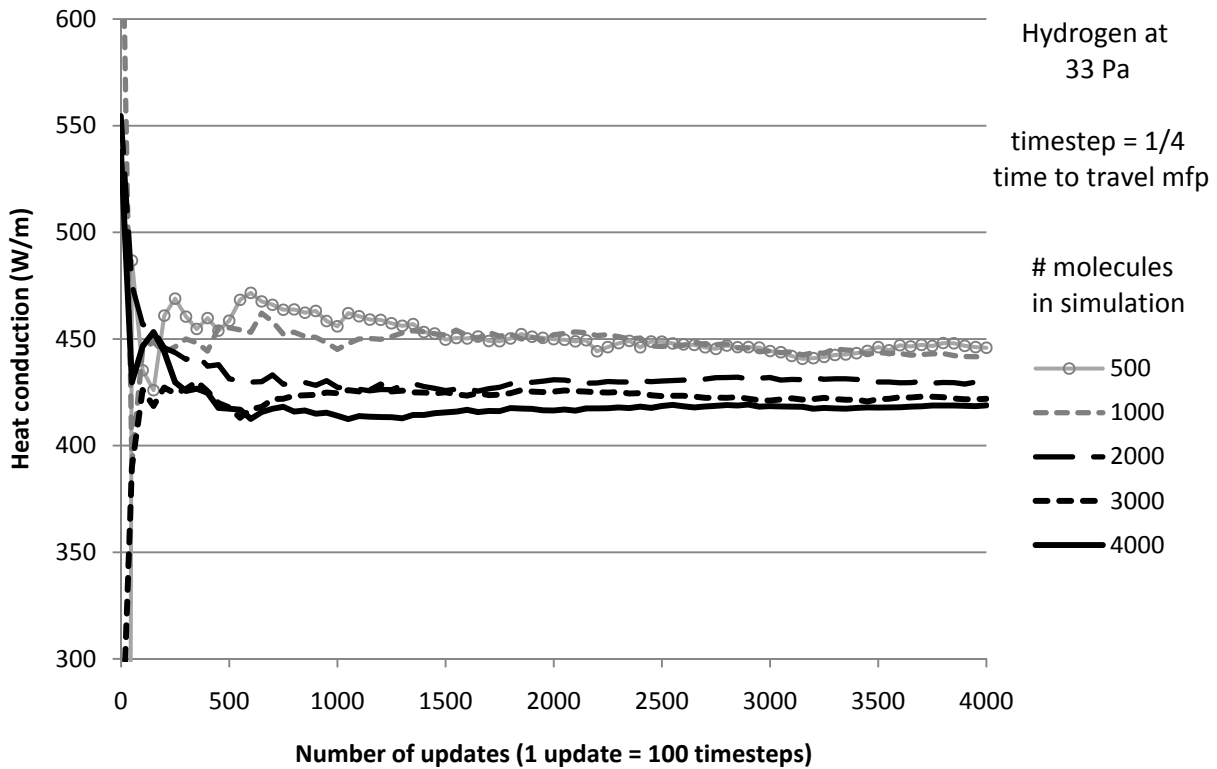


Figure 3.6 Convergence study results – number of molecules

The time step of this study was equal to $\frac{1}{4}$ the mean collision time. In other words, $\frac{1}{4}$ the time required for a molecule with the gas's mean thermal speed to travel one mean free path. Bird advocates time steps less than the mean collision time.

The 4000 molecule results in Figure 3.6 are considered “correct.” This has nothing to do with the heat conduction value that it settles on as time progresses. The reason is that the 4000 molecule case is the most highly discretized case (uses the most molecules). It also has a long simulation time. The goal is to see if fewer numbers of molecules give the same answer as the 4000 molecule case, and use them instead if they do.

Each case in Figure 3.6 appears to converge on a value as time progresses. There is still some scatter in the results, and there always will be in case of a Monte Carlo simulation. The 500 and 1000 molecule cases settle around 440 W/m, the 2000 molecule case at 430 W/m, and the 3000 and 4000 molecule cases at 420 W/m. The 3000 molecule case is selected for the next study.

Figure 3.7 investigates the length of the time step. The 3000 molecule, $\frac{1}{4}$ time step case of Figure 3.6 is compared to 3000 molecule $\frac{1}{2}$, 1, and 2 time step cases. Once again, the number refers to the fraction of the time step required to travel one mean free path for a molecule traveling at the mean thermal speed of the gas. The $\frac{1}{4}$ step is considered the most highly discretized and therefore giving the “correct” value. The $\frac{1}{2}$ and $\frac{1}{4}$ cases give nearly the same value. The 1 and 2 cases give higher heat conduction values.

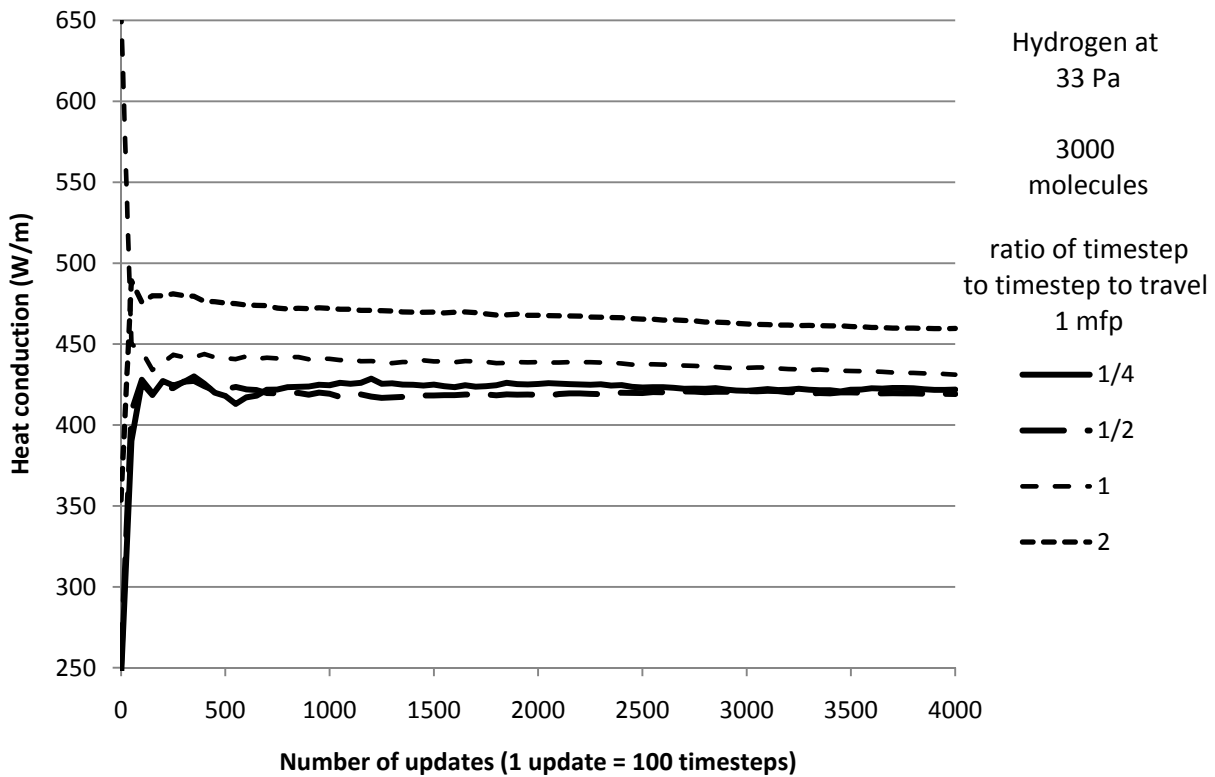


Figure 3.7 Convergence study results – time step

At this point it looks like 3000 molecules and time step equal to $\frac{1}{2}$ the mean collision time lead to the same heat conduction value at 33 Pa as a more highly discretized simulation. Figure 3.8 checks this at 5.5 Pa.

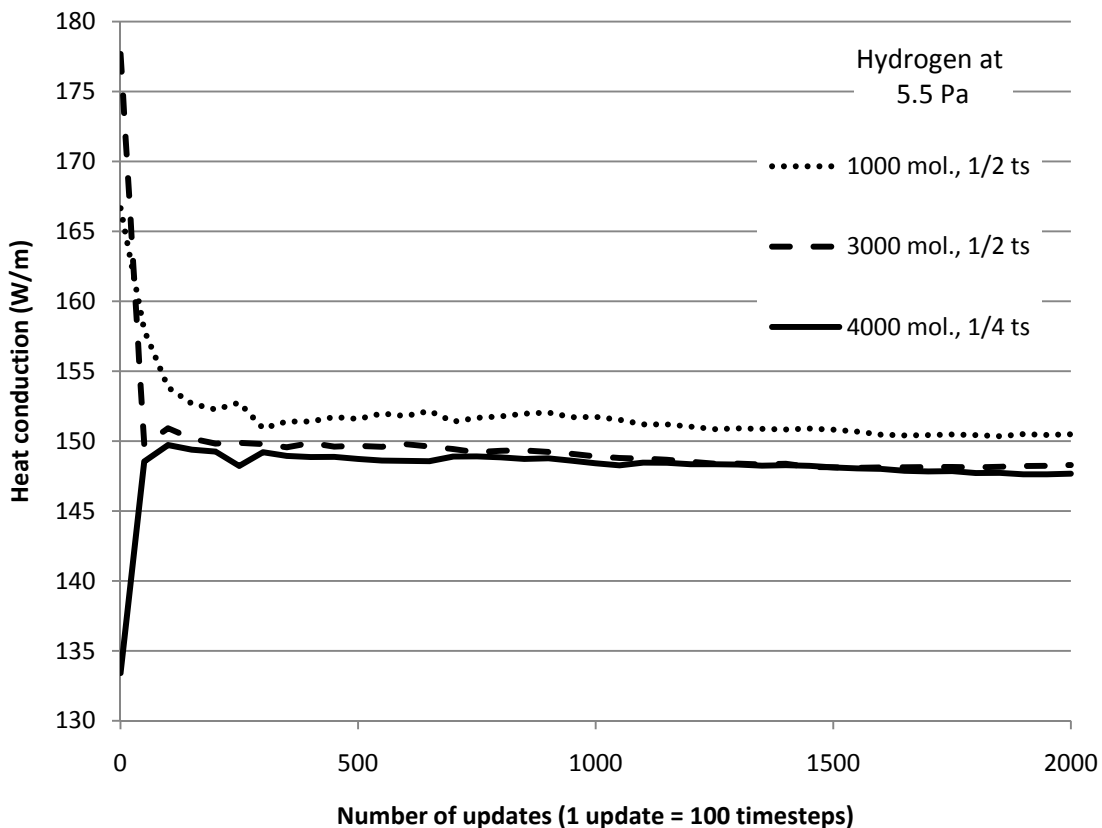


Figure 3.8 Convergence study results – time step and number of molecules at 5.5 Pa

The 3000 molecule, $\frac{1}{2}$ time step results are indistinguishable from the 4000 molecule, $\frac{1}{4}$ time step results at this pressure. Interestingly the 1000 molecule results are closer to the 4000 molecule results at this pressure than they were at 33 Pa. This phenomenon is investigated further in Figure 3.9, where 4000 molecule, $\frac{1}{4}$ time step results are compared to 1000 molecule, $\frac{1}{2}$ time step results at 0.7 Pa.

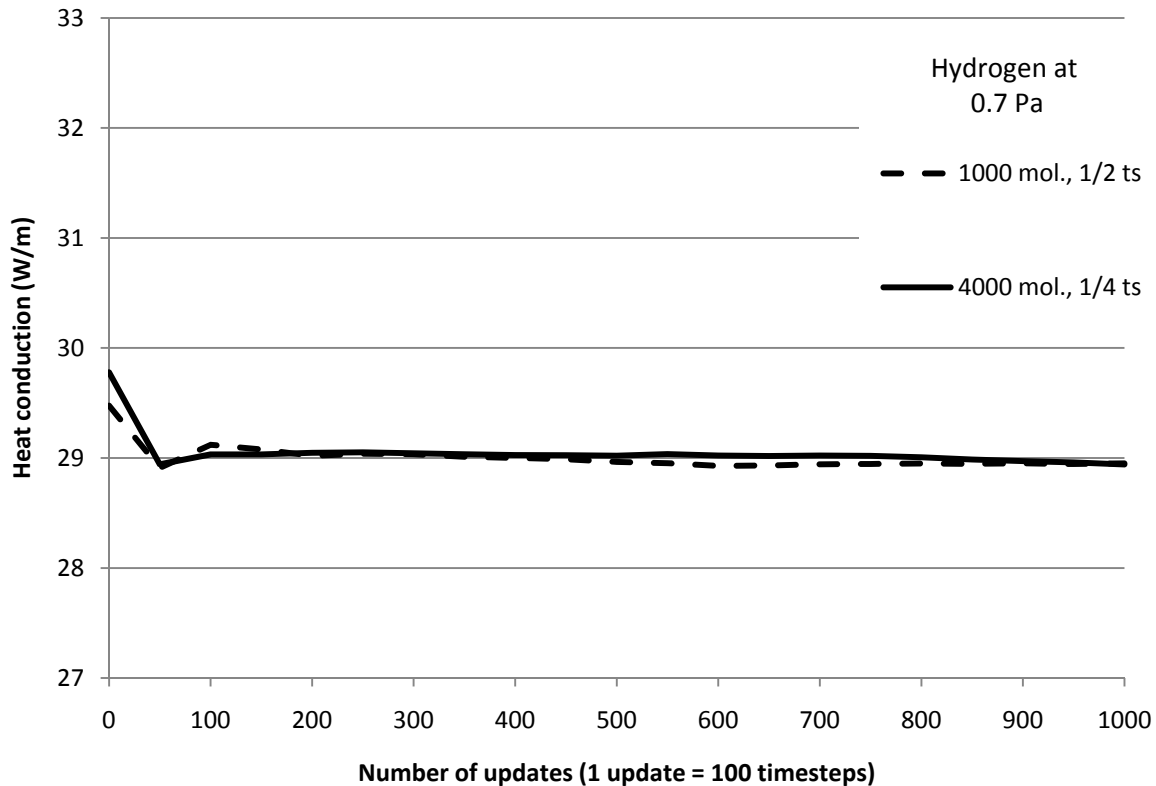


Figure 3.9 Convergence study results – time step and number of molecules at 0.7 Pa

At 0.7 Pa there is little difference between the 1000 molecule $\frac{1}{2}$ timestep results and the 4000 molecule, $\frac{1}{4}$ time step results. This trend of increased agreement at increased rarefaction means that fewer molecules could be used at low pressures to give correct results, but conversely that 3000 molecules will most likely be insufficient to give correct results at pressures higher than 33 Pa. The goal of this research is to predict transition regime data, however, and 33 Pa is already beyond that range.

Next the number of cells is considered. Figure 3.10 shows 10 Pa and 58 Pa results for 10, 20 and 50 cells with varying numbers of simulated molecules per cell. The reason these studies are run at larger pressures is that they were completed before the decision was made to make the other pressures the test cases. The figure indicates that, regardless of the number of cells used, there should at least 100 molecules per cell at higher pressures. 10 cell results are higher than 20 and 50 cell results at 58 Pa, so the usage of 20 cells and 3000 molecules (150 molecules/cell) is justified.

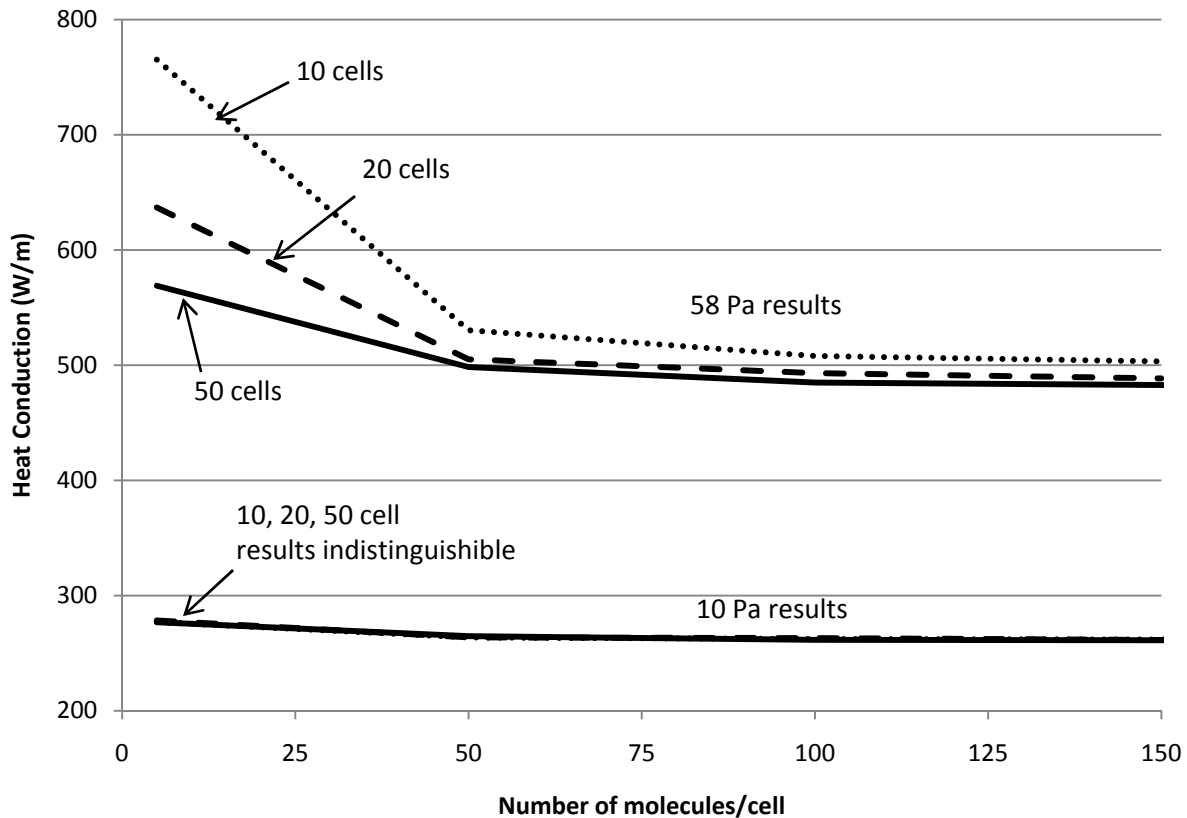


Figure 3.10 Convergence study results – number of cells

The final aspect of this convergence study is to determine at what update (1 update = 100 timesteps) the results are considered converged. Looking at the 3000 molecule, $\frac{1}{2}$ time step, 20 cell results of Figures 3.7, 3.8, and 3.9, the update at which the initial oscillation flattens out decreases with pressure. In Figure 3.9 (0.7 Pa), at the 100th update the results are flattening out. In Figure 3.8 (5 Pa), it's at about 600 updates. In Figure 3.7 (33 Pa), it's at about 1000 updates. Plotting these results on a figure as a function of inverse Knudsen number generates a correlation that can be used to determine the number of updates that must pass for any gas at pressures up to 33 Pa in this research before steady flow is reached and sampling the flow can begin. This correlation is shown in Figure 3.11.

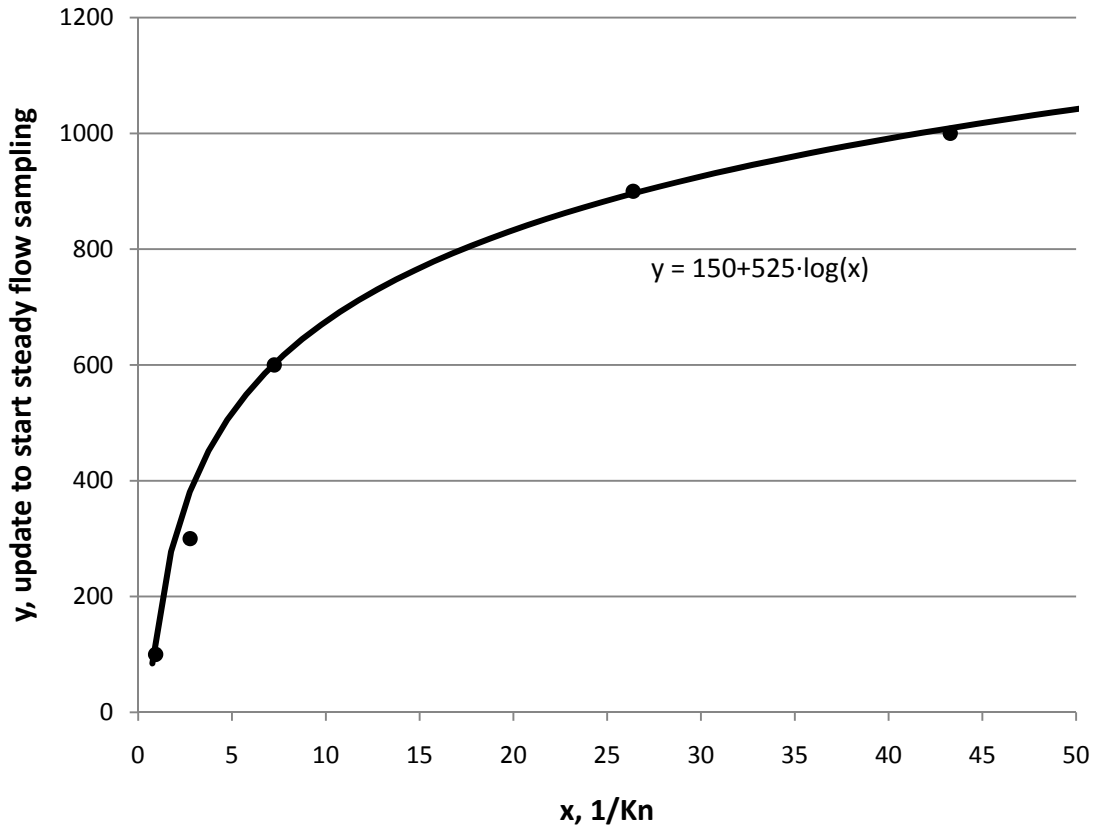


Figure 3.11 Convergence study results – number of updates that should pass before steady flow sampling begins

Additional simulations were run at 2 Pa and 20 Pa to see if they predicted update start times that coincided with the other data. Their points are plotted above and they are close to the values predicted by the correlation.

DSMC CONVERGENCE SUMMARY

The DSMC analysis for all pressures, gases, and gas mixtures in this research uses 20 cells, 400 subcells, and 3000 molecules. At each pressure, the mean collision time is calculated and the time step is set to ½ that value. At each pressure, the inverse Knudsen number is calculated and used in the correlation in Figure 3.11 to determine how many updates must elapse (where 1 update = 100 time steps) before the flow is sampled for results. This sampling period (not mentioned before) is 300 updates after sampling starts, with 1 sample taken every 10 updates. The final heat conduction value is the average of

the 30 data points taken during this period. This discretization of time and space is expected to give reliable and consistent DSMC results through 33 Pa.

Figures of results at higher pressures (5-60 Pa) in this section show a trend in their results. As the number of molecules increase, or the number of cells increase, or the size of the time steps decrease, the converged heat conduction value occurs at a lower value (to a point). Therefore, if care were not taken in the choice of these parameters it would be easy to select parameters that give too high a heat conduction value at these pressures. This is an alternate explanation for why the DSMC method give values “too high” as it nears the continuum regime, as is the case of O’Shea et al.’s work shown in Figure 2.8. Their explanation is that it was difficult to get good DSMC inputs for the gases at these higher pressures. Instead, it may have been that they didn’t use enough molecules or divide space and time finely enough in their simulation.

A hypothesis as to why this occurs at higher pressures relates directly to what’s happening physically in the gas as rarefaction decreases. As rarefaction decreases, heat conduction is more and more a function of intermolecular collisions instead of molecule-wall collisions. Therefore whatever model is being used to predict heat conduction near the continuum must accurately model intermolecular collisions. If not enough molecules are used to model the system, or the time step is too large, it may be that the collision rate is less than it should be. In the case of DSMC, if the molecules aren’t colliding with each other their trajectory continues straight to the walls to exchange energy with them, as in free molecular heat conduction. The equation for free molecular heat conduction predicts much higher heat conduction than exists in the continuum regime for continuum regime pressures. Therefore the hypothesis is that DSMC models that aren’t discretized finely enough will show more evidence of free-molecular flow than they should at higher pressures, leading to increased heat conduction values.

Testing this would mean comparing the collision rate of DSMC to an externally determined “correct” collision rate. In this non-equilibrium case it would be difficult to find a good source for what the correct collision rate is. The focus of this research is getting reliable DSMC results in the transition regime, so an investigation of this phenomenon is outside the scope of work.

CHAPTER IV

Testing

This chapter begins with an overview of parabolic trough receiver heat loss testing and describes how heat conduction measurements are determined from total heat loss values. Temperature, pressure, and power measurements are described. The temperature measurement section is extensive because incorrect temperature measurements caused unreliable data initially. Issues relevant to vacuum systems are discussed. Safety considerations are described. An uncertainty analysis is performed to estimate the uncertainty in the heat conduction data. Finally, test hardware is listed.

HEAT CONDUCTION TEST OVERVIEW

The concentric cylinder, gas heat conduction results were determined from heat loss tests on a parabolic trough receiver on NREL's Heat Loss Test Stand, shown in Figures 4.1 -4.3.

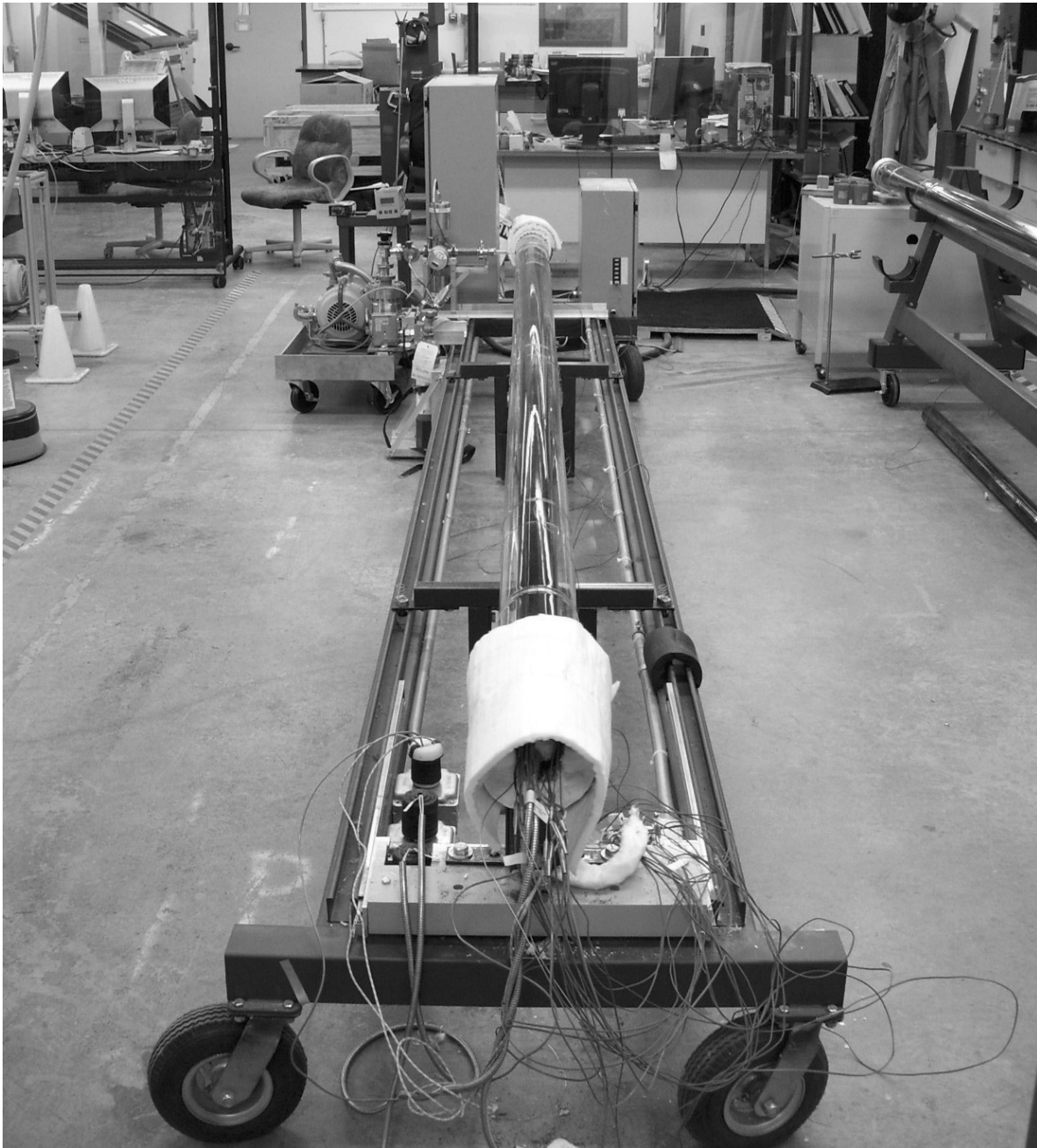


Figure 4.1 NREL's Heat Loss Test Stand, front view



Figure 4.2 NREL's Heat Loss Test Stand, side view

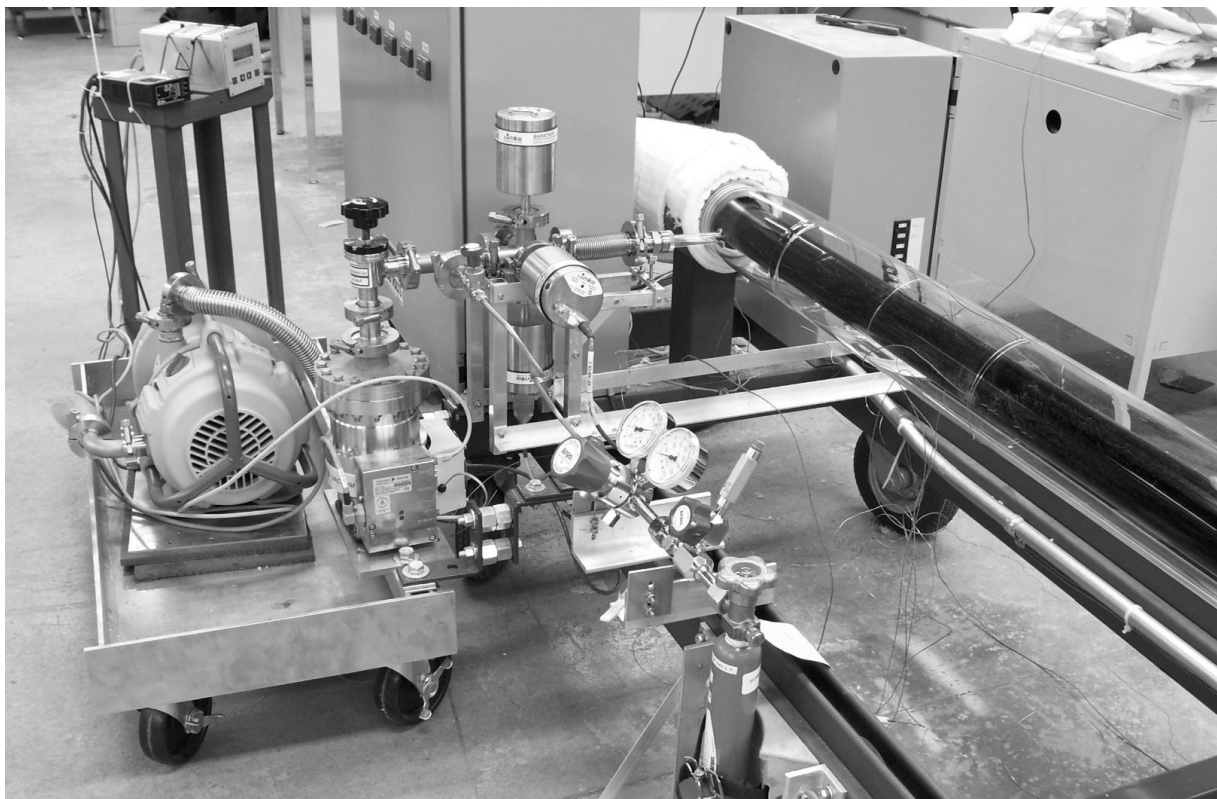


Figure 4.3 Vacuum and gas-delivery system

This test stand was designed to test the total heat loss of parabolic trough receivers. Burkholder et al. [4] first documented test results with this stand, and Burkholder and Kutscher have produced two NREL Technical Reports [53, 54] documenting performance of state-of-the-art parabolic trough receivers. Emittances determined from heat loss tests were recently compared to emittances determined by other laboratories for the same receivers in a blind round-robin study with good agreement [55].

Parabolic trough receivers are typically evacuated so that total heat loss reported for these tests is radiative heat loss. The calculation of gas heat conduction involves the subtraction of the radiative heat loss from the total heat loss, as shown in Figure 4.4.

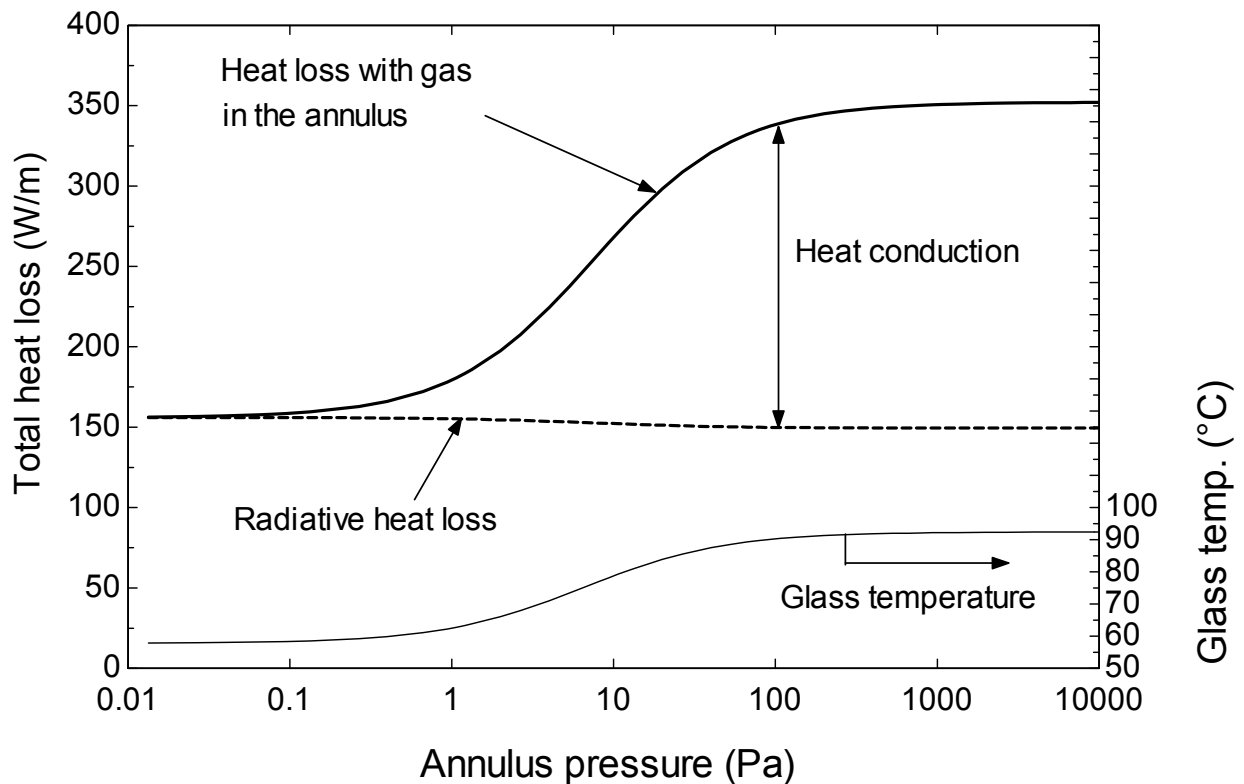


Figure 4.4 Calculating heat conduction

Most studies of concentric cylinder heat conduction control the temperature of the inner and outer surface, and so a test is run with no gas in the annulus to determine the radiative heat loss. This value is then subtracted from all future measurements to determine the heat conduction. While controlling the outer surface temperature is practical for the relatively small wire-in-tube apparatuses of most previous

studies, the large 4 m long, 12.5 cm diameter glass envelope of the parabolic trough receiver makes this difficult and was not attempted in this study. Therefore as gas is added to the annulus the glass envelope temperature rises and the radiative heat loss slightly decreases, as shown in Figure 4.4. There isn't one radiation value that can be subtracted from all total heat loss measurements to find the heat conducted. However, the radiative heat loss can be determined for each measurement. It's possible to put thin layers of insulation around the glass surface and test the radiative heat loss at various glass temperatures to create a correlation between glass temperature and radiative heat loss. This was the approach in Burkholder et al. [7]. However, an easier approach used in this research was to determine the emittance of the absorber surface from heat loss tests with an evacuated annulus and calculate the radiative heat loss. The temperature of the absorber, temperature of the inner surface of the glass, and the emittance can be used to calculate the radiative heat loss using equation 4.1 [56].

$$q_{radiation} = \frac{\sigma A_{abs} (T_{abs,Kelvin}^4 - T_{gl,Kelvin}^4)}{\frac{1}{\epsilon_{abs}} + \frac{1 - \epsilon_{gl}}{\epsilon_{gl}} \left(\frac{r_{abs}}{r_{gl}} \right)} \quad (4.1)$$

where

σ is the Stefan-Boltzmann constant

A_{abs} is the surface area of the absorber

$T_{abs,Kelvin}$, $T_{gl,Kelvin}$ are the temperatures (K) of the absorber and inner glass surface

ϵ_{abs} , ϵ_{gl} are the emittances of the absorber and glass

r_{abs} , r_{gl} are the radii of the absorber and the glass

The test stand uses electric resistance heaters on the inside of the receiver absorber to bring the absorber up to a desired test temperature; in this case, 350°C. Once the absorber reaches 350°C and steady state is achieved (typically 2-6 hours depending on the gas), power transducers measure the electrical power at 5 second intervals for 15 minutes. The power required is the total heat loss, which is normalized by the receiver length. The heat conduction is backed out using the procedure just described.

The receiver is 4.08 m long at 350°C (4.06 m at 23°C) with a stainless steel absorber inner/outer diameter of 6.6/7.0 cm. A test proceeds by placing two 2.17 m long, 5.4 cm outer diameter copper pipes with internal heaters into the receiver—one copper pipe per end. Spacers protruding from the copper pipe center it in the absorber and prevent it from touching the absorber surface. The copper pipe evens out the temperature distribution generated by three internal electric resistance heaters. Two of the heaters are 200 W, 3-cm-long, stainless-steel-sheathed, coiled cable heaters whose surfaces contact the interior of the copper pipe. These heaters are referred to as “coil heaters.” The third heater is a 2000 W, 2.12 m (2.01 m heated-length) inconel-sheathed cartridge heater suspended along the cylindrical axis of the copper pipe using inconel spacers. The cartridge heater is fully inserted into the copper pipe so that its inner-most end, shown in Figure 4.5, is flush with the inner-most end of the copper pipe. When the copper pipe is inserted into the absorber, one coil heater ends up just inside the receiver while the other is adjacent to it but just outside the receiver’s edge. The inner coil heater compensates for end-loss effects, while the outer coil heater creates a zero temperature gradient on the copper pipe between the coil heaters. The cartridge heater supplies most of the thermal energy to the system. Power transducers measure heater output. The total heat loss is based on the sum of the powers of the two inner-most coil heaters and the two cartridge heaters.

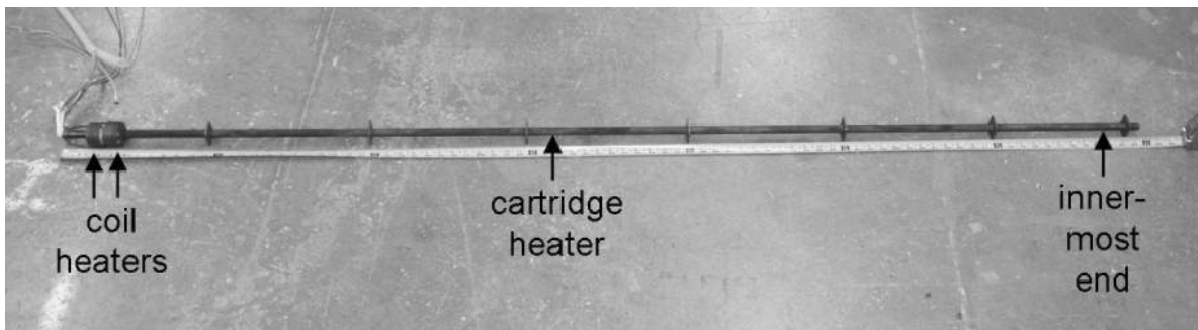


Figure 4.5 Cartridge heater and coil heaters

Figure 4.6 shows the heaters inside the copper pipe, ready for insertion into one end of the receiver.



Figure 4.6 Heaters inside copper pipe

Thermocouples measure the temperature of the copper pipe, stainless-steel absorber tube, and glass envelope at the locations shown in Figure 4.7. Only one-half the receiver is shown but all thermocouples and locations are mirrored about the center. Numbering convention goes from left to right, so Cu 4 is one meter away from the center, Cu 6 is on the far right end, etc.

Excepting Abs 1, Abs 8, Cu 1, Cu 2, Cu 5, and Cu 6, each measurement is the average of 4 thermocouples placed circumferentially: top-bottom-side-side.

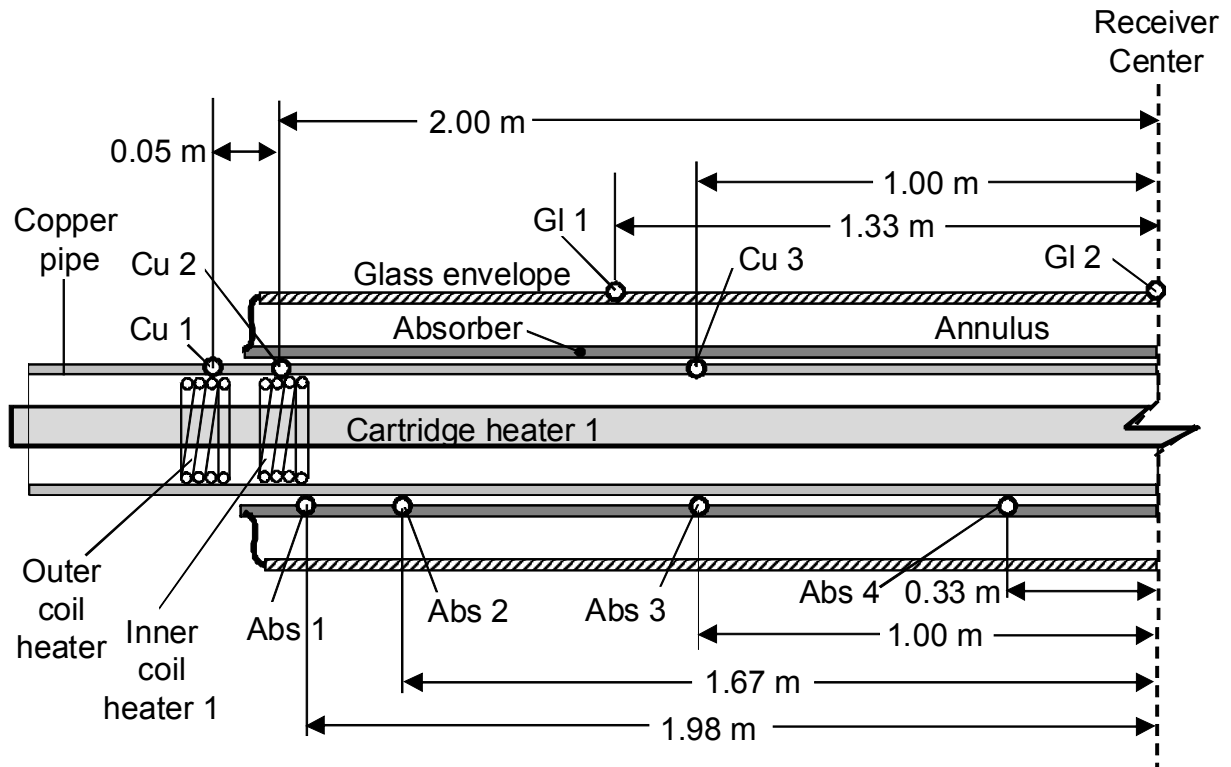


Figure 4.7 Thermocouple locations

Wires attach thermocouples to the copper and glass surfaces. The thermocouples measuring absorber temperatures spring out from the copper pipe to contact the absorber surface, as shown in Figure 4.8.

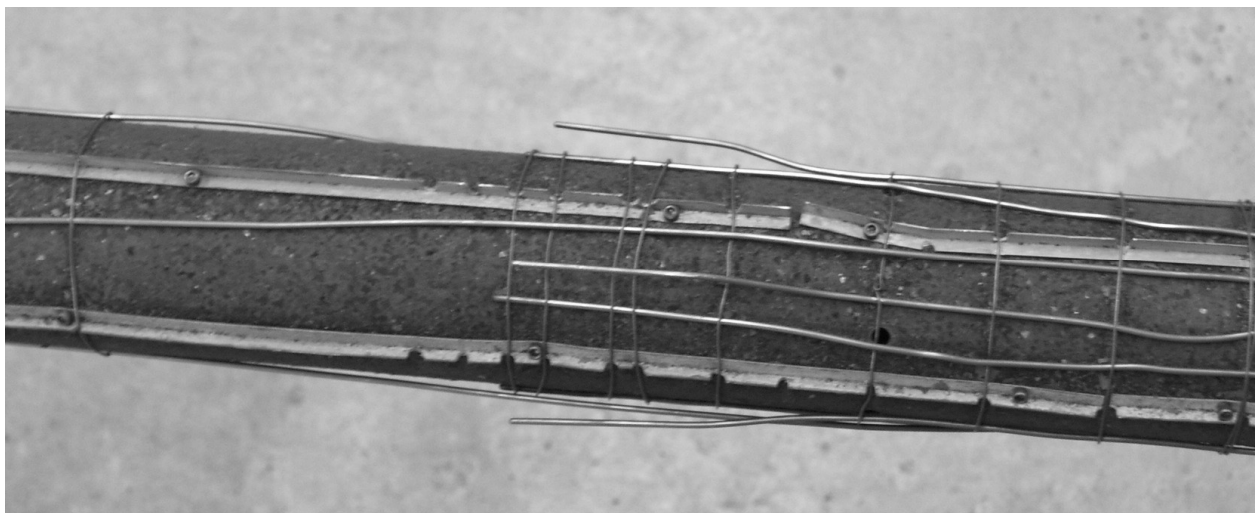


Figure 4.8 Thermocouples spring out from the copper pipe to contact the inside of the absorber surface

A jig is used to ensure that the absorber thermocouples are bent correctly to ensure good contact with the absorber surface.

The parabolic trough receiver was specially made for this testing. Normally the manufacturer (in this case, Schott) adds getters to the annulus and seals the glass envelope after baking it out to ensure the vacuum. This receiver was supplied with no getters and a glass port through which the annulus could be pumped down or filled with gas. This port and its attachment to the gas delivery/vacuum system are shown in Figure 4.9.

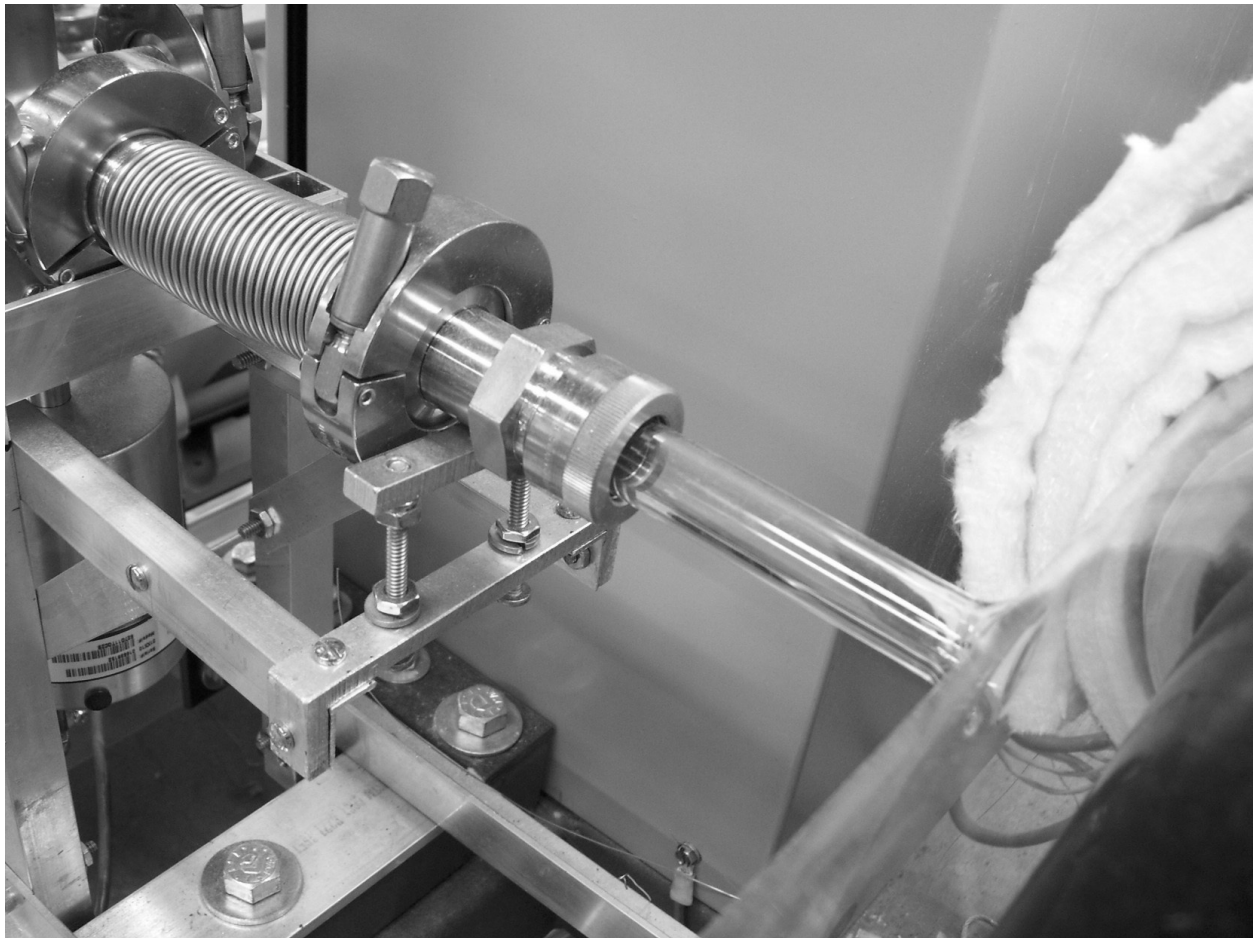


Figure 4.9 Connection between 1 cm i.d. glass port and gas delivery system

A dry roughing pump decreases the receiver annular pressure from atmospheric to 0.133 Pa, and then a turbo pump reduces the pressure to less than 0.00133 Pa. Three MKS Baratron capacitance manometer pressure gages with complementary ranges measured pressure during testing.

Ultra-high purity (5 ppm) xenon, argon, and hydrogen were used in the tests. The gas mixtures were specially prepared by research grade commercial gas supplier Airgas with small molar fraction uncertainties. All mixtures required CGA 350 regulators for flammable gases. The regulators were single stage with brass/nickel diaphragms to prevent off-gassing. A purge assembly was placed between the regulator and the gas cylinder to vent air that would otherwise be caught between the tank and regulator and contaminate the system.

All seals in the gas delivery/vacuum system shown in Figure 4.3 are Viton® to handle high temperatures. The vacuum connections are stainless steel Kurt J. Lesker products.

PARABOLIC TROUGH RECEIVER SPECIFICATIONS

Table 4.1 lists dimensions of the parabolic trough receiver of this research. Dimensions are calculated at the test temperature of 350°C. Dimensioned drawings and measurements give high confidence in these values so no uncertainty is associated with the radii and a 0.5 cm uncertainty is associated with the annular length.

Table 4.1 Parabolic trough receiver specifications

Total length (m):	4.08
Annulus length (m):	4.02
Absorber inner radius (m):	0.033
Absorber outer radius (m):	0.035
Glass inner radius (m):	0.0595
Glass outer radius (m):	0.0625

The absorber tube is stainless steel covered with a selective surface that has an aluminum oxide coating. The glass envelope is made of borosilicate glass and is coated with a silica anti-reflective coating. A bellows exists between the glass envelope and absorber to allow the absorber to lengthen as its temperature rises. This thin bellows is the only solid heat conduction path from the absorber tube to the glass. It's designed to minimize heat conduction and the ends of the bellows are heavily insulated during testing to further minimize this value.

TEMPERATURE MEASUREMENT

Inconel sheathed, mineral-insulated, ungrounded Omega type K thermocouples with special limits of error (1.1°C or 0.4 % of reading, whichever is greater) were used for all temperature measurements. More than 40 thermocouples were used in this experiment so it was not possible to check the calibration of each one, though it's known that errors associated with installation of the thermocouples are often much larger than calibration errors [57]. Nevertheless three were calibrated at 90°C at the Solar Radiation Research Laboratory, and then sent out to another calibration lab where they were calibrated at 90°C and 350°C. Laboratory findings verified the manufacturer accuracy claims. These calibrated thermocouples were compared to the readings of all the other thermocouples in a boiling water bath and in an alumina powder in a small, high temperature furnace and all readings, except for two thermocouples, were consistent with $\pm 2^\circ\text{C}$ at 350°C. Those two thermocouples were discarded.

When parabolic trough receiver testing began in 2007 the absorber temperature was measured with 4 thermocouples – two on the ends and two in the middle. Infrared images of the copper pipe showed a uniform surface temperature so it was believed that the absorber was heated uniformly. In 2008 4 thermocouples became 8, and presently 24 are used to measure the temperature. The reason for this increase is that repeated testing has shown that temperature gradients exist circumferentially and longitudinally and these gradients should be captured in the measurements.

Figure 4.10 shows the cartridge heater inside the copper pipe, which is inside a section of a receiver tube with no glass envelope around it. There is a 12 mm gap between the cartridge heater and the inner edge of the copper pipe, and a 6 mm gap between the copper pipe and the absorber tube.

Rayleigh number calculations place the heat transfer between the cartridge heater and the copper pipe on the edge between conduction and convection, and predict that conduction will govern between the copper pipe and the absorber.

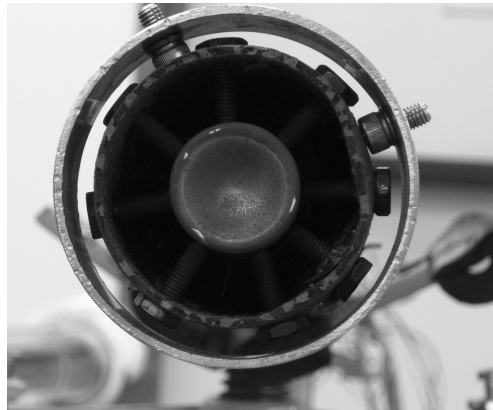


Figure 4.10 Picture showing spacing between cartridge heater and copper pipe, and copper pipe and absorber tube

Thermocouples placed near the top of the absorber tube during tests read 5-15° more than they read on the bottom. In other words, depending on where the thermocouple was placed the experimenter would think that the whole absorber tube was somewhere between 345°C and 360°C.

To address this circumferential gradient baffles were installed on the cartridge heater and the outer surface of the copper pipe, as shown in Figure 4.11.

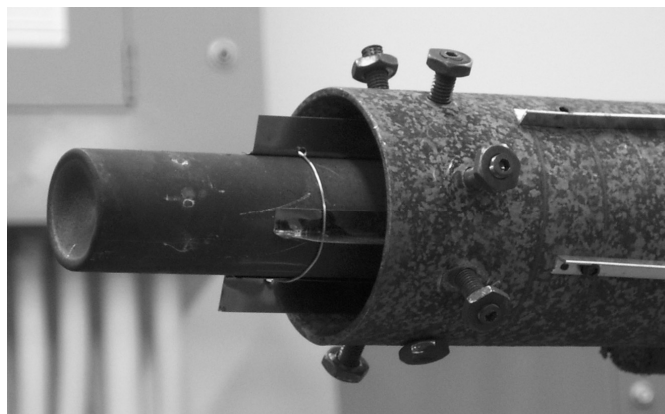


Figure 4.11 Baffles to prevent natural convection installed on cartridge heater and copper pipe.

Subsequent tests showed much less circumferential variation: 0-5°C. Nevertheless, more thermocouples were added so that the circumferential variation is known at 6 of the 8 measurement absorber temperature locations along the absorber tube (Abs 2 – Abs 7).

Longitudinal variation remained unchanged. Typically the central longitudinal sections of the heater are warmer than the ends, so absorber temperature readings one meter from the center tend to be about 2-8°C warmer than the reading in the middle of the absorber. Heater power is varied until the average of all the temperature readings is 350°C, so cooler sections lose a little less heat, the warmer sections lose a little more, and they balance out.

There was a more serious issue with this temperature measurement method that became apparent during higher heat loss tests. A long-standing puzzle for results in Burkholder et al. [7] was why experimental data matched heat conduction predicted with argon and xenon's thermal conductivity in the continuum but severely undershot modeled hydrogen results. The answer became clear in a set of tests where one heating assembly (heaters, copper pipe, thermocouples) was placed inside an absorber tube that had no glass envelope. This allowed access to the outer surface of the absorber. Grooves were milled into the outer surface and thermocouples were placed in the grooves. These thermocouples had excellent contact with the absorber surface and were relied on to provide the correct absorber temperature. Some insulation was placed around the absorber, the heaters were turned on, and the temperatures given by the thermocouples inside the absorber were compared to the temperatures given by the thermocouples outside the absorber.

At low heat loss values, the temperatures agreed within the uncertainty limits of the thermocouples. As the heat flow increased, the inner thermocouples read 2...3...then 10°C higher than the outer thermocouples. A thermocouple energy balance model showed that it was heated by convection and radiation more than the absorber surface. Better thermal contact with the absorber wall would have mitigated this problem to a large extent. It's difficult to access these thermocouples, however. The ones on the ends of the heating assembly slide in to the absorber almost two meters, and as mentioned before there's only a 6 mm gap between the copper pipe and the absorber surface.

Different thermocouple shielding and contact configurations were attempted, as shown in Figure 4.12. Radiation shields placed on the copper pipe didn't decrease the radiative heating of the thermocouple by much, and attempts to limit thermal exchange to that solely between the thermocouple surface and the absorber surface were futile.

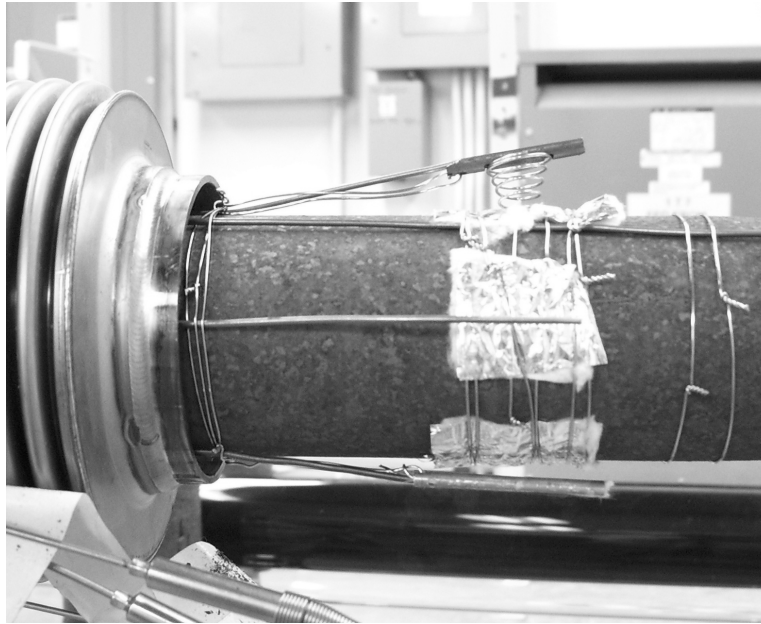


Figure 4.12 Attempted thermocouple shielding and contact configurations

In the end, the thermocouples and copper pipe were left bare (as in Figure 4.8) and an empirical correction was relied on to calculate the correct absorber temperature from the measured temperatures. More thermocouples were placed on the surface of the absorber, and three different levels of insulation were placed on the absorber tube as the copper pipe temperature was varied from 100-500°C. The test was repeated 5 times, where between each test the heater was removed, thermocouples were bent to the correct configuration, the heaters were reinserted and insulation was reapplied. Figure 4.13 shows the levels of insulation applied to the bare absorber. These levels were chosen to duplicate the thermal resistance of an evacuated receiver and a receiver that loses more and more heat due to a gas in the annulus. There was no way, however, to duplicate the heat loss that would be induced by even a 500th of an atmosphere of hydrogen because even that small amount conducts more heat than air at atmospheric pressure.

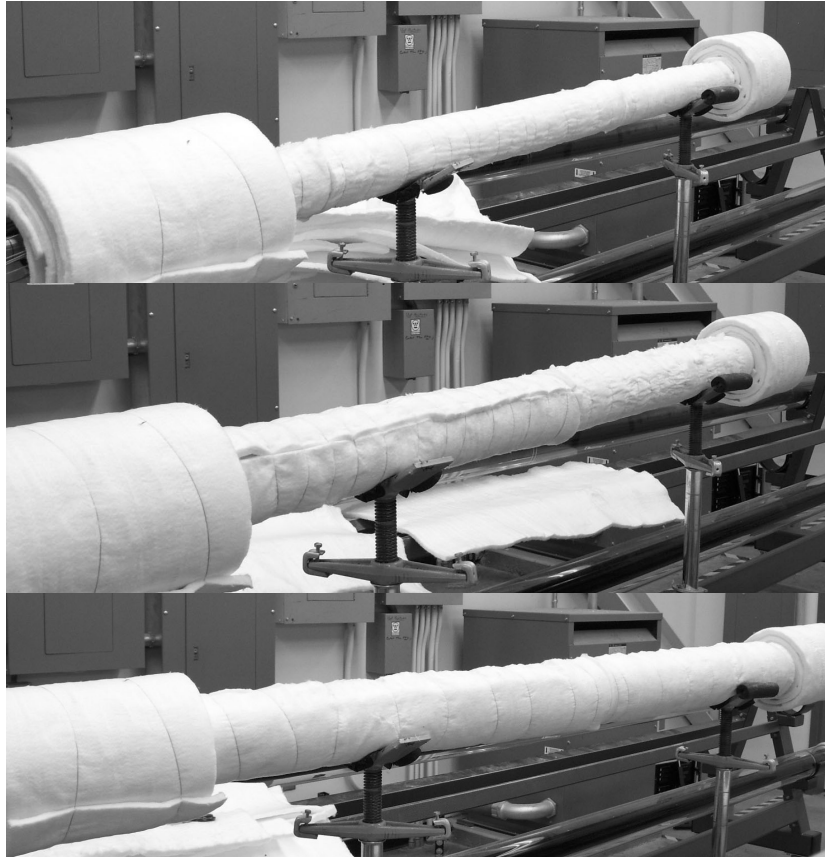


Figure 4.13 1, 2, and 3 layers of insulation to required different amounts of heat loss at a given copper pipe temperature .

The required correction is multivariate – it depends primarily on the difference in between the measured copper pipe temperature and the measured temperature of the inner absorber surface. The larger this temperature difference, the larger the heat flow, the larger the correction required. But it also depends on the copper temperature: the higher the copper temperature, the higher the correction.

Figure 4.14 shows the results of the study.

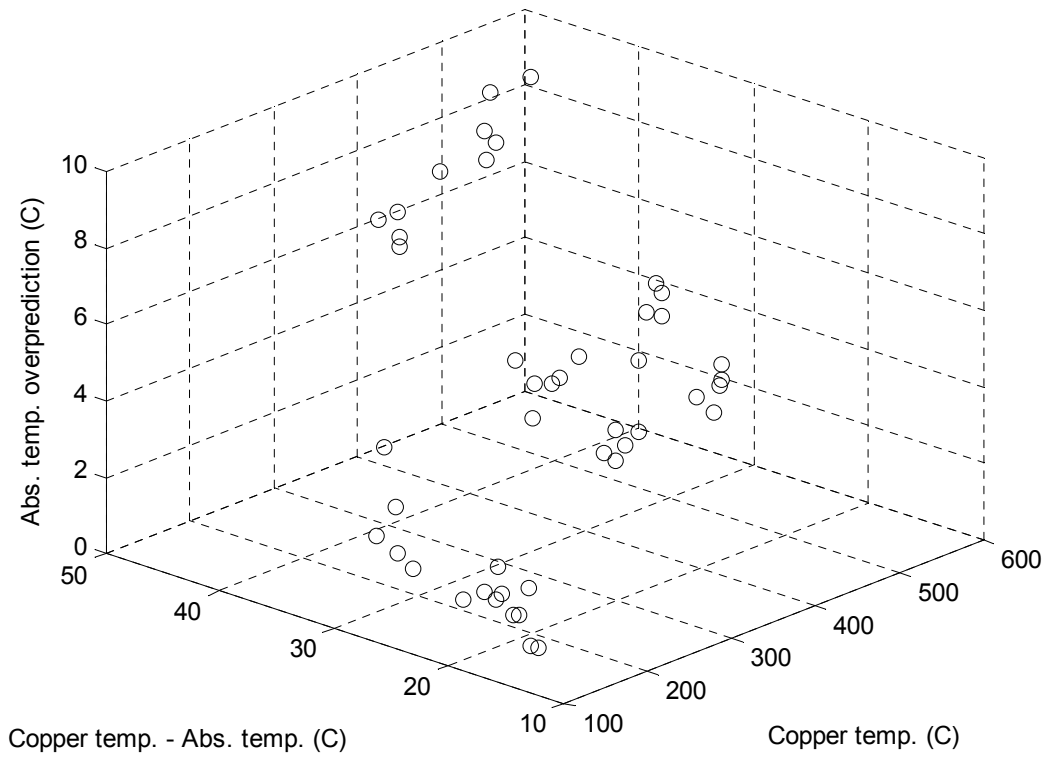


Figure 4.14 Data gathered in absorber temperature over-prediction study

A two-variable linear regression was required. The result of the regression is

$$O_p = -2.1825 + 0.0042 \cdot T_{Cu} + 0.1575 \cdot \Delta T \quad (4.2)$$

where

O_p is the over-prediction of the absorber temperature from measured readings ($^{\circ}\text{C}$)

T_{Cu} is the measured copper temperature ($^{\circ}\text{C}$)

ΔT is the measured copper temperature – measured absorber temperature ($^{\circ}\text{C}$)

The regression is expected to be valid for 100°C - 500°C copper temperatures and ΔT s 10 - 50°C .

The confidence interval of the correlation was determined from equation 4.3 [58]

$$w(\hat{y}_{\text{regf}}) = \pm t_{\alpha/2, n-p} \sqrt{\hat{\sigma}^2 \mathbf{x}_0' (\mathbf{X}' \mathbf{X})^{-1} \mathbf{x}_0} \quad (4.3)$$

where:

$t_{\alpha/2, n-p}$ is the value of the t distribution with $n-2$ degrees of freedom at a confidence level of $(1 - \alpha)$

p is the number of coefficients estimated from data

$\hat{\sigma}^2$ is the standard error of regression

\mathbf{x}_o is a vector of independent variables at which uncertainty is calculated

\mathbf{x}_o' is the transposed vector independent variables

\mathbf{X} is a matrix of independent variables, or measured x values and powers used in regression model

The regression is plotted with its confidence interval in Figure 4.15. It predicts that for low heat conduction values associated with pure xenon and argon the measured absorber temperature over-predicts (is greater than) the real absorber temperature by only 1-3°C. For most of the gas mixtures it predicts that the measured absorber temperature is actually 5-8°C higher than the real value. Hydrogen at high pressures is the worst case: the absorber temperature is actually 10-15°C less than the measured reading. This is the reason for the confusing data in Burkholder et al. [7]. At low heat conduction values the absorber temperature reading was essentially correct, but the 350°C absorber in the hydrogen test was actually 335°C and therefore did not cause as much heat conduction as expected.

The uncertainty in the correlation is $\pm 1^\circ\text{C}$ for most heat conduction cases except hydrogen. The heat flow associated with hydrogen causes large $T_{\text{Cu}} - T_{\text{abs}}$ values ($\approx 80^\circ\text{C}$) which will result in a correlation uncertainty of $\pm 2^\circ\text{C}$. This uncertainty is convolved with the thermocouple calibration uncertainty to yield a total measured absorber temperature uncertainty of $\pm 2-3^\circ\text{C}$. The data acquisition SNAP-AITM modules that process the thermocouple readings and provide cold-junction temperature compensation have accuracies of 0.1% or less, so their contribution to the convolved uncertainty above is negligible. Uncertainty in the absorber temperature in this research is conservatively estimated to be $\pm 3^\circ\text{C}$, while the glass temperature is $\pm 1^\circ\text{C}$.

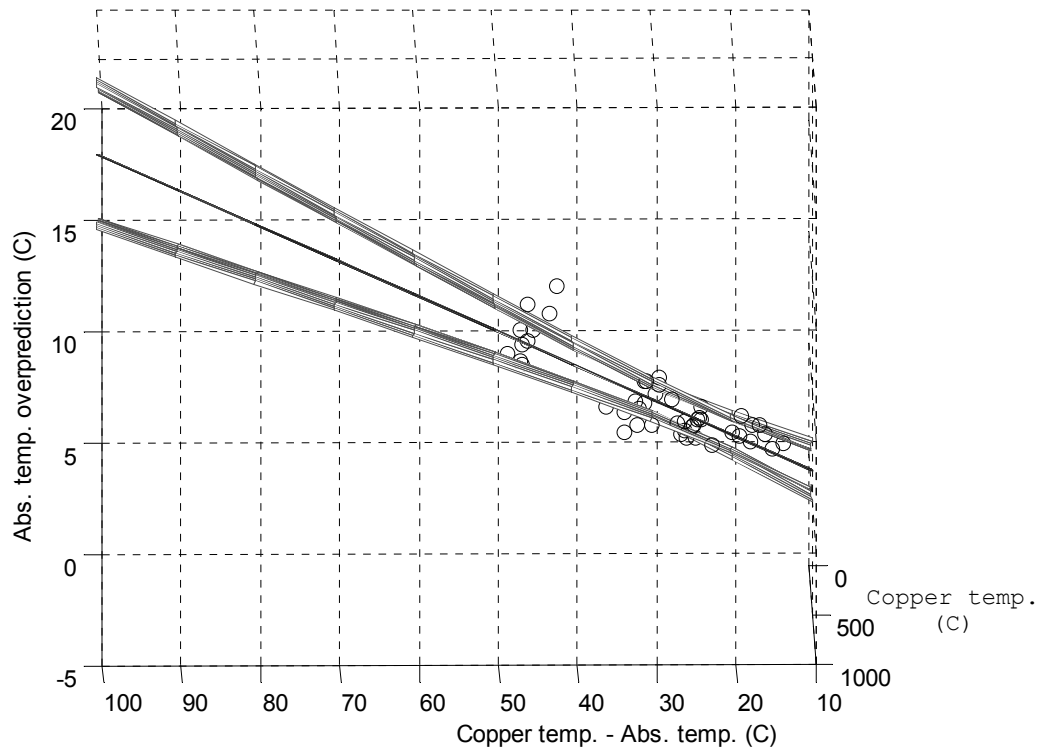


Figure 4.15 Regression result with confidence interval

POWER MEASUREMENT

The SCR power controllers in the data acquisition system are single cycle, variable time base. The power to the heaters is governed by on/off pulses from the controller. When the heaters receive an “on” pulse (which lasts milliseconds), they are fully on (≈ 2000 W). When off, fully off. To supply 200 W, one “on” pulse is followed by 9 “off” intervals. This understanding of how power is supplied to the heaters is crucial for picking the correct full scale range of the power transducer. Even though only 500 W (roughly 250 W/m) might be expected in one test, the transducer still needs to be able to measure the full-scale range of the heater (2000 W). This wasn’t understood early on and some poor data and burned out transducers were the result.

The transducers had to reliably average the power coursing through the heater for the reasons described above. Ohio Semitronics PC5 watt transducers handle this type of waveform. They have a manufacturer-claimed accuracy, checked by calibration at SRRL, of $\pm 0.5\%$ of their full-scale range. This

translates into ± 10 W for the 2000 W model (chosen to match the maximum heater power), which normalized by length becomes ± 5 W/m. Data acquisition SNAP AOA modules read in the 4-20 mA output signals from the transducers and send this to the computer to be processed into the heat loss measurement. The accuracy of these modules is 0.1% which causes a negligible contribution to the ± 5 W/m uncertainty.

Earlier testing used 4000 W heaters instead of 2000 W heaters, which consequently used larger full-scale transducers that resulted in uncertainties of ± 10 W/m instead of the present ± 5 W/m. The desire for less uncertainty in the heat loss measurement of this research led to the design and purchase of lower power heater cores.

PRESSURE MEASUREMENT

Tested pressures in this research span 6 orders of magnitude, from 0.1 Pa to 10,000 Pa. Three different full-scale MKS Type 627D Baratron® temperature regulated capacitance manometers were selected to measure the pressure. Their full-scale values are 0.1 torr, 10 torr, and 1000 torr (13.33 Pa, 1333 Pa, 133.3 kPa). These gauges calculate pressure based on changes in capacitance caused by the deflection of a diaphragm due to the momentum of impinging molecules – they do not give gas composition dependent readings (except for minor corrections due to thermal transpiration, which will be discussed later). Manufacturer claimed accuracy is 0.12% of reading, and calibration at SRRL for the two larger scale transducers that supports this as long as the gauges are zeroed properly before use. Figure 4.3 shows that only one gauge (0.1 torr) is oriented such that its port to the annulus is pointing down. The calibration of the other two transducers were checked in horizontal and upside-down configurations and compared to right-side-up values and determined the same as long as the gauges were zeroed in their orientation of use. The uncertainty induced by the MKS PDR 2000 gauge controller that process the signal from the gauges and sends it to the computer for data-logging is about 0.1%. Both of these values are so small that uncertainty in the pressure readings was decided negligible.

One aspect of using temperature regulated manometers is that the volume near the diaphragm can be considered at the regulated temperature when the gas pressure is low. This affects the

momentum of the molecules and means that the pressure measured by the diagram is not the pressure of the gas in the volume of interest. This is called thermal transpiration and Poulter et al. [59] show that it's a function of gas pressure, composition, temperature difference, and the diameter of the tube connecting the two volumes. The diameter is 1 cm in this case (see Figure 4.9). In the case of this research, where the gauge volume temperature is less than the temperature of the gas in the annulus, it will cause the gauge to read low relative to what actually exists in the annulus. Poulter et al. provide a detailed calculation showing how to correct for the effect, and the correction for pressures and gases in this research is about 2% for pressures less than 1 Pa and 1% for pressures between 1 Pa and 15 Pa. After this there is no correction. All pressures and data presented here have already been corrected for thermal transpiration.

BAKING OUT AND OFF-GASSING

The annulus of the receiver and the internal volume of the gas delivery system comprise a vacuum system. All components of vacuum systems are at some point exposed to atmospheric pressure and during this time molecules adsorb on to their surfaces. Handling components also contaminates them. Molecules and contaminants slowly desorb from the surfaces when exposed to vacuum. This process is accelerated with increasing temperature. Eventually, most of the adsorbed molecules desorb, so that "off-gassing" is small. Thus it is common to "bake-out" vacuum systems before use to ensure that adsorbed molecules and contaminants don't desorb into the volume and affect test results.

The receiver annulus volume is more than 25 L. This is a large volume for a vacuum system. The initial bake out period took about three weeks where for 8-12 hours a day the absorber temperature was raised to 450°C. The glass envelope was insulated so that the glass temperature was maintained at 200°C during these bake-out periods. The off-gassing rate gradually declined from more than 0.2 Pa/hour to less than 0.01 Pa/hour. Off-gassing at this level does not affect test results. But because of off-gassing the annulus was evacuated between each data point, and at the start of every test day the system was allowed to come to steady state, which takes about four hours, and during this time the system was baked out and the off-gassing rate was checked before tests began.

THE GASES

Airgas supplied nine gases for this research. The pure gases – hydrogen, argon, xenon – were research grade purity (5 ppm). The gas mixtures molar fractions were

Hydrogen/Argon mixtures:	10.0% H ₂ /90.0% Ar	25.0% H ₂ /75.0% Ar	50.0% H ₂ /50.0% Ar
Hydrogen/Xenon mixtures:	11.2% H ₂ /88.8% Xe	27.2% H ₂ /72.8% Xe	52.5% H ₂ /47.5% Xe

All mixtures were supplied with certificates of analysis that showed that the accuracy of the smaller fraction molar component was $\pm 1\%$. For instance, the 10% molar fraction of H₂ in the 10% H₂/90% Ar mixture is actually $10.0\% \pm 0.1\%$. The Sherman formula was used to evaluate whether this caused a significant difference in heat conduction and its effect was deemed negligible.

SAFETY

Many of these tests involved hydrogen in an enclosed (by glass) space at elevated temperatures. There were concerns that if there were a leak of air into the annulus the gas mixture could explode. These safety concerns were taken seriously, and a Safe Operating Procedure (SOP) was generated. This SOP is presented in Appendix D. It took more than a year-and-a-half of iterations between safety, management, and this researcher before approvals were granted. Getting approval to begin testing was a milestone in this research.

Several things have to go wrong for there to be an accident in these tests. First and foremost there needs to be a leak into the annulus. Hundreds of hours were spent baking out and testing the vacuum, and sources of leaks were determined at that time and fixed. Pressure is monitored in the annulus at all times. If the pressure begins rising quickly, power is shut off and it's investigated. The area around the glass stem port into the annulus is fragile (Figure 4.9) and care was taken to make sure that as this area moves as little as possible due to thermal expansion and pump vibration.

If there were a leak during testing with hydrogen (there wasn't, by the way), air would rush in and for possibly a millisecond or two the volume percentage of hydrogen in the annulus would be in its flammable range of 4-75%. During that millisecond, if there were an ignition source (and pains were taken to make sure there wasn't) the gas would ignite. However, the amount of hydrogen in these mixtures is so small that the volume percentage of hydrogen after the air rushes in quickly becomes less than 1% for most of the gas mixtures and pressures investigated in this research.

But suppose there was a leak, air rushed in, and during the brief flammable period an ignition source came from somewhere (hydrogen's auto ignition temperature is 550°C, so the 350°C absorber is too cold to ignite it). The gas ignites. What are the consequences?

The United States Nuclear Regulatory Commission has created an Excel® spreadsheet titled "Estimating Pressure Increase and Explosive Energy Release Associated with Explosions" [60]. After the user enters the type of fuel, how much there is, and whether it's in an enclosed space or not, the program outputs the energy of the explosion. For about 90% of the pressures investigated in this research the amount of energy involved in the explosion would have been equivalent to the energy of 20 apples falling 1 meter to land on one's head. Ouch. But not catastrophic. And this energy would have been distributed over the 4 meter length of the receiver. For the last 10%, though, a significant amount of explosive energy existed (equivalent to the combustion energy of *only* a thimbleful of gasoline). These tests were completed without mishap, and I'm grateful for that.

HEAT CONDUCTION TEST PROCEDURE

The test procedure has already been generally described, and a step-by-step procedure is given in the Safe Operation Procedure in Appendix D. This section's goal is to lay out a best practice procedure for getting good data. Not all data, especially data gathered in the beginning, was taken this way. Repeatability tests show that the early data are good, but this procedure provides more likelihood that at the end of a 16 hour testing day 3 or 4 reliable data points will have been gathered.

- 1) Bake out for two days. It's important to remove whatever adsorbed molecules from previous tests are in the gas delivery system or in the annulus. Bake-out absorber temperature should be above the test temperature. 450°C was used, typically.
- 2) Attach the new gas cylinder, and add roughly 10,000 Pa of the new gas to the annulus. Increase the absorber temperature to test temperature and let this gas mixture sit in the annulus. During this time it will be adsorbing and desorbing from the chamber walls. It will also be knocking out whatever gas molecules from the previous tests are still adsorbed on the walls. Let the gas sit at temperature for several hours and then pump it out.
- 3) Bake out again for about 6 hours.
- 4) Commence the tests. Equivalent results were achieved starting at high pressure and working down to low pressure, or starting low and working up high.

In a typical test:

- 1) The pumps are valved off from the annulus. Pressure is monitored for about 30 minutes to see if significant rates of off-gassing (>0.01 Pa/hour) are occurring.
- 2) The gas cylinder valve is opened, the pressure regulator valve is opened, and finally the valve to the annulus is opened slowly.
- 3) Once the desired pressure of gas is added to the annulus, the valves are closed in reverse order.
- 4) The PID temperature set points are entered and the system is allowed to come to steady state, defined as an average absorber temperature of 350°C that changes by less than 0.5°C over a 15 minute interval. The glass envelope temperature should be constant, too. This usually takes between 3-5 hours.
- 5) At steady state, gather data for 15 minutes every 5 seconds. Data collection is continuous anyway, but the time of steady-state is recorded in a log book as well as other descriptors of the test.
- 6) Before another test is started, open the valve to the pumps and evacuate the system.

- 7) At the end of the testing day, the pumps are turned on (roughing pump first, then turbo pump), the valve to the annulus is opened, and the chamber is evacuated.

UNCERTAINTY CALCULATION

Figure 4.16 shows the heaters involved in the heat loss test.

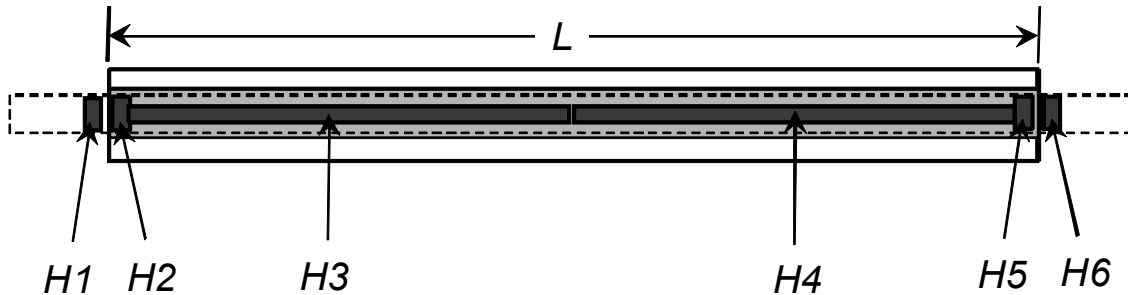


Figure 4.16 Heaters in the experimental set-up

$H1$, $H2$, $H5$, $H6$ are coil heaters associated with end losses. These values are typically small. $H3$ and $H4$ are the cartridge heaters that provide most of the heat to the system. The heat loss is calculated from the following equation:

$$HL = \frac{H2 + H3 + H4 + H5 + \frac{k_{Cu} A_{Cu}}{\Delta x} (T_{Cu1} - T_{Cu2}) + \frac{k_{Cu} A_{Cu}}{\Delta x} (T_{Cu6} - T_{Cu5})}{L} \quad (4.4)$$

where

k_{Cu} is the thermal conductivity of copper

A_{Cu} is the cross-sectional area of the copper pipe

Δx is the distance between T_{Cu1} and T_{Cu2} , and T_{Cu5} and T_{Cu6} , see Figure 4.7

T_{Cu1} , T_{Cu6} are the copper pipe temperatures immediately outside the receiver, see Figure 4.7

T_{Cu2} , T_{Cu5} are the copper pipe temperatures immediately inside the receiver, see Figure 4.7

L is the length of the annulus

H1 and H6 are controlled to make $T_{Cu1} = T_{Cu2}$ and $T_{Cu6} = T_{Cu5}$, creating adiabatic boundaries that prevent heat conduction along the copper pipe. There are uncertainties with these temperatures ($\pm 2^\circ\text{C}$), however, so they are included in the heat loss equation.

Uncertainty analysis is calculated with the differential analysis method (see equation 2.24) where the derivatives of the function are taken with respect to each variable and the root-sum-of-the square method combines contributions of the variables. The variables are assumed to be uncorrelated.

The uncertainty in the heat loss simplifies to

$$U_{HL}^2 = 2 \cdot \left(\left(\frac{1}{L} \right)^2 \Delta H_{coil}^2 \right) + 2 \cdot \left(\left(\frac{1}{L} \right)^2 \Delta H_{cart}^2 \right) + 4 \cdot \left(\left(\frac{k_{Cu} \cdot A_{Cu}}{\Delta x \cdot L} \right)^2 \Delta T_{Cu}^2 \right) + \left(\frac{XX}{L^2} \right) \Delta L^2 \quad (4.5)$$

$$XX = H2 + H3 + H4 + H5 + \frac{k_{Cu} A_{Cu}}{\Delta x} (T_{Cu1} - T_{Cu2}) + \frac{k_{Cu} A_{Cu}}{\Delta x} (T_{Cu6} - T_{Cu5})$$

where

ΔH_{coil} is the uncertainty associated with $H2$ and $H5$, $\pm 2.5 \text{ W}$

ΔH_{cart} is the uncertainty associated with $H3$ and $H4$, $\pm 10 \text{ W}$

ΔT_{Cu1} is the uncertainty associated with T_{Cu1} , T_{Cu2} , T_{Cu5} , and T_{Cu6} , $\pm 2^\circ\text{C}$

ΔL is the uncertainty associated with the annulus length, $\pm 0.005 \text{ m}$

No uncertainty is assumed in the other variables.

The uncertainty works out to be $\pm 5 \text{ W/m}$, rounding to the nearest W/m . It's dominated by the uncertainty in the cartridge heater heat loss measurements. This is considered a systematic error – it's not discernible from the measurements. As measurements are taken over time they show some scatter

but Burkholder et al. [54] show that these random, precision errors are two orders of magnitude smaller than the bias errors considered above.

This is the uncertainty of the heat loss measurement, but this research attempts to quantify the heat loss at a certain absorber temperature. The fact that this temperature isn't known exactly causes more uncertainty in the experimental results. Based on the discussion in the Temperature Measurement section of this chapter, the absorber temperature is known to $\pm 3^\circ\text{C}$. A 347°C absorber will radiate and conduct less heat than a 350°C absorber. If there were no gas in the annulus this would be a difference of 4 W/m due to just radiation. If hydrogen near atmospheric pressure were in the annulus, this would be a difference of almost 12 W/m due to radiation and conduction. Figure 4.17 was created by Sherman's model and it estimates the uncertainty in the heat loss measurement from the total amount of heat (radiation and conduction) lost by the receiver.

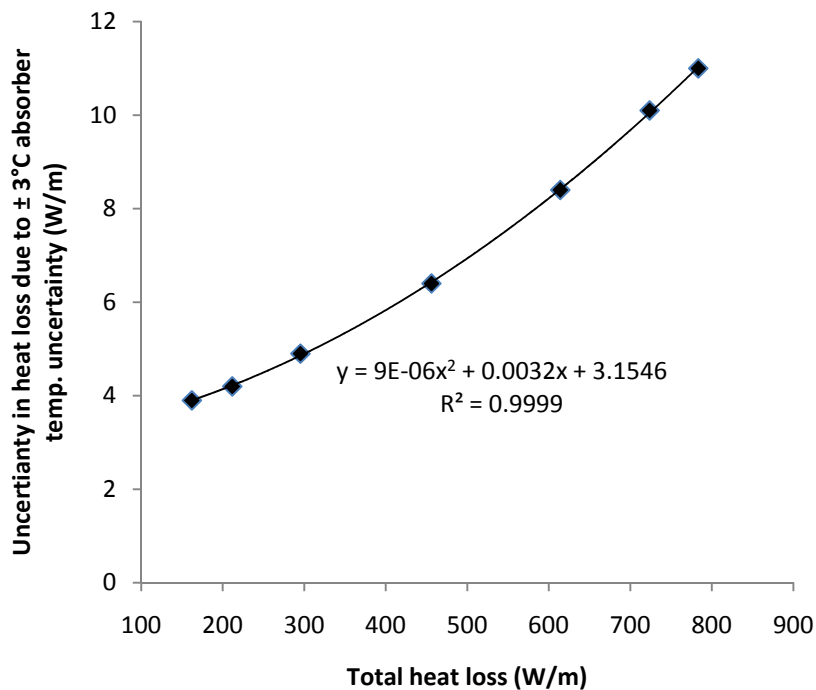


Figure 4.17 Uncertainty in heat loss measurement due to $\pm 3^\circ\text{C}$

This uncertainty is convolved with the ± 5 W/m uncertainty to generate heat loss uncertainties between $\pm 6 - 12$ W/m.

Heat conduction is calculated from two heat loss values:

$$q_c = q_T - q_R \quad (4.6)$$

where

q_c is the heat conduction

q_T is the total measured heat loss

q_R is the radiative heat loss determined from the absorber emittance and glass temperature

The uncertainty of the radiative heat loss measurement is ± 6 W/m, based on the preceding discussion. The uncertainty in the total measured heat loss varies from ± 6 -12 W/m based on the correlation presented in Figure 4.17. This leads to an uncertainty of the heat conduction value between ± 9 -13 W/m, depending on the total amount of heat lost by the system.

EQUIPMENT LIST

The hardware below was used to perform the experiments.

Data acquisition

- 1 routing hub
- 1 Opto 22 ioProject data acquisition software
- 2 Opto 22 Ulitimate i/o SNAP-UP-ADS programmable brains
- 2 Opto 22 A/D module racks
- 14 Opto 22 SNAP AITM 2 channel A-D thermocouple modules
- 3 Opto 22 Dual channel 4-20 mA D-A output modules

Power control and measurement

- 6 Watlow DIN-A-MITE Solid state power controllers – DC10-2050-0000
- 6 Watlow Temperature Limit Controllers – SD3L-HJJA-AARG

6 Ferraz Shawmut 750 V 50 A fuses

2 Ohio Semitronics PC5-107EY25 0-500W power transducer

1 Honeywell Dual-Tec motion sensor

Temperature measurement

50 Omega, alloy 600 sheath, mineral insulated, AF metal transition, ungrounded Type K special limits thermocouples

Heater cores

2 Watlow High temperature Firerod 0.62" diameter, 84.75" length, 208V 2000 W cartridge heater

4 Watlow cable heater 1/8" diameter, coiled i.d. 1.722", coiled length 1", 208V 500W

2 2.17 m copper pipes

Vacuum pumping and pressure measurement

1 Edwards XDS 5 Dry pump

1 Pfeiffer Turbo vacuum pump, Model TMU-26-1

3 MKS 627D Baratron capacitance manometers, 0.1, 10, and 1000 torr full-scale ranges

3 Kurt J. Lesker elbows

2 KJL T's

1 KJL 6-way

1 KJL bellows

1 machined adapter and seal for attachment to glass port on receiver

CHAPTER V

Results

Experimental and modeled results are presented in this chapter. First the accommodation coefficient of hydrogen on the absorber is determined so that it can be used by the models. Pure gas results are presented and the confidence intervals of the models are discussed. Gas mixture results are then presented and compared to modeled results. Both DSMC and Sherman models predict the experimental data in the free molecular, transition, and temperature jump regimes.

HYDROGEN ACCOMMODATION COEFFICIENT ON ABSORBER

As discussed in Chapter II, two heat loss measurement methods are available to determine accommodation coefficients: the free molecule method and the temperature jump method. Hydrogen's accommodation coefficient can be determined on the absorber surface by either method, but in both cases hydrogen's accommodation on the glass envelope must be assumed. Based on Song's correlation [16] $\alpha_{Gl} = 0.25 \pm 25\%$.

The free molecule method is easily applied but first it must be verified that the heat conduction value used in equation 2.3 is a free molecular value. An easy way to check this is to plot heat loss versus pressure. Heat conduction in the free molecular regime is linear with pressure. Figure 5.1 shows a subset of the hydrogen heat conduction results versus pressure.

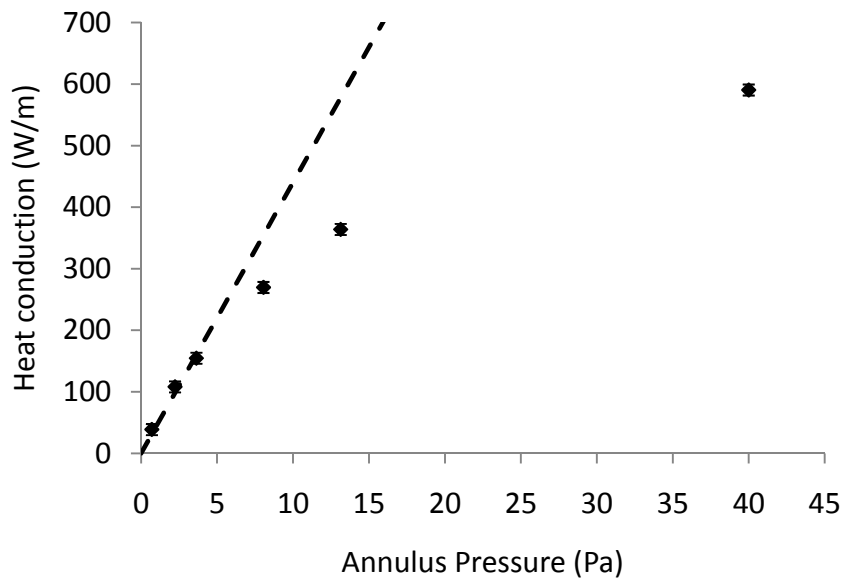


Figure 5.1 Determining the last free molecular heat conduction value to determine hydrogen's accommodation coefficient on the absorber surface.

The heat conduction value near 8 Pa is not on the line. Intermolecular collisions are starting to decrease the efficacy of free molecular heat transport. **Using the heat conduction value at 3.6 Pa the thermal accommodation coefficient of hydrogen on the absorber is $0.34 \pm 23\%$.** More than 80% of

this uncertainty is due to the 25% uncertainty in the glass accommodation coefficient. 23% is close to 25% so the simulations assume all thermal accommodation coefficients are $\pm 25\%$.

The temperature jump method is more involved. Dickens [15] explains it fully. The temperature difference between the absorber surface and glass surface needs to be small. Current methods use $\approx 20^\circ\text{C}$ temperature difference [50]. This is to limit radiative heat transfer and to have better confidence in the average gas temperature and thermophysical properties. The maximum safe temperature for the receiver glass envelope or glass-to-metal seal isn't known, but during bake-out the glass experienced temperatures of 200°C . This limits the maximum temperature of the absorber to about 250°C – it wasn't possible to test the accommodation coefficient with the temperature jump method at an absorber temperature of 350°C . Figure 2.2 shows how accommodation coefficients tend to decrease with temperature. The approach taken was to start at low absorber temperatures and generate a curve, similar to the curves in Figure 2.2, which would allow estimation of the accommodation coefficient on the absorber at 350°C .

Dickens's method must be modified for incomplete accommodation on the outer cylinder surface. Starting with equation 2.8

$$q_{TJ} = \frac{2\pi Lk_{gas}(T_{abs} - T_{gl})}{\ln\left(\frac{r_{gl}}{r_{abs}}\right) + \frac{\gamma_{abs}}{r_{abs}} + \frac{\gamma_{gl}}{r_{gl}}} \quad (2.8)$$

$$q_{TJ} = \frac{2\pi Lk_{gas}(T_{abs} - T_{gl})}{\ln\left(\frac{r_{gl}}{r_{abs}}\right) + \frac{X_{abs}}{P} + \frac{X_{gl}}{P}} \quad (5.1)$$

$$\frac{X_{abs}}{P} = \frac{\gamma_{abs}}{r_{abs}} = \frac{15}{2\pi} \lambda_{STP} \frac{2 - \alpha_{abs}}{2\alpha_{abs} r_{abs}} \quad (5.2)$$

$$\frac{X_{gl}}{P} = \frac{\gamma_{gl}}{r_{gl}} = \frac{\frac{15}{2\pi} \lambda_{STP} \frac{2 - \alpha_{gl}}{2\alpha_{gl}}}{r_{gl}} \quad (5.3)$$

$$\lambda_{STP} = \frac{2\mu_{STP}}{\rho_{STP}\bar{c}} \quad (5.4)$$

$$\bar{c} = \sqrt{\frac{8k_B T}{\pi m}} \quad (5.5)$$

where

STP indicates evaluation at standard temperature and pressure

λ is the mean free path, using equation recommended by Rader [50] and Springer [9]

\bar{c} is the gas's mean thermal speed

k_B is Boltzmann's constant

m is the mass of one molecule

T is the temperature of the gas

All terms in equations 5.1 – 5.5 are known except for X_{abs} and α_{abs} . Dickens explains that X_{abs} can be determined from the slope (m) and y intercept ($b = 1/W_0$) of a line on a figure that plots the inverse heat conduction ($1/W$) versus the inverse pressure ($1/\text{torr}$), as shown in Figure 5.2

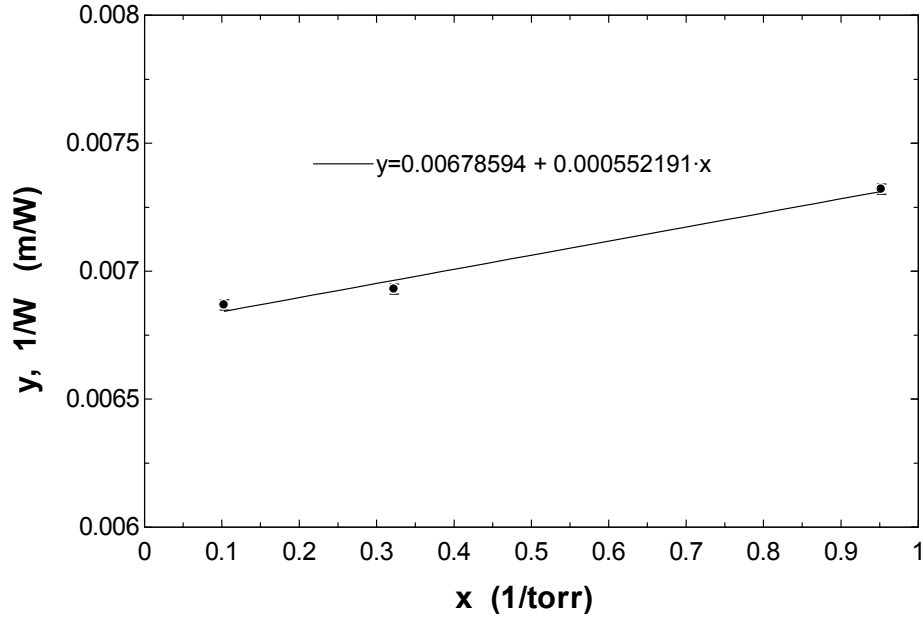


Figure 5.2 Slope and y intercept of 3 hydrogen heat conduction tests at 196°C, at 1.05 torr, 3.1 torr, and 9.7 torr

X_{abs} is related to the slope (m) and y-intercept (b) by

$$W_0 = 1/b \quad (5.6)$$

$$m = \frac{X_{abs} + X_{gl}}{W_0 \ln\left(\frac{r_{gl}}{r_{abs}}\right)} \quad (5.7)$$

X_{abs} is now solved for by the fit, and solution of α_{abs} follows. $\alpha_{abs} = 0.39 \pm 33\%$. Results are very sensitive to the slope of the line and the 25% uncertainty in the glass accommodation coefficient.

Tests were repeated at absorber temperatures of 114°C (2 pressures) and 153°C (3 pressures) and the presents are plotted below.

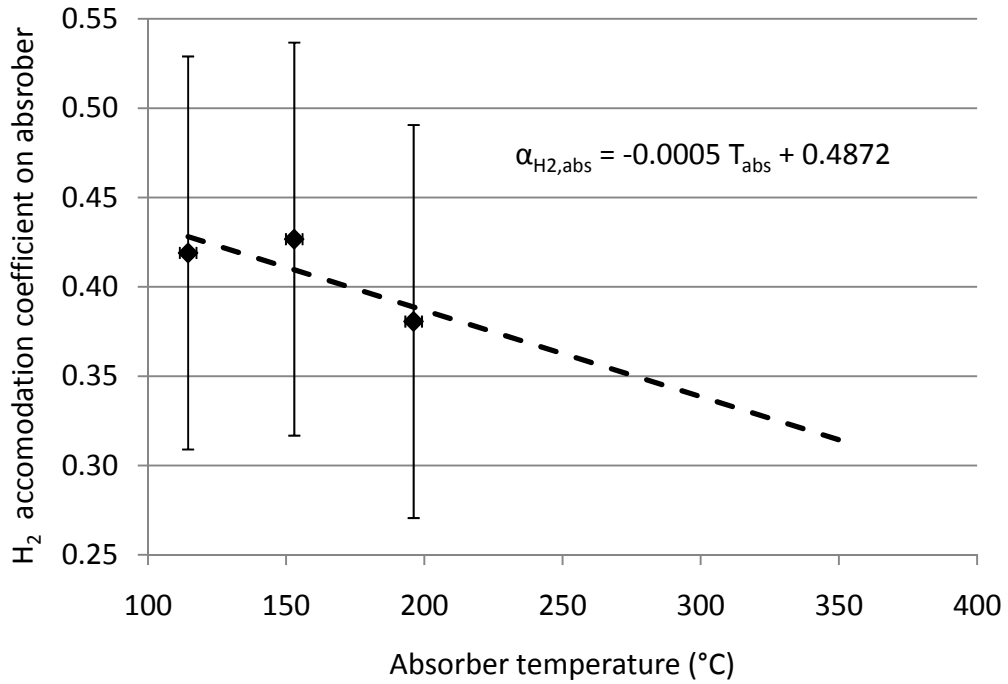


Figure 5.3 Hydrogen accommodation coefficient on absorber trend determined from temperature jump method.

The trend line in Figure 5.3 puts the accommodation coefficient at 0.31 at 350°C. Within uncertainty this is consistent with the 0.34 results from the free molecular method. The uncertainty was slightly less with the free molecular method so simulations will use the 0.34 value.

PURE GAS RESULTS

Experimental results are presented in tabular form in Appendix E.

Figure 5.4 compares the pure hydrogen heat conduction experimental results to modeled results predicted by Sherman's interpolation formula [33] for two cases ($\alpha_{H_2,absorber} = 0.34$, $\alpha_{H_2,glass} = 0.25$; $\alpha_{H_2,absorber} = 0.16$, $\alpha_{H_2,glass} = 0.25$) and Ratzel's model [35] adopted by Dudley [37] and Forristall [5] ($\alpha_{H_2,absorber} = 1$, $\alpha_{H_2,glass} = 1$).

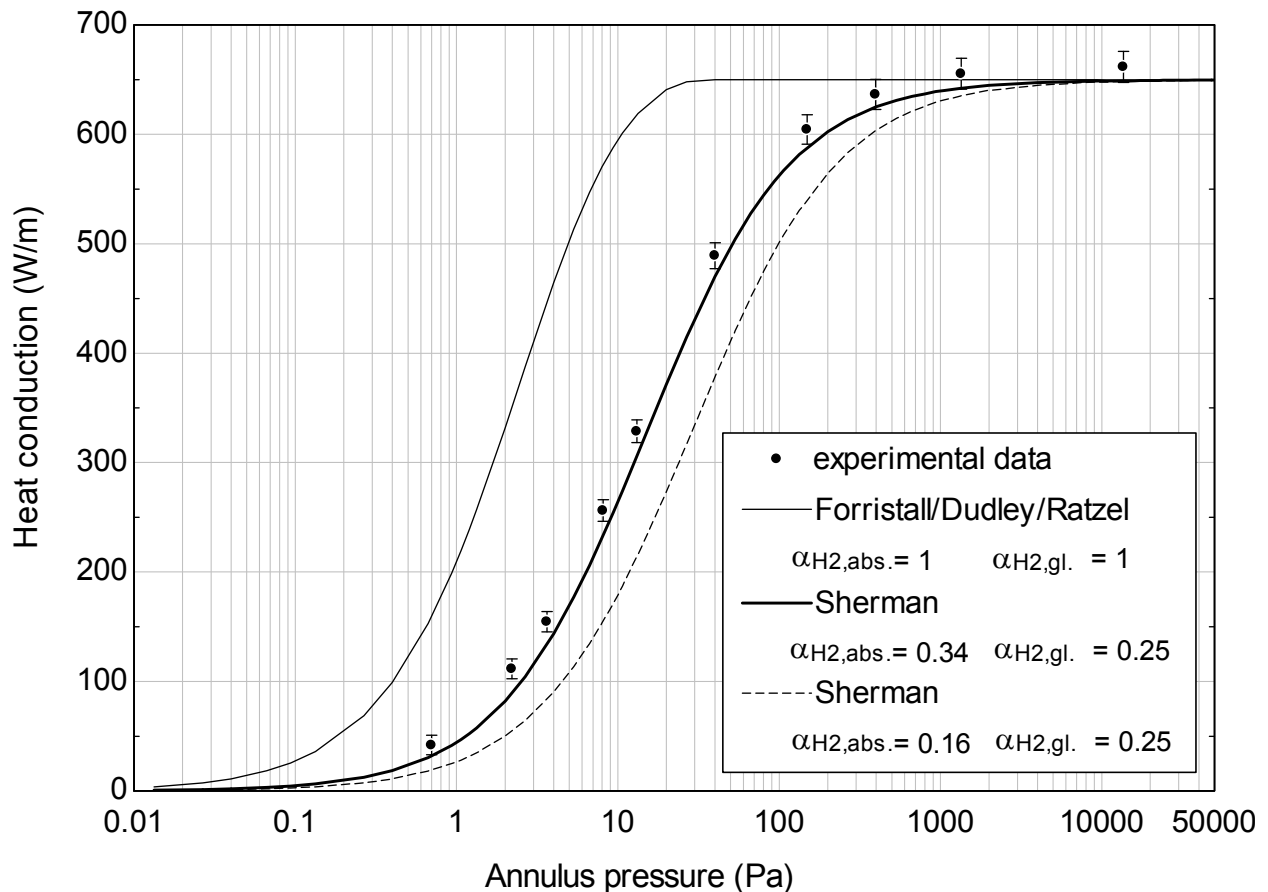


Figure 5.4 Comparison of pure hydrogen results: Sherman, Forristall results and experimental data

Large errors are associated with the Forristall/Dudley/Ratzel model because the assumption of complete thermal accommodation isn't valid for hydrogen on the absorber and glass surfaces. Song et al.'s correlation yields an accommodation coefficient of hydrogen on the absorber of 0.16 ± 0.04 , but Figure 5.4 shows that such a small value doesn't predict experimental data accurately. The Sherman

model that uses a tested accommodation coefficient value of 0.34 on the absorber paired with Song's correlation value of 0.25 on the glass matches most of the experimental data within experimental uncertainty. Figure 5.4 doesn't present the uncertainty bounds of the modeled results. Model results agree with experimental results when the models' confidence intervals are included, as shown by results presented later in this section.

Figure 5.5 compares the pure hydrogen heat conduction experimental results to DSMC model results. All modeled results in this figure used $\alpha_{H_2, \text{absorber}} = 0.34$ and $\alpha_{H_2, \text{glass}} = 0.25$.

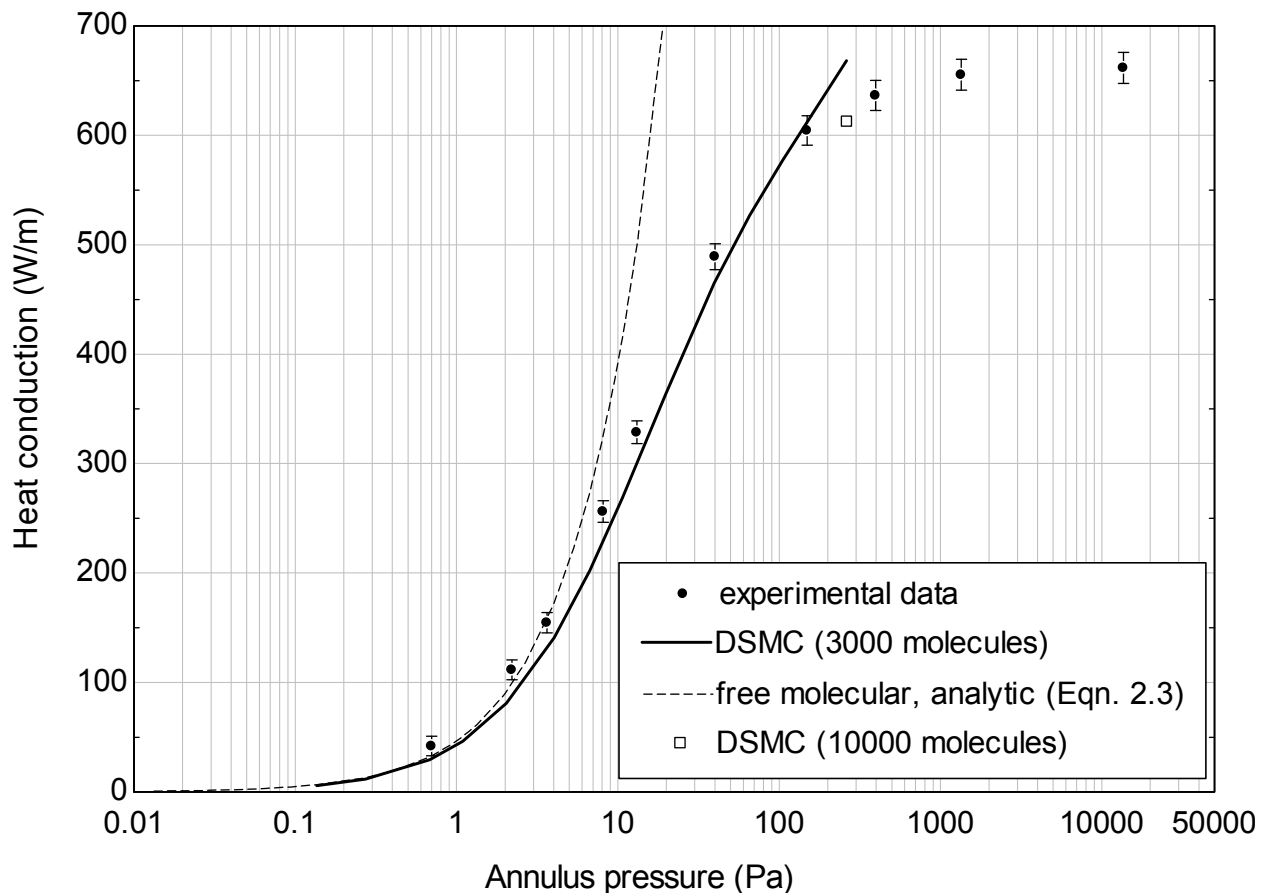


Figure 5.5 Pure hydrogen results: DSMC modeled results and experimental data

DSMC simulation results were determined at the following 13 pressures: 0.1, 0.3, 0.7, 1, 2, 4, 7, 10, 20, 40, 70, 100, and 260 Pa. These pressures are approximate, as the gas pressure is one of the outputs of a DSMC simulation. Each DSMC simulation curve presented in this section was created by linearly interpolating between the results at these pressures. The DSMC convergence study presented in

Chapter III concluded that the use of 20 cells, 400 sub-cells, 3000 molecules, and a time step of $\frac{1}{2}$ the mean collision at each pressure would give reliable results until 33 Pa. DSMC simulations were run at higher pressures to see how well the results that used this discretization matched experimental data near the continuum. The expectation, explained in the DSMC convergence summary of Chapter III and confirmed in Figure 5.5, is that DSMC would predict higher heat conduction results than experimental values at some point above 33 Pa. This is most likely due to insufficient gas and space discretization. This is true of the 3000 molecule 260 Pa DSMC data point in Figure 5.5. If 10,000 molecules had been used at this pressure instead of 3000, a DSMC simulation at 260 Pa would better match the experimental data. The 10,000 molecule simulation data point is shown in Figure 5.5.

The analytic free molecular solution is also presented in Figure 5.5. This solution is correct in the free molecular regime (approximately 4 Pa and less in Figure 5.5). The DSMC results and analytic results are nearly identical for pressures less than 1 Pa in Figure 5.5, and this is sufficient to validate the DSMC model in this regime. At 4 Pa the analytic solution is 14% higher than the DSMC solution. This is the end of the free molecular range so the analytic solution, which assumes no intermolecular collisions, will give a larger heat conduction value than a solution like DSMC which allows for intermolecular collisions even at low pressure.

Figures 5.6 and 5.7 compare hydrogen, argon, and xenon experimental results to Sherman model results. The error bars indicate the 95% confidence intervals of the experimental data, while the dotted lines indicate the 95% confidence interval of Sherman's model. Figure 5.6 shows that all hydrogen experimental results are predicted by Sherman's model within model and experimental uncertainties, while Figure 5.7 shows that argon's and xenon's experimental results are similarly duplicated by Sherman's model. The experimental results in both figures match heat conduction predicted by Fourier's equation near the continuum – this is an important check of the experimental results.

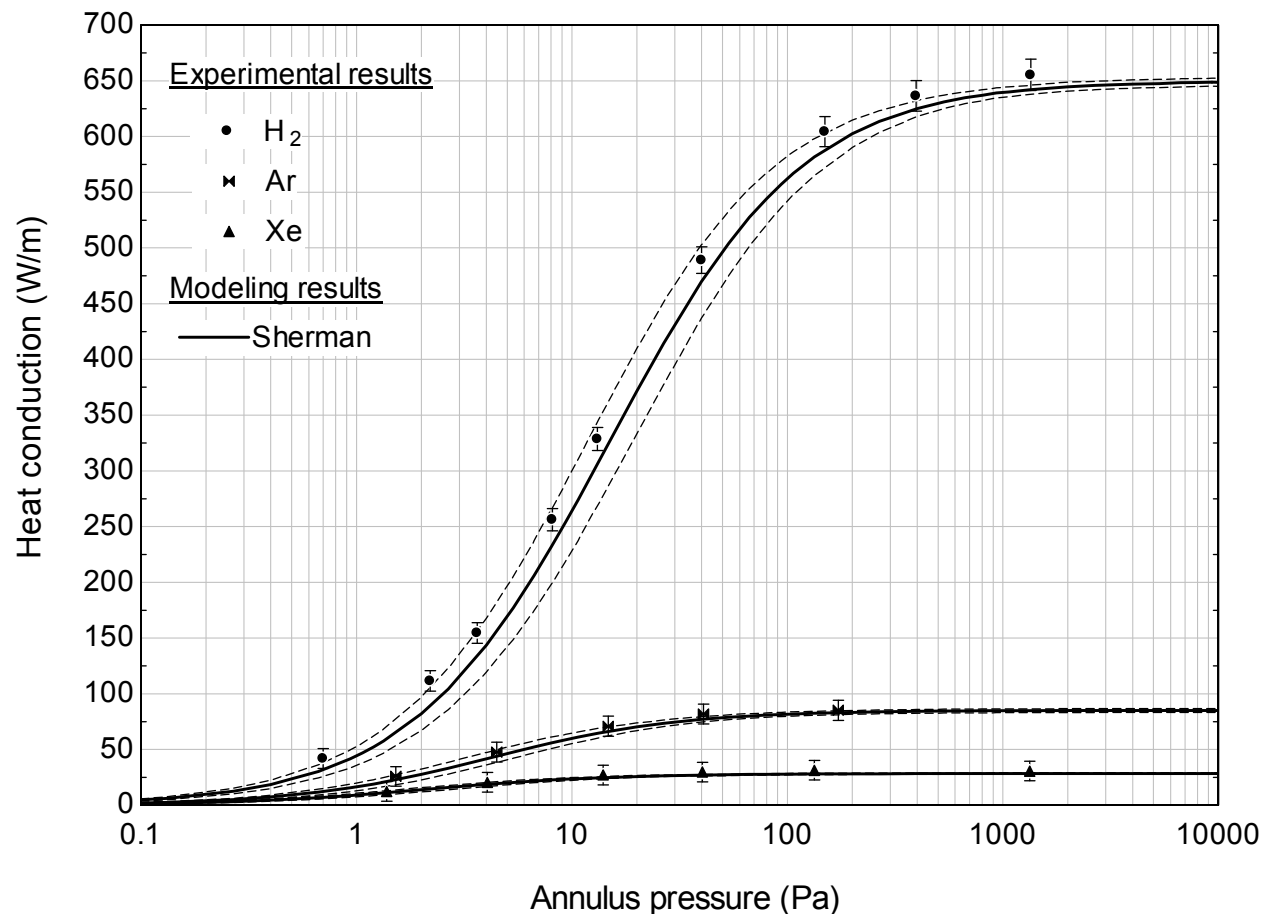


Figure 5.6 Pure gas experimental and Sherman model results

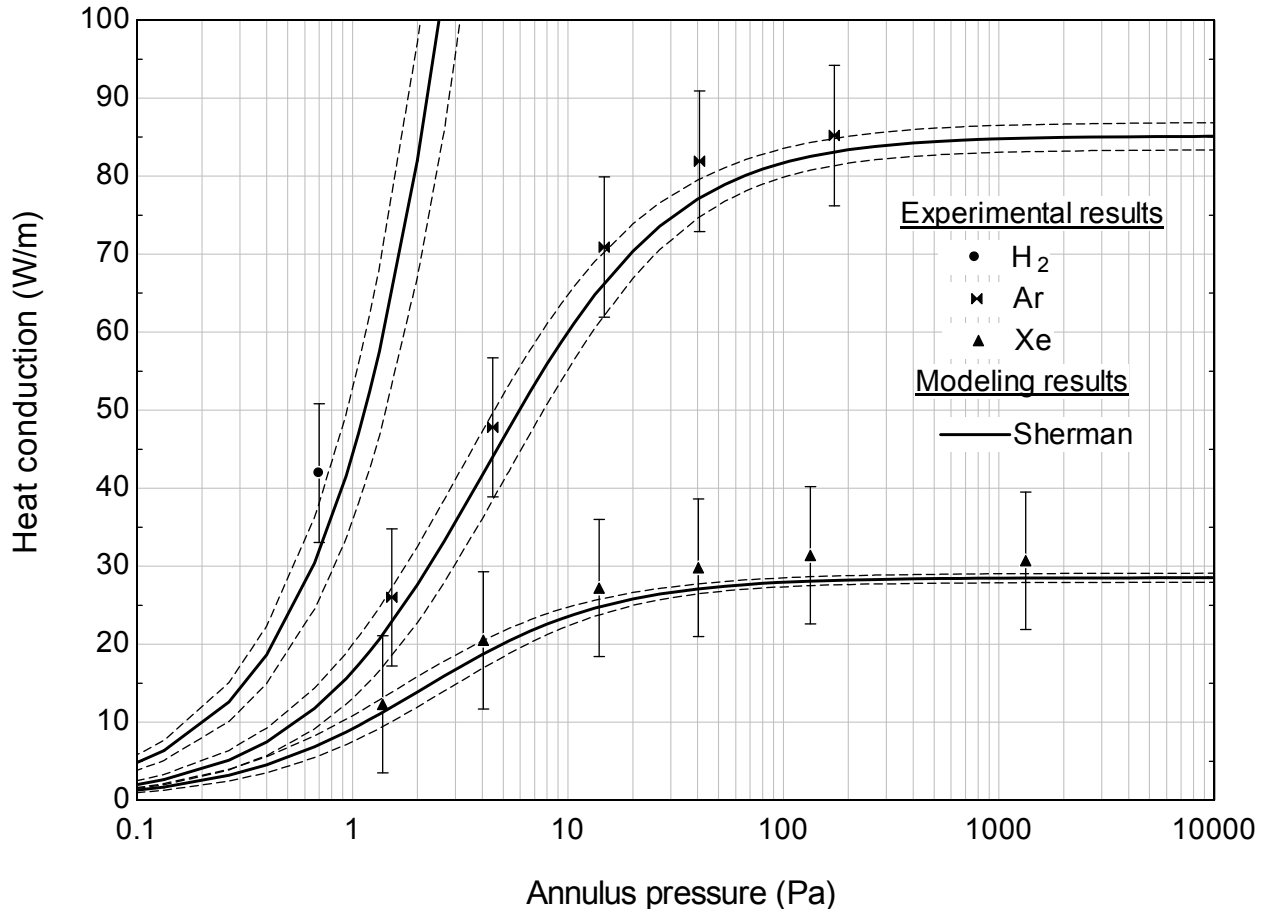


Figure 5.7 Pure gas experimental and Sherman model results, zoomed in to show argon and xenon results

For all data points in Figure 5.6 and 5.7 the Sherman model appears to slightly underpredict the experimental data, though the model results and experimental results still agree within their confidence intervals.

As shown in each figure, the magnitude of the confidence interval for Sherman's model varies as a function of pressure. For example, in Figure 5.6, the confidence interval for the pure hydrogen results is ± 9 W/m at 1 Pa, ± 37 W/m at 10 Pa, ± 21 W/m at 100 Pa, and ± 13 W/m at 1000 Pa. The reason that the confidence interval exhibits this behavior is illustrated in Figure 5.8.

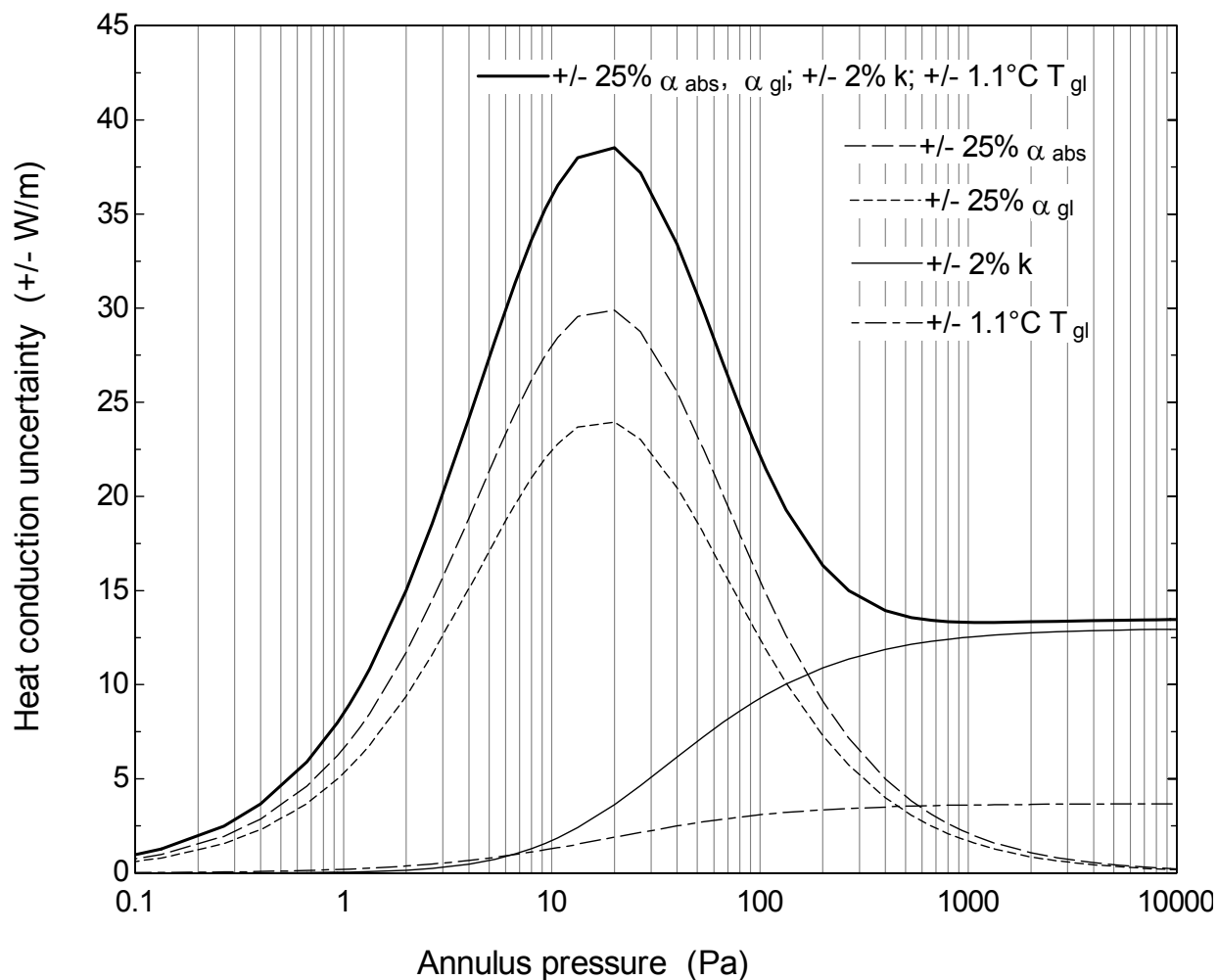


Figure 5.8 Sherman confidence interval contributors for Sherman's pure hydrogen heat conduction results

The top line in Figure 5.8 is the total model uncertainty – the confidence interval values presented in the previous paragraph were determined from the top line. It is the convolution of the four uncertainty lines shown beneath it. Sherman model uncertainties are $\pm 2\%$ for the pure gas thermal conductivities 9 ($\pm 10\%$ for gas mixture), $\pm 25\%$ for the accommodation coefficients, and $\pm 1^\circ\text{C}$ for the glass temperature. The largest contributor to the uncertainty in the transition regime is the accommodation coefficient of hydrogen on the absorber. This is followed closely by uncertainty of the accommodation coefficient on the glass. The $\pm 25\%$ uncertainty of the accommodation coefficients causes the peak model uncertainty in the transition regime. Their effect on the uncertainty decreases as the pressure increases from the

transition regime towards the continuum. Conversely, the 2% uncertainty in the thermal conductivity has little effect early in the transition regime but increases towards the continuum.

Figures 5.9 and 5.10 compare the DSMC results to the pure gas experimental data. The dashed lines again refer to the 95% confidence interval of the modeled results. DSMC simulations were carried out through 260 Pa, though the number of molecules, time step, and grid spacing were based on a maximum pressure of only 33 Pa as investigating transition regime heat conduction was the main focus of this study.

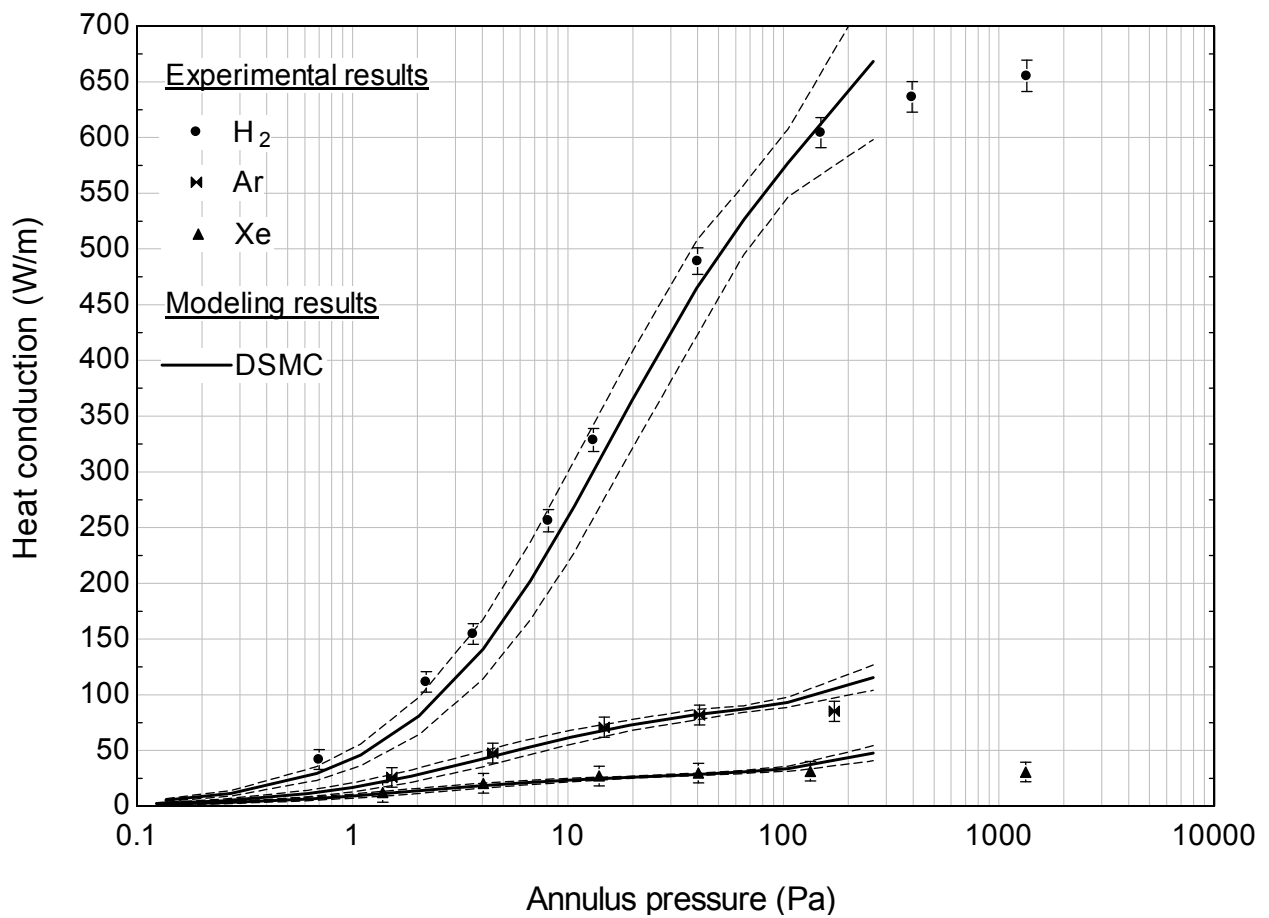


Figure 5.9 Pure gas experimental and DSMC results

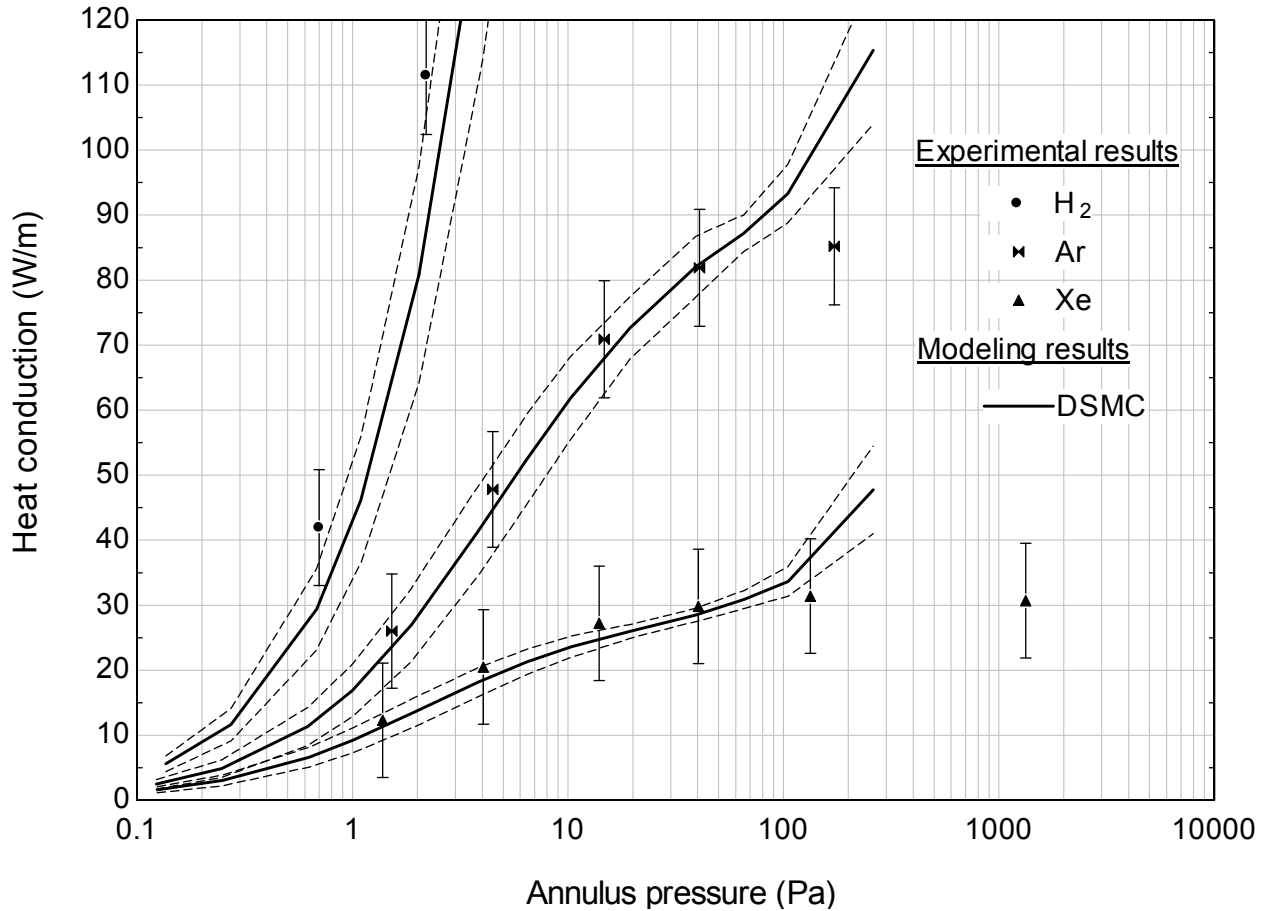


Figure 5.10 Pure gas experimental and DSMC results, zoomed in to investigate argon and xenon results

From free molecular flow up through 40 Pa the DSMC results predict the pure gas experimental results within their respective confidence intervals. Around 100 Pa the DSMC results predict more heat conduction than the experimental results indicate, and this exacerbated at 260 Pa. This is the same behavior observed in Figure 2.8.

Figure 5.11 compares Sherman's confidence interval for hydrogen to that predicted by DSMC. Through much of the free molecular and transition regime the behavior is similar, but around 100 Pa the uncertainty in the DSMC model rapidly increases. Both models use the same accommodation coefficients, so uncertainty in the accommodation coefficients cause the same uncertainty peak around 20 Pa.

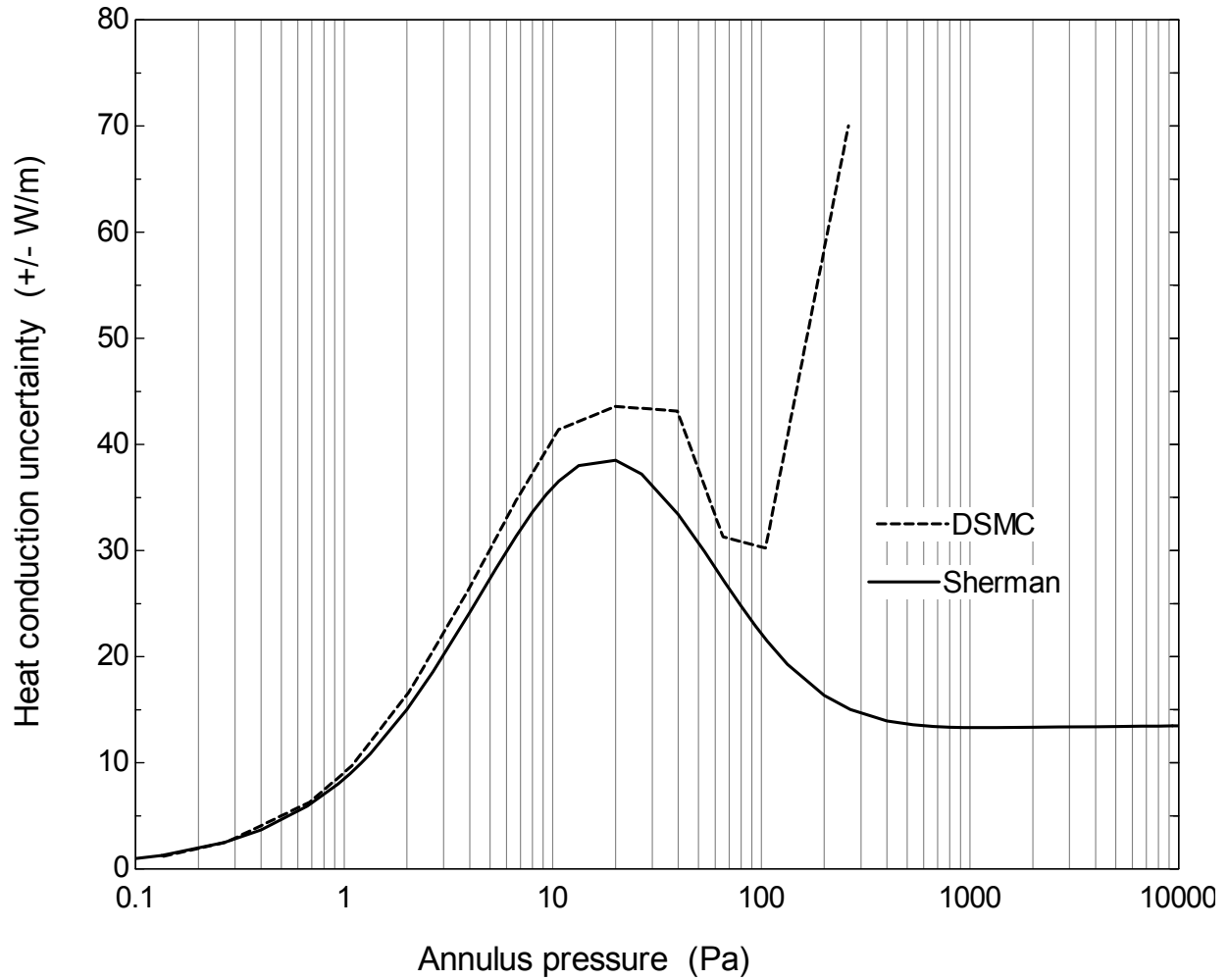


Figure 5.11 Comparison of Sherman and DSMC confidence intervals for the pure hydrogen heat conduction results

To investigate the DSMC uncertainty behavior shown above, the uncertainty of all the DSMC1 model inputs was set to zero. A DSMC1 model was run 10 times with identical inputs, but each time a different random number seed was used to initialize its random number generator. The distribution of the results is shown in Figure 5.12 and compared to a normal distribution.

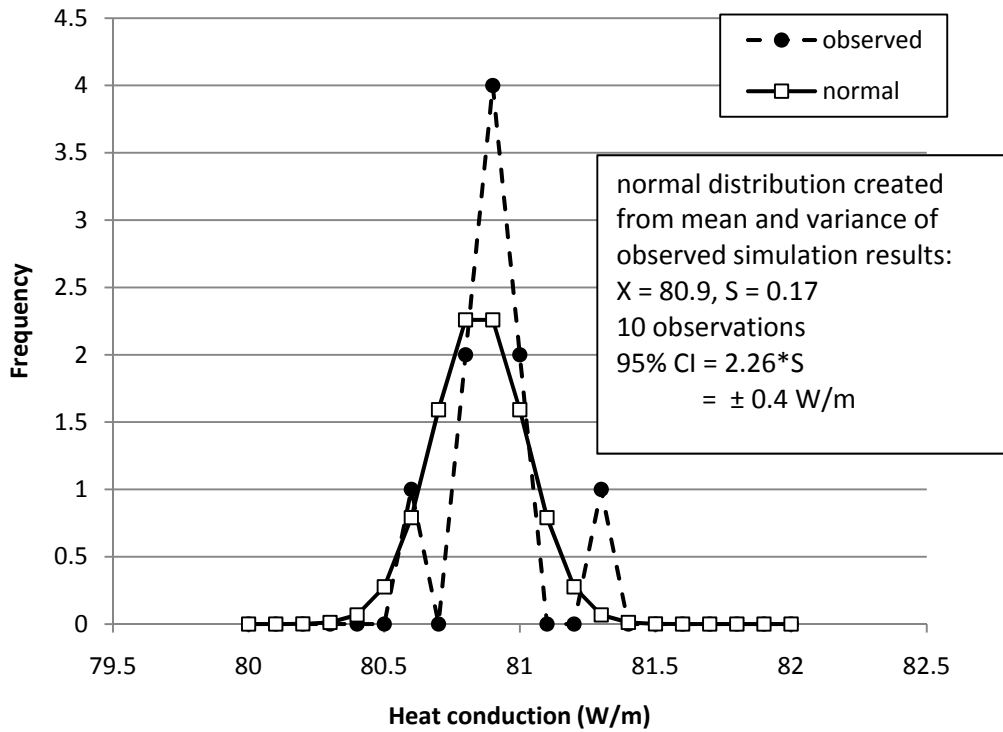


Figure 5.12 Distribution of DSMC1 results from 10 simulations

It's difficult to tell from 10 runs if the spread is a normal distribution. Therefore it's hard to know if the confidence interval calculation shown in the figure is appropriate. Therefore the simulation was re-run 750 times and the spread of the DSMC results was again compared to the normal distribution. The results are shown in Figure 5.13.

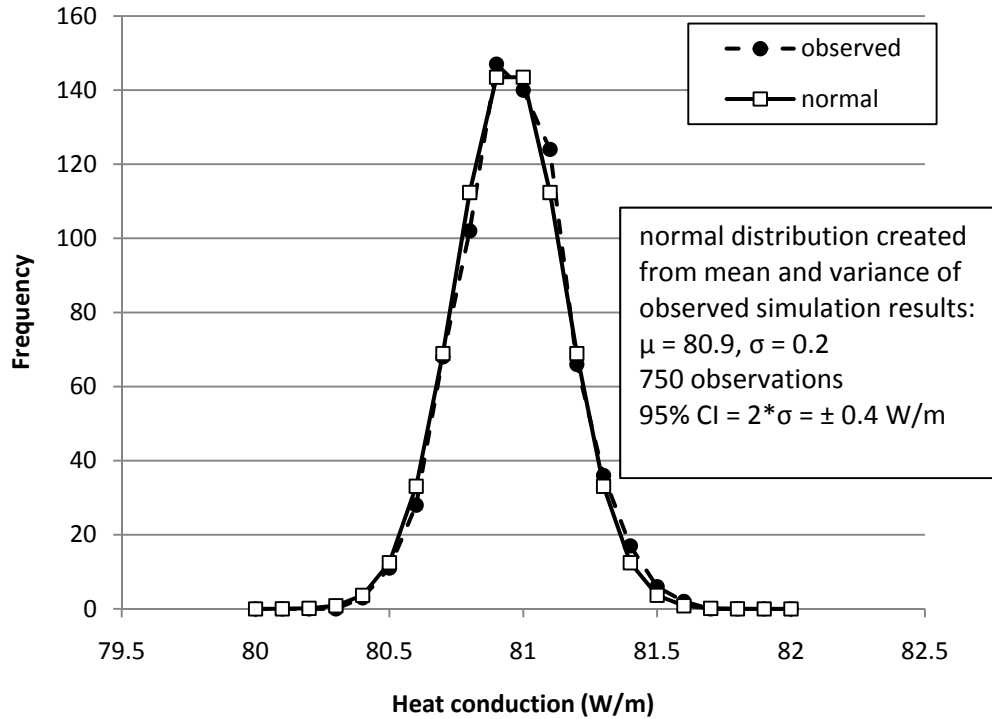


Figure 5.13 Distribution of DSMC1 results from 750 simulations

The distribution is normal. It's appropriate to use estimate the confidence interval from fewer number of simulations assuming that the samples from those simulations are coming from a normally distributed population. For all the pure gas cases, DSMC1 input uncertainties were set to zero and the simulations were allowed to run 10 times at 13 pressures from the free molecular regime to the continuum regime. The standard deviation of the results was taken at each pressure and multiplied by a student t value consistent with 9 degrees of freedom to estimate the 95% confidence interval of the modeled results at that pressure (the same methodology illustrated in Figure 5.12). Figure 5.14 shows the results.

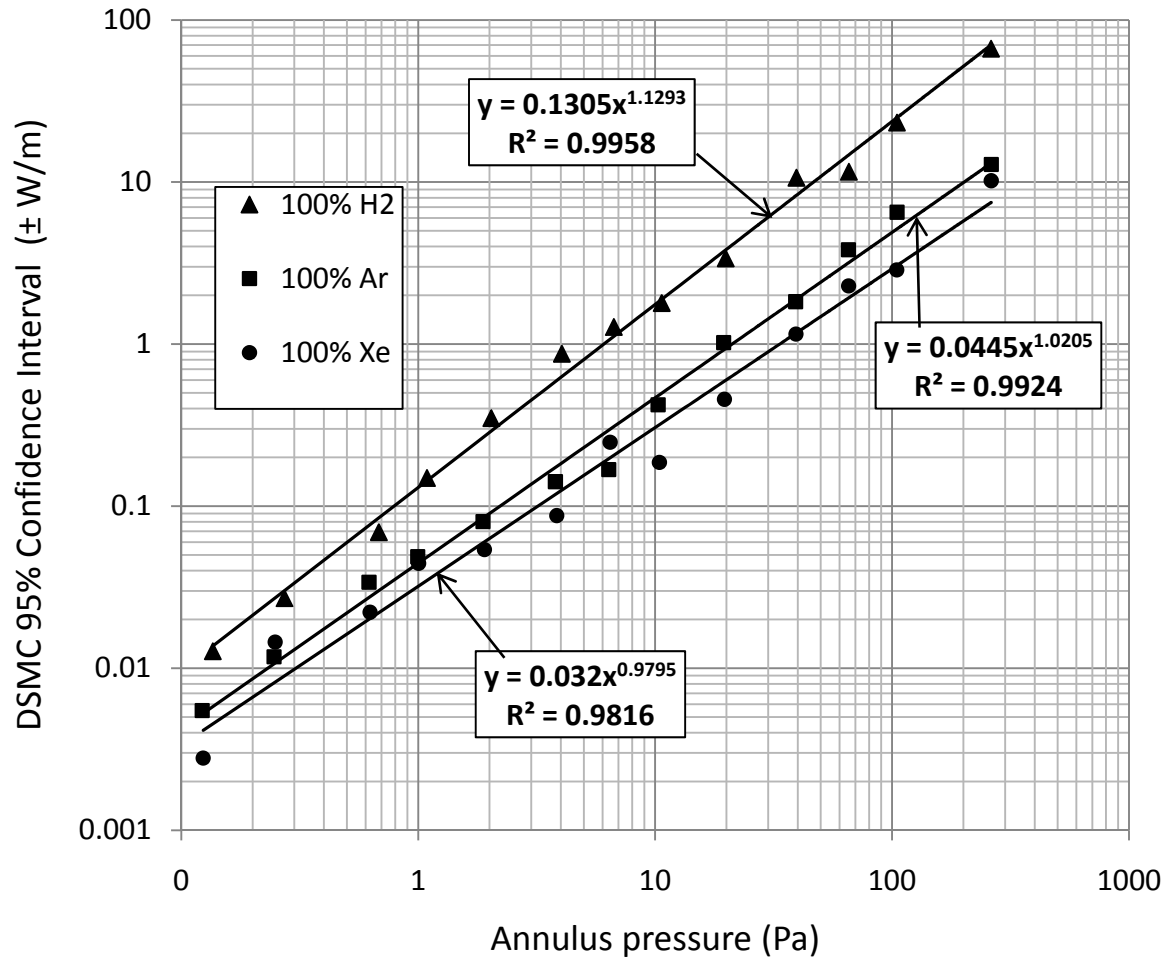


Figure 5.14 Spread of DSMC results with increasing pressure for the pure gases

The magnitude of the confidence interval increases almost linearly with pressure. This can be understood by the fact that each 10 fold increase in pressure means that the number of simulated molecules are being asked to represent 10 times more real molecules. So the effect of any variation in time is magnified at higher pressures. One possible way to prevent this would be increase the number of simulation molecules with pressure.

This confidence interval study was extended to the gas mixtures and final results are plotted in Figure 5.15. The gas mixture results were dependent on the amount of hydrogen, but differences between hydrogen/argon and hydrogen/xenon mixtures were negligible. For this reason Figure 5.15 shows simply the molar fraction of hydrogen without distinguishing whether it's paired with argon or xenon.

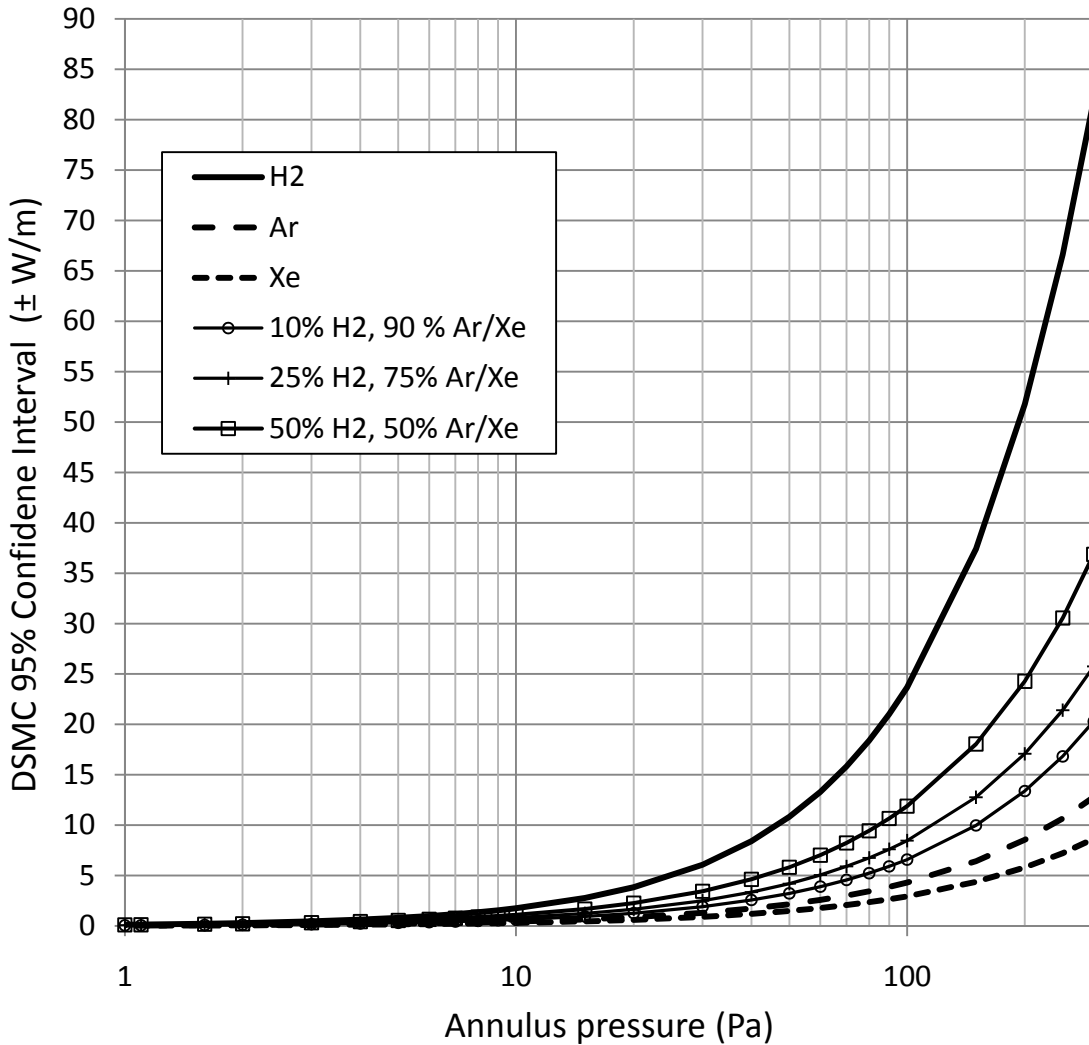


Figure 5.15 Spread of DSMC results with increasing pressure for the pure gases and gas mixtures

Figure 5.15 shows that the confidence intervals associated with the DSMC results increases in magnitude with pressure. This is due to the scatter of the DSMC simulation itself, not associated with uncertainty in its inputs. It's notable that the uncertainties around 30 Pa are ± 7 W/m maximum. It's possible that if a higher pressure were picked for the convergence investigation study then the required number of molecules would have been greater than 3000, and this would have limited the spread of results until higher pressures. For comparison of DSMC results through 33 Pa to experimental results the spread is acceptable.

GAS MIXTURE RESULTS

Hydrogen/argon mixture experimental results are compared to Sherman results in Figure 5.16.

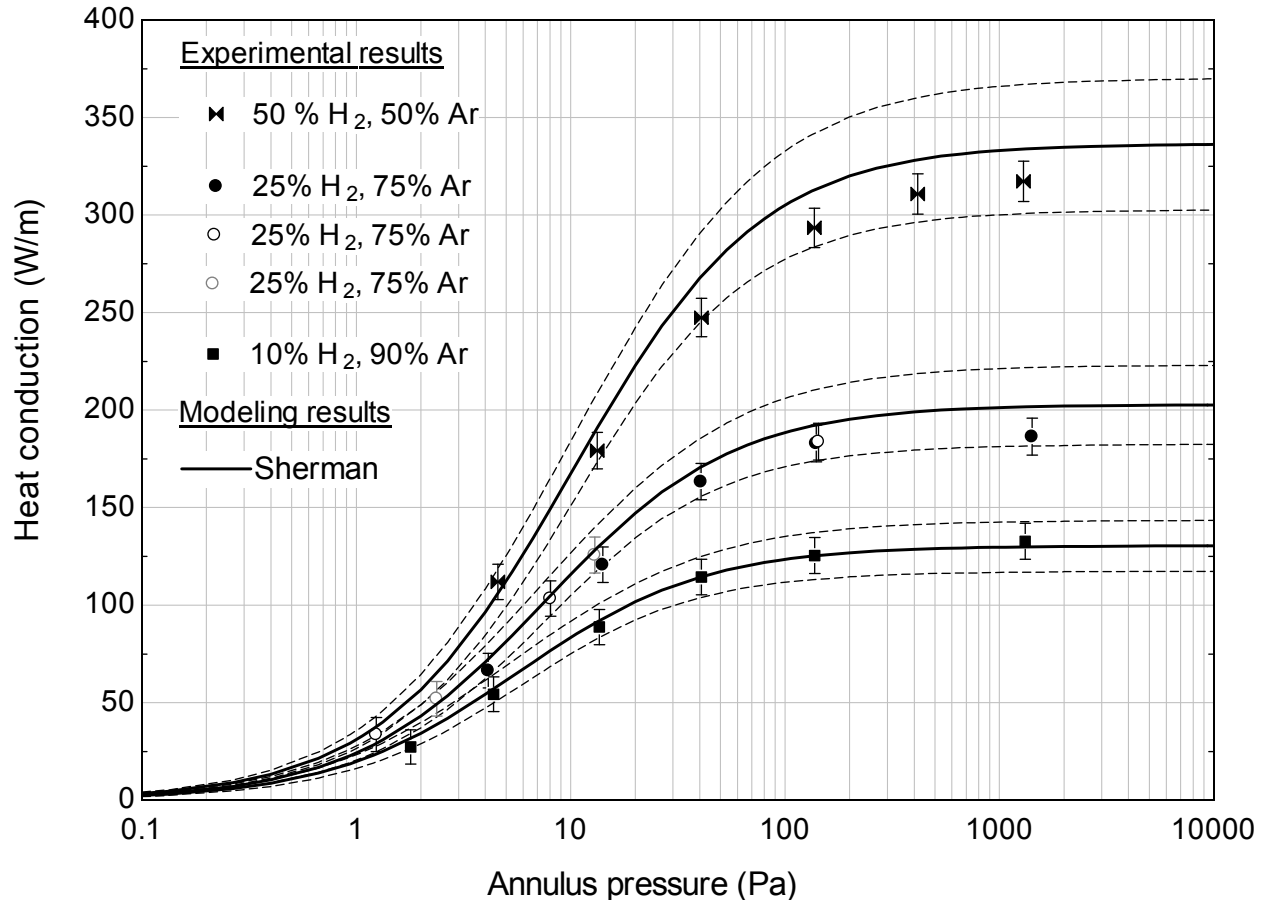


Figure 5.16 Hydrogen/argon gas mixture experimental results compared to Sherman model results

Of note in Figure 5.16 is the repeat of 25% H₂, 75% Ar data points that show test repeatability. Each of these three sets of tests involved removal of the heater cores from the receiver, re-bending the thermocouples to the correct shape, re-attachment of the gas cylinder, another bake-out of the system, re-addition of the gas, etc. Uncertainties for the Sherman formula for these curves are larger in the continuum because uncertainty of the thermal conductivity is $\pm 10\%$ for the gas mixtures instead of $\pm 2\%$ representative of pure gases. The Sherman model shows good agreement with the experimental data.

Figure 5.17 compares the DSMC results to the hydrogen/argon mixture experimental results. Through 40 Pa, and up to 140 Pa, the DSMC results predict the experimental results. The confidence interval of the DSMC results is smaller (meaning less uncertainty) than the confidence interval of the Sherman results in the transition regime because the 10% uncertainty in the gas mixture thermal conductivity (used by the Sherman model) has an effect in a portion of the transition regime.

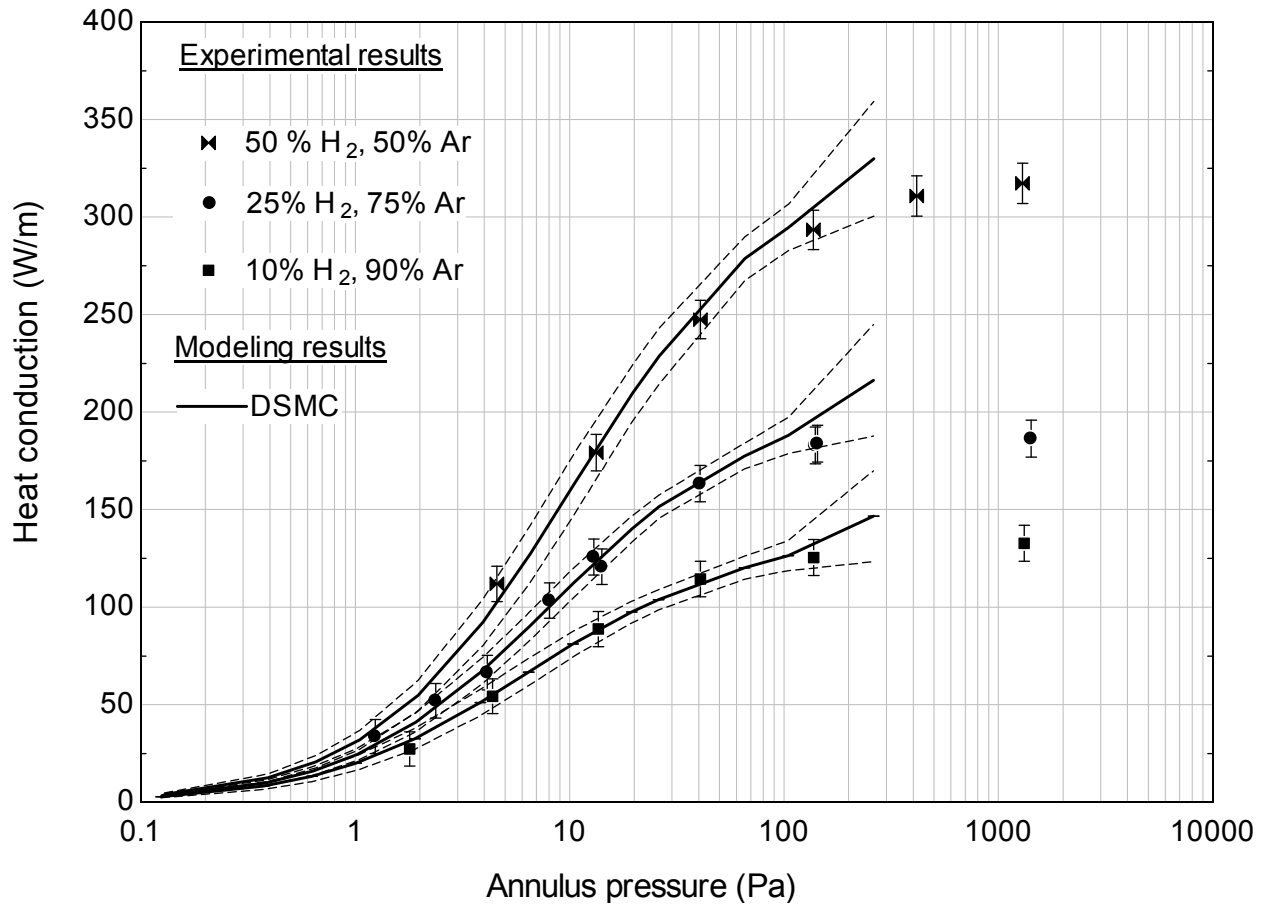


Figure 5.17 DSMC results compared to hydrogen/argon gas mixture experimental results

Hydrogen/xenon mixture experimental results are presented with Sherman model results in Figure 5.18.

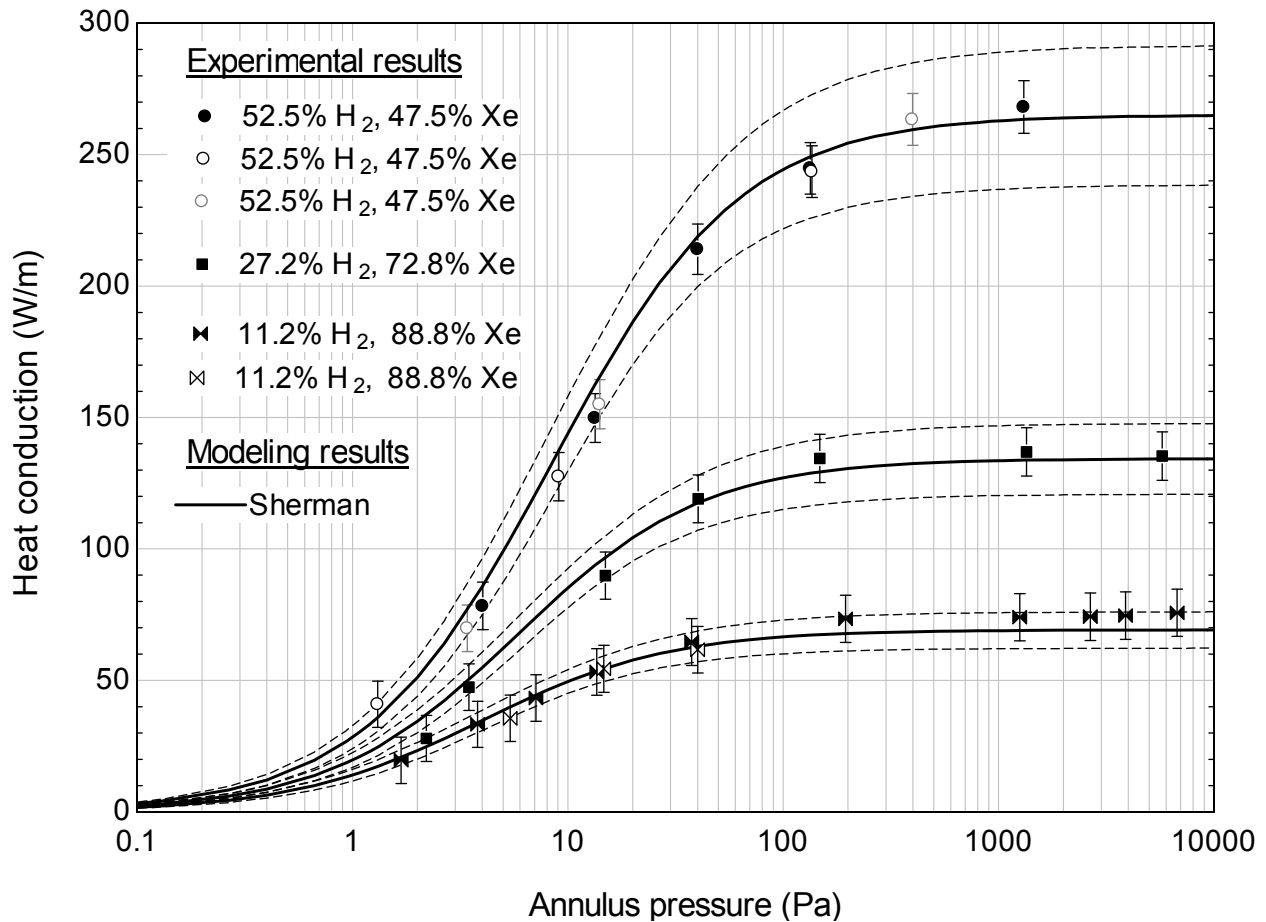


Figure 5.18 Hydrogen/xenon gas mixture experimental results compared to Sherman model results

More repeatability results are presented in Figure 5.18 for the 52.5% H₂, 47.5% Xe results and the 11.2% H₂, 88.8% Xe results. The data show good repeatability. The Sherman model predicts the transition regime and continuum regime experimental data accurately.

Figure 5.19 compares the DSMC results to the hydrogen/xenon mixture experimental results. The DSMC results agree with the experimental results through the transition regime and in to the continuum up to about 200 Pa.

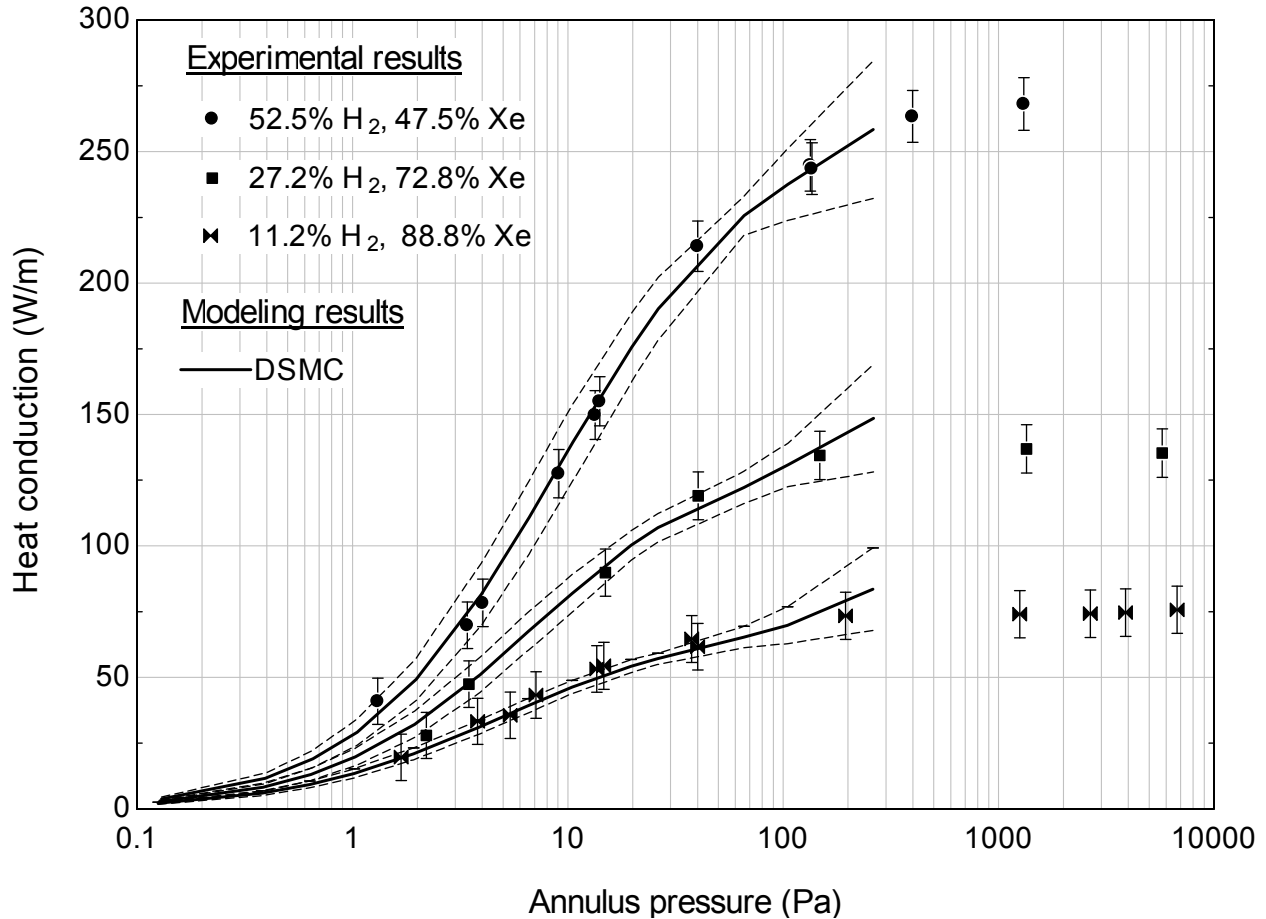


Figure 5.19 Hydrogen/xenon gas mixture experimental results compared to DSMC results

Within uncertainty bounds, the Sherman and DSMC models match all the pure gas and gas mixture experimental data in the free molecular and transition regimes. The Sherman continues to match into the continuum, while the DSMC matches in some areas in the temperature jump regime but starts to deviate as it gets close to the continuum. DSMC seems to have a problem matching the inflection point in the curve that leads results to flattened heat conduction in the continuum. It may be that DSMC simply need to be better discretized (more molecules, shorter time step, more cells) to capture this behavior. The convergence study maximum pressure was 33 Pa, and all DSMC results up to 33 Pa match the experimental data.

Uncertainties being what they are, it's hard to say one model is definitively better than the other at predicting the experimental data for the pure gases or gas mixtures. The only trend that suggests itself is

that Sherman model predicts slightly larger heat conduction values than DSMC for the gas mixtures. This is not true for the pure gases.

For this simple concentric cylinder geometry the Sherman model has some advantages over DSMC: it is less computationally intensive and easier to implement. Both models require reasonable accommodation coefficients to predict free molecular, transition, and temperature-jump regime heat conduction.

One limitation of the Sherman model in this research is the uncertainty associated with the gas mixture thermal conductivity. If this could be known to better than $\pm 10\%$ it would decrease the magnitude of its confidence interval in the late transition, temperature jump, and continuum regimes and that would allow a more stringent comparison with the data.

CHAPTER VI

Conclusions

The Results chapter showed that the Sherman and DSMC models accurately predict argon/hydrogen and xenon/hydrogen gas mixture heat conduction in rarefied heat conduction regimes. This chapter uses the Sherman model to predict heat conduction of inert gas/hydrogen mixtures with larger molar fractions of inert gases than investigated experimentally. These resulting receiver heat losses are entered into the Solar Advisor Model to determine their effect on annual energy production and the levelized cost of energy.

LIMITING HEAT CONDUCTION USING LARGE MOLAR FRACTIONS OF INERT GAS

Ideally the annulus of a parabolic trough receiver is evacuated. In this case heat loss from the receiver is mostly due to radiation from the absorber's low emittance surface, and is consequently low (≈ 150 W/m at 350°C [54]). If a gas is present in the annulus at pressures above 0.1 Pa then the receiver will lose additional energy due to heat conduction through the gas. This research has shown that a receiver can lose an additional 650 W/m, for a total of 800 W/m (650 W/m conduction + 150 W/m radiation) at a typical operation temperature of 350°C depending on the amount of hydrogen in the annulus.

Adding inert gases to hydrogen in the annulus of a parabolic trough receiver reduces the heat conducted. This research has also shown that a simple model – Sherman's model – accurately calculates heat conduction of argon/hydrogen and xenon/hydrogen mixtures in parabolic trough receivers. This model can now be used with confidence in design studies that investigate how larger molar fractions of argon or xenon (or by extension, krypton) in the gas mixture further decrease heat conduction.

Suppose it's determined that 10 Pa of H_2 is the equilibrium pressure of H_2 in the heat transfer fluid. Eventually that 10 Pa will permeate into the annulus. How much xenon should the annulus have to reduce the otherwise 274 W/m of heat loss that hydrogen will induce?

Figure 6.1 shows that 274 W/m can be reduced to 62 W/m with the addition of 90 Pa of xenon (10% molar fraction hydrogen). If more reduction is required, 190 Pa of xenon will reduce the heat conduction to 46 W/m (5% molar fraction hydrogen), or 490 Pa of xenon will reduce it to 35 W/m (2% molar fraction hydrogen).

Figure 6.1 also shows that similar reductions are possible if 10 times more hydrogen, 100 Pa, is in the annulus. 100 Pa of H_2 would cause 567 W/m of heat conduction if alone in the annulus, but when mixed with 900 Pa of xenon the 560 W/m would be reduced to 64 W/m (10% molar fraction hydrogen), or 46 W/m with 1900 Pa xenon (5% molar fraction hydrogen), or 36 W/m with 4900 Pa xenon (2% molar fraction hydrogen).

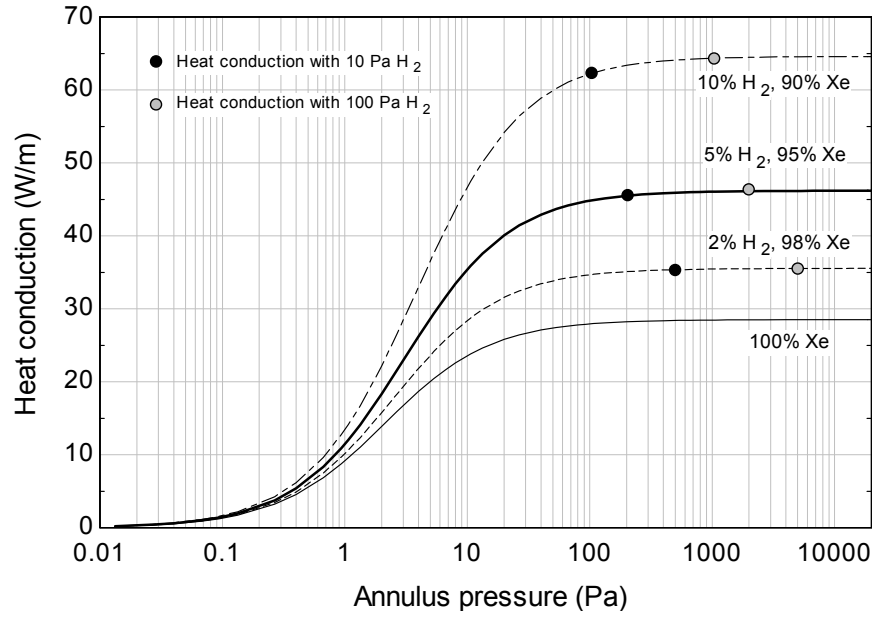


Figure 6.1 Different levels of heat conduction depending on the molar fractions of xenon and hydrogen in the annulus. Absorber at 350°C.

Figure 6.2 shows a similar investigation using argon instead of xenon. Though argon does not reduce heat conduction as much as xenon, it still reduces heat conduction significantly and is cheaper than xenon.

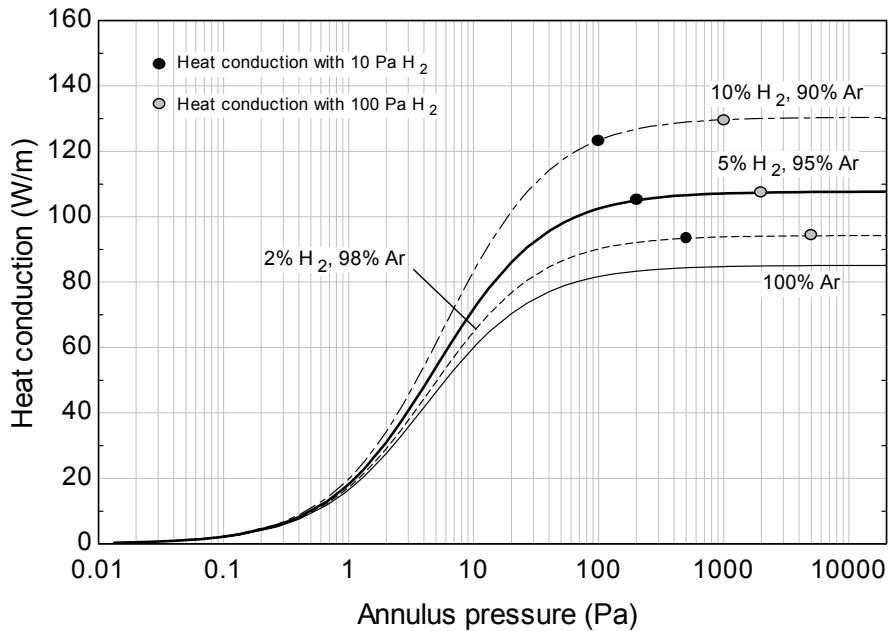


Figure 6.2 Different levels of heat conduction depending on the molar fractions of argon and hydrogen in the annulus. Absorber at 350°C.

NATURAL CONVECTION LIMITS THE TOTAL PRESSURE IN THE ANNULUS

The heat loss in the annulus can be reduced only to a point by adding inert gas. The first limit is obviously the heat conduction that corresponds to pure argon or pure xenon in the annulus, and the second limit is caused by natural convection. Figure 6.3 shows 11.2% H₂, 88.8% Xe heat conduction experimental results up to 50,000 Pa and compares these results to the Sherman formula. The model agrees with the data in the transition regime and agrees in the continuum (within experimental and model uncertainty) but between 5,000 and 10,000 Pa the actual heat loss is more than the model predicts.

Ratzel et al. [35] cite Kraussold [61] for a Raleigh number of 1000 as the criterion for onset of natural convection between concentric cylinders. The Rayleigh number is calculated from [35]

$$N_{Ra} = \frac{c_p \rho^2 g \beta l^3 \Delta T}{\mu k} \quad (6.1)$$

where

c_p is the heat capacity of the gas

ρ is the gas density

g is the gravitational constant

β is the gas's volumetric expansion coefficient

l is the characteristic length, in this case the gap size ($r_2 - r_1$)

ΔT is the temperature difference across the gap ($T_2 - T_1$)

μ is the gas's dynamic viscosity

k is the gas's thermal conductivity

Gas thermophysical properties in the Rayleigh number calculation are evaluated at the film temperature: $(T_2 + T_1)/2$.

The pressures at which the Rayleigh number equals 1000 for xenon and argon for the geometry and temperatures differences of this research are 5,000 Pa and 16,000 Pa, respectively. In other words, the total pressure of the gas mixture in the annulus (which will be predominantly xenon or argon) should

not exceed 5,000 Pa (if xenon is the filler gas) or 16,000 Pa (if argon is the filler gas) lest natural convection will begin increasing the heat conduction. The experimental data for the xenon/hydrogen mixture shown in Figure 6.3 support this conclusion. Argon data is not plotted but shows similar behavior, i.e. 16,000 Pa should be regarded as the maximum allowed annulus pressure.

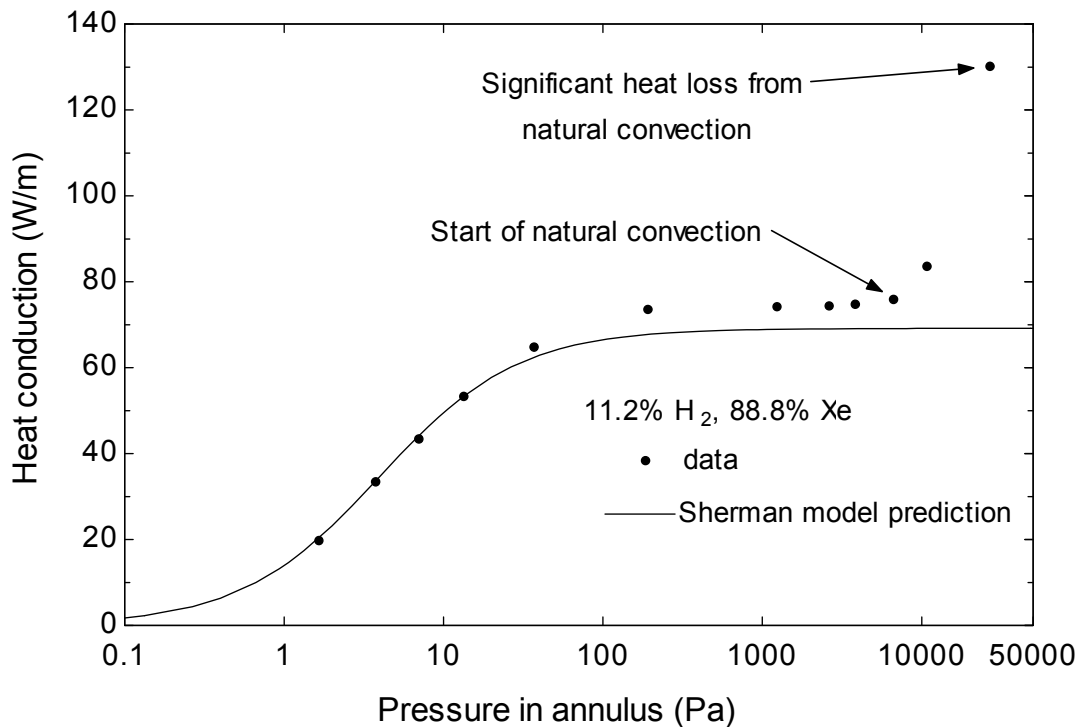


Figure 6.3 Onset of natural convection in the annulus with a xenon/hydrogen mixture in the annulus

EFFECT OF INERT GASES ON PLANT PERFORMANCE

Electricity production of a parabolic trough power plant depends on the thermal energy collected by the solar field. The thermal energy produced by the solar field depends on the insolation, the aperture and optical efficiency of the collectors, and the heat lost by the receivers and piping. Hydrogen can drastically increase the heat lost by the receivers which decreases the total thermal energy produced by the solar field and consequently decreases the electricity produced. A model of a parabolic trough power plant is needed to quantify this effect.

The Solar Advisor Model (SAM) [6] is a performance and economic model designed to give project developers estimates of power production and the levelized cost of energy for various solar technologies. The parabolic trough power plant model in SAM is based on Excelergy [62] which was validated against parabolic trough plant performance data. The SAM results in this section were provided by SAM version 2011.6.30.

Turchi [63] presents a trough reference plant for SAM with costing provided by input from plant developers. The costing for the plant components is summarized in an Excel spreadsheet that is linked through the report. Turchi also created a SAM input file based on the results of the costing study with realistic inputs for the physical model of the plant. This input file is located at [64].

The reference plant of interest is a 100 MWe, wet-cooled, with 6 hrs of thermal energy storage using solar salt located in Blythe, CA. The list of physical and economic inputs to the model is extensive, and description of all the inputs can be found in the User's Guide that comes with the program. Appendix G is a series of screenshots that shows the values related to each of the 14 input screens in the default plant model. The only values varied in this analysis relate to receiver heat loss.

Six different receiver annulus conditions were simulated using the model: evacuated, 100 Pa hydrogen, 1900 Pa xenon, 100 Pa hydrogen with 1900 Pa xenon (5% molar fraction hydrogen), 4900 Pa argon, and 100 Pa hydrogen with 4900 Pa argon (2% molar fraction hydrogen). The predicted net annual energy production and levelized cost of energy for each annulus case is presented in Table 6.1.

Table 6.1 SAM simulation cases and results

Annulus Condition	Total receiver heat loss at 350°C (W/m)	Net annual electricity production (MWh)	Ratio of net annual electricity production to evacuated case	Plant levelized cost of energy, LCOE (¢/kWh)	Difference in LCOE from evacuated case (¢/kWh)
Evacuated	153	374,780	1	20.6	0
1900 Pa Xe	182	367,997	0.98	21.0	+0.4
100 Pa H ₂ & 1900 Pa Xe	199	363,413	0.97	21.2	+0.6
4900 Pa Ar	238	350,693	0.94	22.0	+1.4
100 Pa H ₂ & 4900 Pa Ar	247	347,695	0.93	22.2	+1.6
100 Pa H ₂	720	166,978	0.45	45.7	+25.1

Ideally a plant will have evacuated receivers. However, if hydrogen permeates through into an otherwise evacuated receiver to reside in the annulus at 100 Pa, SAM predicts that plant performance is severely compromised: half the net electricity is produced and the levelized cost of energy more than doubles.

Receivers can be supplied from the manufacturer with a small amount of inert gas in the annulus. A plant using receivers with 1900 Pa of xenon in the annulus will make 98% of the net annual electricity as a plant with evacuated receivers, with an LCOE less than 0.5 cents per kWh higher. This assumes that there is no additional cost to the receiver to add this amount of xenon, and that receiver cost has not decreased (though it should) due to a reduced need for getters in the annulus. Argon (or krypton) could be used instead. Argon conducts more heat than xenon, so a plant with receivers with 4900 Pa of argon in their annuli will make 94% of the net annual electricity as a plant with evacuated receivers, with a levelized cost of energy about 1.5 cents per kWh higher than the evacuated plant. In both cases adding inert gas to the annulus decreases plant performance relative to a plant with evacuated receivers, unless future hydrogen permeation is taken into account.

When 100 Pa of hydrogen permeates in the receivers the performance of a plant with evacuated receivers is severely compromised, as stated before. However, this is not true of plant with inert gases in the receivers' annuli. When 100 Pa of hydrogen permeates into a receiver with 1900 Pa of xenon in the annulus, heat loss is increased minimally (to 199 W/m from 182 W/m) and plant performance decreases slightly (to 97% from 98% of an evacuated plant's net annual electricity production). The heat loss increase and performance decrease for argon receivers is similar.

In summary, though inert gas filled receivers have more heat loss and decreased performance relative to evacuated receivers, they mitigate significant performance penalties that are associated with hydrogen permeation into evacuated receivers. For this reason manufacturers should consider inert gas receivers for parabolic trough power plants where significant hydrogen permeation rates are expected to exist.

BIBLIOGRAPHY

- [1] Moens, L. and D. Blake, "Mechanism of Hydrogen Formation in Solar Parabolic Trough Receivers" National Renewable Energy Laboratory Technical Report, NREL/TP-510-42468, 2008.
- [2] Price, H., R. Forristall, T. Wendelin, A. Lewandowski, T. Moss, C. Gummo, "Field Survey of Parabolic Trough Receiver Performance," Proceedings of ISEC: ASME 2006, Denver, Colorado, July 8-13, 2006.
- [3] Bingham, Carl and B. Meglen. "Spectral Evaluation Experiments of HCEs Feb-Mar 2006," PowerPoint presentation, National Renewable Energy Laboratory, 2006.
- [4] Burkholder, F., H. Price, C. Kutscher, M. Brandemuehl, J. Netter, "Parabolic Trough Receiver Thermal Testing," Proceedings of the ASME Energy Sustainability Conference, Long Beach, California, June 27-30, 2007.
- [5] Forristall, R., "Heat Transfer Analysis and Modeling of a Parabolic Trough Solar Receiver Implemented in Engineering Equation Solver," National Renewable Energy Laboratory Technical Report, NREL/TP-550-34169, 2003.
- [6] SAM (Solar Advisor Model) developed by the National Renewable Energy Laboratory. Available electronically at www.nrel.gov/analysis/sam.
- [7] Burkholder, F., M. Brandemuehl, C. Kutscher, E. Wolfrum, "Heat Conduction of Inert Gas/Hydrogen Mixtures in Parabolic Trough Receivers," Proceedings of the 2nd ASME Energy Sustainability Conference, Jacksonville, Florida, August 10-14, 2008.
- [8] Bomelburg, H., "Heat Loss from Very Thin Heated Wires in Rarefied Gases," Physics of Fluids, Vol. 2, p. 717, 1959.
- [9] Springer, G.S., "Heat transfer in rarefied gases," Advances in Heat Transfer, Vol. 7, pp. 163-218, 1971.
- [10] Bird, G., Molecular Gas Dynamics and the Direct Simulation of Gas Flows, Clarendon Press, Oxford, 1994.
- [11] Kennard, E., Kinetic Theory of Gases, 1st ed. pp. 291-335. McGraw-Hill, New York, 1938.
- [12] Knudsen, Ann. Physik, Vol. 34, p. 593, 1911.
- [13] Harding, G., B. Window, "Free Molecule Thermal Conduction in Concentric Tubular Solar Collectors," Solar Energy Materials Vol. 4, p. 265, 1981.
- [14] Thomas, L., R. Golike, "A Comparative Study of Accommodation Coefficients by the Temperature Jump and Low-Pressure Methods and Thermal Conductivities of He, Ne, and CO₂," The Journal of Chemical Physics, Vol. 22, No. 2, Feb. 1954.
- [15] Dickens, B., "The Effect of Accommodation on Heat Conduction Through Gases," Proceedings of the Royal Society of London. Series A, Containing papers of a mathematical and physical character," Vol. 143, p. 517-540, 1934.
- [16] Song, S. and Yovanovich, M. "Correlation of thermal accommodation coefficient for engineering surfaces," in Fundamentals of conduction and recent developments in contact resistance, M. Imber, G.P. Peterson, and M. Yovanovich (Eds.), Vol 69, The American Society of Mechanical Engineers, United Engineering Center, New York, pp. 107 – 116, 1987.

- [17] Langmuir, I., G. Mackay, "The Dissociation of Hydrogen into Atoms. Part I. Experimental." *Journal of the American Chemical Society*, Vol. 36, pp. 1708-1722, 1914.
- [18] Langmuir, I., "The Dissociation of Hydrogen into Atoms. Part II. Calculation of the Degree of Dissociation and the Heat of Formation." *Journal of the American Chemical Society*, Vol. 37, pp. 417-458, 1915.
- [19] Smoluchowski, M.S., "On Conduction of Heat by Rarefied Gases," *The London, Edinburgh, and Dublin Philosophical Magazine and Journal of Science*, Vol. 46, pp. 192-206, 1898.
- [20] Sheldon, D., G. Springer, "Experimental Study of Rarefied Argon Contained between Concentric Cylinders," *Physics of Fluids*, Vol. 11, No. 6, pp. 1312-1320, 1968.
- [21] Song, S., M. Yovanovich, F. Goodman, "Thermal Gap Conductance of Conforming Surfaces in Contact," *Journal of Heat Transfer*, Vol. 115, pp. 533-540, 1993.
- [22] Beikircher, T., N. Benz, W. Spirkel, "A Modified Temperature-Jump Method for the Transition and Low-Pressure Regime," *Journal of Heat Transfer*, Vol. 120, p. 965, 1998.
- [23] Wilke, C.R., "A Viscosity Equation for Gas Mixtures," *The Journal of Chemical Physics*, Vol. 16, No. 4, pp. 517-519, 1950.
- [24] Kogan, M., *Rarefied Gas Dynamics*, Translated from Russian by Trilling, L., Plenum Press, New York, 1969.
- [25] Braun, D., A. Frohn, "Heat transfer in simple monatomic gases and in binary mixtures of monatomic gases," *International Journal of Heat and Mass Transfer*, Vol. 19, pp. 1329-1335, 1976.
- [26] Braun, D., A. Frohn, "Heat transfer in binary mixtures of monatomic gases for high-temperature difference and for a large Knudsen number range," Paper 13 presented at the 10th International Symposium on Rarefied Gas Dynamics, Aspen, CO, July 19-23, 1976. pp. 149-159.
- [27] Maxwell, J., "Illustrations of the dynamical theory of gases. I. On the motions and collisions of perfectly elastic spheres," *The London, Edinburgh, and Dublin Philosophical Magazine and Journal of Science*, Vol. 19, pp. 19-32, 1860.
- [28] Bhatnagar, P., E. Gross, M. Krook, "A Model for Collision Processes in Gases. I. Small Amplitude Processes in Charged and Neutral One-Component Systems," *Physical Review*, Vol. 94, No. 3, pp. 511-525, 1954.
- [29] Bassanini, P., C. Cercignani, C. Pagani, "Influence of the Accommodation Coefficient on the Heat Transfer in a Rarefied Gas," *International Journal of Heat and Mass Transfer*, Vol. 11, pp. 1359-1369, 1968.
- [30] Lees, L., C.Y. Liu, "Kinetic-Theory Description of Conductive Heat Transfer from a Fine Wire," *Physics of Fluids*, Vol. 5, No. 10, pp. 1137-1148, 1962.
- [31] Hurlbut, F., "Note on Conductive Heat Transfer from a Fine Wire," *Physics of Fluids*, Vol. 7, No. 6, pp. 904-906, 1964.
- [32] Lord, R., "Effect of Incomplete Accommodation on Transition Regime Heat Transfer and Shear," *Physics of Fluids*, Vol. 11, No. 8, pp. 1830-1831, 1968.
- [33] Sherman, F., "A survey of experimental results and methods for the transition regime of rarefied gas dynamics," *Rarefied Gas Dynamics*, pp. 228-260, 1963.

- [34] Bird, G. "Direct Simulation and the Boltzmann Equation," *Physics of Fluids*, Vol. 13, No. 11, pp. 2676-2681, 1970.
- [35] Ratzel, A., Simpson, C. "Heat Loss Reduction Techniques for Annular Solar Receiver Designs," SAND78-1769, Albuquerque, NM, Sandia National Laboratories, 1978.
- [36] Dushman, S., *Scientific Foundations of Vacuum Technique*, J.M. Lafferty, ed., John Wiley and Sons, Inc., New York, 1962.
- [37] Dudley, V., Kolb, G., Sloan, M., and Kearney, D. "Test Results: SEGS LS-2 Solar Collector," SAND94-1884, Albuquerque, NM, Sandia National Laboratories, 1994.
- [38] Bird, R., W. Stewart, E. Lightfoot, *Transport Phenomena*, John Wiley & Sons, New York, 2002.
- [39] Mason, E.A., S.C. Saxena, "Approximate Formula for the Thermal Conductivity of Gas Mixtures," *The Physics of Fluids*, Vol. 1, No. 5, 1958.
- [40] O'Shea, S., R. Collins, "An experimental study of conduction heat transfer in rarefied polyatomic gases," *International Journal of Heat and Mass Transfer*, Vol. 35, No. 12, pp. 3431-3440, 1992.
- [41] Beikircher, T., W. Spirk, "Analysis of Gas Heat Conduction in Evacuated Tube Solar Collectors," *Journal of Solar Energy Engineering*, Vol. 118, pp. 156-161, 1996.
- [42] Dieck, R. H., *Measurement Uncertainty: methods and applications, 4th ed.*, The Instrumentation, Systems, and Automation Society, North Carolina, 2007.
- [43] Helton, J.C., F.J. Davis, "Latin hypercube sampling and the propagation of uncertainty in analyses of complex system," *Reliability Engineering and System Safety*, Vol. 81, pp. 23-69, 2003.
- [44] MATLAB version 2010b, Natick, Massachusetts: The Mathworks, Inc., 2003.
- [45] Stein, M. "Large sample properties of simulations using latin hypercube sampling." *Technometrics*. Vol. 29, No. 2, pp. 143-151, 1987. Correction, Vol. 32, p. 367.
- [46] Richard Perkins, NIST scientist, personal communication 4 May 2011.
- [47] Klein, S. A. (2002). *Engineering Equation Solver (EES) for Microsoft Windows Operating System: Commercial and Professional Versions*. Madison, WI: F-Chart Software.
- [48] Liley, P.E., P.D. Desai "Thermophysical Properties of Refrigerants," ASHRAE, 1993, ISBN 1-1883413-10-9.
- [49] Maxwell, J.C. *The Scientific Papers of James Clark Maxwell*, Vol. 2, Cambridge University Press, London and New York, 1890.
- [50] Rader, D. J., W.M. Trott, J.R. Torczynski, J.N. Casteñeda, T.W. Grasser, "Measurements of Thermal Accommodation Coefficients," SAND2005-6084, Albuquerque, NM and Livermore, CA, Sandia National Laboratories, 2005.
- [51] National Institute of Standards and Technology, [www.nist.gov](http://fluidproperties.nist.gov/thermal.html), 8 May 2011.
<http://fluidproperties.nist.gov/thermal.html>
- [52] National Institute of Standards and Technology, [www.nist.gov](http://nist.gov/calibrations/upload/sp250-49.pdf), 8 May 2011.
<http://nist.gov/calibrations/upload/sp250-49.pdf>

- [53] Burkholder, F., C. Kutscher, "Heat Loss Testing of Solel's UVAC3 Parabolic Trough Receiver," National Renewable Energy Lab Technical Report NREL/TP-550-42394, January 2008. Available electronically at <http://www.nrel.gov/csp/troughnet/pdfs/42394.pdf>
- [54] Burkholder, F., C. Kutscher, "Heat Loss Testing of Schott's 2008 PTR70 Parabolic Trough Receiver," National Renewable Energy Lab Technical Report NREL/TP-550-45633, May 2009. Available electronically at <http://www.nrel.gov/csp/troughnet/pdfs/45633.pdf>
- [55] Dreyer, S., P. Eichel, T. Gnaedig, Z. Hacker, S. Janker, T. Kuckelkorn, K. Silmy, J. Pernpeinter, E. Luepfert, "Heat Loss Measurements on Parabolic Trough Receivers," Proceedings of the SolarPaces Conference, Perpignan, France, September 21-24, 2010.
- [56] Incropera, F., D. Dewitt, Introduction to Heat Transfer, John Wiley & Sons, New York, 2002.
- [57] Moffat, R.J., "Some Experimental Methods for Heat Transfer Studies: Thermocouple Theory and Practice," *Experimental Fluid and Thermal Science*, Vol. 3, pp. 14-32, 1990.
- [58] Montgomery, D., G. Runger, Applied Statistics and Probability for Engineers. John Wiley & Sons, Inc. New York. 1994.
- [59] Poulter, K.F., M.J. Rodgers, P.J. Nash, T.J. Thompson, M.P Perkin, "Thermal transpiration correction in capacitance manometers," *Vacuum*, Vol. 53, No. 6, pp. 311-316, 1983.
- [60] Nuclear Regulatory Commission, www.nrc.gov, 9 May 2011.
http://www.nrc.gov/reading-rm/doc-collections/nuregs/staff/sr1805/15_Explosion_Calculations.xls
- [61] Kraussold, H. "Wärmeabgabe von Zylindrischen Flüssigkeitsschichten bei natürlicher Konvektion," *Forsh Hft. Ver. Dt. Ing.*, 5 (4), 186-191, 1934.
- [62] Price, H., "A Parabolic Trough Solar Power Plant Simulation Model," National Renewable Energy Laboratory Technical Report, NREL/CP-550-33209, January 2003. Available electronically at <http://www.nrel.gov/docs/fy03osti/33209.pdf>
- [63] Turchi, C., "Parabolic Trough Reference Plant for Cost Modeling with the Solar Advisor Model (SAM)," National Renewable Energy Laboratory Technical Report, NREL/TP-550-47605, 2010. Available electronically at <http://www.nrel.gov/docs/fy10osti/47605.pdf>
- [64] NREL Reference Trough Plant and Comparisons via Cost Model SAM-2010-04-12, July 2011, <https://www.nrel.gov/analysis/sam/templates.html>

Appendix A – Review of transition regime experimental results

Year, ref.	Title	Authors	Geo. CC, CS, PP	R _o /R _i or gap	Gases	Knudsen number range	T _{1iss} /T _{cool} - 1	Accommodation coefficient, α		Compares exptl. data to analytic method?	Funded by	Comments
								Hot surf.	Cold surf.			
2011	Transition Regime Heat conduction of Argon/Hydrogen and Xenon/Hydrogen Mixtures in a Parabolic Trough Receiver	Burkholder, F. et al.	CC	1.7 ratio 2.5 cm gap	inert gases, H ₂ , H ₂ - inert mixtures	2e-5 – 25 (i.d.) 5e-5 – 60 (gap)	0.5-0.9	0.3-1	0.3-1	yes	NREL	
1898	On Conduction of Heat by Rarefied Gases ^a	Smoluchowski de Smolan, M.	CC	1.4 ratio 1 mm gap	air, H ₂	2e-5 - 14 (H ₂ , i.d.) 1e-4 - 66 (H ₂ , gap) 2e-5 - 9 (air, i.d.) 1e-4 - 43 (air, gap)	0.1	0.3 (H ₂) 1 (air)	0.3 (H ₂) 1 (air)	Yes, derives temperature jump method and uses it to quantify the temperature discontinuity coefficient. Says this temperature jump method compares favorably to data taken by Mr. Brush.	?	Study focuses on the conduction of heat at very low pressures, specifically investigating the possibility of a temperature discontinuity at the gas/solid surface, necessitating the need for a temperature discontinuity coefficient (TDC). It's possible to remove convection effects by rarefying the gas (gas viscosity remains the same, but the density dependent buoyancy force decreases.) Experimentally he heats a mercury thermometer in a partially evacuated cylinder to 100°C and then plunges it in an ice bath and measures the amount of time for the thermometer temp. to decrease to a certain value. Investigates presence of temperature discontinuity by similar test in cylinders of different radii. Analytically derives value for the TDC. Ratio of TDC to the mean free path is constant. Finds satisfactory agreement between his theory and experiments by Mr. Brush. Explains the temperature discontinuity using the kinetic theory of gases in the following way: the temperature at any point in a gas depends on the mean energy of the gas molecules at that point, and near a solid surface the mean energy of the molecules will not be that of the surface, even if the rebounding molecules completely accommodate to the temperature of the surface due to the incoming molecules with higher energy. Is surprised by how much larger the ratio of the TDC to mean free path is for H ₂ vs air. Suspects it has something to do with the differences in masses of the impacting molecules and the molecules of the surface.

Year	Title	Authors	Geo. CC, CS, PP	R _w /R _i or gap	Gases	Knudsen number range	T _{fil} /T _{cool} - 1	Accommodation coefficient, α		Compares expt. data to analytic method?	Funded by	Comments
								Hot surf.	Cold surf.			
1914	The Dissociation of Hydrogen into Atoms. Part I. Experiment al ¹⁰	Langmuir, Irving and Mackay, G.M.J.								No – but see paper below.		Purpose of paper is to explore at what temperature and pressures molecular heat conduction by H ₂ drastically increases due to the dissociation of H ₂ into hydrogen atoms. For all pressures studied it appears to start between 1500 and 2000 K. This study assumed that H ₂ next to the wire was dissociating at the wire temperature.
1915	The Dissociation of Hydrogen into Atoms. Part II. Calculation of the Degree of Dissociation and the Heat of Formation ^c	Langmuir, Irving	CC	992 ratio	H ₂ N ₂	3e-3 – 1000? (i.d.)	1 – 6 (estimate b/c bulb temp. not stated)	?	?	Yes – provides two methods for calculating the gas temperature about one mean free path away from wire. These two methods give similar temperature drops. However, method requires knowing the total heat conducted through the apparatus first.	Research Laboratory, General Electric Company	At atmospheric pressure saw effect of convection in bulb, but at 200 torr convection effects disappeared. Data from Part I support a large gas temperature discontinuity at the wire surface. Method of temperature drop developed by Smoluchowski are only for small temperature differences and whose radii of curvature are large compared to the mean free path. Present experiments deal with very large temperature drops (1000°C or more) and very small inner radii. Develops simpler less rigorous method, based on Smoluchowski's reasoning. Because outer radius is so much larger than inner radius, discounts temperature discontinuity at outer wire. Assumes Maxwell's velocity distribution function to hold, but acknowledges that especially for small accommodation coefficients this distribution function could be very complex. However, error associated with using it is small. Shows that the temperature jump is directly proportional to the heat flux and the square root of the gas temperature one mean free path away from wire, and inversely proportional to the accommodation coefficient and the gas pressure. Shows experimental evidence of hydrogen dissociating beyond 1200 K. Performs some experiments of heat conduction through H ₂ and N ₂ mixtures at 600 torr at temperatures between 1800 and 3000 K.
1933	The Effect of Accommodation on Heat Conduction Through Gases ^b	Dickens, B.G.	CC	89 Ratio	H ₂ , argon, air, others	5e-4 – 0.005 (H ₂ , i.d.) 0.005-0.05 (Air, i.d.) 0.02 – 0.1 (Ar, i.d.)	0.07	0.36 H ₂ 0.9 Air 0.89 Ar	assm. 1	No, but presents temp. jump method	?	The goal of this paper is to calculate gas thermal conductivity using a platinum wire in a glass cylinder. Because convection effects confound heat loss data at higher pressures, calculates heat loss at lower pressures and then corrects for accommodation and temperature jump.
1935	The Effect of Temperature on the Thermal Conductivity and the Accommodation Coefficient of Hydrogen ^e	Gregory, H.S.	CC	191 Ratio	H ₂	0.002-0.04 (i.d.)	0.03	0.23-0.28 from 0°C to 300°C	assm. 1	No, but presents a temp. jump method.	?	The goal of this paper is show how thermal conductivity and accom. coefficient of H ₂ change with temp. Data shows thermal cond. severely tapering off at 300°C. Uses temp. jump method similar to Dickens to calculate k. See Gregory 1936 for an expansion of Smoluchowski relation to temp. jump for other than monatomic gases
1954	A Comparative Study of Accommodation Coefficients by the Temperature Jump and Low Pressure Methods and Thermal Conductivities of He, Ne, and CO ₂ ^f	Thomas, L.G. and Golike, R.C.	CC	63 ratio	He Ne CO ₂	25 (L.P., i.d.) 0.005 (TJ, i.d.)	0.6 (LP) 0.2 (TJ)	0.17 (He) 0.42 (Ne -40°C) 0.31 (Ne -210 °C) 0.78 (CO ₂)	assm. 1	No, but derives temp. jump method	Office of Ordnance Research and U.S. Office of Naval Research	Goal of paper is to compare α attained by low pressure and temperature jump methods on same material, gas, and test stand. Uses platinum wire. Shows that accommodation increases to a steady state value after 400 minutes after flashing. Shows twice α for a material that wasn't flashed and baked first for He. Need to know filament surface condition. Best reproducible data when surfaces were baked, flashed, and let stand for 12 hours. α decreases slightly with increasing temperature.

Year	Title	Authors	Geo. CC, CS, PP	R _o /R _i or gap	Gases	Knudsen number range	T _{Hot} /T _{Cold} - 1	Accommodation coefficient, α		Compares expt. data to analytic method?	Funded by	Comments
								Hot surf.	Cold surf.			
1959	Heat Loss from Very Thin Heated Wires in Rarefied Gases ⁷	Bomelburg, H.	CC	>10,000 ratio	air	1e-3 – 500 (i.d.)	0.1	air, so close to 1	assm. 1	No	Ballistic Research Laboratory	Wollaston wire suspended in bell jars. Measured resistance and current through wire.
1965	Heat Conduction in Rarefied Gases between Concentric Cylinders ¹¹	Dybbys, A. and Springer G.S.	CC	326	He, Ne, Ar	50-0.03 (i.d.)	0.023	0.2-0.7	assm. 1	Yes - Data compares favorably to Lees and Liu moment method modified by Hurlbut.	Office of Naval Research Advanced Research Projects Agency	Goal is to evaluate Lees and Liu moment method by comparing it to their data. They are using Hurlbut's extension of Lees and Liu to look at incomplete accommodation on the inner radius. Note strong sensitivity of Knudsen number to mean free path and molecular diameter.
1966	Heat Transfer from a Sphere to Rarefied Gas Mixtures ¹	Mikami, H.; Endo, Y.; Takashima Y.	Sphere to ambient	∞	H ₂ , N ₂ , He H ₂ -N ₂ mixtures He-N ₂ mixtures	0.4-0.008 (sphere d.)	0.03	0.3 (H ₂) 0.35 (He) 0.8 (N ₂) Uses special method for mixtures	1 (to ∞)	Yes – Generates expression for Nu = f(Kn, α) and finds mixed gas k and μ and α . Use Liu and Lees method to calculate heat transfer.	Research Laboratory of Nuclear Reactor, Tokyo Institute of Technology	Uses Liu and Lees method to make an expression for the Nusselt number as a function of the Knudsen number and the accommodation coefficient on the sphere surface. Uses Wilke and Mason and Saxena to determine the mixture thermal conductivity. Uses a mixed thermal accommodation coefficient derived from the energy balance that includes mole fraction, pure species accommodation coefficient, and molecular masses. Their method matches data to within 10% in the indicated Knudsen range, with more scatter closer to continuum.
1967	Heat Transfer from Circular Cylinders at Low Reynolds Number. II Experimental Results and Comparison with Theory ¹	Aihara, Y.; Kassoy, D.R.; Libby, P.A.	Wire to ambient	∞	He, N ₂ He-N ₂ mixtures	Kn<0.03 (wire d.)	0.1-0.25	0.8-0.9 (N ₂) 0.03 (He) For mixtures uses mol fraction avg.	1 (to ∞)	Yes – Finds expression for Nusselt based on flow velocity, Re, Pr, Kn, and temperature difference.	Air Force Office of Scientific Research	The initial goal of work was to estimate the amount of a lower molecular weight, higher thermal conductivity gas in a second gas with higher molecular weight, lower thermal conductivity by the amount of heat lost from a wire immersed in turbulent flow of the gases. Their heat loss results were much lower than expected – thermal slip due to much lower α of helium was decreasing heat conduction. Developed theory to accommodate this slip and showed how experimental results fell into their slip limits. Claim accuracy to 5%.
1967	Heat Transfer and Density Distribution Measurements in the Transition Regime ⁸	Teagan, W. and Springer, G.S.	PP	0.13 cm (gap)	Ar, N ₂	0.05-4 (gap)	0.03	0.83	0.83	Yes – compares data to Gross and Ziering 4 and 8 moment models, Lees 4 moment model, and Wang-Chang Uhlenbeck 2 nd approximation. 4 moment models agree with data by 2%, WCU by 5%, and 8 moment models off by 10-20%. Has to apply a correction factor to compare Lees Liu results to nitrogen.	Advanced Research Projects Agency (Ballistic Missile Defense Office)	This report summarizes Teagan's Ph.D. work. He experimentally determines heat flux and density distributions for rarefied gases at rest between two unequally heated parallel plates. "The experimental results for argon were compared with the analytical results of Wang Chang and Uhlenbeck, Gross and Ziering, and Lees. In computing these results the thermal accommodation coefficient measured in the free molecule regime was used with the assumption that its value remained constant over the entire pressure region. The average agreement between heat conduction data and the results for the four moment methods of Lees and Gross-Ziering was about 2%, while the measured density profiles agreed with the results of the analyses within 3%. Both heat conduction and density distribution data differ by ~10-20% from the results of Gross-Ziering's eight-moment method."

Year	Title	Authors	Geo. CC, CS, PP	R _s /R _i or gap (cm)	Gases	Knudsen number range	T _{hot} /T _{cold} - 1	Accommodation coefficient, α		Compares expt. data to analytic method?	Funded by	Comments
								Hot surf.	Cold surf.			
1968	Experimental Study of Rarefied Argon Contained between Concentric Cylinders ¹	Sheldon, D.B and Springer, G.S.	CC	26	Ar	1e-3 - 5 (i.d.)	0.03	0.9	assm. 1	Yes - Compares experimentally derived gas temperature distributions in the transition, temperature jump, and continuum regimes with the temperature distribution predicted by the Lees and Liu, temp. jump, and continuum methods.	Advanced Research Projects Agency (Ballistic Missile Defense Office)	Paper summarizes Sheldon's Ph.D. work. The goal of this work was to measure experimentally the temperature distribution between concentric cylinders in the transition, temperature jump, and continuum regimes and compare to distributions predicted by Lees and Liu, temperature jump, and continuum methods. He only uses argon. Does not present heat conduction results. A moveable wire probe in the annulus measured the temperature at a given radial position. The temp. difference between the cylinders was about 12°C. Makes the following assumptions crucial to comparing data and Lees and Liu prediction in the transition regime: 1) the probe was in the free molecule regime, 2) gas-surface interaction could be described by Knudsen's accommodation coefficient, and 3) the thermal accommodation coefficients at the probe and inner cylinder remained constant. The abstract states: "For Kn > 0.5 agreement between the experimental and calculated [Lees and Liu] equilibrium probe temperatures was within -2.5%. Equilibrium probe temperatures were also compared to local gas temperatures calculated by Smoluchowski's temperature jump approximation, and for Kn < 0.15 agreement was found to be within 1%. In the range of 0.15 < Kn < 0.5 the results of both the moment method and the temperature jump approximation deviated (in opposite directions) from the data by a maximum of 4%."
1968	Mass Transfer Through Rarefied Gas Between Concentric Spheres ¹	Toei, R. Okazaki, M., Uragami, A., and Takaki, Uji	CS	5 ratio	Air, naphthalene	0.015 - 1.5 (i.d.)	0.08	0.9	0.9	Yes - uses Lees and Liu moment method to predict the partial pressure of each species at certain radial positions and compares this to their experimental data. Also compares measured and estimated sublimation rates.	Kyoto University Chemical Engineering Department Kawakami Memorial Foundation	Goal of work was to use kinetic theory to derive equation of mass transfer under reduced pressures, especially for the transition regime, and compare it with experimental results. Equations derived for a small temperature difference using Lees and Liu moment method. Required distribution functions for the diffusing and non-diffusing species. Most experimental results agree with analytic results to within 10%
1969	Heat Transfer to Cylinders in Nitrogen-Helium and Nitrogen-Neon Mixtures ^N	Baccaglioni, G., Kassooy, D.R., Libby, P.A.	Wire to ambient	∞	Ne, He, N ₂ Ne-N ₂ mixtures He-N ₂ mixtures	Kn < 0.03 (wire d.)	0.1-0.25	0.8-0.9 (N ₂) 0.03 (He) 0.1 (Ne) For mixtures uses mol fraction	1 (to ∞)	Yes - finds correlation for Nu same as Aihara in 1967, but new derivation for β. B shows good agreement for N ₂ -Ne mixtures but not N ₂ -He mixtures	Advanced Research Projects Agency (Project Defender)	Mixtures require the calculation of a special slip parameter β. Heuristic rule based on molar averaging by Aihara in 1967 yields analytic results that compare well with experimental results. This paper carries out a more careful and classical derivation of β. Considers nitrogen-neon mixtures because N ₂ and Ne have similar molecular weights, but Ne has an α ≈ 0.1 while N ₂ ≈ 0.9 on tungsten. Uses the same experimental technique of Aihara. N ₂ adsorbed on tungsten wire always affect α for pure species in their tests. One possible reason for the non-agreement of present β theory and experimental results may be non-equilibration between the species temperatures as shown by Goldman and Sirovich 1967.

Year	Title	Authors	Geo. CC, CS, PP	R ₀ /R ₁ or gap (cm)	Gases	Knudsen number range	T _{hot} /T _{cold} - 1	Accommodation coefficient, α		Compares expt. data to analytic method?	Funded by	Comments
								Hot surf.	Cold surf.			
1971	Heat Transfer to Cylinders in Binary Gas Mixtures ^o	Baccaglioni, G., Miller, D., Libby, P.	Wire to ambient, but analyzed as CC	100	Ar-He mixtures	Kn<0.03 (wire d.)	0.2	0.15 (He) 1 (Ar)	1 (to ∞)	Yes – compares temperature slip predicted by extension of Lees-Liu moment method to that given by data	Advanced Research Projects Agency	<p>Paper summarizes Baccaglioni's Ph.D. work. Purpose of this paper is to provide more heat loss data for mixtures of monatomic gases (Ar-He) and the second is to assess non-equilibrium thermodynamic behavior. They do this by extending the Lees-Liu moment method for binary mixtures. They use this method to calculate β which they show to give good agreement with their data. One conclusion from 1969 paper is that when the ratio of molecular weights in a binary mixture is ≈ 1, then the calculation procedure for β of the Baccaglioni 1969 paper is sufficient. However, when the weights are very different, then it isn't accurate.</p> <p>In low Re number flow, the flow field next to the wire is dominated by conduction. This observation led them to believe that they could address this problem as a heat conduction problem between two concentric cylinders. To evaluate the collision intervals use an inverse fifth power force law, where one factor in it is based on coefficient for the unlike molecules, and viscosity coefficients for the like molecules. Outer wall is assumed to perfectly accommodate all molecules. Assumes small temperature differences, but more general equations given first. Equations only applicable to monatomic gases, but could apply to polyatomic gases assuming internal degrees of freedom not important. Solve equations using the Runge-Kutta-Gill procedure with a very fine mesh. "Typically, the average temperature of the poorly accommodated helium relaxes to the temperature of the argon and to the continuum solution only after a distance of order 100 mean free paths."</p> <p>"Generally, we have found that slip effects increase with decreasing thermal accommodation, decreasing pressure, increasing disparate mass ratio, and with increasing concentration of the lighter component."</p> <p>Their accommodation coefficients were determined by experiments with pure gases.</p>
1971	Density Distribution Measurements in Rarefied Gases Contained Between Parallel Plates at High Temperature Differences ^p	Alofs, D., Flagan, R., Springer, G.S.	PP	2.28 cm	He, N ₂	0.03-0.6 (mfp at center plane, and gap distance)	2.7	0.58 He 0.82 N ₂	0.4-0.58 He 0.7-0.82 N ₂	Yes, compares He density results to Lees and Liu method modified for incomplete accommodation at the plates. Largest difference between theory and experiment is about 7% at the hot plate.	United States Atomic Energy Commission	<p>Summarizes Alofs's Ph.D. work. Available data for heat transfer and density distributions between parallel plates are for small temperature differences. Objective of this investigation was to measure local densities of rarefied gases at rest contained between plates at high temperature differences (T_h/T_c = 1 = 2.7). Used luminescence of high energy electrons passing through gas to estimate gas density. Heat transfer measurements made in the free molecule region Kn >= 10 to get accommodation coefficients. Did not bake apparatus during experiments.</p> <p>Helium density measurements compare well to Lees & Liu theory at low pressures and continuum at high pressures. Only compares N₂ data to continuum.</p> <p>Describes work that he could compare data to, but Cercignani and Willis BGK solutions only for complete accommodation. Modifies Lees and Liu method for incomplete accommodation at both surfaces.</p>

Year	Title	Authors	Geo. CC, CS, PP	R _s /R _c or gap (cm)	Gases	Knudsen number range	T _{hot} /T _{cold} - 1	Accommodation coefficient, α		Compares expt. data to analytic method?	Funded by	Comments
								Hot surf.	Cold surf.			
1973	Heat Conduction in Binary Gas Mixtures Between Concentric Cylinders ⁰	Yeh, B.T., Frohn, A.	CC	520 ratio	He, Ar, Kr, Ne, Xe He-Ar mixtures He-Kr Mixtures	1e-3 - 10000 (He, i.d.) 1e-3 - 5000 (Kr, i.d.)	Bath at 26°C, but does not state wire temp., but analysis for small temp. dif.	0.38 (He) 0.65 (Ne) 0.92 (Ar) 0.96 (Kr) 0.97 (Xe)	assm. 1	Yes, uses Lees-Liu moment method to predict heat conduction at small temperature differences, then expands Lees-Liu for monatomic gas mixtures at small temperature differences.	Institut für Allgemeine Mechanik	Summarizes Yeh's Ph.D. work. The molecular heat conduction between concentric cylinders in mixtures of monatomic gases is investigated theoretically and experimentally. Analytic results are obtained for small temperature differences. The heat conduction coefficient in the continuum regime agrees with Chapman-Enskog result for binary mixtures. Uses Maxwell's moment method for analysis, following Lees and Liu. Analytic results agree well with pure species monatomic gases and binary mixtures in the free-molecular, transition, and continuum regimes.
1976	Heat Transfer in Simple Monatomic Gases and in Binary Mixtures of Monatomic Gases ² and Heat Transfer in Binary Mixtures of Monatomic Gases for High- Temperatur e Differences and for a Large Knudsen Number Range ³	Braun, D., Frohn, A.	PP	1 - 20 mm (gap)	He, Ar, Kr, Xe presents He-Ar mixtures	1e-4 - 10 (gap)	0.2-1.0	0.29 (He on SS at 473 K) 0.71 (Ar on SS at 473 K)	0.41 (He on SS at 273 K) 0.75 (Ar on SS at 273 K)	Yes, uses linearized and non-linearized four moment (single species) and eight moment(two species) method of Lees-Liu. The linearized analytic solution deviates significantly (10-25%) from the experimental data depending on the pressure regime. The non-linear equations were solved numerically and agree well with results. Numerical results can be duplicated to within 0.2% for a $\Delta T = 100$ K by an involved analytic method that he presents.	Bundesmini- sterium der Verteidigung	Summarizes Braun's Ph D. work. Investigates conductive heat transfer in pure and binary mixtures of monatomic gases for temperature differences up to 300 K for all pressure regimes. Theoretical results were obtained with the four moment (pure species) and eight moment (two species) solutions of the Boltzmann equation. Experiments were performed in a heat-transfer cell with horizontal flat plates to avoid free-convection currents. Validated test stand by using it to calculate thermal conductivity of pure species in the continuum. Accommodation coefficients calculated for an average temperature in the free molecular regime. - plots show surfaces have unequal accommodation coefficients. Linearized Lees-Liu moment theory shows heat conduction errors of >10% in the free molecular regime, 10% < error <= 25% in the transition and continuum regions for $\Delta T = 200$ K. It's worse for increasing temperature difference. They do show good model agreement with experiment for pure species and binary mixtures at high temperature difference, but this is by numerically solving the non-linear moment equations. Gives an involved approximate analytic solution to the numerical solution. Also measured and modeled density distribution between the plates - model shows good agreement. Both show separation of the gas mixture components as a function of the distance ratio between the hot and cold plates. For He/Ar, and $\Delta T = 200$ K and $Kn \approx 0.6$, this separation of the components is about 7% at $9/10^{th}$ of the way toward the hot plate.
1978	Heat Loss Reduction Techniques for Annular Solar Receiver Designs ¹	Ratzel, A.C., Simpson, C.E.	CC	1.7 ratio 1 cm (gap)	air N ₂ , Ar, Kr, Xe, SF ₆ , Freon C- 318	3e-5 - 0.3 (air, i.d.) 1e-4 - 1 (air, gap) other gases < 1e-5 and $\approx 1e-3$ (only tested other gases at 1e5 and 6.6e3 Pa)	0.6	0.7 - 1, but it is unclear whether analysis uses anything other than $\alpha =$ 1	0.7 - 1, but it is unclear whether analysis uses anything other than $\alpha =$ 1	Yes - compares data to temperature jump method they say Dushman recommends - agrees in transition regime but off by 10% in continuum region	United States Department of Energy	Undertook analytical and experimental work to understand molecular conduction and natural convection in annular receiver geometries. Looked at evacuating annular space, over sizing annular space under partial vacuums and use of gases other than air in annulus. Total heat loss reductions of 10 - 50% depending on method, with evacuation of the annulus the largest reduction. Introduces 1-dimensional heat loss model of HCE that includes a temperature jump molecular conduction model for concentric cylinders. Model takes one accommodation coefficient.

Year	Title	Authors	Geo. CC, CS, PP	R _o /R _i or gap (cm)	Gases	Knudsen number range	T _{Hot} /T _{Cold} - 1	Accommodation coefficient, α		Compares expt. data to analytic method?	Funded by	Comments
								Hot surf.	Cold surf.			
1980	Free Molecule Thermal Conduction in Concentric Tubular Solar Collectors ^U	Harding, G.L.; Window,B.	CC	1.2 ratio 2.6 mm (gap)	H ₂ , He, Ar, CO, N ₂ , and H ₂ O	0.005-0.7 (N ₂ , i.d.) 0.04 – 7 (N ₂ , gap) 0.007 – 1.1 (H ₂ , i.d.) 0.06 – 9.7 (H ₂ , gap)	0.4	for selective surface: 0.85 Ar 0.7-0.8 N ₂ 0.4-0.5 H ₂ 0.4-0.5 He He increases with increasin g temp.	0.84 Ar 0.67 CO 0.35 He 0.27 H ₂ 0.68 N ₂ 1.15 H ₂ O? all values decrease with increasin g temp.	Compares experimental accommodatio n coefficients with those predicted by Baule model, and a Van der Waals coefficient – says they are correlated by no exact correlation. Uses a conduction formula for low pressures that uses an inner and outer accommodatio n coefficient.	Sydney University Research Centre Government of New South Wales Saudi Arabian interests	Determines thermal conduction between two concentric tubes for low pressures of various gases. Found the temperature dependent accommodation coefficients for the gases on a glass surface, a sputtered copper surface, and a metal-carbon selective surface. The accommodation coefficient for the selective surface was close to 1 for all gases except helium and hydrogen. Outer surface was borosilicate glass and the inner cylinder was either borosilicate glass, a 300 nm thick sputtered copper surface, or a stainless-steel-carbon selective surface.
1984	Experimenta l Study of Heat Exchange in a Moderately Rarefied Gas ^V	Kulev, A.N. Shestakov, A.M Borisov, S.F. Semenov, Y.G.	CC	66 ratio	Xe, N ₂ , CO ₂ , NH ₃	0.01 – 1	0.0007	1	1	Yes, compares heat conduction of all gases to Lees-Liu and BGK model by Bassanini, Cercignani, and Pagani (1968)	Ural State University, Sverdlovsk	One reason for the study is the lack of experimental data for the transition between free molecular and continuum regimes, especially for multiatomic gases. Compares Lees-Liu moment method and Bassanini et al. BGK method for small temperature differences to data. Lees-Liu on the same line as the experimental data, BGK about 10% above for Xe (monatomic) data, but over approximates q/q _{fm} for all the other gases. Proposes a modified Lees-Liu solution for small temperature differences. States that this equation compares well, but does not show it graphically. Article translated from Inzhenerno-Fizicheskii Zhurnal
1984	Investigatio n of heat transfer in rarefied gases over a wide range of Knudsen numbers ^W	Semyonon, Y.G., Borisov, S.F., Suetin, P.E.	CC	2 cells: 260 ratio 65 ratio	He, Ne, Ar, Kr, Xe, D ₂ , N ₂ , Air, CO ₂	states full range, but does not display data as function of either pressure or Knudsen number, instead a non- dimensional -ized value A based on Bassanini et al. (1968) moment solution of BGK equation	0.0003	has many, but some notables: H ₂ 0.28 (77K) 0.24 (300 K) He 0.4- 0.5 Ar, Kr, Xe 1 D ₂ 0.45- 0.48	assm. 1	Yes, data agrees well with a linearized BGK moment method	?	Presents experimental results on the heat conduction of rarefied gases using a transient hot-wire technique in the case of small temperature perturbations from the free molecular to the continuum regimes. “ While for the continuum regime it is frequently sufficient to assume the equality of gas and surface temperatures as a boundary condition, for the intermediate and molecular regimes the boundary conditions become more complicated and it is necessary to take into account the nature of energy transfer between the gas molecules and the surface. Thus, the main problem in the description of heat transfer of moderately and highly diffused gases consists in the assignment of boundary conditions.”

Year	Title	Authors	Geo. CC, CS, PP	R _s /R _i or gap (cm)	Gases	Knudsen number range	T _{hot} /T _{cold} - 1	Accommodation coefficient, α		Compares expt. data to analytic method?	Funded by	Comments
								Hot surf.	Cold surf.			
1992	An experimental study of conduction heat transfer in rarefied polyatomic gases ^x	O'Shea, S.J. and Collins, R.E.	CC	1.1	He, benzene, n-hexane	1e-3 – 100 (gap)	0.2	0.88 benzene 0.87 n-hexane	0.87 benzene 0.914 n-hexane	Yes, compares data favorably to a simple empirical fit given by Springer and the Direct Simulation Monte Carlo (DSMC) method. Monte Carlo results start deviating by more than 20% at Kn < 0.1	His Royal Highness Prince Nawaf bin Abdul Aziz of the Kingdom of Saudi Arabia through the Science Foundation for Physics within the University of Sydney	Presents experimental and Monte Carlo simulation results for conduction heat transfer of benzene and of n-hexane over the whole transition range of Knudsen number. They had limited control over surface conditions. Sydney University developed an evacuated tube collector. In unconcentrated sunlight it has stagnation temperatures of 300°C. They want to prevent stagnation temperatures by including a gas in the annulus that adsorbs to the selective surface absorber at low temperatures (thereby evacuating the annulus) but desorbs from the surface at temperatures approaching stagnation, thereby serving as a molecular conduction path to that will conduct heat away from the overheating absorber. During this adsorption, desorption process the Kn number will fluctuate between 100 and 0.1. They define their Kn number by the radial gap. Generally difficult to solve molecular transport problems in the transition regime. Previous experimental heat conduction studies in the transition regime have been limited to simple molecules such as N ₂ and monatomic gases. Uses Bird's direct simulation Monte Carlo Method to analyze the polyatomic gases in transition regime – agrees well from Kn = 100 up to Kn = 0.1 then as it nears continuum up to 25% off. Monte Carlo simulation uses a relaxation model, based on number of collision, to equilibrate rotational and vibrational internal energy states. Uses accommodation coefficients to model gas/boundary collisions. Does not distinguish between internal and translational accommodation coefficients.
1993	Thermal Gap Conductance of Conforming Surfaces in Contact ¹	Song, S., Yovanovich, M.M., Goodman, F.O.	PP	Plates are in contact, so defines an effective gas thickness, δ that is a function of the surface roughness and the mean plate separation	He, Ar, N ₂	Roughly 3e-3 - 2	0.01 – 0.2	for both surfaces, stainless steel smooth and bead-blasted, and nickel smooth and bead-blasted: He 0.55 Ar 0.90 N ₂ 0.78		Yes, presents an Interpolated Simple Kinetic Theory Model which utilizes the temperature jump approximation and Yovanovich's effective gap thickness model.	International Business Machine Corporation (?)	Study looks at heat transfer through gas layers of between two microscopically rough surfaces. Uses the temperature jump approximation and an effective gap distance. Model uses two dimensionless parameters to quantify molecular heat conduction across gap: G, which is the ratio of the rarefied gas resistance to the continuum resistance, and M ² which represents the degree of gas rarefaction. The rarefaction parameter M ² is a modified mean free path (mfp) divided by the gap thickness. The mfp is modified by α at each surface, the ratio of specific heats, and the Prandtl number. Compares model predictions to experiment for relatively small temperature differences. Model agrees well in continuum regime but can differ by an order of magnitude in the transition and free-molecule regimes. Uses the same accommodation coefficient for all temperatures and all surfaces.
1995	Thermal conductivity and accommodation coefficient of spin-polarized atomic-hydrogen gas ²	Yoo, M.J., Greytak, T.J.	CC	5 ratio, 6 mm gap	H	unclear, but some data in transition regime, defines Kn number by the gap distance, not the inner diameter cylinder	0.05-0.1 (ΔT order of 20-40 mK)	Accommodation coefficient on for spin-polarized H upon saturated superfluid He films for 0.2 < T < 0.4 K is given by the expression α = (0.56±0.06)*T	Uses an interpolation model where K _{sat} (T,n) = Q _{sp} /ΔT and K _{sat} = (1/K _{cont} +1/K _{free}) ⁻¹	National Science Foundation	Study focuses on finding the effective thermal conductivity for atomic hydrogen gas between concentric cylinders coated by saturated super-fluid He films. Unclear exactly what pressures were used but some data were in free-molecular and transition regimes. Model agrees within 5% to data.	

Year	Title	Authors	Geo. CC, CS, PP	R ₀ /R ₁ or gap (cm)	Gases	Knudsen number range	T _{Hot} /T _{Cold} - 1	Accommodation coefficient, α		Compares expt. data to analytic method?	Funded by	Comments
								Hot surf.	Cold surf.			
1995	Gas Heat Conduction in Evacuated Flat-Plate Solar Collectors: Analysis and Reduction ^{AA}	Beikircher, T., Benz, N., Spirkel, W.	PP	3 cm (gap)	air, Ar	1e-5 - 1.3 air 1e-5 - 0.01 Ar	0.25	does not state, but for Ar and air close to 1		Yes, presents a modified temperature jump method that can be used with polyatomic gases and gas mixtures. Uses a reduced α to account for different accommodation coefficients at each surface. Derivation applies to small temperature differences.	German Ministry of Research and Technology	Goal of research is to determine experimentally and analytically the molecular heat conduction between an absorber and the casing in an evacuated flat-plate collector. Shows that for small temperature differences the temperature jump method can apply to molecular heat transfer in all pressure regimes. Data agrees well to temperatures-jump theory in the continuum and temperature regimes but outside of error bars in the transition regime by as much as 20% for air. Argon results are only in temperature-jump and continuum regimes. Suggests using Wassiljew relation in the continuum regime for gas mixtures, and then using that thermal conductivity in the temperature jump relation. Reason for gas mixtures is that air will most likely leak in and compromise vacuum. Shows that collectors with inert gases can have less heat loss than collectors with air in them in transition and continuum regimes.
1996	Aerogel and Krypton Insulated Evacuated Flat-Plate Collector for Process Heat Production ^{BB}	Benz, N.; Beikircher, Th.	PP	3.5 cm gap	air, krypton	2e-5 - 230 (gap)	0.23	0.9 (air)	1	Y - modified temperature jump method	German Federal Ministry for Research and Technology and others	Uses a modified temperature jump method by Kennard (Beikircher 95). Looks at gas mixtures in continuum. Uses a reduced α , but unclear what values were used. Model matches data within transition regime within 15% for air. Krypton poor match.
1998	A Modified Temperature-Jump Method for the Transition and Low-Pressure Regime ^{CC}	Beikircher, T., Benz, N., Spirkel, W.	data for plate in tube, but also analyzes CC	10 cm wide plate in 11 cm diameter glass tube	air	1e-4 - 72 using 1.2 cm as the characteristic length	0.40	0.95	0.86	Yes, presents a modified temperature jump method that is adjusted to give the correct free-molecular value for R ₀ = R ₂	?	Proposes a modified temperature jump method for modeling gas heat conduction at arbitrary Kn numbers and for a broad range of geometries. For problems with a single geometric length (PP, CC, CS) the method coincides with 1/Q = 1/Q ₀ + 1/Q _∞ (Sherman's interpolation formula) and Lees and Liu four moment method. This modified method calculates a ΔT_{12} at each wall and a ΔT_{∞} from the Q _∞ solution. For small temperature differences, the temperature dependency of the thermal conductivity and the temperature jumps is neglected and then the formula agrees with Sherman's formula. Method agrees well with data obtained for plate in tube geometry, though still slightly overestimates data as it approaches free-molecular. The mean free path is determined by the average gas temperature and the pressure.

^A Smoluchowski, M.S., "On Conduction of Heat by Rarefied Gases," The London, Edinburgh, and Dublin Philosophical Magazine and Journal of Science, Vol. 46, pp. 192-206, 1898.

^B Langmuir, I., Mackay, G., "The Dissociation of Hydrogen into Atoms. Part I. Experimental." Journal of the American Chemical Society, Vol. 36, pp. 1708-1722, 1914.

^C Langmuir, I., "The Dissociation of Hydrogen into Atoms. Part II. Calculation of the Degree of Dissociation and the Heat of Formation." Journal of the American Chemical Society, Vol. 37, pp. 417-458, 1915.

^D Dickens, B., "The Effect of Accommodation on Heat Conduction Through Gases," Proceedings of the Royal Society of London. Series A, Containing papers of a mathematical and physical character," Vol. 143, p. 517-540, 1934.

^E Gregory, H. "The Effect of Temperature on the Thermal Conductivity and the Accommodation Coefficient of Hydrogen." Proceedings of the Royal Society of London. Series A, Containing papers of a mathematical and physical character, Vol. 149, Issue 866, pp. 35-56, 1935.

^F Thomas, L., Golike, R. "A Comparative Study of Accommodation Coefficients by the Temperature Jump and Low-Pressure Methods and Thermal Conductivities of He, Ne, and CO₂," The Journal of Chemical Physics, Vol. 22, No. 2, Feb. 1954.

^G Bomelburg, H., "Heat Loss from Very Thin Heated Wires in Rarefied Gases," Physics of Fluids, Vol. 2, pp. 717-718, 1959.

^H Dybbs, A., Springer, G. "Heat Conduction Experiments in Rarefied Gases between Concentric Cylinders," Physics of Fluids, Vol. 8, No. 11, pp. 1946-1950.

^I Mikami, H., Endo, Y., Takashima, Y. "Heat Transfer from a Sphere to Rarefied Gas Mixtures," International Journal of Heat and Mass Transfer, Vol. 9, pp. 1435-1448, 1966.

^J Aihara, Y., Kassoy, D., Libby, P. "Heat Transfer from Circular Cylinders at Low Reynolds Numbers. II. Experimental Results and Comparison with Theory," Physics of Fluids, Vol. 10, No. 5, pp. 947-952.

^K Teagan, W., Springer, G. "Heat transfer and density distribution measurements between parallel plates in the transition regime," Report from the Fluid Mechanics Laboratory, Dept. of Mechanical Engineering, Massachusetts Institute of Technology, September 1967.

^L Sheldon, D., Springer, G. "Experimental Study of Rarefied Argon Contained between Concentric Cylinders," Physics of Fluids, Vol. 11, No. 6, pp. 1312-1320, 1968.

^M Toei, R., Okazaki, M., Uragami, A., Takaki, Y., "Mass Transfer Through Rarefied Gas Between Concentric Spheres," Journal of Chemical Engineering of Japan, Vol. 1, No. 2, pp. 125-131, 1968.

^N Baccaglioni, G., Kassoy, D., Libby, P., "Heat Transfer to Cylinders in Nitrogen-Helium and Nitrogen-Neon Mixtures," Physics of Fluids, Vol. 12, No. 7, pp. 1378-1381, 1969.

^O Baccaglioni, G., Miller, D., Libby, P., "Heat Transfer to Cylinders in Binary Gas Mixtures," Physics of Fluids, Vol. 14, No. 11, pp. 2299-2305.

^P Alofs, D., Flagan, R., Springer, G., "Density Distribution Measurements in Rarefied Gases Contained between Parallel Plates at High Temperature Differences," Physics of Fluids, Vol. 14, No. 3, pp. 529-533, 1971.

^Q Yeh, B., Frohn, A., "Heat conduction in binary gas mixtures between concentric cylinders," Physics of Fluids, Vol. 16, No. 6, pp. 801-805, 1973.

^R Braun, D., Frohn, A., "Heat transfer in simple monatomic gases and in binary mixtures of monatomic gases," International Journal of Heat and Mass Transfer, Vol. 19, pp. 1329-1335, 1976.

^S Braun, D., Frohn, A., "Heat transfer in binary mixtures of monatomic gases for high-temperature difference and for a large Knudsen number range," Paper 13 presented at the 10th International Symposium on Rarefied Gas Dynamics, Aspen, CO, July 19-23, 1976. pp. 149-159.

^T Ratzel, A., Simpson, C. "Heat Loss Reduction Techniques for Annular Solar Receiver Designs," SAND78-1769, Sandia National Laboratories, Albuquerque, NM, 1978.

^U Harding, G., Window, B., "Free Molecule Thermal Conduction in Concentric Tubular Solar Collectors," Solar Energy Materials Vol. 4, pp. 265-278, 1981.

^V Kulev, A., Shestakov, A., Borisov, S., Semenov, Y., "Experimental Study of Heat Exchange in a Moderately Rarefied Gas," *Journal of Engineering Physics*, Vol. 49, pp. 1162-1167, Oct. 1985.

^W Semyonov, Y., Borisov, S., Suetin, P., "Investigation of heat transfer in rarefied gases over a wide range of Knudsen numbers," *International Journal of Heat and Mass Transfer*, Vol. 27, No. 10, pp. 1789-1799, 1984.

^X O'Shea, S., Collins, R., "An experimental study of conduction heat transfer in rarefied polyatomic gases," *International Journal of Heat and Mass Transfer*, Vol. 35, No. 12, pp. 3431-3440, 1992.

^Y Song, S., Yovanovich, M., Goodman, F., "Thermal Gap Conductance of Conforming Surfaces in Contact," *Journal of Heat Transfer*, Vol. 115, pp. 533-540, 1993.

^Z Yoo, M., Greytak, T., "Thermal conductivity and accommodation coefficient of spin-polarized atomic-hydrogen gas," *Physical Review B*, Vol. 52, No. 10, pp. 7215-7229, 1995.

^{AA} Beikircher, T., Benz, N., Spirkl, W., "Gas Heat Conduction in Evacuated Flat-Plate Solar Collectors: Analysis and Reduction," *Journal of Solar Energy Engineering*, Vol. 117, pp. 229-235, 1995.

^{BB} Benz, N., Beikircher, T., Aghazadeh, B., "Aerogel and krypton insulated evacuated flat-plate collector for process heat production." *Solar Energy*, Vol. 58, p. 45, 1996.

^{CC} Beikircher, T., Benz, N., "A Modified Temperature-Jump Method for the Transition and Low-Pressure Regime," *Journal of Heat Transfer*, Vol. 120, pp. 965-970, 1998.

Appendix B

EES listing of Sherman Interpolation Formula

"Algorithm to predict 1-D receiver heat loss"

"Uses Sherman interpolation model to calculate gas heat conduction in the transition regime for pure gases and binary mixtures"

"by Frank Burkholder, January 2011"

\$UnitSystem SI MASS DEG PA K J

\$TABSTOPS 0.5 1 1.5 2 cm

"!INPUTS"

"Set directives"

MixtureFlag\$ = 'Yes'

"Yes indicates the gas in annulus is a binary mixture"

EmitFlag\$ = 'No'

"Yes indicates that the user will set the absorber emittance, otherwise it"
"will be estimated from a temperature dependent correlation"

TglassFlag\$ = 'Yes'

"Yes indicates that the user will set the glass temperature, otherwise it"
"will be calculated from h_glass, T_amb, and T_sky"

AccomFlag\$ = 'Yes'

"Yes indicates that the user will enter the accommodation coefficients;"
"if no, Song's correlation (1987) is used"

CalculateKFlag\$ = 'No'

"Yes indicates that the thermal conductivity of the gas mixture will be"
"calculated, otherwise it's user input"

CalcUncertFlag\$ = 'No'

"Yes indicated that the uncertainty in the heat conduction will be"
"calculated"

"Geometry"

Length = 1 [m] "Length of receiver under study"

R_1_o = 3.5 [cm]*convert(cm,m)

"Radius of the outer surface of the absorber"

R_2_i = 5.95 [cm]*convert(cm,m)

"Radius of the inner surface of the glass"

R_2_o = 6.25 [cm]*convert(cm,m)

"Radius of the outer surface of the glass"

"Gases"

"Gas options are Hydrogen, Argon, and Xenon"

Gas\$[1] = 'Hydrogen'

"The gas in the annulus - if this is not a mixture this is the only gas"
"analyzed - if hydrogen in a mixture always make this hydrogen"

Gas\$[2] = 'Argon'

"The second gas in the annulus"

\$IF MixtureFlag\$ = 'Yes'

X[1] = 0.50

"Molar fraction of gas 1"

```

$ELSE
    X[1] = 1 "do not change this value!"
$ENDIF

"Temperatures"
T_1_o_C = 350 [C]          "Temperature of inner cylinder (outer surface)"
$IF TglassFlag$ = 'Yes'
    T_2_o_C = 91.5 [C]    "Temperature of outer cylinder (outer surface)"
$ELSE
    T_amb_C = 22 [C]     "Ambient temperature (for convection to ambient)"
    T_sky_C = 22 [C]    "Sky tempertaure (for radiation to ambient)"
$ENDIF

"Thermal conductivity of gas mixture"
$IF CalculateKFlag$ = 'No'
    k_mix = 0.1191 [W/m-K]
    {0.2826 100% H2, 0.02612 100% Ar, 0.008426 100% Xe}
    {0.04103 10% H2 90% Ar}
    {0.06648 25% H2/ 75% Ar}
    {0.1191 50% H2 50% Ar}
    {0.02092 11.2% H2 88.8% Xe}
    {0.04271 27.2% H2 72.8% Xe}
    {0.09057 52.5% H2 47.5% Xe}
$ENDIF

"Pressure in the annulus"
P_ann = 13.3 [Pa]

"Accommodation coefficients (if AccomFlag$ directive = Yes)"
$IF AccomFlag$ = 'Yes'
    $IF Gas$[1] = 'Hydrogen'
        alpha_Gas1_1 = 0.34 "accommodation coefficient of Gas 1 on surface 1 (inner cylinder)"
        alpha_Gas1_2 = 0.25 "accommodation coefficient of Gas 1 on surface 2 (outer cylinder)"
    $ENDIF
    $IF Gas$[1] = 'Argon'
        alpha_Gas1_1 = 0.66 "accommodation coefficient of Gas 1 on surface 1 (inner cylinder)"
        alpha_Gas1_2 = 0.82 "accommodation coefficient of Gas 1 on surface 2 (outer cylinder)"
    $ENDIF
$ENDIF

```

```

$IF Gas$[1] = 'Xenon'
    alpha_Gas1_1 = 0.76 "accommodation coefficient of Gas 1 on surface 1 (inner cylinder)"
    alpha_Gas1_2 = 0.90 "accommodation coefficient of Gas 1 on surface 2 (outer cylinder)"
$ENDIF
$IF Gas$[2] = 'Hydrogen'
    alpha_Gas2_1 = 0.34 "accommodation coefficient of Gas 1 on surface 1 (inner cylinder)"
    alpha_Gas2_2 = 0.25 "accommodation coefficient of Gas 1 on surface 2 (outer cylinder)"
$ENDIF
$IF Gas$[2] = 'Argon'
    alpha_Gas2_1 = 0.66 "accommodation coefficient of Gas 1 on surface 1 (inner cylinder)"
    alpha_Gas2_2 = 0.82 "accommodation coefficient of Gas 1 on surface 2 (outer cylinder)"
$ENDIF
$IF Gas$[2] = 'Xenon'
    alpha_Gas2_1 = 0.76 "accommodation coefficient of Gas 1 on surface 1 (inner cylinder)"
    alpha_Gas2_2 = 0.90 "accommodation coefficient of Gas 1 on surface 2 (outer cylinder)"
$ENDIF
$ENDIF
"Determine emittance"
$IF EmitFlag$ = 'Yes'
    epsilon_1 = 0.10 "specify absorber emittance, otherwise it will use the emittance as a function of"
    "temperature curve fit below"
$ELSE
    epsilon_1 = 0.0582821 + 0.0000278869 [1/C]*T_1_o_C + 0.0000001851*T_1_o_C^2
$ENDIF
"Material properties"
k_glass = 1.4 [W/m-K] "Thermal conductivity of borosilicate glass"
epsilon_2 = 0.89 "glass emittance"

"!CALCULATIONS"
P_ann = P_ann_torr*convert(torr,Pa)
T_1_o = converttemp(C,K,T_1_o_C)
T_2_i = converttemp(C,K,T_2_i_C)
T_2_o = converttemp(C,K,T_2_o_C)
$IFNOT TglassFlag$ = 'Yes'
    T_amb = converttemp(C,K,T_amb_C)
    T_sky = converttemp(C,K,T_sky_C)
$ENDIF

```

```

R = R# "gas constant"
k = k# "Boltzmann's constant"
sigma = sigma#
X[1]+X[2] = 1 "sum of molar fractions = 1"
Vol_ann = pi*(R_2_i^2-R_1_o^2)*Length "the volume of gas in the annulus, m^3"
Vol_ann_L = Vol_ann*convert(m^3,L) "volume of gas in the annulus, Liters"
P_ann*Vol_ann=n_mix*R*T_mix "depending on the SetPannFlag$, either sets P_ann or n_mix"
duplicate i=1,2
    n[i] = X[i]*n_mix
    MM[i]=MolarMass(Gas$(i))
    mass[i] = n[i]*MM[i]
    P[i]= X[i]*P_ann
    P_torr[i] = P[i]*convert(Pa,torr)
end
T_mix_C = (T_1_o_C+T_2_i_C)/2
T_mix = converttemp(C,K,T_mix_C)

"!Find continuum thermal conductivity of pure species"
P_oo = 660 [torr]*convert(torr,Pa) "atmospheric pressure in Golden, CO"
duplicate i = 1,2
    k[i]=Conductivity(Gas$(i),T=T_mix,P=P_oo)
    mu[i]=Viscosity(Gas$(i),T=T_mix,P=P_oo)
    C_v[i] =Cv(Gas$(i),T=T_mix,P=P_oo)*MM[i]
end

"!Find continuum thermal conductivity of mixture"
$IF MixtureFlag$ = 'Yes'
    "Use the Wilke correlation from Bird, Stewart, and Lightfoot to determine mixture thermal"
    "conductivity in the continuum"
    PHI_1_1= 1/SQRT(8)*1/(1+MM[1]/MM[1])^(1/2)*(1+((mu[1]/mu[1])^(1/2))*(MM[1]/MM[1])^(1/4))^2
    PHI_1_2 = 1/SQRT(8)*1/(1+MM[1]/MM[2])^(1/2)*(1+((mu[1]/mu[2])^(1/2))*(MM[2]/MM[1])^(1/4))^2
    PHI_2_1 = 1/SQRT(8)*1/(1+MM[2]/MM[1])^(1/2)*(1+((mu[2]/mu[1])^(1/2))*(MM[1]/MM[2])^(1/4))^2
    PHI_2_2 = 1/SQRT(8)*1/(1+MM[2]/MM[2])^(1/2)*(1+((mu[2]/mu[2])^(1/2))*(MM[2]/MM[2])^(1/4))^2
    PHI_1 = X[1]*PHI_1_1+X[2]*PHI_1_2
    PHI_2 = X[1]*PHI_2_1+X[2]*PHI_2_2
    $IF CalculateKFlag$ = 'Yes'
        k_mix = (X[1]*k[1])/PHI_1+(X[2]*k[2])/PHI_2

```

```

$ENDIF
k[3] = k_mix
$ELSE
$IF CalculateKFlag$ = 'Yes'
    k_mix = k[1]
$ENDIF
$ENDIF

"!Find the thermal accommodation coefficients"
$IFNOT AccomFlag$ = 'Yes'
    C_0 = -0.57
    C_1 = 6.8 [g/mol]
    MM_Al2O3 = 2*26.98 [g/mol] + 3*16[g/mol] "the antireflective coating on the absorber is"
                                                "aluminum oxide, Al2O3"
    MM_SiO2 = 28.09 [g/mol] + 2*16.00 [g/mol] "the antireflective coatings on the glass is"
                                                "predominantly silica, SiO2"

    mu_Gas1_1 = MM[1]/MM_Al2O3
    mu_Gas1_2 = MM[1]/MM_SiO2
    mu_Gas2_1 = MM[2]/MM_Al2O3
    mu_Gas2_2 = MM[2]/MM_SiO2
    T_0 = 273 [K]
    $IF Gas$[1] = 'Hydrogen'
        M|star_1 = 1.4*MM[1]*convert(kg/kmol,g/mol)
    $ELSE
        M|star_1 = MM[1]*convert(kg/kmol,g/mol)
    $ENDIF
    $IF Gas$[2] = 'Hydrogen'
        M|star_2 = 1.4*MM[2]*convert(kg/kmol,g/mol)
    $ELSE
        M|star_2 = MM[2]*convert(kg/kmol,g/mol)
    $ENDIF

    alpha_Gas1_1 = exp(C_0*((T_1_o-T_0)/T_0))*(M|star_1/(C_1+M|star_1))+
(1-exp(C_0*((T_1_o-T_0)/T_0)))*((2.4*mu_Gas1_1)/(1+mu_Gas1_1)^2)
    alpha_Gas1_2 = exp(C_0*((T_2_i-T_0)/T_0))*(M|star_1/(C_1+M|star_1))+
(1-exp(C_0*((T_2_i-T_0)/T_0)))*((2.4*mu_Gas1_2)/(1+mu_Gas1_2)^2)
    alpha_Gas2_1 = exp(C_0*((T_1_o-T_0)/T_0))*(M|star_2/(C_1+M|star_2))+
(1-exp(C_0*((T_1_o-T_0)/T_0)))*((2.4*mu_Gas2_1)/(1+mu_Gas2_1)^2)

```

```

alpha_Gas2_2 = exp(C_0*((T_2_i-T_0)/T_0))*(M|star_2/(C_1+M|star_2))+1-exp(C_0*((T_2_i-
T_0)/T_0))*((2.4*mu_Gas2_2)/(1+mu_Gas2_2)^2)
$ENDIF

```

```

"!Find free molecular heat conduction"

```

```

A_1 = 2*pi*R_1_o*Length

```

```

Q_FM_1 = (1/alpha_Gas1_1+(R_1_o/R_2_i)*(1/alpha_Gas1_2-1))^(-
1)*(P[1]*(C_v[1]+R/2))/SQRT(2*pi*MM[1]*R*T_mix)*(T_1_o -T_2_i)*A_1

```

```

$IF MixtureFlag$ = 'Yes'

```

```

Q_FM_2 = (1/alpha_Gas2_1+(R_1_o/R_2_i)*(1/alpha_Gas2_2-1))^(-
1)*(P[2]*(C_v[2]+R/2))/SQRT(2*pi*MM[2]*R*T_mix)*(T_1_o -T_2_i)*A_1

```

```

Q_FM = (Q_FM_1+Q_FM_2)

```

```

$ELSE

```

```

Q_FM_2 = 0

```

```

Q_FM = Q_FM_1

```

```

$ENDIF

```

```

"!Find continuum heat conduction"

```

```

Q_oo = (2*pi*Length*k_mix*(T_1_o-T_2_i))/ln(R_2_i/R_1_o)

```

```

"!Find heat conduction by interpolating between the free molecular and continuum solutions using
Sherman's formula"

```

```

1/Q_cond = 1/Q_oo+1/Q_FM

```

```

Q_cond_perm = Q_cond/Length

```

```

"!Find radiative heat transfer across annulus"

```

```

Q_rad = (sigma*A_1*(T_1_o^4-T_2_i^4))/(1/epsilon_1+((1-epsilon_2)/epsilon_2)*(R_1_o/R_2_i))

```

```

"!Find total heat transfer across annulus"

```

```

Q_tot = Q_cond+Q_rad

```

```

Q_tot\m = Q_tot/Length "per meter length"

```

```

"!Find the heat conducted through the glass"

```

```

Q_glasscond = (2*pi*Length*k_glass*(T_2_i-T_2_o))/ln(R_2_o/R_2_i)

```

```

Q_tot = Q_glasscond "steady-state heat transfer"

```

```

DELTAT_gl = T_2_i-T_2_o

```



```

$IFNOT TglassFlag$ = 'Yes'
    "!Find the heat convected to the environment"
    h_oo = Max(5 [W/m2-K], 4.5 [W/m2-K] + 0.012 *T_2_o_C) "Churchill & Chu natural convection"
        "correlation, evaluated to 1st order for T_amb = 23 C and o.d. = 11.5 cm"
    A_2 = 2*pi*R_2_o*Length
    Q_convtoamb = h_oo*A_2*(T_2_o-T_amb)

    "!Find the heat radiated to the environment"
    Q_radosky = sigma*epsilon_2*A_2*(T_2_o^4-T_sky^4)

    "!The heat convected and radiated to environment is equal to that conducted through glass"
    Q_glasscond = Q_convtoamb+Q_radosky
$ENDIF

"!Find the temperature difference between the absorber and glass"
DELTAT = T_1_o-T_2_i

"!Uncertainty calculation"
$IF CalcUncertFlag$ = 'Yes'
    UMHL=UncertaintyOf(Q_cond_perm)
$ELSE
    UMHL = 0 [W/m]
$ENDIF
Qcplus = Q_cond_perm+UMHL
Qcminus = Q_cond_perm-UMHL

```

Appendix C
DSMC1 FORTRAN listing

```
*   DSMC1.FOR
      PROGRAM DSMC1
!-----This is G.A. Bird's DSMC1 described in "Molecular Gas
!-----Dynamics and The Direct Simulation of Gas Flows," Clarendon
!-----Press, Oxford, 1994, with source code on the disk supplied with the
!-----book and corrected with errata available online.
!-----This coded was last modified by F. Burkholder 4/11/2011
!-----to investigate transition regime gas mixture heat conduction
!-----between concentric cylinders for incomplete thermal accommodation
!-----on both surfaces.
!-----Modifications include:
!-----1) Adding code to allow for incomplete thermal accommodation on either
!-----solid surface.
!-----2) Adding code that reads model inputs from a file instead of being
!-----set within this code.
!-----3) Adding code to read in a number from a file to re-initialize the
!-----random number seed in DSMC1.
!-----4) Addition of many comments documenting variable definitions and
!-----describing algorithms.
!-----5) Syntax changes compatible with Fortran 95.

      !Original comments by Bird start with and asterisk, *
      !Comments by FWB start with an explanation point

*-----DSMC1 is general one-dimensional steady flow program
*-----includes options for cylindrical and spherical flows
*-----flow gradients occur only in the direction of the x axis
*-----the x axis becomes the radius in cylindrical and spherical cases
*-----the origin is then at x=0
*-----the axis of a cylindrical flow is along the z axis
*-----in plane flows, there may be a velocity in the y direction
*-----in cylindrical flow, there may be a circumferential velocity
*-----there is an 'inner' (smaller x) and 'outer' (larger x) boundary
*-----each boundary is one of five types
*-----1: an axis or centre (it must then be at x=0)
*-----2: a plane of symmetry or a specularly reflecting surface
*-----3: a solid surface
*-----4: a stream boundary
*-----5: a vacuum
*-----the cell widths may be either uniform or in geometric progression
*-----there may be a constant 'gravitational' acceleration in plane flows
*-----with type 4 or type 5 boundaries
*
*--SI units are used throughout
*
*-----DESCRIPTION OF DATA-----
*
*--the following is set in the PARAMETER statement
*--MNC the number of cells
*--(the other PARAMETER variables must be consistent with the data in
*--SUBROUTINE DATA1, and MNSC can set a default if NSC is not set)
*
*--IFC set to 0 or 1 for uniform or non-uniform cell widths
```

```

*---if IFC=1, set CWR as the ratio of the cell width at the outer
*---boundary to that at the inner boundary (default 0)
*
*--IFX set to 0, 1, or 2 for plane, cylindrical, or spherical flow
*
*--IIS 0 if the initial state is a vacuum, 1 if it is a uniform stream,
*----or 2 for a uniform gradient between two surfaces
*
*--FTMP the stream temperature if IIS=1, or a temperature characteristic
*----of the flow otherwise (of FTMP is not set for IIS= 0 or 2, the
*----default value of 273 is used to set the initial value of CCG(1
*
*--FND the initial number density for IIS=1, the mean value for IIS=2,
*----or need not be set for IIS=0
*
*--FSP(L) the fraction (by number) of species L in the initial stream
*----a value is required for each species, but need not be set for IIS=0
*
*--FNUM the number of real mols. represented by each simulated molecule
*
*--DTM the time step over which the motion and collisions are uncoupled
*
*--NSC the number of sub-cells per cell (MNSC must be at least MNC*NSC)
*----this is optional because MNSC/MNC will be set as the default value
*
*--the following data is required for each boundary
*----K=1 for the inner boundary (lower value of x)
*----K=2 for the outer boundary (higher value of x)
*
*--XB(K) the x coordinate of the boundary (must be positive if IFX>1)
*
*--IB(K) the type code of the boundary
*
*--no further data on the boundary is required if:-
*----IB(K)=1 for an axis or centre (valid for IFX= 1 or 2, and XB(K)=0),
*----IB(K)=2 for a plane of symmetry (if IFX=1) or a specularly
*-----reflecting surface (valid for all IFX values)
*----IB(K)=5 for an interface with a vacuum
*
*--if IB(K)=3 (a solid surface) the following are required:-
*--BT(K) the temperature of the surface (diffuse reflection)
*--BVY(K) the velocity in the y direction (not valid for IFX=2)
*
*--if IB(K)=4 (an interface with an external stream) the reqd. data is:-
*--BFND(K) the number density of the stream
*--BFTMP(K) the temperature
*--BVFX(K) the x (and only) component of the stream velocity
*--BFSP(K,L) the number fraction of species L in the stream
*----a value of BFSP is required for each species
*
*--end of the boundary data
*
*--ISPD (required only for gas mixtures) set to 0 if the diameter,
*----viscosity exponent, and VSS scattering parameter for the
*----cross-collisions are to be set to the mean values, or
*----set to 1 if these quantities are to be set as data
*

```

```

*--the following data must be repeated for each species (L=1 to MNSP)
*
*--SP(1,L) the reference diameter
*--SP(2,L) the reference temperature
*--SP(3,L) the viscosity temperature power law
*--SP(4,L) the reciprocal of the VSS scattering parameter (1. for VHS)
*--SP(5,L) the molecular mass
*
*--ISP(L) the collision sampling group in which the species lies
*----this must be LE.MNSC (not required if MNSG=1)
*
*--ISPR(1,L) the number of rotational degrees of freedom
*--ISPR(2,L) 0, 1 for constant, polynomial rotational relaxation number
*--ISPR(3,L) 0, 1 for common or collision partner species dependent
*----rotational relaxation rate
*
*--SPR(1,L,K) the constant value, or constant in the polynomial for Zr
*----in a collision of species L with species K
*--the following two items are required only if ISPR(2,L)=1
*--SPR(2,L,K) the coefficient of temperature in the polynomial
*--SPR(3,L,K) the coefficient of temperature squared in the polynomial
*
*--end of data for the individual species
*
*--the following data on the cross-collisions is required only if ISPD=1
*--then only for L.NE.M, but L,M data must be repeated for M,L
*
*--SPM(1,L,M) the reference diameter for species L-M collisions
*--SPM(2,L,M) the reference temperature for species L-M collisions
*--SPM(3,L,M) the viscosity temperature power law for species L-M colls.
*--SPM(4,L,M) the reciprocal of the VSS scattering parameter
*
*--end of species data
*
*--GRAV the gravitational acceleration in the x direction (default 0.)
*----this should be non-zero only when IFX=0 (plane flows) and the
*-----boundaries are either type 4 or type 5
*
*--NIS the number of DTM time steps between samplings
*
*--NSP the number of samples between prints
*
*--NPS the number of prints to the assumed start of steady flow
*
*--NPT the number of prints to STOP
*
*-----
*
*      MNM is the maximum number of molecules, MNC is the max number of cells,
*      MNSC is max number of subcells, MNSP is max number of species, MNSG?
*      PARAMETER (MNM=15000,MNC=20,MNSC=400,MNSP=2,MNSG=1)
*
*----MNM is the maximum number of molecules
*----MNC is the maximum number of cells
*----MNSC is the maximum number of sub-cells
*----MNSP is the maximum number of molecular species
*----MNSG is the number of species groups for collision sampling

```

```

*
  DOUBLE PRECISION COL(MNSP,MNSP),MOVT,NCOL,SELT,SEPT,CS(7,MNC,MNSP)
*----COL(M,N) is the number of collisions between species N-M molecules
*----NCOL is the total number of collisions
*----MOVT the total number of molecular moves
*----SELT the total number of pair selections
*----SEPT the sum of collision pair separations
*----CS(N,M,L) sampled information on species L in cell M
*-----N=1 number sum
*-----N=2,3,4 sum of u,v,w
*-----N=5,6,7 sum of u*u,v*v,w*w
*
  DOUBLE PRECISION CSR(MNC,MNSP)
*----CSR(M,L) the sum of the rotational energy of species L in cell M
*
  DOUBLE PRECISION CSH(3,MNC,MNSP)
*----(CSH(N,M,L) higher order sampling in cell M of species L
*-----N=1 sum of u*v
*-----N=2 sum of c**2*u
*-----N=3 sum of rotl. energy*u
*
  DOUBLE PRECISION CSS(8,2,MNSP)
*----CSS(N,M,L) sampled info. on the molecules striking the boundaries
*-----M=1, 2 for the inner, outer boundaries; L is the species
*-----N=1 the number sum
*-----N=2 the sum of the normal momentum of the incident molecules
*-----N=3 the sum of the normal momentum for the reflected molecules
*-----N=4 the sum of the incident parallel momentum in the y direction
*-----N=5 the sum of the incident translational energy
*-----N=6 the sum of the reflected translational energy
*-----N=7 the sum of the incident rotational energy
*-----N=8 the sum of the reflected rotational energy
*
*extra comment
  COMMON /MOLS / NM,PP(MNM),PV(3,MNM),IPL(MNM),IPS(MNM),IR(MNM)
*----NM is the number of molecules
*----PP(M) is the x coordinate molecule M
*----PV(1 to 3,M) u,v,w velocity components of molecule M
*----IPL(M) sub-cell number for molecule M
*----IPS(M) species code number
*----IR(M) cross-reference array (molecule numbers in order of sub-cells)
  COMMON /MOLSR / PR(MNM)
*----PR(M) is the rotational energy of molecule M
  COMMON /CELLS1/ CC(MNC),CG(3,MNC),IC(2,MNC,MNSG),ISC(MNSC),
& CCG(2,MNC,MNSG,MNSG),ISCG(2,MNSC,MNSG),IG(2,MNSG),
& IFC,CWR,AP,RP
*----CC(M) is the cell volume
*----CCG(N,M,L,K) is for collisions between species groups L-K in cell M
*-----N=1 is the maximum value of (relative speed)*(coll. cross-section)
*-----N=2 is the remainder when the selection number is rounded
*----CG(N,M) is the geometry related information on cell M
*-----N=1 the minimum x coordinate
*-----N=2 the maximum x coordinate
*-----N=3 the cell width
*----IC(N,M,L) information on the molecules of species group L in cell M
*-----N=1 (start address -1) of the molecule numbers in the array IR
*-----N=2 the number of molecules in the cell

```

```

*----ISC(M) the cell in which the sub-cell lies
*----ISCG(N,M,L) is the information on species group L in sub-cell M
*-----N=1 (start address -1) of the molecule numbers in the array IR
*-----N=2 the number of molecules in the sub-cell
*----IG(2,M) information on group L molecules (IG(N,L)?)
*-----N=1 (start address -1) of the molecule numbers in the array IR
*-----N=2 the number of molecules in the cell
*----IFC 0,1 for uniform cell width, cell widths in geometric progression
*----CWR the ratio of cell width at outer boundary to that at inner bound.
      COMMON /GAS / SP(5,MNSP),SPM(6,MNSP,MNSP),ISP(MNSP)
*----SP(N,M) information on species M
*-----N=1 the reference cross-section (diameter in the data)
*-----N=2 the reference temperature
*-----N=3 the viscosity-temperature power law
*-----N=4 the reciprocal of the VSS scattering parameter
*-----N=5 the molecular mass
*----SPM(N,M,L) information on the interaction between L-M molecules
*-----N=1 the reference cross-section (diameter in the data)
*-----N=2 the reference temperature
*-----N=3 the viscosity-temperature power law
*-----N=4 the reciprocal of the VSS scattering parameter
*-----N=5 the reduced mass
*-----N=6 the Gamma function of (5/2 - viscosity-temperature power law)
*----ISP(M) the collision sampling group in which species M lies
      COMMON /GASR / SPR(3,MNSP,MNSP),ISPR(3,MNSP),CT(MNC)
*----SPR(N,M,L) information on rotational relaxation properties of a
*-----species M molecule in a collision with a species L molecule
*-----N=1 the const. in the temperature polynomial for the collision numb
*-----N=2 the coefficient of T in this polynomial
*-----N=3 the coefficient of T**2 in this polynomial
*----ISPR(N,M) integer information on rotational properties of species M
*-----N=1 the number of rotational degrees of freedom
*-----N=2 0, 1 for constant, polynomial for relaxation collision number
*-----N=3 0, 1 for a common, collision partner species dependent rate
*----CT(M) the macroscopic temperature in cell M
*
      COMMON /SAMP / COL,NCOL,MOVT,SELT,SEPT,CS,TIME,NPR,NSMP,FND,FTMP,
&
      TIMI,FSP(MNSP),ISPD
*----TIME time
*----NPR the number of output/restart file update cycles
*----NSMP the total number of samples
*----FND the stream number density
*----FTMP the stream temperature
*----FSP(M) the fraction of species M in the stream
*----ISPD relates to the setting of data for colls. between unlike mols.
*----set to 0 if data is set automatically to the mean values
*----set to 1 if the values are set explicitly in the data
      COMMON /SAMPR / CSR
      COMMON /SAMPS / CSS
      COMMON /SAMPH / CSH
*--double precision variables defined above
*
      COMMON /COMP / FNUM,DTM,NIS,NSP,NPS,NPT
*----FNUM is the number of real molecules represented by a simulated mol.
*----DTM is the time step
*----NIS is the number of time steps between samples
*----NSP is the number of samples between restart and output file updates

```

```

*----NPS is the estimated number of samples to steady flow
*----NPT is the number of file updates to STOP

COMMON /MODSF / NSF,SEED
!----NSF is the update where flow measurements begin

COMMON /GEOM1 / IFX,NSC,XB(2),IB(2),BT(2),BVY(2),BFND(2),BFTMP(2),
&&
BVFX(2),BFSP(2,MNSP),BME(2,MNSP),BMR(2,MNSP),IIS,
&&
CW,FW,GRAV
*----IFX 0, 1, or 2 for plane, cylindrical, or spherical flow
*----IIS 0, 1, or 2 if the initial flow is a vacuum, uniform stream, or
*-----a uniform gradient between the values at two solid surfaces
*----NSC the number of sub-cells per cell
*----XB(N) N=1, 2 the location of the inner, outer boundary
*----IB(N) N=1, 2 the type code for the inner, outer boundary
*----no further data is needed if IB=1, 2, or 5
*----if IB=3 (solid surface), the following info. is needed (N as above)
*----BT(N) the temperature of the surface
*----BVY(N) the y velocity component (valid for IFX= 0 or 1)
*----if IB=4 (external gas stream), the following info. (N as above)
*----BFND(N) the number density of the external stream
*----BFTMP(N) the temperature
*----BVFX(N) the x component of the velocity
*----BF(N,L) the fraction of species L in the stream
*----the following are non-data variables that can apply for IB=3, or 4
*----BME(N,L) the number of molecules of species L that enter at each DTM
*----BMR(N,L) the remainder associated with entry number
*----CW the cell width for uniform cells
*----FW the flow width
*----GRAV the gravitational acceleration in the x direction
*

COMMON /CONST / PI,SPI,BOLTZ
*----PI is pi and SPI is the square root of pi
*----BOLTZ is the Boltzmann constant

DOUBLE PRECISION SS(8),RFinit !added FWB

*-----MAIN CODE
CALL INIT1 !Initialize variables and read inputs
RFinit = RF(INT(SEED)) !initialize random number generator
CALL SAMPI1 !Initialize the sampled values
OPEN (5,FILE='QCond.csv',FORM='FORMATTED') !output file

!Update loop
WRITE(*,*) 'DSMC1 running with ',NM,' molecules.'
100 NPR=NPR+1 !update number incrementing
IF (NPR.LE.NPS) CALL SAMPI1 !initializing sampled values until
!sampling starts
DO 200 JJJ=1,NSP !--NSP is the number of samples between updates
!Timestep loop
DO 150 III=1,NIS !--NIS is the number of time steps between
!samples
TIME=TIME+DTM !time incrementing by timestep
CALL MOVE1 !move the molecules
CALL INDEXM !sort the molecules based on their new locations
CALL COLLMR !give molecules the chance to collide

```

```

150     CONTINUE
        !End timestep loop
        CALL SAMPLE1 !sample the flow
200     CONTINUE !One update has been completed
        ! CALL OUT1 if desired, output detailed results to DSMC1.OUT

        !FWB code below outputs pressure and heat conduction to QCond.csv every
10     !updates once the updates are greater than NSF until NPT
        IF (NPR.GE.NSF) THEN
            IF (MOD(NPR,10).EQ.0) THEN
                UD = NPR-NSF
                K = 1 !Surface 1
                A=FNUM/((TIME-TIMI)*2.*PI*XB(K))
                DO 240 N = 1,8
                    SS(N)=0.
240                CONTINUE
                    DO 255 N = 1,8
                        DO 250 L=1,MNSP
                            SS(N)=SS(N)+CSS(N,K,L)
250                        CONTINUE
                            SS(N)=SS(N)*A
255                CONTINUE
                    Prs1 = SS(2)+SS(3)
                    QWpml = -1.*(SS(5)+SS(6)+SS(7)+SS(8))*2.*PI*XB(K)
                    WRITE(*,*) '#',UD,'P:',Prs1,'H1:',QWpml !output to screen
                    WRITE(5,*) UD,',',Prs1,',',QWpml
                END IF
            END IF
            IF (NPR.LT.NPT) GO TO 100 !continue if not at last update
            !End update loop
            CLOSE (5) !close output file
            WRITE(*,*) 'DSMC1 simulation completed.'
            STOP
            END
*-----END MAIN CODE

*   INIT1.FOR
        !Subroutine initializes values
        SUBROUTINE INIT1
            PARAMETER (MNM=15000,MNC=20,MNSC=400,MNSP=2,MNSG=1)
            DOUBLE PRECISION COL(MNSP,MNSP),MOVT,NCOL,SELT,SEPT,CS(7,MNC,MNSP)
            DOUBLE PRECISION CSR(MNC,MNSP)
            COMMON /MOLS / NM,PP(MNM),PV(3,MNM),IPL(MNM),IPS(MNM),IR(MNM)
            COMMON /MOLSR / PR(MNM)
            COMMON /CELLS1/ CC(MNC),CG(3,MNC),IC(2,MNC,MNSG),ISC(MNSC),
&
&
                CCG(2,MNC,MNSG,MNSG),ISCG(2,MNSC,MNSG),IG(2,MNSG),
                IFC,CWR,AP,RP
            COMMON /GAS / SP(5,MNSP),SPM(6,MNSP,MNSP),ISP(MNSP)
            COMMON /GASR / SPR(3,MNSP,MNSP),ISPR(3,MNSP),CT(MNC)
            COMMON /SAMP / COL,NCOL,MOVT,SELT,SEPT,CS,TIME,NPR,NSMP,FND,FTMP,
&
                TIMI,FSP(MNSP),ISPD
            COMMON /SAMPR / CSR
            COMMON /COMP / FNUM,DTM,NIS,NSP,NPS,NPT
            COMMON /GEOM1 / IFX,NSC,XB(2),IB(2),BT(2),BVY(2),BFND(2),BFTMP(2),
&
                BVFX(2),BFSP(2,MNSP),BME(2,MNSP),BMR(2,MNSP),IIS,

```



```

&
COMMON /CONST / PI,SPI,BOLTZ
CW,FW,GRAV
*--set constants
PI=3.141592654
SPI=SQRT(PI)
BOLTZ=1.380622E-23
*--set data variables to default values that they retain if the data
*----does not reset them to specific values
NSC=MNSC/MNC ! sets the number of sub-cells per cell
FND=0. ! initial number density
FTMP=273. ! the stream temperature if IIS=1, or temp char. or flow
GRAV=0. ! no gravity
IFC=0 ! uniform cell width selected
DO 100 N=1,2
  XB(N)=0. ! coordinates of boundary
  IB(N)=5 ! type code of boundary
  BT(N)=0. ! boundary temperature
  BVY(N)=0. ! boundary speed in y direction
  BFND(N)=0. ! number density of stream if coming out of boundary
  BFTMP(N)=0. ! the stream temperature
  BVFX(N)=0. ! the x and only component of the stream velocity
  DO 50 L=1,MNSP ! for each species
    ISP(L)=1 ! all species in collision sampling group 1
    FSP(L)=0. ! the fraction of the species in the stream
    BFSP(N,L)=0. ! the fraction of species in the stream
    BME(N,L)=0. !number of mol. of species L that enter at DTM
    BMR(N,L)=0. ! the remainder associated with entry number
50  CONTINUE
100  CALL DATA1 !Reads model inputs
*--set additional data on the gas
ISPD = 0 !Determine collision cross section, viscosity exponent, &
!VSS scattering parameter from pure gas quantities
IF (MNSP.EQ.1) ISPD=0 !if the number of species = 1 then no
!cross-collisions so ISPD not needed
DO 200 N=1,MNSP !for each species
  DO 150 M=1,MNSP !for each species
    IF ((ISPR(3,N).EQ.0).AND.(M.NE.N)) THEN !if the rotational
!relaxation rate (RRR) is common, and not comp. = species
    SPR(1,N,M)=SPR(1,N,N) !the constant in the RRR, it sets 1
!with 2 to 1 with 1, and 2 with 1 equal to 2 with 2
    SPR(2,N,M)=SPR(2,N,N) !the coefficient of temp in the RRR,
! similar to above
    SPR(3,N,M)=SPR(3,N,N) !the coefficient of temp^2 in the RRR,
! similar to above
  END IF
  IF ((ISPD.EQ.0).OR.(N.EQ.M)) THEN ! if the diameter (coll.
!cross- sect), visc exponent, and VSS scattering param are set
!as mean values (species dep), or identical species
    SPM(1,N,M)=0.25*PI*(SP(1,N)+SP(1,M))**2 !Coll. cross-sect.
! for N,M coll.
*--the collision cross section is assumed to be given by eqn (1.35)
    SPM(2,N,M)=0.5*(SP(2,N)+SP(2,M)) !ref. temp. for N,M col.
    SPM(3,N,M)=0.5*(SP(3,N)+SP(3,M)) !visc. temperature power
! law for N,M collisions
    SPM(4,N,M)=0.5*(SP(4,N)+SP(4,M)) !the reciprocal of VSS
! scattering parameter for N,M collisions

```

```

*--mean values are used for ISPD=0
      ELSE ! if the collision cross section, visc exp, and
          !VSS scat. not set as mean values (so ISPD = 1), not used
          SPM(1,N,M)=PI*SPM(1,N,M)**2 !collision cross section is set
          ! SPM(2,N,M), SPM(3,N,M), and SPM(4,N,M) need to be set here
*--the cross-collision diameter is converted to the cross-section
      END IF
      SPM(5,N,M)=(SP(5,N)/(SP(5,N)+SP(5,M)))*SP(5,M) !reduced mass
          !for the coll.
*--the reduced mass is defined in eqn (2.7)
      SPM(6,N,M)=GAM(2.5-SPM(3,N,M)) !moment of gamma function with
          ! the viscosity temp coeff - listed in book pg 92
150      CONTINUE
200      CONTINUE

*--initialise variables
      TIME=0. !time initialize to 0
      NM=0 !number of molecules
      NPR=0 !NPR the number of output/restart file update cycles
      NCOL=0 !--NCOL is the total number of collisions
      MOVMT=0. !--MOVMT the total number of molecular moves
      SELT=0. !--SELT the total number of pair selections
      SEPT=0. !--SEPT the sum of collision pair separations
      DO 300 M=1,MNSP !for each species
          DO 250 N=1,MNSP !for each species
              COL(M,N)=0. !COL(M,N) is the number of coll. between
                  !species N-M molecules
250          CONTINUE
300          CONTINUE
      FW=XB(2)-XB(1) !FW the flow width, radius 2 - radius 1
      CG(1,1)=XB(1) !cell 1 minimum coordinate is set to boundary 1
      IF (IFC.EQ.0) THEN ! if uniform cell width
          CW=FW/MNC !cell width is the flow width divided by the max
              !number of cells
*--CW is the uniform cell width
          ELSE
              RP=CWR**(1./(MNC-1.))
*--RP is the ratio in the geometric progression
              AP=(1.-RP)/(1.-RP**MNC)
*--AP is the first term of the progression
          END IF
          DO 400 M=1,MNC !for each cell
              CT(M)=FTMP !cell M temperature to FTMP
*--the macroscopic temperature is set to the freestream temperature
              IF (M.GT.1) CG(1,M)=CG(2,M-1) ! if not the first cell set
                  ! the minimum boundary of cell M to the maximum boundary of
                  ! cell M-1
              IF (IFC.EQ.0) THEN ! if uniform cell widths
                  CG(2,M)=CG(1,M)+CW !set the max. boundary to the minimum
                      !boundary + CW
              ELSE
                  CG(2,M)=CG(1,M)+FW*AP*RP**(M-1) !not used
              END IF
              CG(3,M)=CG(2,M)-CG(1,M) !find the cell width
              IF (IFX.EQ.0) CC(M)=CG(3,M) !not used
*--a plane flow has unit cross-sectional area
              IF (IFX.EQ.1) CC(M)=PI*(CG(2,M)**2-CG(1,M)**2) !cell vol.

```

```

      ! = pi*(ro^2-ri^2)*1
*--a cylindrical flow has unit length in the axial direction
      IF (IFX.EQ.2) CC(M)=(4./3.)*PI*(CG(2,M)**3-CG(1,M)**3)!not used
*--a spherical flow occupies the full sphere
      DO 350 L=1,MNSG !for each collision species group
        DO 320 K=1,MNSG !for each collision species group
          CCG(2,M,L,K)=RF(0) !remainder after rounding - 0 to 1
          CCG(1,M,L,K)=SPM(1,1,1)*300.*SQRT(FTMP/300.) !max value of
            !* coll speed *collision cross section is set to species 1
            !with itself
*----CCG(N,M,L,K) is for collisions between species groups L-K in cell M
*----N=1 is the maximum value of (relative speed)*(coll. cross-section)
*----N=2 is the remainder when the selection number is rounded
320          CONTINUE
350          CONTINUE
*--the maximum value of the (rel. speed)*(cross-section) is set to a
*--reasonable, but low, initial value and will be increased as necessary
400          CONTINUE
            IF (IFC.EQ.1) THEN !geometric progression
              AP=(1.-RP)/AP
              RP=LOG(RP)
*--AP and RP are now the convenient terms in eqn (12.1)
            END IF
*--set sub-cells
            DO 500 N=1,MNC !for each cell
              DO 450 M=1,NSC !for each subcell
                L=(N-1)*NSC+M
                ISC(L)=N !array shows which cell each subcell L resides in
450              CONTINUE
500              CONTINUE
                IF (IIS.GT.0) THEN !IIS = 2 for uniform gradient
*--if IIS=1 generate initial gas with temperature FTMP, or
*--if IIS=2 generate initial gas as a uniform gradient between two
*---surfaces (!valid only if IB(1)=3 and IB(2)=3, which is true in this case)
                  IF (IIS.EQ.2.AND.(IB(1).NE.3.OR.IB(2).NE.3)) THEN
                    WRITE (*,*) ' IIS=2 IS AN ILLEGAL OPTION IN THIS CASE '
                    STOP
                  END IF
                DO 550 L=1,MNSP ! for each species
                  REM=0
                  IF (IIS.EQ.1) VMP=SQRT(2.*BOLTZ*FTMP/SP(5,L)) !if gas is all
                    !uniform temperature
*--VMP is the most probable speed in species L, see eqns (4.1) and (4.7)
                DO 520 N=1,MNC ! for each cell
                  IF (IIS.EQ.2) THEN !for the uniform gradient
                    PROP=(N-0.5)/FLOAT(MNC) !determines the gradient
                    VEL5=BVY(1)+PROP*(BVY(2)-BVY(1)) !sets the velocity
                    TMPS=BT(1)+PROP*(BT(2)-BT(1)) !sets the temperature
                    FNDS=FND*0.5*(BT(1)+BT(2))/TMPS !sets the number density
                    VMP=SQRT(2.*BOLTZ*TMPS/SP(5,L)) !the most probable speed
                  ELSE
                    FNDS=FND
                    TMPS=FTMP
                  END IF
                A=FNDS*CC(N)*FSP(L)/FNUM+REM
*--A is the number of simulated molecules of species L in cell N to
*--simulate the required concentrations at a total number density of FND

```

```

        IF (N.LT.MNC) THEN
            MM=A
            REM=(A-MM)
*--the remainder REM is carried forward to the next cell
        ELSE
            MM=NINT(A)
        END IF
        IF (MM.GT.0) THEN
            DO 505 M=1,MM
                IF (NM.LT.MNM) THEN
*--round-off error could have taken NM to MNM+1
                    NM=NM+1
                    IPS(NM)=L !IPS(NM) saves whether the molecule is
                    !species 1 or 2
                    IF (IFX.EQ.0) PP(NM)=CG(1,N)+RF(0)*(CG(2,N)-CG(1,N))
                    !not used
                    IF (IFX.EQ.1) PP(NM)=SQRT(CG(1,N)**2+RF(0)*(CG(2,N)**2
&                                     -CG(1,N)**2))
                    !--PP(NM) is the x coordinate molecule NM
                    IF (IFX.EQ.2) PP(NM)=(CG(1,N)**3+RF(0)*(CG(2,N)**3-CG(
&                                     1,N)**3))**0.3333333
                    !not used for cylindrical geometry
                    IPL(NM)=(PP(NM)-CG(1,N))*(NSC-.001)/CG(3,N)
&                                     +1+NSC*(N-1) !--IPL(NM) sub-cell number for
                    !molecule NM
*--species, position, and sub-cell number have been set
                    DO 502 K=1,3
                        CALL RVELC(PV(K,NM),A,VMP) !--PV(1 to 3,NM) u,v,w
                        !velocity components of molecule NM
502                    CONTINUE
                    IF (IIS.EQ.2) PV(2,NM)=PV(2,NM)+VELS
*--velocity components have been set
*--set the rotational energy
                    IF (ISPR(1,L).GT.0) CALL SROT(PR(NM),TMPS,ISPR(1,L))
                    !set rotational energy
                    END IF
505                    CONTINUE
                    END IF
520                    CONTINUE
550                    CONTINUE
                    END IF
                    ! WRITE (*,99001) NM
                    !99001 FORMAT ('DSMC1 using ',I6,' molecules for the simulation.')
*--calculate the number of molecules that enter at each time step
                    DO 600 N=1,2
                        IF (IB(N).EQ.4) THEN
*--entering! no entering molecules - this section not used
                            DO 560 L=1,MNSP
                                VMP=SQRT(2.*BOLTZ*BFTMP(N)/SP(5,L))
*--VMP is the most probable speed in species L, see eqns (4.1) and (4.7)
                                IF (N.EQ.1) SC=BVFX(N)/VMP
                                IF (N.EQ.2) SC=-BVFX(N)/VMP
*--SC is the inward directed speed ratio
                                IF (ABS(SC).LT.10.1) A=(EXP(-SC*SC)+SPI*SC*(1.+ERF(SC)))
&                                     /(2.*SPI)
                                IF (SC.GT.10.) A=SC
                                IF (SC.LT.-10.) A=0.

```

```

*--A is the non-dimensional flux of eqn (4.22)
      IF (IFX.EQ.1) A=A*2.*PI*XB(N) !cylindrical flow
      IF (IFX.EQ.2) A=A*4.*PI*XB(N)**2
      BME(N,L)=BFND(N)*BFSP(N,L)*A*VMP*DTM/FNUM
      WRITE (*,*) ' entering mols ',BME(N,L)
560      CONTINUE
      END IF
600      CONTINUE
      RETURN
      END
* end of INIT1

* MOVE1.FOR
      SUBROUTINE MOVE1 !the NM molecules are moved over DTM
      PARAMETER (MNM=15000,MNC=20,MNSC=400,MNSP=2,MNSG=1)
      DOUBLE PRECISION COL(MNSP,MNSP),MOVT,NCOL,SELT,SEPT,CS(7,MNC,MNSP)
      DOUBLE PRECISION CSS(8,2,MNSP),DIFF
      COMMON /MOLS / NM,PP(MNM),PV(3,MNM),IPL(MNM),IPS(MNM),IR(MNM)
      COMMON /MOLSR / PR(MNM)
      COMMON /CELLS1/ CC(MNC),CG(3,MNC),IC(2,MNC,MNSG),ISC(MNSC),
&
&
      CCG(2,MNC,MNSG,MNSG),ISCG(2,MNSC,MNSG),IG(2,MNSG),
      IFC,CWR,AP,RP
      COMMON /GAS / SP(5,MNSP),SPM(6,MNSP,MNSP),ISP(MNSP),ALPH(MNSP,2)
      COMMON /GASR / SPR(3,MNSP,MNSP),ISPR(3,MNSP),CT(MNC)
      COMMON /SAMP / COL,NCOL,MOVT,SELT,SEPT,CS,TIME,NPR,NSMP,FND,FTMP,
&
&
      TIMI,FSP(MNSP),ISPD
      COMMON /SAMPS / CSS
      COMMON /COMP / FNUM,DTM,NIS,NSP,NPS,NPT
      COMMON /GEOM1 / IFX,NSC,XB(2),IB(2),BT(2),BVY(2),BFND(2),BFTMP(2),
&
&
      BVFX(2),BFSP(2,MNSP),BME(2,MNSP),BMR(2,MNSP),IIS,
      CW,FW,GRAV
      IF (ABS(GRAV).GT.1.E-6) THEN
          IGRAV=1
      ELSE
          IGRAV=0 !used, no gravity
      END IF
      IFT=-1
*--a negative IFT indicates that molecules have not entered at this step
      N=0 !initialize which molecule its working on
100      N=N+1
      IF (N.LE.NM) THEN
          IF (IFT.LT.0) AT=DTM !time step set to DTM
          IF (IFT.GT.0) AT=RF(0)*DTM !not used, no entering molecules
*--the time step is a random fraction of DTM for entering molecules
150      MOVT=MOVT+1 !keeps track of the number of moves
          MSC=IPL(N)!--IPL(N) sub-cell number for molecule N, so MSC is
          !the subcell number
          MC=ISC(MSC) !the cell which the subcell resides in - this is
          !where the molecule starts
*--MC is the initial cell number
          XI=PP(N) !the initial radial position of the molecule
          IF ((XI+0.00001*CG(3,1)).LT.XB(1)).OR.
&
&
          (XI-0.00001*CG(3,MNC)).GT.XB(2)) THEN !checks to see if
          ! molecule in the annulus
          !
          WRITE (*,*) ' MOL ',N,' OUTSIDE FLOW ',XI
          CALL REMOVE(N)
          GO TO 100

```

```

END IF
DX=PV(1,N)*AT !moves in radial direction (x)
IF (IGRAV.EQ.1) DX=DX+0.5*GRAV*AT*AT !not used
IF (IFX.GT.0) DY=PV(2,N)*AT !move in tangent direction (y)
IF (IFX.EQ.2) DZ=PV(3,N)*AT !not used
X=XI+DX !finds new radial location (x)
IF (IFX.NE.0) THEN
*--cylindrical or spherical flow
*--first check for inner boundary interactions
    IF (IB(1).NE.1) THEN !true
*--there can be no interaction with an axis or centre
    IF (X.LT.XB(1)) THEN !if radial pos. < inner radius
        CALL RBC(IFX,XI,DX,DY,DZ,XB(1),S1) !determine fractional
        !length of the trajectory in annulus
        IF (S1.LT.1.) THEN !collision with inner boundary,
        !S1 < 1 because not all trajectory lies in annulus
        IF (IB(1).GT.3) THEN !not used, molecule leaves flow
            CALL REMOVE(N)
            GO TO 100
        END IF
        DX=S1*DX !displacement in radial direction, x
        DY=S1*DY !displacement in tangential direction, y
        DZ=S1*DZ !displacement in longitudinal direction, z
        CALL AIFX(IFX,XI,DX,DY,DZ,X,PV(1,N),PV(2,N),PV(3,N))
        !the frame of reference has been rotated with regard
        !to the point of intersection with the inner surface
        IF (IB(1).EQ.2) THEN !not used
            PV(1,N)=-PV(1,N)
            PP(N)=XB(1)+0.001*CG(3,1)
            AT=AT*(1.-S1)
            GO TO 150 !finish moving molecule over the remaining
            !time step
        END IF
        IF (IB(1).EQ.3) THEN !used, molecule reflects from the
        !solid surface of boundary 1
        !FWB modified section to include incomplete accommodation
        Spec = IPS(N) !determines molecule species (1 or 2)
        Bound = 1 !surface 1
        AccomCoef = ALPH(Spec,Bound) !the accommodation
        !coefficient of that species on that surface
        RandNum = RF(0) !uniform random number between 0 and 1
        IF (RandNum.GT.AccomCoef) THEN !specular reflection
            !incident quantities on surface 1 incremented
            CSS(1,1,Spec)=CSS(1,1,Spec)+1. !the number sum of
            !molecules striking the boundary is increased by 1
            CSS(2,1,Spec)=CSS(2,1,Spec)-SP(5,Spec)*PV(1,N) !sum
            !of normal momentum (m*Vnormal) of incident molecules
            !incremented on surface 1 (PV(1,N) negative)
            CSS(4,1,Spec)=CSS(4,1,Spec)+SP(5,Spec)*(PV(2,N)-BVY(
            1)) !sum of the incident parallel momentum in
            !the y-direction
            CSS(5,1,Spec)=CSS(5,1,Spec)+0.5*SP(5,Spec)
            *(PV(1,N)**2+(PV(2,N)-BVY(1))**2+PV(3,N)**2) !sum of
            ! incident translation energy, 1/2 m*Vtot^2
            CSS(7,1,Spec)=CSS(7,1,Spec)+PR(N) !summing incident
            ! rotational energy, PR(M) is the rotational energy of
            ! molecule M

```

```

        PV(1,N)=-PV(1,N) !specular reflection
        !the molecule is moved just off the boundary
        PP(N)=XB(1)+0.001*CG(3,1)
        IPL(N)=1
        AT=AT*(1.-S1)
        !reflected quantities on surface 1 incremented
        CSS(3,1,Spec)=CSS(3,1,Spec)+SP(5,Spec)*PV(1,N) !sum
        !of normal momentum (m*Vnormal) of reflected molecules
        !incremented on surface 1 (negative PV negative)
        CSS(6,1,Spec)=CSS(6,1,Spec)-0.5*SP(5,Spec)
        *(PV(1,N)**2+(PV(2,N)-BVY(1))**2+PV(3,N)**2)
        !sum of reflected translation energy, 1/2 m*Vtot^2
        CSS(8,1,Spec)=CSS(8,1,Spec)-PR(N)
        !summing reflected rotational energy, PR(M) is the
        !rotational energy of molecule M
    ELSE !diffuse reflection
        CALL REFLECT1(N,1)!diffuse reflection from surface
        AT=AT*(1.-S1)!AT is the remaining in the time step
        !for this molecule
    END IF
    GO TO 150 !finish moving molecule over the remaining
    !time step
    !End FWB modified section
END IF
END IF
END IF
END IF
RR=X*X+DY*DY+(IFX-1)*DZ*DZ !The resultant vector is
!sqrt(x^2+dy^2)=RR
!molecule always starts out at y = 0, so DY^2 is its length
IF (RR.GT.XB(2)*XB(2)) THEN !if rad. pos. > than outer radius
    CALL RBC(IFX,XI,DX,DY,DZ,XB(2),S1) !determine fractional
    !length of the trajectory in annulus
    IF (S1.LT.1.) THEN !collision with outer boundary, S1 < 1
    !because not all trajectory lies in annulus
        IF (IB(2).GT.3) THEN !molecule leaves flow
            CALL REMOVE(N)
            GO TO 100
        END IF
        DX=S1*DX !displacement in radial direction, x
        DY=S1*DY !displacement in tangential direction, y
        DZ=S1*DZ !displacement in longitudinal direction, z
        CALL AIFX(IFX,XI,DX,DY,DZ,X,PV(1,N),PV(2,N),PV(3,N))
*--the frame of reference has been rotated with regard to the point of
*----intersection with the outer surface
        IF (IB(2).EQ.2) THEN !not used
*--specular reflection from the boundary
            PV(1,N)=-PV(1,N)
            PP(N)=XB(2)-0.001*CG(3,1)
            AT=AT*(1.-S1)
            GO TO 150
        END IF
        IF (IB(2).EQ.3) THEN !used, coll. with solid boundary 2
            !FWB modified section to include incomplete accommodation
            Spec = IPS(N) !determines molecule species (1 or 2)
            Bound = 2 !surface 2
            AccomCoef = ALPH(Spec,Bound) !the accommodation

```

```

!coefficient of that species on that surface
RandNum = RF(0) !uniform random number between 0 and 1
IF (RandNum.GT.AccomCoef) THEN !specular reflection
  !incident quantities on surface 2 incremented
  CSS(1,2,Spec)=CSS(1,2,Spec)+1. !the number sum of
  !molecules striking the boundary is increased by 1
  CSS(2,2,Spec)=CSS(2,2,Spec)+SP(5,Spec)*PV(1,N) !sum
  !of normal momentum (m*Vnormal) of incident molecules
  !incremented on surface 1 (negative PV negative)
  CSS(4,2,Spec)=CSS(4,2,Spec)+SP(5,Spec)*(PV(2,N)-BVY(
  2)) !sum of the incident parallel momentum in the
  ! y-direction
  CSS(5,2,Spec)=CSS(5,2,Spec)+0.5*SP(5,Spec)
  *(PV(1,N)**2+(PV(2,N)-BVY(2))**2+PV(3,N)**2) !sum
  !of incident translation energy, 1/2 m*Vtot^2
  CSS(7,2,Spec)=CSS(7,2,Spec)+PR(N) !summing incident
  !rotational energy, PR(M) is the rotational energy of
  !molecule M
  PV(1,N)=-PV(1,N) !specular reflection
  !the molecule is moved just off the boundary
  PP(N)=XB(2)-0.001*CG(3,MNC)
  IPL(N)=MNSC
  AT=AT*(1.-S1)
  !reflected quantities on surface 2 incremented
  CSS(3,2,Spec)=CSS(3,2,Spec)-SP(5,Spec)*PV(1,N)
  !reflected momentum
  CSS(6,2,Spec)=CSS(6,2,Spec)-0.5*SP(5,Spec)
  *(PV(1,N)**2+(PV(2,N)-BVY(2))**2+PV(3,N)**2)
  !sum of reflected translational energy
  CSS(8,2,Spec)=CSS(8,2,Spec)-PR(N) !sum of reflected
  !rotational energy
ELSE !diffuse reflection
  CALL REFLECT1(N,2)!diffuse reflection from surface
  AT=AT*(1.-S1)!AT is the remaining in the time step
  !for this molecule
END IF
GO TO 150 !finish moving molecule over remaining time
  !step
  !End FWB modified section
END IF
END IF
END IF
  *--calculate the end of the trajectory
  CALL AIFX(IFX,XI,DX,DY,DZ,X,PV(1,N),PV(2,N),PV(3,N))
  * plane flow
  *--molecule N at XI is moved by DX to X
  ELSE IF (X.LT.XB(1).OR.X.GT.XB(2)) THEN !for plane geometry
    IF (X.LT.XB(1)) K=1
    IF (X.GT.XB(2)) K=2
  *--intersection with inner, outer boundary for K=1, 2
  IF (IB(K).EQ.2) THEN
  *--specular reflection from the boundary (eqn (11.7))
    X=2.*XB(K)-X
    PV(1,N)=-PV(1,N)
  END IF
  IF (IB(K).GT.3) THEN
  *--molecule leaves flow

```



```

        CALL REMOVE(N)
        GO TO 100
    END IF
    IF (IB(K).EQ.3) THEN
*--AT is the remaining in the time step for this molecule
        AT=AT-(XB(K)-XI)/PV(1,N)
*--molecule reflects from the surface
        CALL REFLECT1(N,K)
        GO TO 150
    END IF
*--no boundary interactions
    END IF
* now has to determine the cell and subcell it moved to
    IF (X.LT.CG(1,MC).OR.X.GT.CG(2,MC)) THEN
*--the molecule has moved from the initial cell
    IF (IFC.EQ.0) THEN !if uniform cell widths then
        MC=(X-XB(1))/CW+0.99999 !find the new cell
    ELSE
        XD=(X-XB(1))/FW+1.E-6
        MC=1.+(LOG(1.-XD*AP))/RP
*--the cell number is calculated from eqn (12.1)
    END IF
    IF (MC.LT.1) MC=1
    IF (MC.GT.MNC) MC=MNC
*--MC is the new cell number (note avoidance of round-off error)
    END IF
    MSC=((X-CG(1,MC))/CG(3,MC))*(NSC-.001)+1+NSC*(MC-1)
*--MSC is the new sub-cell number
    IF (MSC.LT.1) MSC=1
    IF (MSC.GT.MNSC) MSC=MNSC
    IPL(N)=MSC !resets the subcell it's in
    PP(N)=X !resets its radial position
    IF (IGRAV.EQ.1) PV(1,N)=PV(1,N)+GRAV*AT !not used
    GO TO 100 !end of loop, go back up to the next molecule
ELSE IF (IFT.LT.0) THEN
    IFT=1 !not used
*--new molecules enter
    CALL ENTER1 !not used
    N=N-1
    GO TO 100
END IF
RETURN
END

* ENTER1.FOR !not used
SUBROUTINE ENTER1
*--new molecules enter at boundaries
* PARAMETER (MNM=10000,MNC=200,MNSC=2000,MNSP=2,MNSG=1)
PARAMETER (MNM=15000,MNC=20,MNSC=400,MNSP=2,MNSG=1)
DOUBLE PRECISION COL(MNSP,MNSP),MOV,T,NCOL,SELT,SEPT,CS(7,MNC,MNSP)
COMMON /MOLS / NM,PP(MNM),PV(3,MNM),IPL(MNM),IPS(MNM),IR(MNM)
COMMON /MOLSR / PR(MNM)
COMMON /CELLS1/ CC(MNC),CG(3,MNC),IC(2,MNC,MNSG),ISC(MNSC),
& CCG(2,MNC,MNSG,MNSG),ISCG(2,MNSC,MNSG),IG(2,MNSG),
& IFC,CWR,AP,RP
COMMON /GAS / SP(5,MNSP),SPM(6,MNSP,MNSP),ISP(MNSP)
COMMON /GASR / SPR(3,MNSP,MNSP),ISPR(3,MNSP),CT(MNC)

```

```

COMMON /SAMP / COL,NCOL,MOV,T,SELT,SEPT,CS,TIME,NPR,NSMP,FND,FTMP,
&
TIMI,FSP(MNSP),ISPD
COMMON /COMP / FNUM,DTM,NIS,NSP,NPS,NPT
COMMON /GEOM1 / IFX,NSC,XB(2),IB(2),BT(2),BVY(2),BFND(2),BFTMP(2),
&
BVFX(2),BFSP(2,MNSP),BME(2,MNSP),BMR(2,MNSP),IIS,
&
CW,FW,GRAV
COMMON /CONST / PI,SPI,BOLTZ

DO 100 N=1,2
*--consider each boundary in turn
DO 50 L=1,MNSP
*--consider each species in turn
A=BME(N,L)+BMR(N,L)
M=A
BMR(N,L)=A-M
*--M molecules enter, remainder has been reset
IF (M.GT.0) THEN
VMP=SQRT(2.*BOLTZ*BFTMP(N)/SP(5,L))
IF (ABS(BVFX(N)).GT.1.E-6) THEN
IF (N.EQ.1) SC=BVFX(N)/VMP
IF (N.EQ.2) SC=-BVFX(N)/VMP
FS1=SC+SQRT(SC*SC+2.)
FS2=0.5*(1.+SC*(2.*SC-FS1))
END IF
* the above constants are required for the entering distn. of eqn (12.5)
DO 10 K=1,M
IF (NM.LT.MNM) THEN
NM=NM+1
*--NM is now the number of the new molecule
IF (ABS(BVFX(N)).GT.1.E-6) THEN
QA=3.
IF (SC.LT.-3.) QA=ABS(SC)+1.
2
U=-QA+2.*QA*RF(0)
*--U is a potential normalised thermal velocity component
UN=U+SC
*--UN is a potential inward velocity component
IF (UN.LT.0.) GO TO 2
A=(2.*UN/FS1)*EXP(FS2-U*U)
IF (A.LT.RF(0)) GO TO 2
*--the inward normalised vel. component has been selected (eqn (12.5))
IF (N.EQ.1) PV(1,NM)=UN*VMP
IF (N.EQ.2) PV(1,NM)=-UN*VMP
ELSE
IF (N.EQ.1) PV(1,NM)=SQRT(-LOG(RF(0)))*VMP
IF (N.EQ.2) PV(1,NM)=-SQRT(-LOG(RF(0)))*VMP
*--for a stationary external gas, use eqn (12.3)
END IF
CALL RVELC(PV(2,NM),PV(3,NM),VMP)
*--a single call of RVELC generates the two normal velocity components
IF (ISPR(1,L).GT.0) CALL SROT(PR(NM),BFTMP(N),ISPR(1,L))
IF (N.EQ.1) PP(NM)=XB(1)+0.001*CG(3,1)
IF (N.EQ.2) PP(NM)=XB(2)-0.001*CG(3,MNC)
*--the molecule is moved just off the boundary
IPS(NM)=L
IF (N.EQ.1) IPL(NM)=1
IF (N.EQ.2) IPL(NM)=MNSC
ELSE

```

```

                WRITE (*,*)
&' WARNING: EXCESS MOLECULE LIMIT - RESTART WITH AN INCREASED FNUM'
                END IF
10             CONTINUE
                END IF
50             CONTINUE
100            CONTINUE
                RETURN
                END

* REFLECT1.FOR !diffuse reflection of molecule N from surface K
SUBROUTINE REFLECT1(N,K)
PARAMETER (MNM=15000,MNC=20,MNSC=400,MNSP=2,MNSG=1)
DOUBLE PRECISION COL(MNSP,MNSP),MOVT,NCOL,SELT,SEPT,CS(7,MNC,MNSP)
DOUBLE PRECISION CSS(8,2,MNSP)
COMMON /MOLS / NM,PP(MNM),PV(3,MNM),IPL(MNM),IPS(MNM),IR(MNM)
COMMON /MOLSR / PR(MNM)
COMMON /CELLS1/ CC(MNC),CG(3,MNC),IC(2,MNC,MNSG),ISC(MNSC),
&
&
                CCG(2,MNC,MNSG,MNSG),ISCG(2,MNSC,MNSG),IG(2,MNSG),
                IFC,CWR,AP,RP
COMMON /GAS / SP(5,MNSP),SPM(6,MNSP,MNSP),ISP(MNSP)
COMMON /GASR / SPR(3,MNSP,MNSP),ISPR(3,MNSP),CT(MNC)
COMMON /SAMP / COL,NCOL,MOVT,SELT,SEPT,CS,TIME,NPR,NSMP,FND,FTMP,
&
                TIMI,FSP(MNSP),ISPD
COMMON /SAMPS / CSS
COMMON /COMP / FNUM,DTM,NIS,NSP,NPS,NPT
COMMON /GEOM1 / IFX,NSC,XB(2),IB(2),BT(2),BVY(2),BFND(2),BFTMP(2),
&
                BVFX(2),BFSP(2,MNSP),BME(2,MNSP),BMR(2,MNSP),IIS,
                CW,FW,GRAV
COMMON /CONST / PI,SPI,BOLTZ
L=IPS(N) ! determines which species it is
*----sample the surface properties due to the incident molecules
*----CSS(N,M,L) sampled info. on the molecules striking the boundaries
*-----M=1, 2 for the inner, outer boundaries; L is the species
*-----N=1 the number sum
*-----N=2 the sum of the normal momentum of the incident molecules
*-----N=3 the sum of the normal momentum for the reflected molecules
*-----N=4 the sum of the incident parallel momentum in the y direction
*-----N=5 the sum of the incident translational energy
*-----N=6 the sum of the reflected translational energy
*-----N=7 the sum of the incident rotational energy
*-----N=8 the sum of the reflected rotational energy
CSS(1,K,L)=CSS(1,K,L)+1. !the number sum of molecules striking
!the boundary is increased by 1
IF (K.EQ.1) CSS(2,K,L)=CSS(2,K,L)-SP(5,L)*PV(1,N) !sum of normal
!momentum (m*Vnormal) of incident molecules incremented on surface 1
!(negative PV negative)
IF (K.EQ.2) CSS(2,K,L)=CSS(2,K,L)+SP(5,L)*PV(1,N) !on surface 2
CSS(4,K,L)=CSS(4,K,L)+SP(5,L)*(PV(2,N)-BVY(K)) !sum of the
!incident parallel momentum in the y-direction
CSS(5,K,L)=CSS(5,K,L)+0.5*SP(5,L)
&
                *(PV(1,N)**2+(PV(2,N)-BVY(K))**2+PV(3,N)**2) !sum of
!incident translation energy, 1/2 m*Vtot^2
CSS(7,K,L)=CSS(7,K,L)+PR(N) !summing incident rotational energy,
!PR(M) is the rotational energy of molecule M
*--Diffuse reflection
VMP=SQRT(2.*BOLTZ*BT(K)/SP(5,L))

```

```

*--VMP is the most probable speed in species L, see eqns (4.1) and (4.7)
  IF (K.EQ.1) PV(1,N)=SQRT(-LOG(RF(0)))*VMP
  IF (K.EQ.2) PV(1,N)=-SQRT(-LOG(RF(0)))*VMP
*--the normal velocity component has been generated (eqn(12.3))
  CALL RVELC(PV(2,N),PV(3,N),VMP)
*--a single call of RVELC generates the two parallel velocity components
  PV(2,N)=PV(2,N)+BVY(K)
  IF (ISPR(1,L).GT.0) CALL SROT(PR(N),BT(K),ISPR(1,L))
  IF (K.EQ.1) PP(N)=XB(1)+0.001*CG(3,1)
  IF (K.EQ.2) PP(N)=XB(2)-0.001*CG(3,MNC)
*--the molecule is moved just off the boundary
  IF (K.EQ.1) IPL(N)=1
  IF (K.EQ.2) IPL(N)=MNSC
*--sample the surface properties due to the reflected molecules
  IF (K.EQ.1) CSS(3,K,L)=CSS(3,K,L)+SP(5,L)*PV(1,N)
  IF (K.EQ.2) CSS(3,K,L)=CSS(3,K,L)-SP(5,L)*PV(1,N)
  CSS(6,K,L)=CSS(6,K,L)-0.5*SP(5,L)
  &      *(PV(1,N)**2+(PV(2,N)-BVY(K))**2+PV(3,N)**2)
  CSS(8,K,L)=CSS(8,K,L)-PR(N)
  RETURN
  END

*   REMOVE.FOR
  SUBROUTINE REMOVE(N)
*--remove molecule N and replace it by molecule NM
  PARAMETER (MNM=15000,MNC=20,MNSC=400,MNSP=2,MNSG=1)
  COMMON /MOLS / NM,PP(MNM),PV(3,MNM),IPL(MNM),IPS(MNM),IR(MNM)
  COMMON /MOLSR / PR(MNM)
  PP(N)=PP(NM)
  DO 100 M=1,3
    PV(M,N)=PV(M,NM)
100  CONTINUE
  PR(N)=PR(NM)
  IPL(N)=IPL(NM)
  IPS(N)=IPS(NM)
  NM=NM-1
  N=N-1
  RETURN
  END

*   SAMPI1.FOR
  SUBROUTINE SAMPI1
*--initialises all the sampling variables
  PARAMETER (MNM=15000,MNC=20,MNSC=400,MNSP=2,MNSG=1)
  DOUBLE PRECISION COL(MNSP,MNSP),MOVT,NCOL,SELT,SEPT,CS(7,MNC,MNSP)
  DOUBLE PRECISION CSR(MNC,MNSP)
  DOUBLE PRECISION CSS(8,2,MNSP)
  DOUBLE PRECISION CSH(3,MNC,MNSP)
  COMMON /SAMP / COL,NCOL,MOVT,SELT,SEPT,CS,TIME,NPR,NSMP,FND,FTMP,
  &      TIMI,FSP(MNSP),ISPD
  COMMON /SAMPR / CSR
  COMMON /SAMPS / CSS
  COMMON /SAMPH / CSH
  COMMON /COMP / FNUM,DTM,NIS,NSP,NPS,NPT

  NSMP=0 !number of samples set to 0
  TIMI=TIME !initial time of sample

```

```

    DO 200 L=1,MNSP !for each species
      DO 50 N=1,MNC !for each cell
*--CS(M,N,L) sampled information on species L in cell N
*----M=1 number sum
*----M=2,3,4 sum of u,v,w
*----M=5,6,7 sum of u*u,v*v,w*w
      CS(1,N,L)=1.E-6
      DO 20 M=2,7
        CS(M,N,L)=0.
20      CONTINUE
*--(CSH(M,N,L) higher order sampling in cell N of species L
*----M=1 sum of u*v
*----M=2 sum of c**2*u
*----M=3 sum of rotl. energy*u
      DO 40 M=1,3
        CSH(M,N,L)=0.
40      CONTINUE
*--CSR(N,L) the sum of the rotational energy of species L in cell N
      CSR(N,L)=0.
50      CONTINUE
*--CSS(M,N,L) sampled info. on the molecules striking the boundaries
*----N=1, 2 for the inner, outer boundaries; L is the species
*----M=1 the number sum
*----M=2 the sum of the normal momentum of the incident molecules
*----M=3 the sum of the normal momentum for the reflected molecules
*----M=4 the sum of the incident parallel momentum in the y direction
*----M=5 the sum of the incident translational energy
*----M=6 the sum of the reflected translational energy
*----M=7 the sum of the incident rotational energy
*----M=8 the sum of the reflected rotational energy
      DO 100 N=1,2
        CSS(1,N,L)=1.E-6
        DO 60 M=2,8
          CSS(M,N,L)=0.
60      CONTINUE
100     CONTINUE
200     CONTINUE
      RETURN
      END

*  SAMPLE1.FOR
      SUBROUTINE SAMPLE1
*--sample the molecules in the flow.
      PARAMETER (MNM=15000,MNC=20,MNSC=400,MNSP=2,MNSG=1)
      DOUBLE PRECISION COL(MNSP,MNSP),MOVT,NCOL,SELT,SEPT,CS(7,MNC,MNSP)
      DOUBLE PRECISION CSR(MNC,MNSP)
      DOUBLE PRECISION CSH(3,MNC,MNSP)

      COMMON /MOLS / NM,PP(MNM),PV(3,MNM),IPL(MNM),IPS(MNM),IR(MNM)
      COMMON /MOLSR / PR(MNM)
      COMMON /CELLS1/ CC(MNC),CG(3,MNC),IC(2,MNC,MNSG),ISC(MNSC),
&
&
&                CCG(2,MNC,MNSG,MNSG),ISCG(2,MNSC,MNSG),IG(2,MNSG),
&                IFC,CWR,AP,RP
      COMMON /SAMP / COL,NCOL,MOVT,SELT,SEPT,CS,TIME,NPR,NSMP,FND,FTMP,
&
&                TIMI,FSP(MNSP),ISPD
      COMMON /SAMPR / CSR
      COMMON /SAMPH / CSH

```

```

COMMON /COMP / FNUM,DTM,NIS,NSP,NPS,NPT
NSMP=NSMP+1 !increment the number of samples taken
DO 100 NN=1,MNSG !for each gas species
  DO 50 N=1,MNC !for each cell
    L=IC(2,N,NN)
    IF (L.GT.0) THEN
      DO 10 J=1,L
        K=IC(1,N,NN)+J
        M=IR(K)
        I=IPS(M)
        CS(1,N,I)=CS(1,N,I)+1
        CSQ=0.
        DO 5 LL=1,3
          CS(LL+1,N,I)=CS(LL+1,N,I)+PV(LL,M)
          CS(LL+4,N,I)=CS(LL+4,N,I)+PV(LL,M)**2
          CSQ=CSQ+PV(LL,M)**2
5        CONTINUE
        CSR(N,I)=CSR(N,I)+PR(M)
        CSH(1,N,I)=CSH(1,N,I)+PV(1,M)*PV(2,M)
        CSH(2,N,I)=CSH(2,N,I)+CSQ*PV(1,M)
        CSH(3,N,I)=CSH(3,N,I)+PR(M)*PV(1,M)
10       CONTINUE
      END IF
50     CONTINUE
100    CONTINUE
      RETURN
      END

* OUT1.FOR
  SUBROUTINE OUT1
*--output a progressive set of results to file DSMC.OUT.
  PARAMETER (MNM=15000,MNC=20,MNSC=400,MNSP=2,MNSG=1)
  DOUBLE PRECISION COL(MNSP,MNSP),MOVT,NCOL,SELT,SEPT,CS(7,MNC,MNSP)
  DOUBLE PRECISION CSR(MNC,MNSP)
  DOUBLE PRECISION CSS(8,2,MNSP)
  DOUBLE PRECISION CSH(3,MNC,MNSP)
  CHARACTER*9 FNAME
  COMMON /MOLS / NM,PP(MNM),PV(3,MNM),IPL(MNM),IPS(MNM),IR(MNM)
  COMMON /MOLSR / PR(MNM)
  COMMON /CELLS1/ CC(MNC),CG(3,MNC),IC(2,MNC,MNSG),ISC(MNSC),
& CCG(2,MNC,MNSG,MNSG),ISCG(2,MNSC,MNSG),IG(2,MNSG),
& IFC,CWR,AP,RP
  COMMON /GAS / SP(5,MNSP),SPM(6,MNSP,MNSP),ISP(MNSP)
  COMMON /GASR / SPR(3,MNSP,MNSP),ISPR(3,MNSP),CT(MNC)
  COMMON /SAMP / COL,NCOL,MOVT,SELT,SEPT,CS,TIME,NPR,NSMP,FND,FTMP,
& TIMI,FSP(MNSP),ISPD
  COMMON /SAMPR / CSR
  COMMON /SAMPS / CSS
  COMMON /SAMPH / CSH
  COMMON /GEOM1 / IFX,NSC,XB(2),IB(2),BT(2),BVY(2),BFND(2),BFTMP(2),
& BVFX(2),BFSP(2,MNSP),BME(2,MNSP),BMR(2,MNSP),IIS,
& CW,FW,GRAV
  COMMON /COMP / FNUM,DTM,NIS,NSP,NPS,NPT
  COMMON /CONST / PI,SPI,BOLTZ
  DOUBLE PRECISION VEL(3),SMU(3),SVEL(3,MNC),SN,SM,SMCC,SRDF,SRE,TT,
& TROT,DBOLTZ,SS(8),SUV,SCCU,SRU,SUU
  COMMON /OP / QC(2),Ps(2) !FWB added

```

```

DBOLTZ=BOLTZ

FNAME = 'DSMC.OUT'
OPEN (4,FILE=FNAME,FORM='FORMATTED')
WRITE(4,*) 'ModelINPUTS '
WRITE(4,*) IFX,IIS,FTMP,FND,FSP(1),FNUM,DTM,XB(1),XB(2),IB(1),
&BT(1),BVY(1),IB(2),BT(2),BVY(2),SP(1,1),SP(2,1),SP(3,1),SP(4,1),
&SP(5,1),ISPR(1,1),SPR(1,1,1),ISPR(2,1),NIS,NSP,NPS,NPT
WRITE(4,*) ' '
WRITE(4,*) 'ModelPARAMETERS '
WRITE(4,*) MNM,MNC,MNSC,MNSP,MNSG
WRITE(4,*) ' '
WRITE(4,*) ' FLOW SAMPLED FROM TIME ',TIMI,' TO TIME ',TIME
WRITE(4,*) ' COLLISIONS:-'
WRITE(4,99001) ((IDINT(COL(M,L)),M=1,MNSP),L=1,MNSP)
99001 FORMAT (5I12)
WRITE(4,*) ' TOTAL NUMBER OF SAMPLES ',NSMP
WRITE(4,*) NM,' MOLECULES'
WRITE(4,*) MOVT,' TOTAL MOLECULAR MOVES'
IF (NCOL.GT.0) THEN
    WRITE(4,*) INT(SELT),' SELECTIONS ',INT(NCOL),
&          ' COLLISION EVENTS, RATIO ',REAL(NCOL/SELT)
    IF (NCOL.GT.0) WRITE(4,*) ' MEAN COLLISION SEPARATION ',
&          REAL(SEPT/NCOL)
END IF
DO 100 K=1,2 !for each boundary
    IF (IB(K).EQ.3) THEN
        IF (K.EQ.1) WRITE(4,*) ' INNER SURFACE PROPERTIES '
        IF (K.EQ.2) WRITE(4,*) ' OUTER SURFACE PROPERTIES '
        IF (IFX.EQ.0) A=FNUM/(TIME-TIMI)
        IF (IFX.EQ.1) A=FNUM/((TIME-TIMI)*2.*PI*XB(K))
        !for cylindrical flow
        IF (IFX.EQ.2) A=FNUM/((TIME-TIMI)*4.*PI*XB(K)*XB(K))
        DO 20 N=1,8
            SS(N)=0.
            DO 10 L=1,MNSP
                SS(N)=SS(N)+CSS(N,K,L)
10          CONTINUE
20          CONTINUE
        WRITE(4,*) ' SAMPLE FRACTION SPECIES 1, SPECIES 2....'
        WRITE(4,99002) SS(1),(CSS(1,K,L)/SS(1),L=1,MNSP)
99002 FORMAT (F12.1,6F12.6)
        DO 40 N=1,8
            SS(N)=SS(N)*A
40          CONTINUE
        WRITE(4,*) ' NUM FLUX INC PRESS REFL PRESS SHEAR STR '
        WRITE(4,99003) (SS(N),N=1,4)
99003 FORMAT (6E12.5)
        Ps(K) = SS(2)+SS(3) !FWB added
        WRITE(4,*)
& ' INC TR EN REFL TR EN INC ROT EN REFL ROT EN NET HEAT FLUX '
        WRITE(4,99003) (SS(N),N=5,8),SS(5)+SS(6)+SS(7)+SS(8)
        IF (K.EQ.1) THEN
            QC(K) = -1*(SS(5)+SS(6)+SS(7)+SS(8))*2*PI*XB(K) !FWB added
        ELSE
            QC(K) = (SS(5)+SS(6)+SS(7)+SS(8))*2*PI*XB(K) !FWB added
        ENDIF
    END DO

```

```

      END IF
100  CONTINUE
      WRITE (4,*) 'SAMPLES'
      WRITE (4,*) ' CELL      N SP 1      N SP 2      ETC '
      DO 200 N=1,MNC
          WRITE (4,99004) N,(IDINT(CS(1,N,L)),L=1,MNSP)
200  CONTINUE
99004 FORMAT (' ',I6,5I9)
      WRITE (4,*) ' FLOWFIELD_PROPERTIES'
      WRITE (4,*)
& ' CELL      X COORD      DENSITY      TR TEMP      ROT TEMP      OV_TEMP      U
&          V          W      SHEAR STRESS      HEAT FLUX'
*--first the mixture properties
      DO 400 N=1,MNC
          A=FNUM/(CC(N)*NSMP)
          SN=0.
          SM=0.
          DO 250 K=1,3
              SMU(K)=0.
250  CONTINUE
          SMCC=0.
          SRE=0.
          SRDF=0.
          SUV=0.
          SUU=0.
          SCCU=0.
          SRU=0.
          DO 300 L=1,MNSP
              SN=SN+CS(1,N,L)
*--SN is the number sum
*--CS(M,N,L) sampled information on species L in cell N
*----M=1 number sum
              SM=SM+SP(5,L)*CS(1,N,L)
*--SM is the sum of molecular masses
              DO 260 K=1,3
                  SMU(K)=SMU(K)+SP(5,L)*CS(K+1,N,L)
*--SMU(1 to 3) are the sum of mu, mv, mw
260  CONTINUE
                  SMCC=SMCC+(CS(5,N,L)+CS(6,N,L)+CS(7,N,L))*SP(5,L)
*--SMCC is the sum of  $m(u^{**2}+v^{**2}+w^{**2})$ 
                  SRE=SRE+CSR(N,L)
*--SRE is the sum of rotational energy
                  SRDF=SRDF+ISPR(1,L)*CS(1,N,L)
*--SRDF is the sum of the rotational degrees of freedom
                  SUU=SUU+SP(5,L)*CS(5,N,L)
*--SUU is the sum of  $m*u*u$ 
                  SUV=SUV+SP(5,L)*CSH(1,N,L)
*--SUV is the sum of  $m*u*v$ 
                  SCCU=SCCU+SP(5,L)*CSH(2,N,L)
*--SCCU is the sum of  $m*c^{**2}*u$ 
                  SRU=SRU+CSH(3,N,L)
*--SRU is the sum of rotl. energy * u
300  CONTINUE
                  DENN=SN*A
*--DENN is the number density, see eqn (1.34)
                  DEN=DENN*SM/SN
*--DEN is the density, see eqn (1.42)

```



```

        DO 350 K=1,3
            VEL(K)=SMU(K)/SM
            SVEL(K,N)=VEL(K)
350    CONTINUE
*--VEL and SVEL are the stream velocity components, see eqn (1.43)
        UU=VEL(1)**2+VEL(2)**2+VEL(3)**2
        TT=(SMCC-SM*UU)/(3.D00*DBOLTZ*SN)
*--TT is the translational temperature, see eqn (1.51)
        IF (SRDF.GT.1.E-6) TROT=(2.D00/DBOLTZ)*SRE/SRDF
*--TROT is the rotational temperature, see eqn (11.11)
        TEMP=(3.D00*TT+(SRDF/SN)*TROT)/(3.+SRDF/SN)
*--TEMP is the overall temperature, see eqn (11.12)
        CT(N)=TEMP
        TXY=-DENN*SUV/SN
*--TXY is the xy component of shear stress (see eqn (12.13))
        QX=DENN*(0.5*SCCU-SUV*VEL(2)-(SUU-SM*VEL(1)**2+0.5*SMCC+SRE)
&        *VEL(1)+SRU)/SN
*--QX is the x component of the heat flux vector (see eqn (12.14))
        XC=0.5*(CG(1,N)+CG(2,N))
*--XC is the x coordinate of the midpoint of the cell
        WRITE (4,99005) N,XC,DEN,TT,TROT,TEMP,VEL(1),VEL(2),VEL(3),TXY,
&        QX
99005    FORMAT (' ',I5,F10.4,1P,E12.4,0P,6F10.4,2E12.4)
400    CONTINUE

        WRITE (4,*)
        DO 500 L=1,MNSP
*--now the properties of the separate species
        WRITE (4,*) ' SPECIES ',L
        WRITE (4,*)
&        ' CELL    X COORD        N DENS        DENSITY        TTX        TTY        T
&        TZ      TR TEMP      ROT TEMP      TEMP      U DIF VEL V DIF VEL W DIF VEL '
        DO 450 N=1,MNC
            A=FNUM/(CC(N)*NSMP)
            DENN=CS(1,N,L)*A
*--DENN is the partial number density
            DEN=SP(5,L)*DENN
*--DEN is the partial density, see eqn (1.13)
            DO 420 K=1,3
                VEL(K)=CS(K+1,N,L)/CS(1,N,L)
*--VEL defines the average velocity of the species L molecules
420    CONTINUE
            UU=VEL(1)**2+VEL(2)**2+VEL(3)**2
            TTX=(SP(5,L)/DBOLTZ)*(CS(5,N,L)/CS(1,N,L)-VEL(1)**2)
            TTY=(SP(5,L)/DBOLTZ)*(CS(6,N,L)/CS(1,N,L)-VEL(2)**2)
            TTZ=(SP(5,L)/DBOLTZ)*(CS(7,N,L)/CS(1,N,L)-VEL(3)**2)
*--the component temperatures are based on eqn (1.30)
            TT=(SP(5,L)/(3.D00*DBOLTZ))
&            *((CS(5,N,L)+CS(6,N,L)+CS(7,N,L))/CS(1,N,L)-UU)
*--TT is the translational temperature, see eqn (1.29)
            IF (ISPR(1,L).GT.0) THEN
                TROT=2.D00*CSR(N,L)/(ISPR(1,L)*DBOLTZ*CS(1,N,L))
            ELSE
                TROT=0.
            END IF
*--TROT is the rotational temperature, see eqn (11.10)
            TEMP=(3.D00*TT+ISPR(1,L)*TROT)/(3.+ISPR(1,L))

```

```

        DO 440 K=1,3
            VEL(K)=VEL(K)-SVEL(K,N)
*--VEL now defines the diffusion velocity of species L, see eqn (1,45)
440      CONTINUE
            XC=0.5*(CG(1,N)+CG(2,N))
            WRITE (4,99006) N,XC,DENN,DEN,TTX,TTY,TTZ,TT,TROT,TEMP,VEL(1),
&          VEL(2),VEL(3)
99006    FORMAT (' ',I5,F9.4,1P,2E12.4,0P,9F10.4)
450      CONTINUE
500      CONTINUE
            CLOSE (4)
            RETURN
            END

*      SROT.FOR
        SUBROUTINE SROT(PR,TEMP,IDF)
*--selects a typical equilibrium value of the rotational energy PR at
*----the temperature TEMP in a gas with IDF rotl. deg. of f.
        COMMON /CONST / PI,SPI,BOLTZ
        IF (IDF.EQ.2) THEN
            PR=-LOG(RF(0))*BOLTZ*TEMP
*--for 2 degrees of freedom, the sampling is directly from eqn (11.22)
        ELSE
*--otherwise apply the acceptance-rejection method to eqn (11.23)
            A=0.5*IDF-1.
50          ERM=RF(0)*10.
*--the cut-off internal energy is 10 kT
            B=((ERM/A)**A)*EXP(A-ERM)
            IF (B.LT.RF(0)) GO TO 50
            PR=ERM*BOLTZ*TEMP
        END IF
        RETURN
        END

*      RBC.FOR
        SUBROUTINE RBC(IFX,XI,DX,DY,DZ,R,S)
*----calculates the trajectory fraction S from a point at radius XI with
*----displacements DX, DY, and DZ to a possible intersection with a
*----surface of radius R, IFX=1, 2 for cylindrical, spherical geometry
            DD=DX*DX+DY*DY !hypotenuse length formed by DX and DY
            IF (IFX.EQ.2) DD=DD+DZ*DZ !not used
            B=XI*DX/DD
            C=(XI*XI-R*R)/DD
            A=B*B-C
            IF (A.GE.0.) THEN
*--find the least positive solution to the quadratic
                A=SQRT(A)
                S1=-B+A
                S2=-B-A
                IF (S2.LT.0.) THEN
                    IF (S1.GT.0.) THEN
                        S=S1
                    ELSE
                        S=2.
                    END IF
                ELSE IF (S1.LT.S2) THEN
                    S=S1
                END IF
            END IF
        END

```

```

        ELSE
            S=S2
        END IF
    ELSE
        S=2.
*--setting S to 2 indicates that there is no intersection
    END IF
    RETURN
END

*   AIFX.FOR
    SUBROUTINE AIFX(IFX,XI,DX,DY,DZ,X,U,V,W)
*----calculates the new radius and realigns the velocity components in
*----cylindrical (IFX=1) and spherical (IFX=2) flows
    IF (IFX.EQ.1) THEN !used
        DR=DY
        VR=V
    ELSE IF (IFX.EQ.2) THEN
        DR=SQRT(DY*DY+DZ*DZ)
        VR=SQRT(V*V+W*W)
    END IF
    A=XI+DX
    X=SQRT(A*A+DR*DR) !calculates new radius
    S=DR/X !sin theta = this ratio
    C=A/X !cos theta = this ratio
    B=U !old radial velocity saved in B
    U=B*C+VR*S !rotation about z-axes
    V=-B*S+VR*C !now u in radial direction and v perpendicular to that
    IF (IFX.EQ.2) THEN ! not used
        VR=V
        A=6.2831853*RF(0)
        V=VR*SIN(A)
        W=VR*COS(A)
    END IF
    RETURN
END

*   ERF.FOR
    FUNCTION ERF(S)
*--calculates the error function of S
    B=ABS(S)
    IF (B.GT.4.) THEN
        D=1.
    ELSE
        C=EXP(-B*B)
        T=1./(1.+0.3275911*B)
        D=1.-(0.254829592*T-0.284496736*T*T+1.421413741*T*T*T-
& 1.453152027*T*T*T*T+1.061405429*T*T*T*T*T)*C
    END IF
    IF (S.LT.0.) D=-D
    ERF=D
    RETURN
END

*   INDEXM.FOR !sorts molecules into cells and subcells based on radial
!position
    SUBROUTINE INDEXM

```

```

*--the NM molecule numbers are arranged in order of the molecule groups
*--and, within the groups, in order of the cells and, within the cells,
*--in order of the sub-cells
*
  PARAMETER (MNM=10000,MNC=200,MNSC=2000,MNSP=2,MNSG=1)
  PARAMETER (MNM=15000,MNC=20,MNSC=400,MNSP=2,MNSG=1)

  COMMON /MOLS / NM,PP(MNM),PV(3,MNM),IPL(MNM),IPS(MNM),IR(MNM)
  COMMON /CELLS1/ CC(MNC),CG(3,MNC),IC(2,MNC,MNSG),ISC(MNSC),
&
&
  COMMON /GAS / SP(5,MNSP),SPM(6,MNSP,MNSP),ISP(MNSP)
*--Initializations
  DO 200 MM=1,MNSG !for each collision group species
*--IG(2,M) information on group L molecules (IG(N,L)?)
*----N=1 (start address -1) of the molecule numbers in the array IR
*----N=2 the number of molecules in the collision group
  IG(2,MM)=0 !the number of molecules in the collision group = 0
  DO 50 NN=1,MNC !for each cell
*--IC(N,M,L) information on the molecules of species group L in cell M
*----N=1 (start address -1) of the molecule numbers in the array IR
*----N=2 the number of molecules in the cell
  IC(2,NN,MM)=0 !the number of molecules of group type MM in
  !cell NN = 0
50  CONTINUE
  DO 100 NN=1,MNSC !for each subcell
*--ISCG(N,M,L) is the information on species group L in sub-cell M
*----N=1 (start address -1) of the molecule numbers in the array IR
*----N=2 the number of molecules in the sub-cell
  ISCG(2,NN,MM)=0 !the number of molecules of group type MM in
  !subcell NN
100 CONTINUE
200 CONTINUE
  DO 300 N=1,NM !for each molecule
  LS=IPS(N) !LS tells which molecule species it is
  MG=ISP(LS)!ISP(LS) the collision sampling group in which
  !species LS lies
  IG(2,MG)=IG(2,MG)+1 !Increment the number of molecules in that
  !collision group
  MSC=IPL(N) !The subcell it's in is, IPL(N) sub-cell number for
  !molecule N
  ISCG(2,MSC,MG)=ISCG(2,MSC,MG)+1 !Increment the number of
  !molecules in that subcell
  MC=ISC(MSC) !find which cell the subcell resides in
  IC(2,MC,MG)=IC(2,MC,MG)+1 !Increment the number of molecules in
  !that cell in that collision group
300 CONTINUE
*--number in molecule groups in the cells and sub-cells have been counted
  M=0
  DO 400 L=1,MNSG !for each collision group
  IG(1,L)=M
*--the (start address -1) has been set for the groups
  M=M+IG(2,L) !the start address for the next group is the start
  !number of this group plus the number of molecules in this group
400 CONTINUE
  DO 600 L=1,MNSG
  M=IG(1,L) !find the start address of that group
  DO 450 N=1,MNC !for each cell

```

```

        IC(1,N,L)=M !set the starting address of that collision group
        ! in that cell
        M=M+IC(2,N,L) !find the next starting address by adding
        !the number of molecules in this cell that are part of the same
        !collision group
450     CONTINUE
*--the (start address -1) has been set for the cells
        M=IG(1,L) !reset the start address to what it was for this group
        DO 500 N=1,MNSC !for each subcell
            ISCG(1,N,L)=M !find the start address of that subcell for
            !that collision species
            M=M+ISCG(2,N,L) !find the next start address based on the old
            !start address+the number of molecules of this collision
            !species in this cell
            ISCG(2,N,L)=0 !set the num. of molecules in this subcell to 0
500     CONTINUE
600     CONTINUE
*--the (start address -1) has been set for the sub-cells
        DO 700 N=1,NM !for each molecule
            LS=IPS(N) !find which species it is
            MG=ISP(LS)!find which collision group it's in
            MSC=IPL(N) !which sub-cell it's in
            ISCG(2,MSC,MG)=ISCG(2,MSC,MG)+1 !increment the number of mol.
            !in that subcell of that collision group
            K=ISCG(1,MSC,MG)+ISCG(2,MSC,MG) !the counter is the start
            !address of that subcell plus the number of molecules in that
            !subcell
            IR(K)=N !IR(M) cross-reference array linking molecule number
            !to subcell start address
*--the molecule number N has been set in the cross-reference array
700     CONTINUE
        RETURN
        END

*   SELECT.FOR
        SUBROUTINE SELECT
*--selects a potential collision pair and calculates the product of the
*--collision cross-section and relative speed
        PARAMETER (MNM=15000,MNC=20,MNSC=400,MNSP=2,MNSG=1)
        COMMON /MOLS / NM,PP(MNM),PV(3,MNM),IPL(MNM),IPS(MNM),IR(MNM)
        COMMON /CELLS1/ CC(MNC),CG(3,MNC),IC(2,MNC,MNSG),ISC(MNSC),
&
&
        CCG(2,MNC,MNSG,MNSG),ISCG(2,MNSC,MNSG),IG(2,MNSG),
        IFC,CWR,AP,RP
        COMMON /GAS / SP(5,MNSP),SPM(6,MNSP,MNSP),ISP(MNSP)
        COMMON /CONST / PI,SPI,BOLTZ
        COMMON /ELAST / VRC(3),VRR,VR,L,M,LS,MS,CVR,MM,NN,N
        K=INT(RF(0)*(IC(2,N,NN)-0.001))+IC(1,N,NN)+1
        !Multiply the number of molecules in cell N of collision group NN
        !by a random number from 0 to 1, then make it an integer - that picks
        !one molecule in the collision group (randomly).
        ! Then it adds that value to the address number to find the starting
        !address of that molecule in that collision group
        L=IR(K)
*--the first molecule L has been chosen at random from group NN in cell
100     MSC=IPL(L) !finds which subcell the molecule is in
        IF ((NN.EQ.MM.AND.ISCG(2,MSC,MM).EQ.1).OR.
&
&
        (NN.NE.MM.AND.ISCG(2,MSC,MM).EQ.0)) THEN

```

```

*--if MSC has no type MM molecule find the nearest sub-cell with one
  NST=1 !setting up a counter to search adjacent sub-cells
  NSG=1
150  INC=NSG*NST !this sets increment (first time thru went up one)
      NSG=-NSG !sets the search direction
      NST=NST+1 !ups the subcell increment
      MSC=MSC+INC !defines the subcell to look in
      IF (MSC.LT.1.OR.MSC.GT.MNSC) GO TO 150 ! keep looking if going
        !outside subcell range
      IF (ISC(MSC).NE.N.OR.ISCG(2,MSC,MM).LT.1) GO TO 150 !keep
        !looking if in a different in cell or if the number of molecules
        !of type MM in the cell is 0
        !possible to get stuck in an infinite loop here
      END IF
*--the second molecule M is now chosen at random from the group MM
*--molecules that are in the sub-cell MSC
  K=INT(RF(0)*(ISCG(2,MSC,MM)-0.001))+ISCG(1,MSC,MM)+1
  !Multiply the number of molecules in subcell MSC (in cell N) of
  !collision group MM by a random number from 0 to 1, then make it
  !an integer - that picks one molecule in the collision group
  M=IR(K) !find the molecule number using the cross-reference array
  IF (L.EQ.M) GO TO 100
*--choose a new second molecule if the first is again chosen
*
  DO 200 K=1,3
    VRC(K)=PV(K,L)-PV(K,M) !Calculate the difference in the velocity
    !components between the two colliding molecules--VRC(3) are the
    !pre-collision components of the relative velocity
200  CONTINUE
*--VRC(1 to 3) are the components of the relative velocity
  VRR=VRC(1)**2+VRC(2)**2+VRC(3)**2 !relative speed squared
  VR=SQRT(VRR) !relative speed
*--VR is the relative speed
  LS=IPS(L) !find which species one of the molecules is
  MS=IPS(M) !the the species of the other molecule
  CVR=VR*SPM(1,LS,MS)*((2.*BOLTZ*SPM(2,LS,MS))/(SPM(5,LS,MS)*VRR))
  &  ***(SPM(3,LS,MS)-0.5))/SPM(6,LS,MS) !CVR is the relative
  ! speed * the collision cross section
*--SPM(N,M,L) information on the interaction between L-M molecules
*----N=1 the reference cross-section (diameter in the data)
*----N=2 the reference temperature
*----N=3 the viscosity-temperature power law
*----N=4 the reciprocal of the VSS scattering parameter
*----N=5 the reduced mass
*----N=6 the Gamma function of (5/2 - viscosity-temperature power law)
*--the collision cross-section is based on eqn (4.63)
  RETURN
  END

* ELASTIC.FOR
  SUBROUTINE ELASTIC
*--generate the post-collision velocity components.
  PARAMETER (MNM=15000,MNC=20,MNSC=400,MNSP=2,MNSG=1)
  !FWB added below to check conservation of energy and momentum
  DOUBLE PRECISION KEi,LMxi,LMyi,LMzi,KEf,LMxf,LMyf,LMzf
  DOUBLE PRECISION DKE,DLMx,DLMy,DLMz
  !end FWB section

```

```

COMMON /MOLS / NM,PP(MNM),PV(3,MNM),IPL(MNM),IPS(MNM),IR(MNM)
COMMON /GAS / SP(5,MNSP),SPM(6,MNSP,MNSP),ISP(MNSP)
COMMON /CONST / PI,SPI,BOLTZ
COMMON /ELAST / VRC(3),VRR,VR,L,M,LS,MS,CVR,MM,NN,N
DIMENSION VRCP(3),VCCM(3)
*--VRCP(3) are the post-collision components of the relative velocity
*--VCCM(3) are the components of the centre of mass velocity
RML=SPM(5,LS,MS)/SP(5,MS) !red. mass/the mol. mass of species MS
RMM=SPM(5,LS,MS)/SP(5,LS) !red. mass/the mol. mass of species LS
DO 100 K=1,3
    VCCM(K)=RML*PV(K,L)+RMM*PV(K,M) !the components of the
    !center-of-mass velocity
100 CONTINUE
!FWB added section
!Find pre-collision KE and linear momentum
KEi = 0. !initialize
LMxi = 0. !initialize
LMyi = 0. !initialize
LMzi = 0. !initialize
KEi = 0.5*SP(5,LS)*(PV(1,L)**2+PV(2,L)**2+PV(3,L)**2)+0.5*SP(5,MS)
& *(PV(1,M)**2+PV(2,M)**2+PV(3,M)**2)
LMxi = SP(5,LS)*PV(1,L)+SP(5,MS)*PV(1,M)
LMyi = SP(5,LS)*PV(2,L)+SP(5,MS)*PV(2,M)
LMzi = SP(5,LS)*PV(3,L)+SP(5,MS)*PV(3,M)
!End FWB section
*--VCCM defines the components of the centre-of-mass velocity, eqn (2.1)
IF (ABS(SPM(4,LS,MS)-1.)<.1.E-3) THEN !if the reciprocal of
    !VSS scattering parameter for N,M collisions is 0
*--use the VHS logic
*--see p. 222 for a description below
    B=2.*RF(0)-1.
*--B is the cosine of a random elevation angle
    A=SQRT(1.-B*B)
    VRCP(1)=B*VR
    C=2.*PI*RF(0)
*--C is a random azimuth angle
    VRCP(2)=A*COS(C)*VR
    VRCP(3)=A*SIN(C)*VR
ELSE
*--use the VSS logic
    B=2.*(RF(0)**SPM(4,LS,MS))-1.
*--B is the cosine of the deflection angle for the VSS model, eqn (11.8)
    A=SQRT(1.-B*B)
    C=2.*PI*RF(0)
    OC=COS(C)
    SC=SIN(C)
    D=SQRT(VRC(2)**2+VRC(3)**2)
    IF (D.GT.1.E-6) THEN
        VRCP(1)=B*VRC(1)+A*SC*D
        VRCP(2)=B*VRC(2)+A*(VR*VRC(3)*OC-VRC(1)*VRC(2)*SC)/D
        VRCP(3)=B*VRC(3)-A*(VR*VRC(2)*OC+VRC(1)*VRC(3)*SC)/D
    ELSE
        VRCP(1)=B*VRC(1)
        VRCP(2)=A*OC*VRC(1)
        VRCP(3)=A*SC*VRC(1)
    END IF
*--the post-collision rel. velocity components are based on eqn (2.22)

```

```

      END IF
*--VRCP(1 to 3) are the components of the post-collision relative vel.
      DO 200 K=1,3
          PV(K,L)=VCCM(K)+VRCP(K)*RMM
          PV(K,M)=VCCM(K)-VRCP(K)*RML
200    CONTINUE
      !FWB added section
      !Find post-collision KE and linear momentum
      KEf = 0. !initialize
      LMxf = 0. !initialize
      LMyf = 0. !initialize
      LMzf = 0. !initialize
      KEf = 0.5*SP(5,LS)*(PV(1,L)**2+PV(2,L)**2+PV(3,L)**2)+0.5*SP(5,MS)
& *(PV(1,M)**2+PV(2,M)**2+PV(3,M)**2)
      LMxf = SP(5,LS)*PV(1,L)+SP(5,MS)*PV(1,M)
      LMyf = SP(5,LS)*PV(2,L)+SP(5,MS)*PV(2,M)
      LMzf = SP(5,LS)*PV(3,L)+SP(5,MS)*PV(3,M)
      !Compare pre and post collision values
      DKE = 0.
      DLMx = 0.
      DLMy = 0.
      DLMz = 0.
      !See if kinetic energy and momentum conserved
      DKE = KEf-KEi
      DLMx = LMxf-LMxi
      DLMy = LMyf-LMyi
      DLMz = LMzf-LMzi
      !End FWB section
      RETURN
      END

*   RVELC.FOR
      SUBROUTINE RVELC(U,V,VMP)
*--generates two random velocity components U and V in an equilibrium
*--gas with most probable speed VMP (based on eqns (C10) and (C12))
      A=SQRT(-LOG(RF(0)))
      B=6.283185308*RF(0)
      U=A*SIN(B)*VMP
      V=A*COS(B)*VMP
      RETURN
      END

*   GAM.FOR
      FUNCTION GAM(X)
*--calculates the Gamma function of X.
      A=1.
      Y=X
      IF (Y.LT.1.) THEN
          A=A/Y
      ELSE
50      Y=Y-1
          IF (Y.GE.1.) THEN
              A=A*Y
              GO TO 50
          END IF
      END IF
      GAM=A*(1.-0.5748646*Y+0.9512363*Y**2-0.6998588*Y**3+

```



```

&      0.4245549*Y**4-0.1010678*Y**5)
RETURN
END

*   COLLMR.FOR
      SUBROUTINE COLLMR
*--calculates collisions appropriate to DTM in a gas mixture
*   PARAMETER (MNM=10000,MNC=200,MNSC=2000,MNSP=2,MNSG=1)
      PARAMETER (MNM=15000,MNC=20,MNSC=400,MNSP=2,MNSG=1)
      DOUBLE PRECISION COL(MNSP,MNSP),MOVT,NCOL,SELT,SEPT,CS(7,MNC,MNSP)
      DOUBLE PRECISION CSR(MNC,MNSP)
      COMMON /MOLS / NM,PP(MNM),PV(3,MNM),IPL(MNM),IPS(MNM),IR(MNM)
      COMMON /MOLSR / PR(MNM)
      COMMON /CELLS1/ CC(MNC),CG(3,MNC),IC(2,MNC,MNSG),ISC(MNSC),
&
&
&      CCG(2,MNC,MNSG,MNSG),ISCG(2,MNSC,MNSG),IG(2,MNSG),
      IFC,CWR,AP,RP
      COMMON /GAS / SP(5,MNSP),SPM(6,MNSP,MNSP),ISP(MNSP)
      COMMON /GASR / SPR(3,MNSP,MNSP),ISPR(3,MNSP),CT(MNC)
      COMMON /SAMP / COL,NCOL,MOVT,SELT,SEPT,CS,TIME,NPR,NSMP,FND,FTMP,
&
&      TIMI,FSP(MNSP),ISPD
      COMMON /SAMPR / CSR
      COMMON /COMP / FNUM,DTM,NIS,NSP,NPS,NPT
      COMMON /CONST / PI,SPI,BOLTZ
      COMMON /ELAST / VRC(3),VRR,VR,L,M,LS,MS,CVR,MM,NN,N
*--VRC(3) are the pre-collision components of the relative velocity
      DO 100 N=1,MNC !for each cell
*--consider collisions in cell N
      DO 50 NN=1,MNSG !for each collision group
      DO 20 MM=1,MNSG !for each collision group
      SN=0. !set the number sum to zero
      DO 10 K=1,MNSP !for each species
          IF (ISP(K).EQ.MM) SN=SN+CS(1,N,K)!if the collision group
          !for this group is equal to the collision group of this loop,
          !add the number density for that group to this cell
          !-CS(1,N,K) sampled number density of species K in cell N
10      CONTINUE
          IF (SN.GT.1.) THEN !if the number density is more than 1
          !molecule per m3
          AVN=SN/FLOAT(NSMP) !NSMP the total number of samples
          ELSE
          AVN=IC(2,N,MM) !the number density in this cell for this
          !collision group
          END IF
*--AVN is the average number of group MM molecules in the cell
          ASEL=0.5*IC(2,N,NN)*AVN*FNUM*CCG(1,N,NN,MM)*DTM/CC(N)
&
&          +CCG(2,N,NN,MM)
          !IC(2)is the number density in the cell of species p, AVN is the
          !average number density of species q, FNUM is the number
          !density, CCG(1,N,NN,MM) see below
*----CCG(N,M,L,K) is for collisions between species groups L-K in cell M
*----N=1 is the maximum value of (relative speed)*(coll. cross-section)
*----N=2 is the remainder in the sel. pairs when the sel. number is rounded
*--ASEL is the number of pairs to be selected, see eqn (11.5)
          NSEL=ASEL
          CCG(2,N,NN,MM)=ASEL-NSEL
          IF (NSEL.GT.0) THEN
              IF (( (NN.NE.MM) .AND. (IC(2,N,NN) .LT.1 .OR. IC(2,N,MM) .LT.1) )

```

```

&      .OR.((NN.EQ.MM).AND.(IC(2,N,NN).LT.2))) THEN
      !if number densities less than 1 molecule per m3
      CCG(2,N,NN,MM)=CCG(2,N,NN,MM)+NSEL
*--if there are insufficient molecules to calculate collisions,
*--the number NSEL is added to the remainder CCG(2,N,NN,MM)
      ELSE !there are sufficient molecules to calculate
      !collisions
      CVM=CCG(1,N,NN,MM) !max val of rel speed*collcross
      !section for NN MM collision
      SELT=SELT+NSEL !SELT the total number of pair selections
      DO 12 ISEL=1,NSEL !for each collision pair
        CALL SELECT !the produce of the relative and collision
        ! cross section, CVR, is returned
        IF (CVR.GT.CVM) CVM=CVR
*--if necessary, the maximum product in CVM is upgraded
        IF (RF(0).LT.CVR/CCG(1,N,NN,MM)) THEN
*--the collision is accepted with the probability of eqn (11.6)
          NCOL=NCOL+1
          SEPT=SEPT+ABS(PP(L)-PP(M)) !--SEPT the sum of
          !collision pair separations, increments by the
          !difference of the radial position of molecule N
          !with molecule M
          COL(LS,MS)=COL(LS,MS)+1.D00 !COL(M,N) is the number
          !of collisions between species N-M molecules
          COL(MS,LS)=COL(MS,LS)+1.D00 !COL(M,N) is the number
          !of collisions between species N-M molecules
          IF (ISPR(1,LS).GT.0.OR.ISPR(1,MS).GT.0) CALL INELR
          !if number of rotational degrees of freedom of either
          !molecule greater than 0
*--ISPR(N,M) integer information on rotational properties of species M
*----N=1 the number of rotational degrees of freedom
*----N=2 0, 1 for constant, polynomial for relaxation collision number
*----N=3 0, 1 for a common, collision partner species dependent rate
*--bypass rotational redistribution if both molecules are monatomic
*---see Section 11.3
          CALL ELASTIC !rotational energy first accounted for,
          !which changes velocities, then an elastic collision is
modeled
          END IF
12      CONTINUE
          CCG(1,N,NN,MM)=CVM !max val of rel speed*collcross
          !section for NN MM collision
          END IF
20      CONTINUE
50      CONTINUE
100     CONTINUE
        RETURN
      END

*   INELR.FOR
      SUBROUTINE INELR
*--adjustment of rotational energy in a collision
      PARAMETER (MNM=15000,MNC=20,MNSC=400,MNSP=2,MNSG=1)
      COMMON /MOLSR / PR(MNM)
      COMMON /GAS   / SP(5,MNSP),SPM(6,MNSP,MNSP),ISP(MNSP)
      COMMON /GASR  / SPR(3,MNSP,MNSP),ISPR(3,MNSP),CT(MNC)

```

```

COMMON /ELAST / VRC(3),VRR,VR,L,M,LS,MS,CVR,MM,NN,N
DIMENSION IR(2)
*--IR is the indicator for the rotational redistribution
ETI=0.5*SPM(5,LS,MS)*VRR !1/2*mr*relspeed^2 ,interesting reduced form
*--ETI is the initial translational energy
ECI=0.
*--ECI is the initial energy in the active rotational modes
ECF=0.
*--ECF is the final energy in these modes
ECC=ETI
*--ECC is the energy to be divided
XIB=2.5-SPM(3,LS,MS) ! 2.5 minus the viscosity-temperature power
!law for translational modes, LS molecules with MS molecules
*--XIB is the number of modes in the redistribution
IRT=0 !saying no redistribution
*--IRT is 0,1 if no,any redistribution is made
DO 100 NSP=1,2
*--consider the molecules in turn, for each molecule
IF (NSP.EQ.1) THEN !if the first molecule
K=L !the species
KS=LS
JS=MS
ELSE
K=M
KS=MS
JS=LS
END IF
IR(NSP)=0
*--ISPR(N,M) integer information on rotational properties of species M
*----N=1 the number of rotational degrees of freedom
*----N=2 0, 1 for constant, polynomial for relaxation collision number
*----N=3 0, 1 for a common, collision partner species dependent rate
IF (ISPR(1,KS).GT.0) THEN !if the number of rotational degrees
!of freedom of species KS>0
IF (ISPR(2,KS).EQ.0) THEN !if ISPR(2,KS)=0 use a constant
!relaxation collision number
ATK=1./SPR(1,KS,JS)
ELSE
ATK=1./((SPR(1,KS,JS)+SPR(2,KS,JS)*CT(N)+SPR(3,KS,JS)*CT(N)
& **2) !--CT(N) the macroscopic temperature in cell N
END IF
*--SPR(1,L,K) the constant value, or constant in the polynomial for Zr
*----in a collision of species L with species K
*--the following two items are required only if ISPR(2,L)=1
*--SPR(2,L,K) the coefficient of temperature in the polynomial
*--SPR(3,L,K) the coefficient of temperature squared in the polynomial
*--ATK is the probability that rotation is redistributed to molecule L,
*--it's the reciprocal of the relaxation collision number
!--XI is the sum of the average degrees of freedom
!--XIA is the square with subscript a on 229, it is one or
!more terms in 5.42
!--XIB is the square with subscript b on 229, is the remaining
!terms
*--PR(K) is the rotational energy of molecule K
IF (ATK.GT.RF(0)) THEN
IRT=1 !there will be energy re-distribution
IR(NSP)=1 !this was 0, now it's 1 for this molecule

```

```

        ECC=ECC+PR(K) !--ECC is the rotational energy to be divided,
        ! PR(K) is the rotational energy of molecule K
        ECI=ECI+PR(K) !--ECI is the energy in the active rotational
        ! modes
        XIB=XIB+0.5*ISPR(1,KS) !--XIB is the average number of modes
        ! in the redistribution of the energy of both molecules,
        !ISPR(1,KS is the number of rotational degrees of freedom of
        ! molecule KS, XIB is the sum of the rotational energy modes of
        ! both molecules
        END IF
    END IF
100  CONTINUE
!--apply the general Larsen-Borgnakke distribution function
    IF (IRT.EQ.1) THEN !if re-distributing
        DO 150 NSP=1,2 !for each molecule
            IF (IR(NSP).EQ.1) THEN !if the energy is to be re-distributed
                IF (NSP.EQ.1) THEN !if the first molecule
                    K=L
                    KS=LS
                ELSE
                    K=M
                    KS=MS
                END IF
                XIB=XIB-0.5*ISPR(1,KS) !removing half of the rotational
                !modes, but for this molecule
!--half of the the current molecule's rotational energy modes is removed
                ! from the total (avg) modes in the collision
                IF (ISPR(1,KS).EQ.2) THEN !if this molecule has two
                !rotational modes
                    ERM=1.-RF(0)**(1./XIB) !equation 5.46, the ratio of the
                    !new rotational energy to the total energy that is to
                    ! be divided
                ELSE
                    XIA=0.5*ISPR(1,KS) !the number of avg. rotational degrees
                    !of freedeom of species KS, becomes XIA
                    CALL LBS(XIA-1.,XIB-1.,ERM) !call Larsen-Borgnakke
                    !function to select a Larsen-Borgnakke energy ratio using
                    !eqn (11.9)
                END IF
                PR(K)=ERM*ECC !the rotational energy of this molecule is set
                ! by the available fraction of rotational energy(ERM) times
                !the total energy
                ECC=ECC-PR(K)
!--the available energy is reduced accordingly
                ECF=ECF+PR(K) !the final energy in the rotational modes
            END IF
150  CONTINUE
            ETF=ETI+ECI-ECF
!--ETF is the post-collision translational energy
!--adjust VR and, for the VSS model, VRC for the change in energy
            A=SQRT(2.*ETF/SPM(5,LS,MS)) !the calculated relative velocity
            IF (ABS(SPM(4,LS,MS)-1.).LT.1.E-3) THEN !if the reciprocal of
            !VSS scattering parameter for LS,MS collisions is zero
                VR=A !--VR, the relative speed, is the the calculated relative
                ! velocity
            ELSE
                DO 160 K=1,3

```

```

VRC(K)=VRC(K)*A/VR !--VRC(3) are the pre-collision
!components, modified as a result of the inelastic collision,
!of the relative velocity, are scaled by the ratio of the
!new relative velocity of the old relative velocity
160    CONTINUE
      VR=A
      END IF
      END IF
      RETURN
      END

*   LBS.FOR
      SUBROUTINE LBS(XMA,XMB,ERM)
*--selects a Larsen-Borgnakke energy ratio using eqn (11.9)
*--XMA is XIA-1, XMB is XIB-1
100   ERM=RF(0) !the ratio of new rotational energy to ECC
      IF (XMA.LT.1.E-6.OR.XMB.LT.1.E-6) THEN
          IF (XMA.LT.1.E-6.AND.XMB.LT.1.E-6) RETURN
          IF (XMA.LT.1.E-6) P=(1.-ERM)**XMB
          IF (XMB.LT.1.E-6) P=(1.-ERM)**XMA
      ELSE
          P=((XMA+XMB)*ERM/XMA)**XMA*((XMA+XMB)*(1.-ERM)/XMB)**XMB
      END IF
      IF (P.LT.RF(0)) GO TO 100
      RETURN
      END

*   RF.FOR
      FUNCTION RF(IDUM)
*--generates a uniformly distributed random fraction between 0 and 1
*----IDUM will generally be 0, but negative values may be used to
*-----re-initialize the seed
      SAVE MA,INEXT,INEXTP
      PARAMETER (MBIG=1000000000,MSEED=161803398,MZ=0,FAC=1.E-9)
      DIMENSION MA(55)
      DATA IFF/0/
      IF (IDUM.LT.0.OR.IFF.EQ.0) THEN
          IFF=1
          MJ=MSEED-IABS(IDUM)
          MJ=MOD(MJ,MBIG)
          MA(55)=MJ
          MK=1
          DO 50 I=1,54
              II=MOD(21*I,55)
              MA(II)=MK
              MK=MJ-MK
              IF (MK.LT.MZ) MK=MK+MBIG
              MJ=MA(II)
50          CONTINUE
          DO 100 K=1,4
              DO 60 I=1,55
                  MA(I)=MA(I)-MA(1+MOD(I+30,55))
                  IF (MA(I).LT.MZ) MA(I)=MA(I)+MBIG
60          CONTINUE
100         CONTINUE
          INEXT=0
          INEXTP=31

```

```

END IF
200  INEXT=INEXT+1
    IF (INEXT.EQ.56) INEXT=1
    INEXTP=INEXTP+1
    IF (INEXTP.EQ.56) INEXTP=1
    MJ=MA(INEXT)-MA(INEXTP)
    IF (MJ.LT.MZ) MJ=MJ+MBIG
    MA(INEXT)=MJ
    RF=MJ*FAC
    IF (RF.GT.1.E-8.AND.RF.LT.0.99999999) RETURN
    GO TO 200
END

*   DATA1.FOR
    SUBROUTINE DATA1
*--defines the data for a particular run of DSMC1.FOR.
    PARAMETER (MNM=15000,MNC=20,MNSC=400,MNSP=2,MNSG=1)
    DOUBLE PRECISION COL(MNSP,MNSP),MOVT,NCOL,SELT,SEPT,CS(7,MNC,MNSP)
    CHARACTER*9 FNAME
    COMMON /GAS / SP(5,MNSP),SPM(6,MNSP,MNSP),ISP(MNSP),ALPH(MNSP,2)
    COMMON /GASR / SPR(3,MNSP,MNSP),ISPR(3,MNSP),CT(MNC)
    COMMON /CELLS1/ CC(MNC),CG(3,MNC),IC(2,MNC,MNSG),ISC(MNSC),
    & CCG(2,MNC,MNSG,MNSG),ISCG(2,MNSC,MNSG),IG(2,MNSG),
    & IFC,CWR,AP,RP
    COMMON /SAMP / COL,NCOL,MOVT,SELT,SEPT,CS,TIME,NPR,NSMP,FND,FTMP,
    & TIMI,FSP(MNSP),ISPD
    COMMON /COMP / FNUM,DTM,NIS,NSP,NPS,NPT
    COMMON /GEOM1 / IFX,NSC,XB(2),IB(2),BT(2),BVY(2),BFND(2),BFTMP(2),
    & BVFX(2),BFSP(2,MNSP),BME(2,MNSP),BMR(2,MNSP),IIS,
    & CW,FW,GRAV
    COMMON /MODSF / NSF,SEED

    FNAME = 'DSMC.IN'
    OPEN (10,FILE=FNAME) !no FORM = FORMATTED
    READ(10,*) IFX,IIS,FTMP,FND,FSP(1),FSP(2),FNUM,DTM,XB(1),XB(2),
    & IB(1),BT(1),BVY(1),IB(2),BT(2),BVY(2),SP(1,1),SP(2,1),SP(3,1),
    & SP(4,1),SP(5,1),SP(1,2),SP(2,2),SP(3,2),SP(4,2),SP(5,2),
    & ISPR(1,1),ISPR(1,2),ISPR(2,1),ISPR(2,2),SPR(1,1,1),SPR(1,1,2),
    & SPR(1,2,1),SPR(1,2,2),NIS,NSP,NPS,NSF,NPT,ALPH(1,1),ALPH(1,2),
    & ALPH(2,1),ALPH(2,2),SEED
    CLOSE(10)

*--set data (must be consistent with PARAMETER variables)
!   IFX=1
*--it is a cylindrical flow
!   IIS=2
*--there is a uniform gradient between the two surfaces
!   FTMP=482.98
*--FTMP is the temperature (K)
!   FND=7.998E20
*--FND is the number density
!   FSP(1)=0.10
!   FSP(2)=0.90
*--FSP(N) is the number fraction of species N
!   FNUM=1.939E15
*--FNUM is the number of real molecules represented by a simulated mol.
!   DTM=1.677e-6 !1.108E-7 is 0.5
*--DTM is the time step, 2.5 e-6 default, 1e-6 Xe, 1e-7 H2

```

```

!      XB(1)=0.035
!      XB(2)=0.0595
*--the simulated region is from x=XB(1) to x=XB(2)
!      IB(1)=3
!      BT(1)=623.1
!      BVY(1)=0.
*--the inner wall is stationary at a temperature of 623 K
!      IB(2)=3
!      BT(2)=342.86
!      BVY(2)=0.
*--the outer boundary is at 353 K and is stationary
!Gas specific inputs
!H2
!      SP(1,1)=2.92E-10
!      SP(2,1)=273.
!      SP(3,1)=0.67
!      SP(4,1)=0.7407
!      SP(5,1)=3.44E-27
!Ar
!      SP(1,2)=4.17E-10
!      SP(2,2)=273.
!      SP(3,2)=0.81
!      SP(4,2)=0.7143
!      SP(5,2)=66.3E-27
!Xe
!      SP(1,2)=5.74E-10
!      SP(2,2)=273.
!      SP(3,2)=0.85
!      SP(4,2)=0.6944
!      SP(5,2)=218E-27

*--SP(1,N) is the molecular diameter of species N
*--SP(2,N) is the reference temperature of species N
*--SP(3,N) is the viscosity-temperature index of species N
*--SP(4,N) is the reciprocal of the VSS scattering parameter of species N
*--SP(5,N) is the molecular mass of species N

!      ISPR(1,1)=2 !2 dof H2
!      ISPR(1,2)=0 !0 dof Xe,Ar
!      ISPR(2,1)=0 !H2
!      ISPR(2,2)=0 !Xe,Ar
!      SPR(1,1,1)=5. !H2 with H2
!      SPR(1,1,2)=5. !H2 with Xe,Ar
!      SPR(1,2,1)=0. !Xe,Ar with H2
!      SPR(1,2,2)=0. !Xe with Xe or Ar with Ar

!--ISPR(1,N) is the number of degrees of freedom of
! species N, 2 for H2,0 of Xe
*--SPR(1,N,K) is the constant in the polynomial for the rotational
*--relaxation collision number of species N in collision with species K
*--ISPR(2,N) is 0,1 for constant, polynomial for collision number
*--set ISPR(3,N) here for how to calculate partner species dependent
*--rotational relaxation rate (0=common) (1=species dependent) if not
!--mean desired
!      NIS=5
*--NIS is the number of time steps between samples
!      NSP=20

```

```
*--NSP is the number of samples between restart and output file updates
!     NPS=200 !200 good
*--NPS is the number of updates to reach assumed steady flow
!     NSF=810
!     NPT=1010 !2000 good
*--NPT is the number of file updates to STOP
!     ALPH(1,1)=0.34 !accomm coeff of hydrogen on abs (surface 1)
!     ALPH(1,2)=0.25 !accomm coeff of hydrogen on gl (surface 2)
!     ALPH(2,1)=0.66 !accomm coeff of argon on abs (surface 1)
!     ALPH(2,2)=0.82 !accomm coeff of argon on glass (surface 2)
!     ALPH(2,1)=0.76 !accomm coeff of xenon on abs (surface 1)
!     ALPH(2,2)=0.90 !accomm coeff of xenon on gl (surface 2)
!     SEED = -1000000 !seed for DMSC's random number generator
RETURN
END
```


SOP #: 827

Center #: 5500

Revision #: 2

Revision Date: 4/7/11

Safe Operating Procedure for:
**Receiver Hydrogen Permeation Testing
And
Receiver Heat Loss Testing with Hydrogen/Hydrogen Mixtures**

Emergency Shutdown Procedures:

In case of an emergency, there are two large disconnect switches. One is on the east wall labeled with a large sign "Main Power HCE Receiver Test Stand #1 Disconnect" and the second is on the west wall labeled "Test Stand #2 Receiver Hydrogen Permeation Test Emergency Shutoff." Turning off the power will de-energize the system for the indicated test stand. The data acquisition systems are powered by UPS on the floor near the desk and should be left on to monitor the system until the outer temperature glass temperature is below 50°C.

SIGNATURES

Concurrence:

Frank Burkholder, Principal Author

Date

Greg Glatzmaier, Author

Date

Chuck Kutscher, Line Manager

Date

Maureen Jordan, EHS Office Director

Date

Approval:

Dave Mooney, 5500 Center Director

Date

Administrative Notes:

1. This Safe Operating Procedure (SOP) shall be read and signed by all authorized workers
2. A list of authorized personnel shall be kept as an appendix
3. This procedure shall be updated when necessary (refer to ES&H procedure 6-6.2 for details on management of change)
4. This procedure shall be reviewed annually by the author

Safety Contact Information

Designated Area Representative:	Judy Netter	Phone:	x-6258
ESH Point of Contact:	Lee Ann Holwager	Phone:	x-3231
Building Area Engineer (BAE):	Steve Nixon	Phone:	x-7374
Line Manager:	Chuck Kutscher	Phone:	x-7521
SOP Coordinator	Teri Spinuzzi	Phone:	x-3818
Center Director:	Dave Mooney	Phone:	x-6782
Medical:	Services	Phone:	x-6522
	Reception	Phone:	x-6525
Emergencies:	From a site phone	Phone:	x-1234
	From a cell phone:	Phone:	303-384-6811

1.0 Introduction

Activity description:

This SOP addresses 2 different experiments that involve heat loss from parabolic trough receivers resulting from the presence of hydrogen (Experiment #1) and hydrogen mixtures (Experiment #2) in the receiver's annulus. A brief overview of the reason for these experiments is given below, followed by descriptions of the two experiments.

Overview

Parabolic trough power plants offer an attractive option for near-term, utility-scale renewable electricity generation. With over 10,000 MW of planned installation by 2015, this technology will provide sustainable electricity to U.S. and global markets. Parabolic trough power plants are based on the single axis parabolic reflector, which reflects and concentrates sunlight to a receiver located at the focal line. The concentrated sunlight is absorbed by the receiver's absorber and heats a heat transfer fluid (HTF) flowing within the absorber tube. Thermal energy within the heated HTF is used to generate steam for Rankine cycle power generation or can be stored for later use.

The absorber tube of the receiver is surrounded by a glass tube that seals to the absorber tube with bellows at both ends. The enclosed volume between the glass and receiver tube forms a 25 liter annulus that is normally evacuated to less than 0.0001 torr to minimize heat conduction/convection between the receiver tube and ambient air. This is less than 1/5,000,000th of atmospheric pressure (1 atm = 660 torr 5400 feet above sea level).

The heat transfer fluid (HTF) used in the plants is Therminol VP-1™. VP-1™ is a eutectic mixture of two organic compounds, biphenyl and diphenyl oxide. The fluid is thermally stable to a maximum temperature of 390 °C. Its vapor pressure at 390 °C is about 10 atmospheres. Its freezing point is 12 °C. These thermal properties allow VP-1™ to perform as the heat transfer fluid in parabolic trough power plants with a normal operating temperature range of 293 – 393 °C. Its low freezing point minimizes the risk of freezing in the solar collector field when the plant is off-sun.

At temperatures near 393 °C, the organic components of the HTF undergo a variety of degradation reactions that produce hydrogen as a byproduct. The hydrogen is transported throughout the power plant to all components that contain HTF. Its high permeability in metals allows it to permeate through the steel walls of the expansion tank, steam generator, piping and receiver tubes. Hydrogen that permeates through the absorber tube wall establishes an equilibrium pressure within the annular volume of the HCE.

The occurrence of hydrogen within the annular volumes of the receivers results in degradation of their thermal performance. Hydrogen conducts significant amounts of heat from the absorber to the glass envelope at hydrogen pressures greater than 0.05 torr. The suspected hydrogen equilibrium pressure in receivers is about 1 torr. The estimated decrease in annual thermal energy output from a solar field with 1 torr hydrogen pressure in all the receivers is 20%. Two approaches are being investigated to prevent this performance decrease.

Modeling analysis has shown that if the HTF is free of hydrogen, hydrogen within the annuli will permeate out through the absorber and through the walls of the two bellows at a rate that reduces the hydrogen pressure in the HCEs to acceptable levels below 0.001 torr. This effect may be the basis of methods to permanently remove hydrogen from the receiver annuli and thereby maximize the performance and power output of power plants that use VP-1™ as the HTF. This approach is being investigated in Experiment #1.

Modeling has also shown that the heat loss due to the presence of hydrogen can be almost completely eliminated if a low conductivity inert gas, like xenon, is present in the annulus as well. This approach is investigated in Experiment #2.

Experiment #1: Permeation testing of hydrogen at 400°C

Testing of parabolic trough receivers will be conducted to determine time constants for the reduction of hydrogen partial pressure in the receiver annulus resulting from the permeation of hydrogen through the receiver absorber tube and its end bellows. The tests will be performed at the design receiver tube operating temperature of 400 °C. The receiver is heated by two 4,800 W Incoloy-sheathed electrical cartridge heaters and four 600 W cable heaters in a system identical to the system already used for receiver heat loss testing (see Receiver Heat Loss Testing SOP). This work differs from the existing receiver heat-loss work and SOP in that a small amount of hydrogen (and hydrogen alone) is introduced to the receiver annulus before the test begins, and its pressure is monitored during the test period as it slowly permeates out. Modeling suggests that 14 hours will be required to go from the starting hydrogen pressure of about 0.3 torr (1/660th of atmospheric pressure) to 0.1 torr. However, testing may occur with hydrogen pressures up to 500 torr. Therefore this test will take several days and involve warm-up and cool-down periods. Testing will be monitored at all times.

Experiment #2: Heat loss testing of hydrogen, hydrogen/argon and hydrogen/xenon gas mixtures at 350°C and 450°C.

This testing is identical to that described above except for three differences: 1) not just hydrogen, but hydrogen/argon or hydrogen/xenon mixtures are placed in the annulus, 2) absorber temperatures of 350°C and 450°C are investigated, and 3) testing lasts 1 day (not several days), with the heat loss measured at several pressures during the test period. The goal of this testing is to measure the steady-state heat-loss at a specified absorber temperature with a gas of a desired composition in the annulus at a specified pressure.

The heat loss of three pure gases will be investigated: hydrogen (H₂), argon (Ar), and xenon (Xe). The heat loss of six gas mixtures will also be investigated:

Mixtures of Argon and Hydrogen
90%Ar/10%H₂, 75%Ar/25%H₂, 50%Ar/50%H₂

Mixtures of Xenon and Hydrogen
90%Xe/10%H₂, 75%Xe/25%H₂, 50%Xe/50%H₂

The heat losses will be tested at absorber temperatures of 350°C and 450°C. For all the tests besides the pure hydrogen tests, the test pressures are: 0.0001, 0.004, 0.001, 0.004, 0.01, 0.03, 0.06, 0.1, 0.2, 0.5, 1, 2, 5, 10, and 100 torr. The pure hydrogen tests include the aforementioned pressures as well as 200, 300, 400, and 500 torr. A table listing all of these tests and the amount of hydrogen in the annulus of each test is provided in Appendix III.

Location Description: FTLB Lab 118-1

Organization Involved: Center 5500, Electricity, Resources & Building Systems Integration

2.0 Summary of Hazards

2.a. Primary Hazards and Controls

Electrical:	<input type="checkbox"/> No	<input checked="" type="checkbox"/> Yes	List: The heaters and associated control panel have a 240/208 V electrical power source. The total heater rating is approximately 10 kW.
Describe the controls for this potential hazard:			
<p>Electrical service was designed and installed in compliance with National Electrical Code (NEC) requirements and NREL requirements. Power wiring on the test rig has been inspected by an NREL Electrician. The test rig is hardwired through a suitably rated disconnect switch. All power wiring is properly enclosed.</p> <p>Work (repair/maintenance) shall not be conducted on energized systems apart from basic trouble shooting with standard test equipment.</p> <p>When performing diagnostics or zero energy verification after LOTO has been applied, electrical/arc flash PPE meeting a Hazard Risk Category 1 shall be worn. This PPE consists of the following:</p> <ul style="list-style-type: none"> ➤ Long sleeve shirt and pants or coveralls with a minimum Arc Rating of 4 ➤ Arc rated face shield ➤ Safety glasses with side shields ➤ Hard hat ➤ Hearing protection (ear inserts) ➤ Dielectric gloves with leather protectors (dielectric gloves must have been tested within the last 6 months) <p>When performing visual non-contact inspections where energized conductors are exposed, electrical/arc flash PPE meeting a Hazard Risk Category 0 shall be worn. This PPE consists of the following:</p>			

- Long sleeve shirt and pants made of cotton or other non-melting material
- Safety glasses with side shields
- Hearing protection (ear inserts)
- Leather gloves

If diagnostics, zero energy verification or visual non-contact inspections are being conducted then establish a Limited Approach Boundary at 3'6" and an Arc Flash Boundary at 4'.

If work will be conducted on the test stand, then the 208V disconnect switch for that test stand shall be locked and tagged out by the user, and a zero energy verification shall be performed before work commences. Equipment specific LOTO procedures for each of the test stands can be found in Appendix IV..

Hazardous Chemical/Materials:

No

Yes

List: Small amounts gas containing hydrogen or hydrogen mixtures will be used for testing.

Describe the controls for this potential hazard:

Prevention of hydrogen ignition during testing is accomplished in three ways:

1. **Air (oxygen) is not present in the annulus.** Neither Experiment #1 nor Experiment #2 call for experiments with air. The glass envelope of the receiver seals the receiver annulus from the atmosphere. Measures used to ensure air (oxygen) is not introduced into the annulus involve the following:
 - Using new receiver tubes. These tubes are designed to maintain a relative vacuum for tens of years.
 - Visual inspection of the glass ensuring there is no damage
 - Visual inspection that the stainless steel tube is >1/4 inch from the glass ensuring a thermal bridge is not created and potentially cracking the glass
 - The annulus is pumped down ensuring there is a negligible amount of air in the space before testing
 - A vacuum is held on the annulus for a period of ≥2 hours before the hydrogen/hydrogen mixture is added ensuring there are no leaks in the system

If something unforeseen does occur where a leak does develop and air is introduced into the annulus the hydrogen-air mixture still shouldn't ignite because of the following:

2. **There are no ignition sources.** As shown in Appendix II, hydrogen's auto-ignition temperature is 565°C. The maximum absorber temperature investigated in Experiment #1 is 400°C, and 450°C in Experiment #2. The heaters are equipped with overheat relays which will automatically shut down the power to the heaters if a temperature of 500°C is detected at the heaters or at the stainless steel tube.

The absorber tube is bonded and grounded to the test frame by 4 independent methods: the two support wires and the two ground wires from the copper pipes inserted into the receiver. This bonding and grounding ensures that no static sparks could develop that would ignite the hydrogen. The continuity of the bonding and grounding has been tested.

But if somehow there was an air leak *and* an ignition source, the hydrogen-air mixture still would likely not ignite. The reason for this is:

3. **Such small amounts of hydrogen are used that the percentage of hydrogen in the resulting hydrogen-air mixture would be less than hydrogen's lower flammability limit of 4% in all but 14 of the 280 tests.** To illustrate, consider the following example. Suppose that the glass stem connecting to the vacuum system were to break off during testing (though

measures have already been taken to prevent stresses to this component and thereby prevent this from happening). Suddenly there would be a 1.5 cm diameter hole through the glass envelope into the annulus. The pressure differential would cause air to rush in, preventing hydrogen from leaking out until the pressure inside the annulus reached atmospheric pressure. The amount of time this would take depends on the size of the hole. For a 1.5 cm diameter hole, modeling suggests that it should take about 0.5 seconds. For a smaller hole (0.2 cm) it would take about 30 seconds. During this filling period, and only during this filling period for most tests, is there a chance for the volumetric percentage of hydrogen in the hydrogen-air mixture to be in the 4%-75% flammability range.

Experiment #1 involves a maximum initial hydrogen pressure in the annulus of 1 torr. If there were a leak and air rushed in, this hydrogen would get squished down to an equivalent volume of only 0.04 L. (Of course hydrogen still occupies the entire volume, but this method shows the volume that the hydrogen in the annulus would occupy if it were at atmospheric pressure.) The remainder of the 25 L annulus would be air, so the volumetric % of hydrogen would be $0.04/25 = 0.2\%$. This is far below the lower flammability limit of 4%. However, during the air fill period (0.5 seconds – 30 seconds) the percentage must go from 100% hydrogen to 0.2% hydrogen. It's during this time period that an ignition source would be required to ignite the small amount of hydrogen present in the annulus. If hydrogen pressures greater than 10 torr are used during testing then the hydrogen-air mixture will exceed 1% by volume, 25% of the flammable limit up to concentrations within the flammable range (4 – 75% by volume).

Experiment #2 involves testing a variety of gas mixtures at various pressures; Appendix III lists the hydrogen percentage if there were a leak for the 139 test cases. Each of these test cases will be repeated twice (350°C and 450°C), a total of 278 tests. The hydrogen partial pressures are low enough so that in 254 of the 278 tests the hydrogen percentage of the resulting hydrogen-air mixture in the case of a leak would be less than 1%, four times less than the 4% flammability limit. Of the remaining 24 tests, 10 still result in hydrogen percentages of less than 4%, while the remaining 14 would fall in the flammability range. These tests will be performed after sufficient experience has been gained with system so there is greater assurance that there will not be any leaks or ignitions sources during these tests. The 24 tests that have a potential hydrogen/air mixture of $\geq 1\%$ shall be conducted fully attended.

If there were a leak into the annulus, the increase in pressure would be immediately obvious to the operator, as would the “sucking” sound created as the receiver filled with air. In this case the operator should shut the experiment off and wait for the system to cool down. Do not enter the test area and contact your EHS POC.

Eventually the hydrogen gas in the annulus for both tests must be vented. Prior to the hydrogen being vented an inert fill gas (Argon or Nitrogen) will be added to the annulus to bring the mixture below its lower flammability limit and then the gas mixture will be pumped out and into the fume hood.

The quantity of hydrogen and the six hydrogen mixtures will be limited in the lab to one lecture size cylinder of each. At the end of each days use the cylinder of hydrogen/hydrogen mixture shall be stored in the flammable gas cabinet located in the laboratory.

High Temperatures:

No

Yes

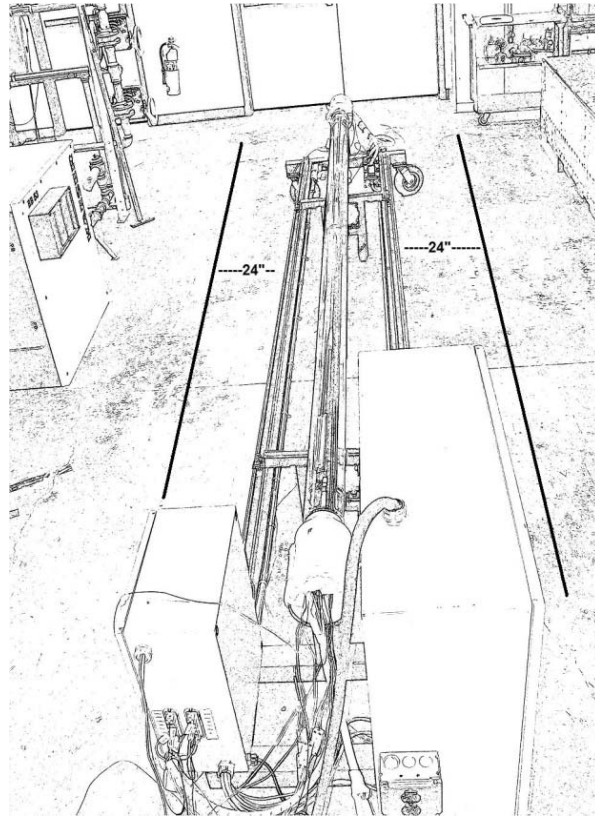
List: The absorber tube is heated to a maximum of 450 °C.

Describe the controls for this potential hazard:

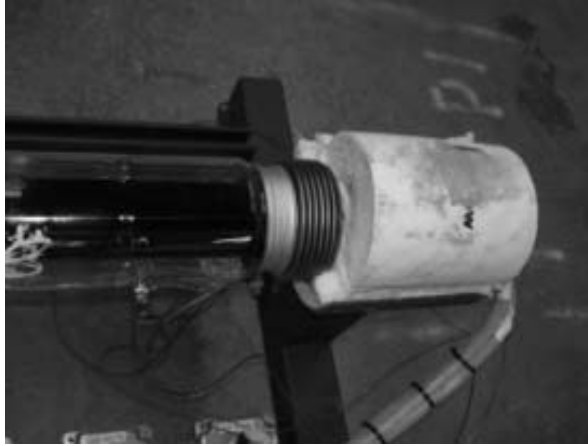
The absorber tube is heated by electric heaters placed inside of it. These heaters have conservative maximum power settings within the program software (Watlow, Labview, Opto22) that limits their maximum power to 80% of their capacity. Besides limiting absorber temperature, this increases the heater lifetimes. The heaters also have over-temperature control hardware to prevent runaway system operation in case of operator inattention. If the temperature of the heater, copper pipe or absorber surface ever goes above 500°C, relay switches permanently shut off power to the system.

This happens independently of the operator.

Precautions will be taken to prevent ignition of adjacently located combustible materials. These include keeping a combustible free, 24-inch clearance around all heated surfaces. Housekeeping will be a priority at the start and end of each day to prevent accumulation of any combustibles in the test area.



High-temperature surfaces could cause serious burns. Where possible, insulation is installed (e.g., ceramic fiber disk on receiver tube ends). Caution tape is placed on the floor to indicate regions where high temperature surfaces might be contacted. The surface most likely to be contacted is the glass surface whose temperature will be between 50°C and 200°C in Experiments #1 and #2.



The test area is bounded by laboratory walls on the east, south and west sides. Doors on the south wall have been modified to be for emergency exit only so no one can enter into the test area.



Partitions with signage will be placed at the north boundary of the test area during testing and will remain in place after a test is concluded and the hardware is cooling down to ambient temperature. The signs will state that an experiment is in progress and “Do Not Enter.” Traffic entering the west side of the lab will be directed away from the test area by the partition. For test stand #1, located on the east side of the room, a motion sensor with a manual override monitors the test area when unattended activities are allowed. This motion sensor cuts power to the entire system if there is unauthorized entry to the test area. For test stand #2, located on the west side of the room, a photo sensor with electronic override through LabView monitors the test area when unattended activities are allowed. This photo sensor cuts power to all heaters if there is unauthorized entry to the test area.



Appropriate PPE (refer to section 2.c. for listing of PPE) will be used when entry into the test area is made during testing and the cool-down periods.

High Pressure:	<input type="checkbox"/> No	<input checked="" type="checkbox"/> Yes	List: Hydrogen, hydrogen mixtures, argon and nitrogen gases will be provided to the test from compressed gas cylinders.
----------------	-----------------------------	---	---

Describe the controls for this potential hazard:

All standard procedures will be used and followed for mounting, securing and operating compressed gas cylinders. Pressure regulators will limit the delivery pressure of the gases to less than 12 psi. Two valves isolate the gas cylinder from the receiver annulus. The pressure regulator is one valve, and another valve in the vacuum system is the second one. Both valves must be open for gas to flow from the gas cylinder to the receiver annulus.

Over pressurization of the receiver tube is controlled by the constant monitoring of the pressure by the worker during filling activities. Additionally the potential for over pressurization is controlled by the gas delivery pressure being limited to 12 psi and the vacuum pump operating during filling operations.

For Experiment #1, the compressed gas cylinder will be removed from the testing area after filling operations. This may be possible for Experiment #2 as well, but if multiple tests are to be performed in a day the cylinder will remain in the test area until testing is complete that day. Cylinders of hydrogen and hydrogen mixtures will be stored in the gas cabinet located in the laboratory at the end of each days use.

Low Pressure:	<input type="checkbox"/> No	<input checked="" type="checkbox"/> Yes	List: The HCE annulus will be under vacuum.
---------------	-----------------------------	---	---

Describe the controls for this potential hazard:

The vacuum puts the tube glass under compression, the design condition of the receivers. If the tube glass fails, implosion would produce glass shards that would first implode on to the receiver surface, and then drop to the floor. Though we have never had a failure in the laboratory, experience indicates this as the primary failure mode of receivers in the field.

The receiver glass will be inspected prior to testing to assure it is free of damage that might contribute to unexpected failure. Items to inspect include possible chips, cracks and other imperfections in the glass. The test carriage will be adequate to maintain appropriate alignment and

support of the tube at temperature. Identical tubes have been tested in this lab, at other laboratories, and in the field with good results.

HCE Bowing:

No

Yes

List: After the heaters are inserted in the HCE, the stainless steel will bow down slightly towards the glass.

Describe the controls for this potential hazard:

A slight bowing effect is normal and duplicates the bowing of the absorber tube in the field due to the HTF flowing within it. However, if the stainless steel sags excessively so that its surface is only ¼” away from the HCE glass, the test on the HCE will not be performed, or if it occurs during testing, it will be aborted.

This condition creates a thermal bridge between the stainless steel and the glass and can cause the glass to break from unequal thermal expansion of the glass.



Attended and Unattended Operations:

No

Yes

List: Unattended operation of experiments #1 and #2 are limited.

Describe the controls for this potential hazard:

All test that where, if there were an air leak into the annulus, the **hydrogen/air mixture would be ≥1% by volume** shall be **attended**.

Unattended operations are permitted only for the tests where, if there were an air leak into the annulus, the **hydrogen/air mixture would be <1% by volume**. Unattended operations are limited to 2 hour increments and may not occur consecutively.

New tubes must be attended during initial heat-up to confirm integrity. If at any time the worker has a question about a receiver, they shall conduct the test in an attended mode.

For unattended operations on test stand #1, push the green motion sensor “on” button to activate the motion sensor. For unattended operations on test stand #2, switch on the photo sensor button using its control button in LabView. For either case, ensure the “Caution Do Not Enter Thermal Hazard” signs are in place and pull the divider closer to the operator’s station to close access to the test area.

2.b. Administrative Controls:


Authorized users: a list of current authorized users is attached as Appendix I

User Training: Before performing experiments under this SOP, workers will:

- Review the content of this SOP;
- Review Trough Receiver Test Manual
- Receive instruction on working in this lab from the DAR;
- Receive instruction from principle authors of this SOP;
- Sign off on the Authorized Users Page, in Appendix I of this SOP;
- Review the operators manual for the roughing pump and turbo pump.
- Complete NREL Health and Safety Training:
 - Chemical Safety
 - Waste Minimization
 - Lockout/Tagout
 - Qualified Electrical Worker – Required for anyone trouble shooting, performing zero energy verification or working on an electrical system.
 - CPR – Required for anyone trouble shooting or working on an electrical system

2.c. Personal Protective Equipment (this section complies with OSHA’s requirement for a Certificate of Hazard Assessment under 29CFR1910.132)

Activity	PPE	Comments
General lab PPE – Accessing any part of the lab	<ul style="list-style-type: none"> ➤ Safety glasses with side shields ➤ Work boots or closed toe/closed heel shoes ➤ Long pants, no shorts 	

<p>Accessing the test area during testing, heat up or cool down periods</p>	<ul style="list-style-type: none"> ➤ General lab PPE ➤ Thermally insulating gloves ➤ Leather jacket and bib ➤ All cotton or other non-melting clothing ➤ Face shield with forehead protection 	
<p>Handling receivers</p>	<ul style="list-style-type: none"> ➤ General building PPE ➤ Leather gloves 	
<p>Performing diagnostics or zero energy verification on heater syst</p>	<ul style="list-style-type: none"> ➤ Long sleeve shirt and pants or coveralls with a minimum Arc Rating of 4 ➤ Arc rated face shield ➤ Safety glasses with side shields ➤ Hard hat ➤ Hearing protection (ear inserts) ➤ Dielectric gloves with leather protectors (dielectric gloves must have been tested within the last 6 months) 	<p>See section 2.a. Electrical</p>
<p>Performing visual non-contact inspections where energized conductors are exposed</p>	<ul style="list-style-type: none"> ➤ Long sleeve shirt and pants made of cotton or other non-melting material ➤ Safety glasses with side shields ➤ Hearing protection (ear inserts) ➤ Leather gloves 	<p>See section 2.a. Electrical</p>

3.0 Environmental Hazards and Controls

Are air and water emissions a concern?	<input checked="" type="checkbox"/> No	<input type="checkbox"/> Yes	List: No air or water emission concerns will be generated with these experiments.
Describe the environmental controls for this hazard:			
Not Applicable			

Will hazardous waste be generated?	<input checked="" type="checkbox"/> No	<input type="checkbox"/> Yes	List: No hazardous wastes will be generated with these experiments
Describe the methods for proper waste handling and disposal:			
Not Applicable			
Is waste minimization necessary?	<input checked="" type="checkbox"/> No	<input type="checkbox"/> Yes	List: There is little to no waste generated with these experiments.
Describe the methods to be utilized for waste minimization:			
Not Applicable			

4.0 ASSEMBLY/OPERATIONAL PROCEDURES

Though the operational procedures for Experiment #1 (Permeation Testing) and Experiment #2 (Inert gas – hydrogen mixture heat loss testing) are similar, there are enough minor differences to list them separately below.

Experiment #1 – Permeation testing

The testing procedure involves the following major steps:

- I. Receiver set-up
- II. Adding gas to the annulus
- III. Testing
- IV. Cool-down
- V. Repeat of steps III-IV for a number of days
- VI. Removing gas from annulus
- VII. Removing receiver from test stand

The steps are described in more detail below.

- I) **Receiver set-up**
 - a. Ensure receiver glass supports are up and place receiver on test stand.
 - b. Place heaters inside receiver.
 - c. Check receiver sag. If closer than ¼” to glass, do not test.
 - d. Check glass envelope for chips or cracks. If anything looks worn or suspect, do not test.
 - e. Loop absorber support wires around the ends of the absorber.
 - f. Slowly lower glass supports until absorber support wires are supporting entire weight of receiver.
 - g. Check that support wires are nestled in grooves on absorber ends and in the grooves on the test stand.
 - h. Turn on the data acquisition system. If pressure measurement is desired, ensure that the pressure gauges are at their operating temperature. This usually required the pressure gauges to be on the night before the test.

- II) **Adding gas to the annulus**
 - a. Attach vacuum system to the glass stem, ensuring that vacuum system o-ring seal is supported by the vacuum system stand.
 - b. Attach nitrogen and hydrogen gas cylinders to vacuum system. Keep the pressure regulator valves closed, but open valves that isolate vacuum system from the lines to the gas cylinders.
 - c. Turn on the roughing pump and pump the annulus down. Refer to the Edwards roughing pump manual for operating instructions.

- d. After pumping annulus down to the limit of the pump's vacuum pressure (0.05 torr), check that the system holds a vacuum.
- e. Fill the system to 500 torr of nitrogen, then pump the system back down to 0.05 torr. Repeat twice. This assures that the remaining gas in the annulus is more than 99.999999% nitrogen (or argon).
- f. Allow hydrogen to flow in to annulus to 1 torr. Pump back down to 0.05 torr. Repeat 4 times.
- g. Fill annulus once again to a pressure of hydrogen that once heated will meet the desired test pressure not to exceed 500 torr (or slightly less so that pressure is at its desired concentration after the gas heats up to an average temperature of about 300°C). The annulus gas should now be at least 99.999% hydrogen.
- h. Valve off nitrogen and hydrogen gas cylinders and remove from system.
- i. Valve off roughing pump and turn it off.

III) Testing

- a. Ensure that all signage and partitions are in place and the test area is clear of personnel and combustible material. "Do Not Enter" signs are located on the south doors and on the partitions.
- b. Remove any combustible items that are near the receiver.
- c. Make all necessary heater and thermocouple connections.
- d. Turn main switch "On"
- e. Use system software (Labview, Opto22, Watlow) to initiate heating to desired absorber temperature of 400°C. Monitor system and room air temperatures in the process.
- f. Watch absorber during warm-up and testing to assure that steel tube does not get closer than ¼" to glass. If it does, abort test.
- g. Staff will remain behind operator's desk unless something specific with the test stand requires the operator's attention. Staff may enter testing area briefly wearing aforementioned PPE.
- h. Test will be attended at all times when the power to the heaters is on.

IV) Cool down

- a. After the prescribed test period, operator will initiate cool down from the data acquisition system. This entails turning the heaters off and watching system temperatures decrease.
- b. System must be monitored during initial cool down to verify proper operation.
- c. Once the glass temperature is less than 75°C, the operator may shut off the main power to the system, turn off the data acquisition system, and leave. If testing is not finished, barriers should be left in place and signage should indicate that hydrogen is left in the annulus overnight.
- d. The operator may leave for the evening.

V) Repeat of steps III-IV for a number of days

- a. The permeation testing requires a number of days of tests. The goal of this testing is to find the total time needed for the glass temperature to decrease to about 80°C. This corresponds to a hydrogen pressure of about 0.001 torr.
- b. Steps III and IV are repeated until this occurs.

VI) Removing remaining hydrogen gas from annulus

- a. There will little hydrogen gas remaining in the annulus after these tests. However, before pumping the remaining hydrogen gas out it should be mixed with argon or nitrogen as safe practice.
- b. Allow system to cool to an absorber temperature of about 150°C.
- c. Attach the argon or nitrogen cylinder to the test stand.
- d. Allow argon or nitrogen to bleed into the annulus.
- e. Pump out gas mixture, venting to the fume hood.
- f. Turn off pump, allow about 500 torr of argon or nitrogen into the annulus.
- g. Vent system to atmosphere.

VII) Removing receiver from test stand

- a. Reinstall tube supports on test stand before unplugging heaters and TC's and then removing heaters. Remove wire absorber loop supports from receiver ends.
- b. The receiver can then be removed and a new receiver installed. Two people are required to handle the receivers.

Experiment #2 – Inert gas/hydrogen heat loss testing

The testing procedure involves the following major steps:

- I. Receiver set-up
- II. Baking out system as absorber reaches 350°C or 450°C.
- III. Adding gas to the annulus
- IV. Steady-state testing
- V. Repeat of steps III-IV
- VI. Cool-down/Removing gas from annulus
- VII. Removing receiver from test stand

The steps are described in more detail below

I) Receiver set-up

- a. Ensure receiver glass supports are up and place receiver on test stand.
- b. Place heaters inside receiver.
- c. Check receiver sag. If closer than ¼" to glass, do not test.
- d. Check glass envelope for chips or cracks. If anything looks worn or suspect, do not test.
- e. Loop absorber support wires around the ends of the absorber.
- f. Slowly lower glass supports until absorber support wires are supporting entire weight of receiver.
- g. Check that support wires are nestled in grooves on absorber ends and in the grooves on the test stand.
- h. Turn on the data acquisition system. Ensure that the pressure gauges are at their operating temperature. This usually required the pressure gauges to be on the night before the test.

II) Baking out system as absorber reaches 350°C or 450°C

- a. The vacuum system and absorber need to be baked out (evacuated while roughing and turbo pump are in operation) as they approach the desired test temperature before the gas is added to the annulus. This assures that any gases that are adsorbed on the absorber surface at room temperature (that wouldn't be pumped out at room temperature) are evacuated from the annulus at the test temperatures.
- b. Ensure that all signage and partitions are in place and the test area is clear of personnel and combustible material. "Do Not Enter" signs are located on the south doors and on the partitions.
- c. Remove any combustible items that are near the receiver.
- d. Make all necessary heater and thermocouple connections.
- e. Attach vacuum system to the glass stem, ensuring that vacuum system o-ring seal is supported by the vacuum system stand.
- f. Attach the gas cylinder with mixture of interest to the vacuum system. Keep the pressure regulator valve closed, but open valve that isolates vacuum system from the line to the gas cylinder.
- g. Turn main switch "On"
- h. Turn on the roughing pump and let it run.

- i. After pumping annulus down to the limit of the roughing pump's vacuum pressure (0.05 torr), check that the system holds a vacuum.
- j. If the system holds the vacuum, turn on the turbo pump while leaving the roughing pump running. Follow the operation procedures of the Pfeiffer Turbo Pump manual.
- k. After 10 minutes or so, valve off the pumps and see if the system still holds a vacuum. The pressure in the annulus should slowly increase due to the off-gassing of the absorber and glass.
- l. Use system software (Labview, Opto22, Watlow) to initiate heating to desired absorber temperature of 350°C or 450°C. Monitor system pressure and temperatures in the process.
- m. Once the system has reached the desired test temperature, allow it to bake out at temperature as long as it takes so that when the pumps are isolated from the system the pressure increase in the annulus due to off-gassing is minimal. Discussions with vacuum experts indicate this should take anywhere from 30 min to 2 hours.
- n. Once this is achieved, the turbo pump may be turned off and allowed to spin down, followed by the roughing pump.

III) **Adding gas to the annulus**

- a. Be sure valves to pumps and the pipe to the hydrogen gas mixture cylinder are closed.
- b. Open the gas mixture pressure regulator. The second valve now controls the amount of gas reaching the annulus.
- c. Slowly open the second valve connecting the hydrogen gas mixture cylinder to the annulus. Allow the desired pressure of gas to bleed in, then close the second valve followed by the first valve (the pressure regulator). The desired gas mixtures and pressures are listed in Appendix III.

IV) **Steady-state testing**

- a. The gas entering will decrease the absorber temperature. This absorber temperature must be brought back up to the desired test temperature (350°C or 450°C) using the computer software and then the system must be allowed to come to steady-state. This will take 1-2 hours.
- b. Once the system has achieved steady state (less than 0.5°C change in 15 minutes), record data for another 15 minutes.

V) **Repeat of steps III-IV**

- a. Data on as many pressures as possible will be gathered on a single day. Previous experience with receiver heat loss testing indicates that 5-6 data points are possible during one day.
- b. Repeat steps III and IV.

VI) **Cool-down/Removing gas from annulus**

- a. After the prescribed test period, operator will initiate cool down from the data acquisition system. This entails turning the heaters off and watching system temperatures decrease.
- b. System must be monitored during cool down to verify proper operation.
- c. Once the absorber temperature is less than 150°C, remove the hydrogen mixture gas cylinder and attach an argon gas cylinder.
- d. Allow argon to bleed into the annulus slowly until the annulus pressure is about 500 torr.
- e. Use the roughing pump to pump the diluted hydrogen gas mixture out the fume hood.
- f. Once again allow argon to bleed into the annulus to about 500 torr.
- g. Turn the roughing pump off and vent the system to atmosphere.
- h. Once the glass temperature is less than 75°C, the operator may leave.

VII) Removing receiver from test stand

- a. Reinstall tube supports on test stand before unplugging heaters and TC's and then removing heaters. Remove wire absorber loop supports from receiver ends.
- b. The receiver can then be removed and a new receiver installed. Two people are required to handle the receivers.

5.0 EMERGENCY INFORMATION

1) Describe emergency exits.

There are 3 emergency exits out of the FTLB Lab 118-1 and they are located:

- South end of room, exits into hallway
- West side of room, exits into hallway
- North end of room, exits into Lab 118-2

2) Building Evacuation/Assembly Area

In event of building evacuation gather in the south east parking lot. Make contact with a fire marshal team member.

3) Emergency Electrical Shutoff

Refer to the Emergency Shutdown Procedures found on page 1 of this document.

4) The Eyewash And Safety Shower Station location.

The hazards within FTLB Lab 118-1 do not specifically require and eyewash or shower, however an operational eyewash can be found at the utility sink located in the north west corner of the room. The nearest safety shower is located in the hallway between lab 119 and lab 121.

5) If exiting the lab out the west double doors, the Fire Pull alarm station will be to your left just as you exit the hallway door going into the **main** (high ceiling) hallway.

6) The Nearest Fire Extinguishers are Located at each of the exit doors.

8. REFERENCES

- Operators manual for roughing pump
- Operators manual for turbo pump
- Trough Receiver Test Manual
- Receiver Heat Loss Testing SOP
- NREL Chemical Safety Procedure; 6-4.6
- NREL Compressed Gas Safety Procedure; 6-4.7

- NREL Electrical Safety Procedure; 6-4.15
- NREL Lockout/Tagout Procedure; 6-4.16

Document Revision History

Revision: 2	Date Created: 1/04/10	Last Approval Date: 1/26/10
	Date of Last Revision: 3/25/11	

Reason for Change

Revision:	Sec/Para Changed	Change Made:	Date
0	N/A	Initial Issue of Document	1/4/2010
1	1 st page, section 2a	Better indicates location of each emergency shut-down switch and describes how to activate unattended operation sensors for each test stand.	3/25/2011
2	2a	Added LOTO description, modified upper hydrogen pressure range for permeation test	4/7/2011

Appendix I – Authorized Personnel

(By signing this document, the authorized worker is acknowledging that they have read and understood this SOP)

Worker Printed Name	Center # / Contractor	Authorized to:	Worker Signature	Signature of Authorizing Manager
Frank Burkholder	5500	<input type="checkbox"/> Hydrogen Permeation Testing <input checked="" type="checkbox"/> Heat Loss Testing with Hydrogen/Hydrogen Mixtures <input type="checkbox"/> Other		
Greg Glatzmaier	5500	<input checked="" type="checkbox"/> Hydrogen Permeation Testing <input type="checkbox"/> Heat Loss Testing with Hydrogen/Hydrogen Mixtures <input type="checkbox"/> Other		
Judy Netter	5500	<input checked="" type="checkbox"/> Hydrogen Permeation Testing <input checked="" type="checkbox"/> Heat Loss Testing with Hydrogen/Hydrogen Mixtures <input type="checkbox"/> Other		
Mike Martinez	5500	<input checked="" type="checkbox"/> Hydrogen Permeation Testing <input type="checkbox"/> Heat Loss Testing with Hydrogen/Hydrogen Mixtures <input type="checkbox"/> Other		
		<input type="checkbox"/> Hydrogen Permeation Testing <input type="checkbox"/> Heat Loss Testing with Hydrogen/Hydrogen Mixtures <input type="checkbox"/> Other		
		<input type="checkbox"/> Hydrogen Permeation Testing <input type="checkbox"/> Heat Loss Testing with Hydrogen/Hydrogen Mixtures <input type="checkbox"/> Other		
		<input type="checkbox"/> Hydrogen Permeation Testing <input type="checkbox"/> Heat Loss Testing with Hydrogen/Hydrogen Mixtures <input type="checkbox"/> Other		
		<input type="checkbox"/> Hydrogen Permeation Testing <input type="checkbox"/> Heat Loss Testing with Hydrogen/Hydrogen Mixtures <input type="checkbox"/> Other		
		<input type="checkbox"/> Hydrogen Permeation Testing <input type="checkbox"/> Heat Loss Testing with Hydrogen/Hydrogen Mixtures <input type="checkbox"/> Other		
		<input type="checkbox"/> Hydrogen Permeation Testing <input type="checkbox"/> Heat Loss Testing with Hydrogen/Hydrogen Mixtures <input type="checkbox"/> Other		
		<input type="checkbox"/> Hydrogen Permeation Testing <input type="checkbox"/> Heat Loss Testing with Hydrogen/Hydrogen Mixtures <input type="checkbox"/> Other		
		<input type="checkbox"/> Hydrogen Permeation Testing <input type="checkbox"/> Heat Loss Testing with Hydrogen/Hydrogen Mixtures <input type="checkbox"/> Other		
		<input type="checkbox"/> Hydrogen Permeation Testing <input type="checkbox"/> Heat Loss Testing with Hydrogen/Hydrogen Mixtures <input type="checkbox"/> Other		

**APPENDIX II:
MSDS for Hydrogen**

MATERIAL SAFETY DATA SHEET

SECTION 1. PRODUCT IDENTIFICATION

PRODUCT NAME: Hydrogen, compressed
CHEMICAL NAME: Hydrogen **FORMULA:** H₂
SYNONYMS: None
MANUFACTURER: Air Products and Chemicals, Inc.
7201 Hamilton Boulevard
Allentown, PA 18195-1501
PRODUCT INFORMATION: 1-800-752-1597
MSDS NUMBER: 1009 **REVISION:** 4
REVISION DATE: June 1994

SECTION 2. COMPOSITION/INFORMATION ON INGREDIENTS

Hydrogen is sold as pure product >99%

CAS NUMBER: 1333-74-0

EXPOSURE LIMITS:

OSHA: None

ACGIH: Simple asphyxiant

SECTION 3. HAZARD IDENTIFICATION

EMERGENCY OVERVIEW

Hydrogen is a flammable, colorless, odorless, compressed gas packaged in cylinders at high pressure. It poses an immediate fire and explosive hazard when concentrations exceed 4%. It is much lighter than air and burns with an invisible flame. High concentrations that will cause suffocation are within the flammable range and must not be entered.

EMERGENCY TELEPHONE NUMBERS

(800) 523-9374 Continental U.S., Canada, and Puerto Rico

(610) 481-7711 other locations

POTENTIAL HEALTH EFFECTS INFORMATION:

INHALATION: Asphyxiant. It should be noted that before suffocation could occur, the lower flammability limit of hydrogen in air would be exceeded possibly causing both an oxygen-deficient and explosive atmosphere. Exposure to moderate concentrations may cause dizziness, headache, nausea and unconsciousness. Exposure to atmospheres containing 8-10% or less oxygen will quickly bring about unconsciousness without warning leaving individuals unable to protect themselves. Lack of sufficient oxygen may cause serious injury or death.

EYE CONTACT: None
SKIN CONTACT: None
CHRONIC EFFECTS: None
OTHER EFFECTS OF OVEREXPOSURE: None

EXPOSURE INFORMATION:

ROUTE OF ENTRY: Inhalation
TARGET ORGANS: None
EFFECT: Asphyxiation (suffocation)
SYMPTOMS: Exposure to an oxygen-deficient atmosphere (<19.5%) may cause dizziness, drowsiness, nausea, vomiting, excess salivation, diminished mental alertness, loss of consciousness, and death.

MEDICAL CONDITIONS AGGRAVATED BY OVEREXPOSURE: None

CARCINOGENIC POTENTIAL: Hydrogen is not listed by NTP, OSHA or IARC.

SECTION 4. FIRST AID

INHALATION: Persons suffering from lack of oxygen should be removed to fresh air. If victim is not breathing, administer artificial respiration. If breathing is difficult, administer oxygen. Obtain prompt medical attention.

SKIN CONTACT: None

EYE CONTACT: None

INGESTION: None

NOTES TO PHYSICIAN: None

SECTION 5. FIRE AND EXPLOSION

FLASH POINT: Flammable gas	AUTOIGNITION: 565.5_C (1050_F)	FLAMMABLE LIMITS: LOWER: 4% UPPER: 74%
--------------------------------------	--	--

EXTINGUISHING MEDIA: CO₂, dry chemical, water spray or fog for surrounding area. Do not extinguish until hydrogen source is shut off.

HAZARDOUS COMBUSTION PRODUCTS: None

SPECIAL FIRE FIGHTING INSTRUCTIONS: Evacuate all personnel from danger area. Immediately cool container with water spray from maximum distance, taking care not to extinguish flames. If flames are accidentally extinguished, explosive re-ignition may occur. Stop flow of gas if without risk while continuing cooling water spray.

UNUSUAL FIRE AND EXPLOSION HAZARDS: Burns with a pale blue, nearly invisible flame. Hydrogen is easily ignited with low-ignition energy, including static electricity. Hydrogen is lighter than air and can accumulate in the upper sections of enclosed spaces. Pressure in a container can build up due to heat, and it may rupture if pressure relief devices should fail to function.

SECTION 6. ACCIDENTAL RELEASE MEASURES

Evacuate immediate area. Eliminate any possible sources of ignition, and provide maximum explosion-proof ventilation. Shut off source of hydrogen, if possible. If leaking from cylinder, or valve, call the Air Products' emergency phone number. The presence of a hydrogen flame can be detected by approaching cautiously with an outstretched straw broom to make the flame visible.

SECTION 7. HANDLING AND STORAGE

STORAGE: Specific requirements are listed in NFPA 50A. Cylinder storage locations should be well-protected, well-ventilated, dry, and separated from combustible materials. Cylinders should never knowingly be allowed to reach a temperature exceeding 125 °F (52 °C). Cylinders of hydrogen should be separated from oxygen cylinders or other oxidizers by a minimum distance of 20 ft., or by a barrier of noncombustible material at least 5 ft. high having a fire resistance rating of at least 1 hour.

Cylinders should be stored upright with valve protection cap in place and firmly secured to prevent falling or being knocked over. Protect cylinders from physical damage; do not drag, roll, slide or drop. Use a suitable hand truck for cylinder movement. Post "No Smoking or Open Flames" signs in the storage areas. There should be no sources of ignition. All electrical equipment should be explosion proof in the storage and use areas. Storage areas must meet national electric codes for class 1 hazardous areas.

HANDLING: Do not "open" hydrogen cylinder valve before connecting it, since self-ignition may occur. Hydrogen is the lightest gas known and may collect in the top of buildings with out proper ventilation. It may leak out of a system which is gas-tight for air or other gases. Leak check system with leak detection solution, never with flame. If user experiences difficulty operating cylinder valve, discontinue use and contact supplier. Use only approved CGA connections. DO NOT USE ADAPTERS. Never insert an object (e.g., wrench, screwdriver, pry bar, etc.) into valve cap openings. Doing so may damage valve, causing a leak to occur. Use an adjustable strap wrench to remove over-tight or rusted caps. Never strike an arc on a compressed gas cylinder or make a cylinder a part of an electrical circuit.

SPECIAL PRECAUTIONS: Use piping and equipment adequately designed to withstand pressures to be encountered. Use a check valve or other protective apparatus in any line or piping from the cylinder to prevent reverse flow.

SECTION 8. PERSONAL PROTECTION/EXPOSURE CONTROLS

ENGINEERING CONTROLS: Provide natural or explosion-proof ventilation adequate to ensure hydrogen does not reach its lower explosive limit of 4%.

RESPIRATORY PROTECTION:

General Use: None

Emergency Use: Air supplied respirators are required in oxygen-deficient atmospheres. Before entering area you must check for flammable or oxygen-deficient atmospheres.

PROTECTIVE GLOVES: Work gloves are recommended when handling cylinders.

EYE PROTECTION: Safety glasses are recommended when handling cylinders.

OTHER PROTECTIVE EQUIPMENT: Safety shoes are recommended when handling cylinders.

SECTION 9. PHYSICAL AND CHEMICAL PROPERTIES

APPEARANCE AND STATE: Colorless gas at normal temperature and pressure.

ODOR: Odorless

MOLECULAR WEIGHT: 2.016

BOILING POINT (1 atm): -423.0 °F (-252.8 °C)

SPECIFIC GRAVITY (Air =1): 0.06960

FREEZING POINT/MELTING POINT: -434.5 °F (-259.2 °C)

VAPOR PRESSURE (at 70 °F): Not applicable

GAS DENSITY (At 70 °F (21.1 °C) and 1 atm): 0.00521 lb/ft³ (0.08342 kg/m³)

SOLUBILITY IN WATER (Vol/Vol at 60 °F (15.6 °C): 0.019

SPECIFIC VOLUME (At 70 °F (21.1 °C) and 1 atm): 192 ft³/lb (11.99m³/kg)

SECTION 10. REACTIVITY/STABILITY

CHEMICAL STABILITY: Stable

CONDITIONS TO AVOID: None

INCOMPATIBILITY (Materials to Avoid): Oxidizing agents. Some steels are susceptible to hydrogen embrittlement at high pressures and temperatures.

REACTIVITY:

- A) **HAZARDOUS DECOMPOSITION PRODUCTS:** None
- B) **HAZARDOUS POLYMERIZATION:** Will not occur.

SECTION 11. TOXICOLOGICAL INFORMATION

Hydrogen is a simple asphyxiant.

SECTION 12. ECOLOGICAL INFORMATION

No adverse ecological effects are expected. Hydrogen does not contain any Class I or Class II ozone depleting chemicals (40 CFR Part 82). Hydrogen is not listed as a marine pollutant by DOT (49 CFR Part 171).

SECTION 13. DISPOSAL

WASTE DISPOSAL METHOD: Do not attempt to dispose of residual or unused product in the cylinder. Return to supplier for safe disposal.

Residual product within process system may be vented at a controlled rate, to the atmosphere through a vent stack that discharges to an elevated point. This stack should be in an isolated area away from ignition sources.

SECTION 14. TRANSPORTATION

DOT/IMO SHIPPING NAME: Hydrogen, compressed

HAZARD CLASS: 2.1 (Flammable Gas)

IDENTIFICATION NUMBER: UN1049

PRODUCT RQ: None

SHIPPING LABEL(s): Flammable gas.

PLACARD (When required): Flammable gas.

SPECIAL SHIPPING INFORMATION: Cylinder should be transported in a secure upright position in a well ventilated truck. NEVER TRANSPORT IN PASSENGER COMPARTMENT OF A VEHICLE.

Shipment of compressed gas cylinders which have not been filled with the owner's consent is a violation of Federal law (49 CFR Part 173.301 (b)).

SECTION 15. REGULATORY INFORMATION

U.S. FEDERAL REGULATIONS:

EPA - ENVIRONMENTAL PROTECTION AGENCY

CERCLA: Comprehensive Environmental Response, Compensation, and Liability Act of 1980 (40 CFR Parts 117 and 302):

Reportable Quantity (RQ): None

SARA: Superfund Amendment and Reauthorization Act

SECTION 302/304: Requires emergency planning on threshold planning quantities (TPQ) and release reporting based on reportable quantities (RQ) of EPA's extremely hazardous substances (40 CFR Part 355).

Extremely Hazardous Substances: None

Threshold Planning Quantity (TPQ): None

SECTIONS 311/312: Require submission of material safety data sheets (MSDSs) and chemical inventory reporting with identification of EPA defined hazard classes (40 CFR Part 370). The hazard classes for this product are:

IMMEDIATE:	No	PRESSURE:	Yes
DELAYED:	No	REACTIVITY:	No
		FLAMMABLE:	Yes

SECTION 313: Requires submission of annual reports of release of toxic chemicals that appear in 40 CFR Part 372.

Hydrogen does not require reporting under Section 313

40 CFR PART 68: Risk Management for Chemical Accidental Release. Requires the development and implementation of risk management programs at facilities that manufacture, use, store, or otherwise handle regulated substances in quantities that exceed specified thresholds.

Hydrogen is not listed as a regulated substance. However, any process that involves a flammable gas on site in one location, in quantities of 10,000 pounds (4,553 kg) or greater, is covered under this regulation.

TSCA: Toxic Substance Control Act: Hydrogen is listed on the TSCA inventory.

OSHA - OCCUPATIONAL SAFETY AND HEALTH ADMINISTRATION:

29 CFR 1910.119: Process Safety Management of Highly Hazardous Chemicals. Requires facilities to develop a process safety management program based on Threshold Quantities (TQ) of highly hazardous chemicals.

Hydrogen is not listed in Appendix A as a highly hazardous chemical. However, any process that involves a flammable gas on site in one location, in quantities of 10,000 pounds (4,553 kg) or greater is covered under this regulation unless it is used as fuel.

SECTION 16. OTHER INFORMATION

OTHER INFORMATION:

NFPA RATINGS:

HEALTH: = 0

FLAMMABILITY: = 4

REACTIVITY: = 0

SPECIAL: = SA (CGA recommends this to designate simple asphyxiant)

HMIS RATINGS:

HEALTH: = 0

FLAMMABILITY: = 4

REACTIVITY: = 0

APPENDIX III: Planned inert gas/hydrogen mixture heat loss tests

Appendix C - All tests listed below performed at 350 °C and 450 °C.									
Highlight cells		1.0%		or greater H2 volumetric percentage if leak into annulus					
Gas/Gas Mixture:		Argon			Gas/Gas Mixture:		Xenon		
% H2:		0%			% H2:		0%		
Comment:		Pure argon testing			Comment:		Pure xenon testing		
Test #	Pressure in annulus (torr)	Volume of H2 in annulus at atm. pressure (L)	% volume H2 if leak into annulus	Qnt. H2 (g)	Test #	Pressure in annulus (torr)	Volume of H2 in annulus at atm. pressure (L)	% volume H2 if leak into annulus	Qnt. H2 (g)
1	0.0001	0	0.0%	0.E+00	16	0.0001	0	0.0%	0.E+00
2	0.0004	0	0.0%	0.E+00	17	0.0004	0	0.0%	0.E+00
3	0.001	0	0.0%	0.E+00	18	0.001	0	0.0%	0.E+00
4	0.004	0	0.0%	0.E+00	19	0.004	0	0.0%	0.E+00
5	0.01	0	0.0%	0.E+00	20	0.01	0	0.0%	0.E+00
6	0.03	0	0.0%	0.E+00	21	0.03	0	0.0%	0.E+00
7	0.06	0	0.0%	0.E+00	22	0.06	0	0.0%	0.E+00
8	0.1	0	0.0%	0.E+00	23	0.1	0	0.0%	0.E+00
9	0.2	0	0.0%	0.E+00	24	0.2	0	0.0%	0.E+00
10	0.5	0	0.0%	0.E+00	25	0.5	0	0.0%	0.E+00
11	1	0	0.0%	0.E+00	26	1	0	0.0%	0.E+00
12	2	0	0.0%	0.E+00	27	2	0	0.0%	0.E+00
13	5	0	0.0%	0.E+00	28	5	0	0.0%	0.E+00
14	10	0	0.0%	0.E+00	29	10	0	0.0%	0.E+00
15	100	0	0.0%	0.E+00	30	100	0	0.0%	0.E+00
Gas/Gas Mixture: 90% Argon / 10% Hydrogen					Gas/Gas Mixture: 75% Argon / 25% Hydrogen				
% H2:		10%			% H2:		25%		
Comment:		gas mixture			Comment:		gas mixture		
Test #	Pressure in annulus (torr)	Volume of H2 in annulus at atm. pressure (L)	% volume H2 if leak into annulus	Qnt. H2 (g)	Test #	Pressure in annulus (torr)	Volume of H2 in annulus at atm. pressure (L)	% volume H2 if leak into annulus	Qnt. H2 (g)
31	0.0001	3.8E-07	0.0%	2.E-08	46	0.0001	9.5E-07	0.0%	4.E-08
32	0.0004	1.5E-06	0.0%	6.E-08	47	0.0004	3.8E-06	0.0%	2.E-07
33	0.001	3.8E-06	0.0%	2.E-07	48	0.001	9.5E-06	0.0%	4.E-07
34	0.004	1.5E-05	0.0%	6.E-07	49	0.004	3.8E-05	0.0%	2.E-06
35	0.01	3.8E-05	0.0%	2.E-06	50	0.01	9.5E-05	0.0%	4.E-06
36	0.03	1.1E-04	0.0%	5.E-06	51	0.03	2.8E-04	0.0%	1.E-05
37	0.06	2.3E-04	0.0%	9.E-06	52	0.06	5.7E-04	0.0%	2.E-05
38	0.1	3.8E-04	0.0%	2.E-05	53	0.1	9.5E-04	0.0%	4.E-05
39	0.2	7.6E-04	0.0%	3.E-05	54	0.2	1.9E-03	0.0%	8.E-05
40	0.5	1.9E-03	0.0%	8.E-05	55	0.5	4.7E-03	0.0%	2.E-04
41	1	3.8E-03	0.0%	2.E-04	56	1	9.5E-03	0.0%	4.E-04
42	2	7.6E-03	0.0%	3.E-04	57	2	1.9E-02	0.1%	8.E-04
43	5	1.9E-02	0.1%	8.E-04	58	5	4.7E-02	0.2%	2.E-03
44	10	3.8E-02	0.2%	2.E-03	59	10	9.5E-02	0.4%	4.E-03
45	100	3.8E-01	1.5%	2.E-02	60	100	9.5E-01	3.8%	4.E-02

Gas/Gas Mixture: 50% Argon / 50% Hydrogen					Gas/Gas Mixture: 90% Xenon / 10% Hydrogen				
% H2: 50%					% H2: 10%				
Comment: gas mixture					Comment: gas mixture				
Test #	Pressure in annulus (torr)	Volume of H2 in annulus at atm. pressure (L)	% volume H2 if leak into annulus	Qnt. H2 (g)	Test #	Pressure in annulus (torr)	Volume of H2 in annulus at atm. pressure (L)	% volume H2 if leak into annulus	Qnt. H2 (g)
61	0.0001	1.9E-06	0.0%	8.E-08	76	0.0001	3.8E-07	0.0%	2.E-08
62	0.0004	7.6E-06	0.0%	3.E-07	77	0.0004	1.5E-06	0.0%	6.E-08
63	0.001	1.9E-05	0.0%	8.E-07	78	0.001	3.8E-06	0.0%	2.E-07
64	0.004	7.6E-05	0.0%	3.E-06	79	0.004	1.5E-05	0.0%	6.E-07
65	0.01	1.9E-04	0.0%	8.E-06	80	0.01	3.8E-05	0.0%	2.E-06
66	0.03	5.7E-04	0.0%	2.E-05	81	0.03	1.1E-04	0.0%	5.E-06
67	0.06	1.1E-03	0.0%	5.E-05	82	0.06	2.3E-04	0.0%	9.E-06
68	0.1	1.9E-03	0.0%	8.E-05	83	0.1	3.8E-04	0.0%	2.E-05
69	0.2	3.8E-03	0.0%	2.E-04	84	0.2	7.6E-04	0.0%	3.E-05
70	0.5	9.5E-03	0.0%	4.E-04	85	0.5	1.9E-03	0.0%	8.E-05
71	1	1.9E-02	0.1%	8.E-04	86	1	3.8E-03	0.0%	2.E-04
72	2	3.8E-02	0.2%	2.E-03	87	2	7.6E-03	0.0%	3.E-04
73	5	9.5E-02	0.4%	4.E-03	88	5	1.9E-02	0.1%	8.E-04
74	10	1.9E-01	0.8%	8.E-03	89	10	3.8E-02	0.2%	2.E-03
75	100	1.9E+00	7.6%	8.E-02	90	100	3.8E-01	1.5%	2.E-02
Gas/Gas Mixture: 75% Xenon / 25% Hydrogen					Gas/Gas Mixture: 50% Xenon / 50% Hydrogen				
% H2: 25%					% H2: 50%				
Comment: gas mixture					Comment: gas mixture				
Test #	Pressure in annulus (torr)	Volume of H2 in annulus at atm. pressure (L)	% volume H2 if leak into annulus	Qnt. H2 (g)	Test #	Pressure in annulus (torr)	Volume of H2 in annulus at atm. pressure (L)	% volume H2 if leak into annulus	Qnt. H2 (g)
91	0.0001	9.5E-07	0.0%	4.E-08	106	0.0001	1.9E-06	0.0%	8.E-08
92	0.0004	3.8E-06	0.0%	2.E-07	107	0.0004	7.6E-06	0.0%	3.E-07
93	0.001	9.5E-06	0.0%	4.E-07	108	0.001	1.9E-05	0.0%	8.E-07
94	0.004	3.8E-05	0.0%	2.E-06	109	0.004	7.6E-05	0.0%	3.E-06
95	0.01	9.5E-05	0.0%	4.E-06	110	0.01	1.9E-04	0.0%	8.E-06
96	0.03	2.8E-04	0.0%	1.E-05	111	0.03	5.7E-04	0.0%	2.E-05
97	0.06	5.7E-04	0.0%	2.E-05	112	0.06	1.1E-03	0.0%	5.E-05
98	0.1	9.5E-04	0.0%	4.E-05	113	0.1	1.9E-03	0.0%	8.E-05
99	0.2	1.9E-03	0.0%	8.E-05	114	0.2	3.8E-03	0.0%	2.E-04
100	0.5	4.7E-03	0.0%	2.E-04	115	0.5	9.5E-03	0.0%	4.E-04
101	1	9.5E-03	0.0%	4.E-04	116	1	1.9E-02	0.1%	8.E-04
102	2	1.9E-02	0.1%	8.E-04	117	2	3.8E-02	0.2%	2.E-03
103	5	4.7E-02	0.2%	2.E-03	118	5	9.5E-02	0.4%	4.E-03
104	10	9.5E-02	0.4%	4.E-03	119	10	1.9E-01	0.8%	8.E-03
105	100	9.5E-01	3.8%	4.E-02	120	100	1.9E+00	7.6%	8.E-02

Gas/Gas Mixture:		Hydrogen						
% H2:		100%						
Comment:		Pure H2 for accommodation coefficient testing						
Test #	Pressure in annulus (torr)	Volume of H2 in annulus at atm. pressure (L)	% volume H2 if leak into annulus	Qnt. H2 (g)				
121	0.0001	3.8E-06	0.0%	2.E-07				
122	0.0004	1.5E-05	0.0%	6.E-07				
123	0.001	3.8E-05	0.0%	2.E-06				
124	0.004	1.5E-04	0.0%	6.E-06				
125	0.01	3.8E-04	0.0%	2.E-05				
126	0.03	1.1E-03	0.0%	5.E-05				
127	0.06	2.3E-03	0.0%	9.E-05				
128	0.1	3.8E-03	0.0%	2.E-04				
129	0.2	7.6E-03	0.0%	3.E-04				
130	0.5	1.9E-02	0.1%	8.E-04				
131	1	3.8E-02	0.2%	2.E-03				
132	2	7.6E-02	0.3%	3.E-03				
133	5	1.9E-01	0.8%	8.E-03				
134	10	3.8E-01	1.5%	2.E-02				
135	100	3.8E+00	15.2%	2.E-01				
136	200	7.6E+00	30.3%	3.E-01				
137	300	1.1E+01	45.5%	5.E-01				
138	400	1.5E+01	60.6%	6.E-01				
139	500	1.9E+01	75.8%	8.E-01				

APPENDIX IV: LOTO Procedures

National Renewable Energy Laboratory LOCKOUT/TAGOUT EQUIPMENT SPECIFIC PROCEDURE

INTRODUCTION	
<p>Caution: Hazardous energy sources shall be under the exclusive control of the authorized worker (or workers) conducting service or maintenance. Zero energy verification shall be achieved and confirmed (by all workers) prior to the commencement of work. Each authorized worker shall apply their own locks & tags to each isolation device. Locks may not be shared. Where required by Lab Level Procedure 6-4.16 (Lockout/Tagout), use this form to document equipment specific procedures, and incorporate with the applicable Safe Operating Procedure (SOP).</p>	
EQUIPMENT INFORMATION	
Equipment Description HCE Receiver Test Stand #1	Manufacturer NREL
Location FTLB 118-01	Center 5500
APPLICATION OF CONTROL	
<p>1. Notify Affected Workers - Before beginning work on equipment or systems, notify users and workers in the area who could be affected by the shutdown. If possible, schedule and coordinate work to minimize interruptions.</p> <p>2. Preparation for Shutdown - The authorized worker shall review the below table and have knowledge of the type and magnitude of the energy, the hazards of the energy to be controlled, and the method or means to control the energy.</p> <p>3. Shutdown Procedure - The machine or equipment shall be turned off or shut down (by an authorized worker) using the following established procedures:</p> <ul style="list-style-type: none"> • Shut down heaters through data acquisition program • Allow heaters to cool down to room temperature • Place disconnect identified in step 1 to the off position • Unplug the 120 V cord coming from the DAC box on the test stand marked with the 120V sticker • Complete energy isolation steps 1 and 2 below 	

Identification of Hazardous Energy		4. Energy Isolation and Lock/Tag Application (as referenced in step 3 above)				5. Stored Energy		6. Verification		
		Type	Magnitude	Type	Location	ID	Required Hardware	Y/N	Required Action	Method
1	Electrical	208 VAC	Disconnect	Disconnect located on east wall	Main Power HCE Receiver Test	Multilock hasp	<input type="checkbox"/> Yes <input checked="" type="checkbox"/> No		Voltage measurement across each phase where line voltage enters equipment	Electrical/Arc Flash PPE meeting Hazard Category 1
2	Electrical	120 VAC	Cord & Plug	Test Stand #1	DAC box on stand marked 120V	Plug cover and Multilock hasp if cord and plug exemption cannot be maintained	<input type="checkbox"/> Yes <input type="checkbox"/> No		Voltage measurement where line voltage enters equipment	Electrical/Arc Flash PPE meeting Hazard Category 1

ADDITIONAL SAFETY MEASURES

Refer to the above table. This space is provided to list additional detailed instructions regarding the steps necessary to relieve any residual or potential energy resident in the system (and to prevent re-accumulation). This space may also be used to list additional details regarding energy isolation or zero energy verification.

Hazard Category 1 PPE includes:

- Long sleeve shirt and long pant s, or coveralls meeting an arc rating of 4
- Face shield with arc rating of 4 and wrap around guarding to protect forehead, ears and neck
- Hard hat, Safety glasses with side shields, and Hearing protection (ear inserts)
- Dielectric gloves with leather protectors

Line Drawing Required by EHS Office Photos Required by EHS Office

REMOVAL PROCEDURE

1. **Area Survey** - Inspect the work area to ensure that nonessential items have been removed and that machine or equipment components are operationally intact and ready for operation.
2. **Preparation** - Check the work area to ensure that all personnel have been safely positioned or removed from the area.
3. **Verification** - Verify that the controls are in the "off" or neutral position.
4. **Notification** - Notify affected employees that the lockout or tagout device(s) have been removed. Notification shall occur prior to the start-up of equipment.
5. **Device Removal** - Remove lockout/tagout devices (as identified in the above table). Device removal shall be performed by the authorized worker who applied the device.

RE-ENERGIZATION (START-UP) PROCEDURE – List the sequence of steps required for restoring equipment to operation.

1. Follow standard equipment start up procedures
- 2.

National Renewable Energy Laboratory
LOCKOUT/TAGOUT EQUIPMENT SPECIFIC PROCEDURE

INTRODUCTION

Caution: Hazardous energy sources shall be under the exclusive control of the authorized worker (or workers) conducting service or maintenance. Zero energy verification shall be achieved and confirmed (by all workers) prior to the commencement of work. Each authorized worker shall apply their own locks & tags to each isolation device. Locks may not be shared. Where required by Lab Level Procedure 6-4.16 (Lockout/tagout), use this form to document equipment specific procedures, and incorporate with the applicable Safe Operating Procedure (SOP).

EQUIPMENT INFORMATION

Equipment Description	HCE Receiver Test Stand #2	Manufacturer	NREL	Model #	N/A
Location	FTLB 118-01	Center	5500	NREL SOP #	751 and 827

APPLICATION OF CONTROL

1. **Notify Affected Workers** - Before beginning work on equipment or systems, notify users and workers in the area who could be affected by the shutdown. If possible, schedule and coordinate work to minimize interruptions.
2. **Preparation for Shutdown** - The authorized worker shall review the below table and have knowledge of the type and magnitude of the energy, the hazards of the energy to be controlled, and the method or means to control the energy.
3. **Shutdown Procedure** - The machine or equipment shall be turned off or shut down (by an authorized worker) using the following established procedures:
 - Shut down heaters through data acquisition program
 - Allow heaters to cool down to room temperature
 - Place disconnect identified in step 1 to the off position
 - Unplug the 120 V cord coming from the box on the test stand marked as "Receiver Hydrogen Permeation Test"
 - Complete energy isolation steps 1 and 2 below

Item	Identification of Hazardous Energy			4. Energy Isolation and Lock/Tag Application (as referenced in step 3 above)			5. Stored Energy		6. Verification	
	Type	Magnitude	Type	Location	ID	Required Hardware	Y/N	Required Action	Method	PPE
1	Electrical	208 VAC	Disconnect	Disconnect located on west wall	Test Stand #2	Multilock hasp	<input type="checkbox"/> Yes <input checked="" type="checkbox"/> No		Voltage measurement across each phase where line voltage enters equipment	Electrical/Arc Flash PPE meeting Hazard Category 1
2	Electrical	120 VAC	Cord & Plug	Test Stand #2	Receiver Hydrogen Permeation Test	Plug cover and Multilock hasp if cord and plug exemption cannot be maintained	<input type="checkbox"/> Yes <input checked="" type="checkbox"/> No		Voltage measurement where line voltage enters equipment	Electrical/Arc Flash PPE meeting Hazard Category 1

ADDITIONAL SAFETY MEASURES

Refer to the above table. This space is provided to list additional detailed instructions regarding the steps necessary to relieve any residual or potential energy resident in the system (and to prevent re-accumulation). This space may also be used to list additional details regarding energy isolation or zero energy verification.

Hazard Category 1 PPE includes:

- Long sleeve shirt and long pant s, or coveralls meeting an arc rating of 4
- Face shield with arc rating of 4 and wrap around guarding to protect forehead, ears and neck
- Hard hat , Safety glasses with side shields, and Hearing protection (ear inserts)
- Dielectric gloves with leather protectors

Line Drawing Required by EHS Office Photos Required by EHS Office

REMOVAL PROCEDURE

1. **Area Survey** - Inspect the work area to ensure that nonessential items have been removed and that machine or equipment components are operationally intact and ready for operation.

2. **Preparation** - Check the work area to ensure that all personnel have been safely positioned or removed from the area.

3. **Verification** - Verify that the controls are in the "off" or neutral position.

4. **Notification** - Notify affected employees that the lockout or tagout device(s) have been removed. Notification shall occur prior to the start-up of equipment.

5. **Device Removal** - Remove lockout/tagout devices (as identified in the above table). Device removal shall be performed by the authorized worker who applied the device.

RE-ENERGIZATION (START-UP) PROCEDURE – List the sequence of steps required for restoring equipment to operation.

1. Follow standard equipment start up procedures
- 2.

Appendix E - Experimental Results in Tabular Form

Gas	P (Pa)	T _{abs} (°C)	T _{gl,i} (°C)	Q _C (W/m)	U _{QC} (±W/m)
H ₂	0.7	348.6	64.9	41.9	8.9
	2.2	348.4	78.2	111.5	9.1
	3.6	349.9	87.9	154.6	9.3
	8.1	351.5	102.6	256.2	9.9
	13.1	350.5	114.0	328.5	10.4
	40.0	352.3	135.3	489.1	11.9
	149.2	350.8	147.8	604.4	13.4
	395.8	351.0	153.0	636.4	13.8
	1347.0	351.0	155.0	655.3	14.1
	13626.0	349.7	155.3	661.7	14.2
Ar	1.5	350.3	63.0	26.0	8.8
	4.5	351.1	67.7	47.8	8.9
	14.7	352.3	72.4	70.9	9.0
	40.8	351.8	73.1	81.9	9.0
	172.3	352.9	74.1	85.2	9.0
Xe	1.4	352.3	60.1	12.3	8.8
	4.1	352.5	62.1	20.5	8.8
	13.9	352.4	63.6	27.2	8.8
	40.3	352.1	64.1	29.8	8.8
	133.3	352.2	64.4	31.4	8.8
	1332.0	352.7	64.6	30.7	8.8
10% H ₂ / 90% Ar	1.8	351.5	63.7	27.2	8.8
	4.4	351.2	68.9	54.3	8.9
	13.6	352.3	75.4	88.7	9.0
	40.7	351.5	78.9	114.4	9.1
	137.3	351.2	81.3	125.4	9.2
	1318.0	350.9	81.7	132.7	9.2
25% H ₂ / 75% Ar	4.1	349.3	70.6	66.4	8.9
	14.1	350.0	80.0	120.7	9.1
	40.6	350.6	87.7	163.3	9.3
	139.8	351.4	91.1	182.9	9.4
	1419.0	352.4	91.2	186.4	9.5
	11692.0	352.5	90.9	188.2	9.5
25% H ₂ / 75% Ar	1.2	347.4	64.1	33.7	8.8
	8.1	348.9	77.3	103.4	9.1
	143.1	350.5	91.3	183.8	9.4
25% H ₂ / 75% Ar	2.4	347.5	68.0	52.0	8.9
	13.0	350.2	81.5	125.7	9.2
50% H ₂ / 50% Ar	4.6	349.7	78.4	111.9	9.1
	13.3	350.5	91.5	179.2	9.4
	40.7	351.7	102.7	247.4	9.8
	136.9	349.5	107.4	293.4	10.1
	415.2	351.0	110.0	310.8	10.3
	1296.0	351.6	111.4	317.3	10.3
	13332.0	351.9	111.9	318.5	10.3

Gas	P (Pa)	T _{abs} (°C)	T _{gl,i} (°C)	Q _C (W/m)	U _{QC} (±W/m)
52.5% H ₂ / 47.5% Xe	4.0	349.9	70.1	78.3	9.0
	13.4	350.2	85.6	149.8	9.3
	40.0	349.0	95.7	214.0	9.6
	133.5	350.4	100.7	244.8	9.8
	1308.0	349.8	103.8	268.1	10.0
52.5% H ₂ / 47.5% Xe	1.3	351.1	65.4	40.9	8.8
	9.1	348.9	81.6	127.5	9.2
	135.9	351.0	101.0	243.5	9.8
52.5% H ₂ / 47.5% Xe	3.4	349.5	71.3	69.8	8.9
	14.0	348.0	86.7	155.0	9.3
	398.6	352.6	103.5	263.4	9.9
27.2% H ₂ / 72.8% Xe	2.2	351.8	63.2	27.9	8.8
	3.5	351.0	66.9	47.4	8.9
	15.0	350.8	74.9	89.8	9.0
	40.2	349.3	80.5	119.0	9.1
	147.7	348.8	83.2	134.4	9.2
	1347.0	348.5	83.3	136.9	9.2
	5746.0	349.0	83.0	135.3	9.2
11.2% H ₂ / 88.8% Xe	1.7	352.0	61.8	19.6	8.8
	3.8	350.9	63.0	33.2	8.8
	7.1	352.2	65.2	43.2	8.9
	13.6	352.1	67.1	53.2	8.9
	37.6	351.7	69.1	64.6	8.9
	194.5	349.7	70.4	73.4	9.0
	1254.0	350.1	70.4	74.0	9.0
	2662.0	350.1	70.2	74.2	9.0
	3880.0	350.3	70.5	74.6	9.0
	6746.0	350.4	71.8	75.7	9.0
	10932.0	350.7	73.1	83.4	9.0
	27198.0	351.0	81.0	130.0	9.2
11.2% H ₂ / 88.8% Xe	5.4	352.9	65.3	35.6	8.8
	14.7	352.3	68.2	54.4	8.9
	40.1	352.3	69.7	61.6	8.9

Hydrogen accommodation coefficient temperature jump tests

	P (torr)	T _{abs} (°C)	T _{gl,i} (°C)	Q _C (W/m)	U _{QC} (±W/m)
H ₂	1.1	195.7	148.0	136.6	9.2
	3.1	196.4	151.0	144.3	9.3
	9.7	196.5	152.0	145.6	9.3
	1.0	152.9	116.0	97.4	9.1
	10.0	152.9	119.0	103.7	9.1
	45.8	152.9	120.0	103.7	9.1
	1.0	115.7	88.8	67.3	8.9
	10.0	113.3	88.2	71.0	9.0

Appendix F

Matlab front end for DSMC1 execution with Latin Hypercube Sampling

```
%
%
%
%Creates a base input file for DSMC1, uses Latin Hypercube Sampling
%to generate DSMC1 files, calls DSMC1, and reads output from DSMC1
%F. Burkholder, May 2011
clear all
close
clc

%INPUTS
%Gases
Gas{1} = 'Hydrogen'; % 'Hydrogen'
Gas{2} = 'Xenon'; % 'Argon','Xenon'
X(1) = 0.112; %Molar fraction of Gas 1

%Geometry
ri = 0.035; %m, inner radius
ro = 0.0595; %m, outer radius
NC = 20; %number of cells - recompile fortran code if
    % different NC desired

%Temperature
AbsTemp = 350; %C, absorber temperature

%Simulation
NumSimMol = 3000; %Desired number of simulated molecules
TSF = 0.5; %Multiply time step based on col. rate by this factor
NIS = 5; % # of time steps between samples
NSP = 20; % # of samples between restart and output file updates
NPS = 200; %update at which to start sampling
NofSF = 300; %the number of updates of steady flow
NumPressures = 13; %number of pressures to simulate
NumCaseatEachP = 20; % # of cases to simulate at each pressure,
    %do not exceed NumLHSBins below

%Latin Hypercube inputs
LHSVarGas1 = 6; %number of LHS variables for Gas 1
LHSVarGas2 = 5; %number of LHS variables for Gas 2
NumLHSBins = 20; %each input divided into this many equal % bins

%Uncertainties 95% CI limit, entered as percentage of mean value
TwoSigmaAccomCoef = 25; % accommodation coefficients
TwoSigmaMolDiam = 0.5; % molecular diameters
TwoSigmaViscTempCoeff = 1; %viscosity temperature coefficient
TwoSigmaIoverScatterParam = 3.5; %inverse of col. scat. parameter
TwoSigmaRotRelaxNum = 40; %Collision rotational relax. number

% 11.2 H2 88.8 Xe
%*****
Pr(1)=0.1333; TGl(1)=58.16;
Pr(2)=0.4; TGl(2)=58.82;
```

```

Pr(3)=0.6666; TGl(3)=59.41;
Pr(4)=1.067;  TGl(4)=60.19;
Pr(5)=2;      TGl(5)=61.66;
Pr(6)=4;      TGl(6)=63.75;
Pr(7)=6.666; TGl(7)=65.4;
Pr(8)=10.67; TGl(8)=66.81;
Pr(9)=20;    TGl(9)=68.33;
Pr(10)=26.6; TGl(10)=68.86;
Pr(11)=66.66; TGl(11)=69.98;
Pr(12)=106.7; TGl(12)=70.29;
Pr(13)=266.6; TGl(13)=70.62;

%CALCULATIONS
%Constants
R = 8314; %J/kmol-K, gas constant
k_Boltz = 1.381e-23; %J/K, Boltmann's constant
N_Avo = 6.022e26; %molecules/kmol Avogadro's number
X(2) = 1-X(1); %molar fraction gas 2
gap = ro-ri; %for Knudsen number calculation

%Initialize Matlab's random number stream
RandStream.setDefaultStream ...
    (RandStream('mt19937ar','seed',sum(100*clock)));

%Determine gas properties
for j = 1:2
    if strcmp(Gas{j},'Xenon')
        %props from App. A, MGD, Bird
        ALPH(j,1)=0.76; %accom. coefficient on absorber (surf 1)
        ALPH(j,2)=0.90; %accom. coefficient on glass (surf 2)
        SP(1,j)=5.65E-10; %SP(1,N), mol. diam. of species N, A3 at ref T
        SP(2,j)=273; %K, the ref. temp. of the molecular diameter, A3
        SP(3,j)=0.85; %the viscosity temperature index, A1, at ref T
        SP(4,j)=0.6944; %the recip. of the VSS scat. param. alpha, A3
        SP(5,j)=218E-27; %kg, the molecular mass, A1
        ISPR(1,j) = 0; %the number of rotational degrees of freedom
        SPR(1,j,1)=0; %SPR(1,N,K) rotation relax. # with spec. 1
        SPR(1,j,2)=0; %SPR(1,N,K) rotation relax. # with spec. 2
        ISPR(2,j)=0; %0,1 for constant, polynomial for collision number
        MM(j) = 131.3; %kg/kmol, molar mass
        MolDiam(j) = SP(1,j); %m, molecular diameter
    end
    if strcmp(Gas{j},'Argon')
        %props from App. A, MGD, Bird
        ALPH(j,1)=0.66; %accom. coefficient on absorber (surf 1)
        ALPH(j,2)=0.82; %accom. coefficient on glass (surf 2)
        SP(1,j)=4.11E-10; %SP(1,N), mol. diam. of species N, A3 at ref T
        SP(2,j)=273; %K, the ref. temp. of the molecular diameter, A3
        SP(3,j)=0.81; %the viscosity temperature index, A1, at ref T
        SP(4,j)=0.7143; %the recip. of the VSS scat. param. alpha, A3
        SP(5,j)=66.3E-27; %kg, the molecular mass, A1
        ISPR(1,j) = 0; %the number of rotational degrees of freedom
        SPR(1,j,1)=0; %SPR(1,N,K) rotation relax. # with spec. 1
        SPR(1,j,2)=0; %SPR(1,N,K) rotation relax. # with spec. 2
        ISPR(2,j)=0; %0,1 for constant, polynomial for collision number
    end
end

```

```

MM(j) = 39.95; %kg/kmol, molar mass
MolDiam(j) = SP(1,j); %m, molecular diameter

end
if strcmp(Gas{j},'Hydrogen')
    %props from App. A, MGD, Bird
    ALPH(j,1)=0.34; %accom. coefficient on absorber (surf 1)
    ALPH(j,2)=0.25; %accom. coefficient on glass (surf 2)
    SP(1,j)=2.88E-10; %SP(1,N), mol. diam. of species N, A3 at ref T
    SP(2,j)=273; %K, the ref. temp. of the molecular diameter, A3
    SP(3,j)=0.67; %the viscosity temperature index, A1, at ref T
    SP(4,j)=0.7407; %the recip. of the VSS scat. param. alpha, A3
    SP(5,j)=3.44E-27; %kg, the molecular mass, A1
    ISPR(1,j) = 2; %the number of rotational degrees of freedom
    SPR(1,j,1)=5; %SPR(1,N,K) rotation relax. # with spec. 1
    SPR(1,j,2)=5; %SPR(1,N,K) rotation relax. # with spec. 2
    ISPR(2,j)=0; %0,1 for constant, polynomial for collision number
    MM(j) = 2.016; %kg/kmol, molar mass
    MolDiam(j) = SP(1,j); %m, molecular diameter

end
SigmaALPH(j,1)=ALPH(j,1)*TwoSigmaAccomCoef/(2*100); %on absorber (s1)
SigmaALPH(j,2)=ALPH(j,2)*TwoSigmaAccomCoef/(2*100); %on glass (s2)
SigmaMolDiam(j) = SP(1,j)*TwoSigmaMolDiam/(2*100);
SigmaViscTempCoeff(j)=SP(3,j)*TwoSigmaViscTempCoeff/(2*100);
SigmaOverScatterParam(j)=SP(4,j)*TwoSigmaOverScatterParam/(2*100);
if strcmp(Gas{j},'Hydrogen')
    SigmaRotRelaxNum(j) = SPR(1,j,j)*TwoSigmaRotRelaxNum/(2*100);
else
    SigmaRotRelaxNum(j) = 0;
end
end

%Create LHS sample
%assumes that Gas{1} is Hydrogen
OutFormat = 1;
%mean values
mu = [ALPH(1,1) ALPH(1,2) SP(1,1) SP(3,1) SP(4,1) SPR(1,1,1)...
      ALPH(2,1) ALPH(2,2) SP(1,2) SP(3,2) SP(4,2)];
%mean value variances
var = [SigmaALPH(1,1)^2 0 0 0 0 0 0 0 0 0 0;...
      0 SigmaALPH(1,2)^2 0 0 0 0 0 0 0 0 0;...
      0 0 SigmaMolDiam(1)^2 0 0 0 0 0 0 0 0;...
      0 0 0 SigmaViscTempCoeff(1)^2 0 0 0 0 0 0 0;...
      0 0 0 0 SigmaOverScatterParam(1)^2 0 0 0 0 0 0;...
      0 0 0 0 0 SigmaRotRelaxNum(1)^2 0 0 0 0 0;...
      0 0 0 0 0 0 SigmaALPH(2,1)^2 0 0 0 0;...
      0 0 0 0 0 0 0 SigmaALPH(2,2)^2 0 0 0;...
      0 0 0 0 0 0 0 0 SigmaMolDiam(2)^2 0 0;...
      0 0 0 0 0 0 0 0 0 SigmaViscTempCoeff(2)^2 0;...
      0 0 0 0 0 0 0 0 0 0 SigmaOverScatterParam(2)^2];
crit = 0.33; %maximum correlation coefficient allowed
Y = eye(LHSVarGas1+LHSVarGas2);
Rc = 1; %initialize value
while (Rc > crit) %assures minimum correlation
    LHC = lhsnorm(mu,var,NumLHSBins,'off');
end

```

```

Rval = corrcoef(LHC);
Rval2 = abs(Rval-Y);
Rc = max(max(Rval2));
end
%correct for accommodation coefficients > 1 or < 0
for i = 1:NumLHSBins
    if LHC(i,1) > 1, LHC(i,1) = 1; end
    if LHC(i,1) < 0, LHC(i,1) = 0; end
    if LHC(i,2) > 1, LHC(i,2) = 1; end
    if LHC(i,2) < 0, LHC(i,2) = 0; end
    if LHC(i,7) > 1, LHC(i,7) = 1; end
    if LHC(i,7) < 0, LHC(i,7) = 0; end
    if LHC(i,8) > 1, LHC(i,8) = 1; end
    if LHC(i,8) < 0, LHC(i,8) = 0; end
end

for k = 1:NumCaseatEachP
    disp(['Case: ' num2str(k,3)])
    for j = 1:NumPressures
        disp(['Pressure: ' num2str(Pr(j),4) ' Pa.']);
        %Initialize arrays for this pressure
        M = zeros(NumCaseatEachP,37);
        Summ = zeros(NumCaseatEachP,41);
        %Estimate the number density from ideal gas law
        T_ave_K = (AbsTemp+TGl(j))/2 + 273.1; %K
        T_abs_K = AbsTemp+273.1; %K
        kmolperm3 = Pr(j)/(R*T_ave_K);
        molecperm3 = kmolperm3*N_Avo; %molecules per m3 = FND
        %Estimate the number of molecules in the annulus
        Vol = pi*(ro^2-ri^2)*1; %m3, volume of 1 meter length of annulus
        NumRealMol = Vol*molecperm3; %number of molecules in the annulus
        NumRealMolperSimMol = round(NumRealMol/NumSimMol);
        IFX = 1; %Cylindrical flow
        IIS = 2; %Starts with uniform gradient between surfaces
        FTMP = T_ave_K; %K, the starting temperature
        %FND calculated from desired pressure and ideal gas law
        FND = molecperm3; %molecules/m3, the total number density
        FSP(1) = X(1); %the number fraction of species 1
        FSP(2) = X(2); %the number fraction of species 2
        FNUM = NumRealMolperSimMol; %real molecules/simulated molecule
        XB(1)=ri; %m, inner wall boundary
        XB(2)=ro; %m, outer wall boundary
        IB(1)=3; %stationary solid wall
        BT(1)=AbsTemp+273.1; %K, inner wall temperature
        BVY(1)=0; %m/s, boundary velocity
        IB(2)=3; %stationary solid wall
        BT(2)=TGl(j)+273.1; %K, outer wall temperature
        BVY(2)=0; %m/s, boundary velocity
        %Estimate mean thermal speed, collision rate, and mean free path
        %of each pure gas
        for i = 1:2
            m_molec(i) = MM(i)/N_Avo; %mass of one molecule
            cbar(i) = sqrt( (8*k_Boltz*T_abs_K)/(pi*m_molec(i)) ); %cbar
            cbarr(i) = sqrt(2)*cbar(i); %mean cr in a collision
            nu(i) = pi*MolDiam(i)^2*molecperm3*X(i)*cbarr(i);
            %nu = mean collision rate , molecules colliding per second
            lambda(i) = cbar(i)/nu(i); %mean free path
        end
    end
end

```

```

        Kn(i) = lambda(i)/gap; %Knudsen number
        InvKn(i) = 1/Kn(i); %Inverse Knudsen number
    end
    %find molar fraction weighted quantities
    nu_mx = X(1)*nu(1)+X(2)*nu(2); %mean collision rate
    lambda_mx = X(1)*lambda(1)+X(2)*lambda(2); %mean free path
    meancoltime_mx = 1/nu_mx; %mean collision time
    Kn_mx = lambda_mx/gap; %Knudsen number of gas mixture
    InvKn_mx = 1/Kn_mx; %Inverse Knudsen of gas mixture
    NSF = round(NPS+max(100,150+525*log10(InvKn_mx))); %update to
        %start sampling
    Rem = mod(NSF,10);
    NSF = NSF-Rem;
    NPT = round(NSF+NofSF); %update at which to stop
    TimeStep = meancoltime_mx*TSF; %s, sets the time step
    DTM = TimeStep; %s, the time step
    SEED = round(-1*rand(1,1)*1000000); %seed to re-init RF in DSMC1
    if OutFormat == 1 %2 hydrogen, 6 LHC columns
        csvwrite('DSMC.IN',[IFX IIS FTMP FND FSP(1) FSP(2) FNUM DTM ...
            XB(1) XB(2) IB(1) BT(1) BVY(1) IB(2) BT(2) BVY(2) LHC(k,3) ...
            SP(2,1) LHC(k,4) LHC(k,5) SP(5,1) LHC(k,9) SP(2,2) ...
            LHC(k,10) LHC(k,11) SP(5,2) ISPR(1,1) ISPR(1,2) ISPR(2,1)...
            ISPR(2,2) LHC(k,6) LHC(k,6) SPR(1,2,1) SPR(1,2,2)...
            NIS NSP NPS NSF NPT LHC(k,1) LHC(k,2) LHC(k,7) LHC(k,8) SEED]);
    end
    tic;
    !twogasnoml.exe
    %run fortran DSMC1 executable
    dt = toc; %record how long the simulation took
    DSMCdata = csvread('QCond.csv');
    P(k,j) = mean(DSMCdata(:,2));
    PCL(k,j) = 2*std(DSMCdata(:,2));
    QC(k,j) = mean(DSMCdata(:,3));
    QCCL(k,j) = 2*std(DSMCdata(:,3));
    QTime(k,j) = dt;
end
end
end

```

Appendix G

Solar Advisor Model Reference Plant Inputs

The screenshot displays the Solar Advisor Model (SAM) software interface. The main window title is "100 MW Phys Trough - NREL Ref Wet Plant". The left sidebar contains a "System Summary" section with various input categories: Climate, Financing, Tax Credit Incentives, Payment Incentives, Annual Performance, Trough System Costs, Solar Field, Collectors (SCAs), Receivers (HCEs), Power Cycle, Thermal Storage, Parasitics, and User Variables. The main content area shows the "System Summary" output table.

System Summary	
Nameplate Capacity	99000 kW
Total Direct Cost	658,286,398.58 \$
Total Installed Cost	824,240,399.66 \$
Total Installed Cost per Capacity	8,325.66 \$/kW
Analysis Period	30 years
Inflation Rate	2.5 %
Real Discount Rate	8 %

File Case Results Simulations Developer Help

100 MW Phys Trough - NREL Ref Wet Plant x 100 MW Phys Trough - NREL Ref Dry Plant 64MW w 0hrs TES - Nevada in 2005 250MW w 6hrs TES - Arizona

Select Technology and Market... [CSP Trough Physical, Independent Power Producer]

System Summary

Climate
 Location: BLYTHE RIVERSIDE CO ARPT, CA
 Lat: 33.6 Long: -114.7 Elev: 119.0 m

Financing
 Analysis: 30 years

Tax Credit Incentives

Payment Incentives

Annual Performance
 Degradation: 0 % per year
 Availability: 96 %

Trough System Costs
 Total Installed: \$ 824,240,400
 Est. per Capacity (\$/MW): \$ 8,326

Solar Field
 Solar Multiple: 2
 Number of Loops: 227
 Aperture Area: 854065

Collectors (SCAs)

Receivers (HCEs)

Power Cycle
 Nameplate: 99 MWe
 Rated efficiency: 0.3774

Thermal Storage
 Storage Hours: 6
 Fluid Volume: 26032

Parasitics

User Variables

Choose Climate/Location

Location: USER/CA BlytheTMY3-747188.csv

Solar Advisor reads weather files in TMY2, TMY3, and EPW format. The default weather file library includes a complete set of TMY2 files for U.S. locations. To add files for other locations, use the web links below to find and download the files, and then click Add/Remove above to help SAM locate them on your computer.

Notes:
 SAM looks for weather files in the specified folders. To change the search folders, click "Add/Remove". The prefix "SAM/" indicates a location from the standard SAM library, and those preceded by "USER/" are stored in your project file to facilitate sharing with other people.

Add/Remove...
 Refresh list
 Copy to project
 Remove from project
 Create TMY3 file
 Location Lookup...

Location Information

City: BLYTHE RIVERSIDE Timezone: GMT -8 Latitude: 33.617 deg
 State: CA Elevation: 119 m Longitude: -114.717 deg

Weather Data Information (Annual)

Direct Normal: 2636.3 kWh/m2 Dry-bulb Temp: 24.3 °C
 Global Horizontal: 2077.4 kWh/m2 Wind Speed: 3.5 m/s

View hourly data...

Web Links

Solar Advisor reads weather files in TMY2, TMY3, and EPW format.
 The default weather file library includes a complete set of TMY2 files for U.S. locations.
 You can use the web links below to find weather data for other locations. After you have downloaded the desired weather files, click Add/Remove above to help SAM locate the downloaded weather files on your computer.

[Best weather data for the U.S. \(1200+ locations in TMY3 format\)](#)
[Best weather data for international locations \(in EPW format\)](#)
[U.S. satellite-derived weather data \(10 km grid cells in TMY2 format\)](#)

File Case Results Simulations Developer Help

100 MW Phys Trough - NREL Ref Wet Plant | 100 MW Phys Trough - NREL Ref Dry Plant | 64MW w 0hrs TES - Nevada in 2005 | 250MW w 6hrs TES - Arizona

Select Technology and Market... [CSP Trough Physical, Independent Power Producer]

System Summary

Climate
 Location: BLYTHE RIVERSIDE CO ARPT, CA
 Lat: 33.6 Long: -114.7 Elev: 119.0 m

Financing
 Analysis: 30 years

Tax Credit Incentives

Payment Incentives

Annual Performance
 Degradation: 0 % per year
 Availability: 96 %

Trough System Costs
 Total Installed: \$ 824,240,400
 Est. per Capacity (\$/kW): \$ 8.326

Solar Field
 Solar Multiples: 2
 Number of Loops: 227
 Aperture Area: 854065

Collectors (SCAs)

Receivers (HCEs)

Power Cycle
 Nameplate: 99 MWe
 Rated efficiency: 0.3774

Thermal Storage
 Storage Hours: 6
 Fluid Volume: 26032

Parasitics

User Variables

General

Analysis Period: 30 years
 Inflation Rate: 2.50 %
 Real Discount Rate: 8.00 %
 Nominal Discount Rate: 10.70 %

Taxes and Insurance

Federal Tax: 35.00 %/year
 State Tax: 8.00 %/year
 Sales Tax: 7.75 %
 Insurance: 0.50 % of installed cost

Salvage Value

Net Salvage Value: 0.00 % of installed cost
 End of Analysis Period Value: \$ 0.00

Property Tax

Assessed Percent: 100.00 % of installed cost
 Assessed Value: \$ 824,240,399.66
 Assessed Value Decline: 0.00 %/year
 Property Tax: 0.00 %/year

Construction Period

Loan	Percent of Installed Costs	Up-Front Fee (%)	Months Prior to Operation	Interest Rate (Annual)	Principal Amount	Interest	Total Construction Financing Cost
Loan 1	0	0	0	0	\$ 0.00	\$ 0.00	\$ 0.00
Loan 2	0	0	0	0	\$ 0.00	\$ 0.00	\$ 0.00
Loan 3	0	0	0	0	\$ 0.00	\$ 0.00	\$ 0.00
Loan 4	0	0	0	0	\$ 0.00	\$ 0.00	\$ 0.00
Loan 5	0	0	0	0	\$ 0.00	\$ 0.00	\$ 0.00
Totals:	0				\$ 0.00	\$ 0.00	\$ 0.00

Note: If you specify construction period loans, the sum of percentages in the Percent of Installed Costs column must equal 100.

Loan Parameters

Installed Cost: \$ 824,240,399.66
 Construction Financing Cost: \$ 0.00
 Principal Amount: \$ 346,180,967.86

Loan Term: 20 years
 Loan Rate: 8 %/year
 Debt Fraction: 42 %
 WACC: 10.71 %

Solution Mode

Specify IRR Target
 Specify First Year PPA Price

Choose Specify IRR Target when you know the minimum IRR and want SAM to calculate a PPA price to meet the target. Choose Specify First Year PPA Price when you know the PPA price (or bid price) and want SAM to calculate the resulting IRR. Note that you can specify an optional annual power price escalation rate and optional hourly payment allocation factors. See help for details.

Specify IRR Target

Minimum Required IRR: 15 %
 PPA Escalation Rate: 1.2 %

Constraint: Require a minimum DSCR
 Minimum Required DSCR: 1.4

Constraint: Require a positive cashflow

Financial Optimization

Allow SAM to pick a debt fraction to minimize the LCOE
 Allow SAM to pick a PPA escalation rate to minimize the LCOE

Specify First Year PPA Price

First Year PPA Price: 0.15 \$/kWh
 PPA Escalation Rate: 0 %/yr

Federal Depreciation

No Depreciation
 5-yr MACRS
 Straight Line (specify years): 7
 Custom (specify percentages): Edit...

State Depreciation

No Depreciation
 5-yr MACRS
 Straight Line (specify years): 7
 Custom (specify percentages): Edit...

File Case Results Simulations Developer Help

100 MW Phys Trough - NREL Ref Wet Plant X 100 MW Phys Trough - NREL Ref Dry Plant 64MW w 0hrs TES - Nevada in 2005 250MW w 6hrs TES - Arizona

Select Technology and Market... [CSP Trough Physical, Independent Power Producer]

System Summary

Climate
Location: BLYTHE RIVERSIDE CO ARPT, CA
Lat: 33.6 Long: -114.7 Elev: 119.0 m

Financing
Analysis: 30 years

Tax Credit Incentives

Payment Incentives

Annual Performance
Degradation: 0 % per year
Availability: 96 %

Trough System Costs
Total Installed: \$ 824,240,400
Est. per Capacity (\$/kW): \$ 8,326

Solar Field
Solar Multiple: 2
Number of Loops: 227
Aperture Area: 854065

Collectors (SCAs)

Receivers (HCEs)

Power Cycle
Nameplate: 99 MWe
Rated efficiency: 0.3774

Thermal Storage
Storage Hours: 6
Fluid Volume: 26032

Parasitics

User Variables

Investment Tax Credit (ITC)

Reduces Depreciation Basis

	Amount	Federal	State
Federal	\$ 0	<input checked="" type="checkbox"/>	<input checked="" type="checkbox"/>
State	\$ 0	<input type="checkbox"/>	<input type="checkbox"/>
	Percentage	Maximum	
Federal	30 %	<input checked="" type="checkbox"/>	<input checked="" type="checkbox"/>
State	0 %	<input type="checkbox"/>	<input type="checkbox"/>

Note:
Depreciation is only allowed for third party-owned projects, so the basis reduction inputs can be ignored for homeowner-owned residential projects.

Production Tax Credit (PTC)

	Amount	Term	Escalation
Federal	Value: 0 \$/kWh	10 years	2 %
State	Value: 0 \$/kWh	10 years	2 %

File Case Results Simulations Developer Help

100 MW Phys Trough - NREL Ref Wet Plant | 100 MW Phys Trough - NREL Ref Dry Plant | 64MW w 0hrs TES - Nevada in 2005 | 250MW w 6hrs TES - Arizona

Select Technology and Market... [CSP Trough Physical, Independent Power Producer]

System Summary

Climate
 Location: BLYTHE RIVERSIDE CO ARPT, CA
 Lat: 33.6 Long: -114.7 Elev: 119.0 m

Financing
 Analysis: 30 years

Tax Credit Incentives

Payment Incentives

Annual Performance
 Degradation: 0 % per year
 Availability: 96 %

Trough System Costs
 Total Installed: \$ 824,240,400
 Est. per Capacity (\$/kW): \$ 8,326

Solar Field
 Solar Multiple: 2
 Number of Loops: 227
 Aperture Area: 854065

Collectors (SCAs)

Receivers (HCEs)

Power Cycle
 Nameplate: 99 MWe
 Rated efficiency: 0.3774

Thermal Storage
 Storage Hours: 6
 Fluid Volume: 26032

Parasitics

User Variables

Investment Based Incentive (IBI)

	Amount	Taxable Incentive		Reduces Depreciation Basis	
		Federal	State	Federal	State
Federal	\$ 0	<input checked="" type="checkbox"/>	<input checked="" type="checkbox"/>	<input type="checkbox"/>	<input type="checkbox"/>
State	\$ 0	<input checked="" type="checkbox"/>	<input checked="" type="checkbox"/>	<input type="checkbox"/>	<input type="checkbox"/>
Utility	\$ 0	<input checked="" type="checkbox"/>	<input checked="" type="checkbox"/>	<input type="checkbox"/>	<input type="checkbox"/>
Other	\$ 0	<input checked="" type="checkbox"/>	<input checked="" type="checkbox"/>	<input type="checkbox"/>	<input type="checkbox"/>
	Percentage	Maximum			
Federal	0 %	\$ 1e+099		<input type="checkbox"/>	<input type="checkbox"/>
State	0 %	\$ 1e+099		<input type="checkbox"/>	<input type="checkbox"/>
Utility	0 %	\$ 1e+099		<input type="checkbox"/>	<input type="checkbox"/>
Other	0 %	\$ 1e+099		<input type="checkbox"/>	<input type="checkbox"/>

Capacity Based Incentive (CBI)

	Amount	Maximum	Taxable Incentive		Reduces Depreciation Basis	
			Federal	State	Federal	State
Federal	0 \$/W	\$ 1e+099	<input checked="" type="checkbox"/>	<input checked="" type="checkbox"/>	<input type="checkbox"/>	<input type="checkbox"/>
State	0 \$/W	\$ 1e+099	<input checked="" type="checkbox"/>	<input checked="" type="checkbox"/>	<input type="checkbox"/>	<input type="checkbox"/>
Utility	0 \$/W	\$ 1e+099	<input checked="" type="checkbox"/>	<input checked="" type="checkbox"/>	<input type="checkbox"/>	<input type="checkbox"/>
Other	0 \$/W	\$ 1e+099	<input checked="" type="checkbox"/>	<input checked="" type="checkbox"/>	<input type="checkbox"/>	<input type="checkbox"/>

Production Based Incentive (PBI)

	Amount	Term	Escalation	Taxable Incentive	
				Federal	State
Federal	Value: 0 \$/kWh	0 years	0 %	<input checked="" type="checkbox"/>	<input checked="" type="checkbox"/>
State	Value: 0 \$/kWh	0 years	0 %	<input checked="" type="checkbox"/>	<input checked="" type="checkbox"/>
Utility	Value: 0 \$/kWh	0 years	0 %	<input checked="" type="checkbox"/>	<input checked="" type="checkbox"/>
Other	Value: 0 \$/kWh	0 years	0 %	<input checked="" type="checkbox"/>	<input checked="" type="checkbox"/>

File Case Results Simulations Developer Help

100 MW Phys Trough - NREL Ref Wet Plant 100 MW Phys Trough - NREL Ref Dry Plant 64MW w 0hrs TES - Nevada in 2005 250MW w 6hrs TES - Arizona

Select Technology and Market... [CSP Trough Physical, Independent Power Producer]

System Summary

Climate
 Location: BLYTHE RIVERSIDE CO ARPT, CA
 Lat: 33.6 Long: -114.7 Elev: 119.0 m

Financing
 Analysis: 30 years

Tax Credit Incentives

Payment Incentives

Annual Performance
 Degradation: 0 % per year
 Availability: 96 %

Trough System Costs
 Total Installed: \$ 824,240,400
 Est. per Capacity (\$/kW): \$ 8,326

Solar Field
 Solar Multiple: 2
 Number of Loops: 227
 Aperture Area: 854065

Collectors (SCAs)

Receivers (HCEs)

Power Cycle
 Nameplate: 99 MWe
 Rated efficiency: 0.3774

Thermal Storage
 Storage Hours: 6
 Fluid Volume: 26032

Parasitics

User Variables

Annual System Performance

System Degradation	Value	0 %
Availability	Value	96 %

Notes:
 System degradation is compounded annually, calculated from the first year output.
 Availability specifies a system's uptime operational characteristics.
 Both are specifiable as annual schedules.

File Case Results Simulations Developer Help

100 MW Phys Trough - NREL Ref Wet Plant | 100 MW Phys Trough - NREL Ref Dry Plant | 64MW w 0hrs TES - Nevada in 2005 | 250MW w 6hrs TES - Arizona

Select Technology and Market... [CSP Trough Physical, Independent Power Producer]

System Summary

Climate
 Location: BLYTHE RIVERSIDE CO ARPT, CA
 Lat: 33.6 Long: -114.7 Elev: 119.0 m

Financing
 Analysis: 30 years

Tax Credit Incentives

Payment Incentives

Annual Performance
 Degradation: 0 % per year
 Availability: 96 %

Trough System Costs
 Total Installed: \$ 824,240,400
 Est. per Capacity (\$/kW): \$ 8,326

Solar Field
 Solar Multiple: 2
 Number of Loops: 227
 Aperture Area: 854065

Collectors (SCAs)

Receivers (HCEs)

Power Cycle
 Nameplate: 99 MWe
 Rated efficiency: 0.3774

Thermal Storage
 Storage Hours: 6
 Fluid Volume: 26032

Parasitics

User Variables

Direct Capital Costs

Site Improvements	854065	m2	28.00 \$/m2	\$ 23,913,814.40
Solar Field	854065	m2	295.00 \$/m2	\$ 251,949,116.00
HTF System	854065	m2	90.00 \$/m2	\$ 76,865,832.00
Storage	1748.81	MWh	81 \$/kWh	\$ 141,653,418.12
Fossil Backup	110	MWe, Gross	0 \$/kWe	\$ 0.00
Power Plant	110	MWe, Gross	946 \$/kWe	\$ 104,060,000.00
Balance of Plant	110	MWe, Gross	0 \$/kWe	\$ 0.00
Contingency				10 % \$ 59,844,218.05
Total Direct Cost				\$ 658,286,398.58

Indirect Capital Costs

	% of Direct Cost	Non-fixed Cost	Fixed Cost	Total
EPC and Owner Costs	14.8 %	\$ 97,426,386.99	\$ 0.00	\$ 97,426,386.99
Land	3.9 %	\$ 25,673,169.54	\$ 0.00	\$ 25,673,169.54
Sales Tax of	7.75 %	applies to	84 % of Direct Cost	\$ 42,854,444.55
Total Indirect Cost				\$ 165,954,001.08

Total Installed Costs

Total Installed Cost	\$ 824,240,399.66
Estimated Total Installed Cost per Net Capacity (\$/kW)	\$ 8,325.66

Operation and Maintenance Costs

	First Year Cost	Escalation Rate (above inflation)
Fixed Annual Cost	0.00 \$/yr	0 %
Fixed Cost by Capacity	69.00 \$/kW-yr	0 %
Variable Cost by Generation	3.00 \$/MWh	0 %
Fossil Fuel Cost	6.00 \$/MMBTU	0 %

Notes

- Escalation rates do not apply to O&M annual schedules, only first year values.
- Fossil fuel cost is not applicable to PV or Dish Stirling systems. Set to zero for these systems.

File Case Results Simulations Developer Help

100 MW Phys Trough - NREL Ref Wet Plant | 100 MW Phys Trough - NREL Ref Dry Plant | 64MW w 0hrs TES - Nevada in 2005 | 250MW w 6hrs TES - Arizona

Select Technology and Market... [CSP Trough Physical, Independent Power Producer]

System Summary

Climate
Location: BLYTHE RIVERSIDE CO ARPT, CA
Lat: 33.6 Long: -114.7 Elev: 119.0 m

Financing
Analysis: 30 years

Tax Credit Incentives

Payment Incentives

Annual Performance
Degradation: 0 % per year
Availability: 96 %

Trough System Costs
Total Installed: \$ 899,146,082
Est. per Capacity (\$/kW): \$ 9,082

Solar Field
Solar Multiple: 2.30332
Number of Loops: 262
Aperture Area: 985749

Collectors (SCAs)

Receivers (HCEs)

Power Cycle
Nameplate: 99 MWe
Rated efficiency: 0.3774

Thermal Storage
Storage Hours: 6
Fluid Volume: 26032

Parasitics

User Variables

Solar Field Parameters

Option 1: Option 2:

Solar multiple: 2
Field aperture: 987540 m²
Row spacing: 15 m
Stow angle: 170 deg
Deploy angle: 10 deg
Number of field subsections: 2
Header pipe roughness: 4.57e-005 m
HTF pump efficiency: 0.85
Freeze protection temp: 150 °C
Irradiation at design: 950 W/m²
Allow partial defocusing: Sequenced:

Heat Transfer Fluid

Field HTF fluid: VP-1
User-defined HTF fluid: Edit...
Design loop inlet temp: 293 °C
Design loop outlet temp: 391 °C
Min single loop flow rate: 1 kg/s
Max single loop flow rate: 12 kg/s
Min field flow velocity: 0.356106 m/s
Max field flow velocity: 4.9655 m/s
Header design min flow velocity: 2 m/s
Header design max flow velocity: 3 m/s
Initial field temperature: 100 °C

Design Point

Single loop aperture: 3762.4 m²
Loop optical efficiency: 0.744601
Total loop conversion efficiency: 0.716894
Total required aperture, SM=1: 427969 m²
Required number of loops, SM=1: 113.749
Actual number of loops: 262
Actual aperture: 985749 m²
Actual solar multiple: 2.30332
Field thermal output: 671.344 MWT

Collector Orientation

Collector tilt: 0 deg
Collector azimuth: 0 deg
Tilt: horizontal=0, vertical=90
Azimuth: equator=0, west=90, east=-90

Mirror Washing

Water usage per wash: 0.6 L/m², aper.
Washes per year: 5

Plant Heat Capacity

Hot piping thermal inertia: 0.2 kWh/K-MWT
Cold piping thermal inertia: 0.2 kWh/K-MWT
Field loop piping thermal inertia: 4.5 Wh/K-m

Land Area

Solar Field Area: 731 acres
Non-Solar Field Land Area Multiplier: 1.3
Total Land Area: 950 acres

Single Loop Configuration

Note: The specification below is only for one loop in the solar field.
Usage tip: To configure the loop, choose whether to edit SCA's, HCE's or defocus order. Select assemblies by clicking one or dragging the mouse over multiple items. Assign types to selected items by pressing keys 1-4.

Number of SCA/HCE assemblies per loop: 8 Edit SCAs Edit HCEs Edit Defocus Order

SCA: 1	SCA: 1	SCA: 1	SCA: 1	SCA: 1	SCA: 1
HCE: 1 DF# 8	HCE: 1 DF# 7	HCE: 1 DF# 6	HCE: 1 DF# 5	HCE: 1 DF# 4	HCE: 1 DF# 3
				SCA: 1	SCA: 1
				HCE: 1 DF# 1	HCE: 1 DF# 2

File Case Results Simulations Developer Help

100 MW Phys Trough - NREL Ref Wet Plant x 100 MW Phys Trough - NREL Ref Dry Plant 64MW w 0hrs TES - Nevada in 2005 250MW w 6hrs TES - Arizona

Select Technology and Market... [CSP Trough Physical, Independent Power Producer]

System Summary

Climate

Location: BLYTHE RIVERSIDE CO ARPT, CA
 Lat: 33.6 Long: -114.7 Elev: 119.0 m

Financing

Analysis: 30 years

Tax Credit Incentives

Payment Incentives

Annual Performance

Degradation: 0 % per year
 Availability: 96 %

Trough System Costs

Total Installed: \$ 899,146,082
 Est. per Capacity (\$/kW): \$ 9,082

Solar Field

Solar Multiple: 2.30332
 Number of Loops: 262
 Aperture Area: 985749

Collectors (SCAs)

Receivers (HCEs)

Power Cycle

Nameplate: 99 MWe
 Rated efficiency: 0.3774

Thermal Storage

Storage Hours: 6
 Fluid Volume: 26032

Parasitics

User Variables

Collector (SCA) Type 1 ▼

Configuration name: SAM/CSP Physical Trough SCAs/Solargenix SGX-1 Choose collector from library...

Collector Geometry

Reflective aperture area	<input type="text" value="470.3"/> m ²	Number of modules per assembly	<input type="text" value="12"/>
Aperture width, total structure	<input type="text" value="5"/> m	Average surface-to-focus path length	<input type="text" value="1.8"/> m
Length of collector assembly	<input type="text" value="100"/> m	Piping distance between assemblies	<input type="text" value="1"/> m

Optical Parameters

Incidence angle modifier coeff 1	<input type="text" value="1"/>	Geometry effects	<input type="text" value="0.98"/>
Incidence angle modifier coeff 2	<input type="text" value="0.0506"/>	Mirror reflectance	<input type="text" value="0.935"/>
Incidence angle modifier coeff 3	<input type="text" value="-0.1763"/>	Dirt on mirror	<input type="text" value="0.95"/>
Tracking error	<input type="text" value="0.994"/>	General optical error	<input type="text" value="0.99"/>

Optical Calculations

Length of single module	<input type="text" value="8.33333"/> m	End loss at design	<input type="text" value="0.99822"/>
Incidence angle modifier	<input type="text" value="1.00247"/>	Optical efficiency at design	<input type="text" value="0.856609"/>

File Case Results Simulations Developer Help

100 MW Phys Trough - NREL Ref Wet Plant | 100 MW Phys Trough - NREL Ref Dry Plant | 64MW w 0hrs TES - Nevada in 2005 | 250MW w 6hrs TES - Arizona

Select Technology and Market... [CSP Trough Physical, Independent Power Producer]

System Summary

Climate
Location: BLYTHE RIVERSIDE CO ARPT, CA
Lat: 33.6 Long: -114.7 Elev: 119.0 m

Financing
Analysis: 30 years

Tax Credit Incentives

Payment Incentives

Annual Performance
Degradation: 0 % per year
Availability: 96 %

Trough System Costs
Total Installed: \$ 899,146,082
Est. per Capacity (\$/kW): \$ 9,082

Solar Field
Solar Multiple: 2.30332
Number of Loops: 262
Aperture Area: 985749

Collectors (SCAs)

Receivers (HCEs)

Power Cycle
Nameplate: 99 MWe
Rated efficiency: 0.3774

Thermal Storage
Storage Hours: 6
Fluid Volume: 26032

Parasitics

User Variables

Receiver (HCE) Type 1

Configuration name: Schott PTR70 2008 Choose receiver from library...

Receiver Geometry

Absorber tube inner diameter	0.066 m	Absorber flow plug diameter	0 m
Absorber tube outer diameter	0.07 m	Internal surface roughness	4.5e-005
Glass envelope inner diameter	0.115 m	Absorber flow pattern	Tube flow
Glass envelope outer diameter	0.12 m	Absorber material type	304L

Parameters and Variations

	Variation 1	Variation 2	Variation 3	Variation 4*
Variant weighting fraction*	0.985	0.01	0.005	0
Absorber Parameters:				
Absorber absorptance	0.96	0.96	0.8	0
Absorber emittance	Table...	0.65	0.65	0
Envelope Parameters:				
Envelope absorptance	0.02	0.02	0	0
Envelope emittance	0.86	0.86	1	0
Envelope transmittance	0.963	0.963	1	0
	<input type="checkbox"/> Broken Glass	<input type="checkbox"/> Broken Glass	<input checked="" type="checkbox"/> Broken Glass	<input type="checkbox"/> Broken Glass
Gas Parameters:				
Annulus gas type	Hydrogen	Air	Air	Hydrogen
Annulus pressure (torr)	0.0001	750	750	0
Heat Loss at Design:				
Estimated avg. heat loss (W/m)	150	1100	1500	0
Optical Effects:				
Bellows shadowing	0.96	0.96	0.96	0.963
Dirt on receiver	0.98	0.98	1	0.98

Note: * The variant weighting fractions and Variation 4 inputs are not part of the library.

Total Weighted Losses

Heat loss at design	166.25 W/m
Optical derate	0.869242

File Case Results Simulations Developer Help

100 MW Phys Trough - NREL Ref Wet Plant | 100 MW Phys Trough - NREL Ref Dry Plant | 64MW w 0hrs TES - Nevada in 2005 | 250MW w

Select Technology and Market... [CSP Trough Physical, Independent Power Producer]

System Summary

Climate
Location: BLYTHE RIVERSIDE CO ARPT, CA
Lat: 33.6 Long: -114.7 Elev: 119.0 m

Financing
Analysis: 30 years

Tax Credit Incentives

Payment Incentives

Annual Performance
Degradation: 0 % per year
Availability: 96 %

Trough System Costs
Total Installed: \$ 899,146,082
Est. per Capacity (\$/kW): \$ 9,082

Solar Field
Solar Multiple: 2.30332
Number of Loops: 262
Aperture Area: 985749

Collectors (SCAs)

Receivers (HCEs)

Power Cycle
Nameplate: 99 MWe
Rated efficiency: 0.3774

Thermal Storage
Storage Hours: 6
Fluid Volume: 26032

Parasitics

User Variables

Plant Capacity

Design gross output	110	MWe
Estimated gross to net conversion factor	0.9	
Estimated net output at design (nameplate)	99	MWe

Note: Parasitic losses typically reduce net output to approximately 90 % of design gross power

Power Block Design Point

Rated cycle conversion efficiency	0.3774
Design inlet temperature	391 °C
Design outlet temperature	293 °C
Boiler operating pressure	100 bar
Fossil backup boiler LHW efficiency	0.9
Steam cycle blowdown fraction	0.013

Plant Control

Low resource standby period	2	hrs
Fraction of thermal power needed for standby	0.2	
Power block startup time	0.5	hr
Fraction of thermal power needed for startup	0.2	
Minimum required startup temp	300	°C
Max turbine over design operation	1.15	
Min turbine operation	0.25	
Minimum power block restart time	1	hr
Turbine Inlet Pressure Control	Fixed pressure	

Cooling System

Condenser type	Evaporative	Hybrid Dispatch
Ambient temp at design	20 °C	Period 1: 0
Ref. Condenser Water dT	10 °C	Period 2: 0
Approach temperature	5 °C	Period 3: 0
ITD at design point	16 °C	Period 4: 0
Condenser pressure ratio	1.0028	Period 5: 0
Min condenser pressure	1.25 inHg	Period 6: 0
Cooling system part load levels	8	Period 7: 0
		Period 8: 0
		Period 9: 0

Note: Hybrid dispatch control parameters refer to the dispatch periods defined on the thermal storage page.

File Case Results Simulations Developer Help

100 MW Phys Trough - NREL Ref Wet Plant x 100 MW Phys Trough - NREL Ref Dry Plant 64MW w 6hrs TES - Nevada in 2005 250MW w 6hrs TES - Arizona

Select Technology and Market... [CSP Trough Physical, Independent Power Producer]

System Summary

Climate
 Location: BLYTHE RIVERSIDE CO ARPT, CA
 Lat: 33.6 Long: -114.7 Elev: 119.0 m

Financing
 Analysis: 30 years

Tax Credit Incentives

Payment Incentives

Annual Performance
 Degradation: 0 % per year
 Availability: 96 %

Trough System Costs
 Total Installed: \$ 899,146,082
 Est. per Capacity (\$/kW): \$ 9,082

Solar Field
 Solar Multiple: 2.30332
 Number of Loops: 262
 Aperture Area: 985749

Collectors (SCAs)

Receivers (HCEs)

Power Cycle
 Nameplate: 99 MWe
 Rated efficiency: 0.3774

Thermal Storage
 Storage Hours: 6
 Fluid Volume: 26032

Parasitics

User Variables

Storage System

Full load hours of TES: 6 hr
 Storage volume: 26032 m3
 TES Thermal capacity: 1748.81 MWh
 Parallel tank pairs: 2
 Tank height: 20 m
 Tank fluid min height: 1 m
 Tank diameter: 28.7859 m
 Min fluid volume: 1301.6 m3
 Tank loss coeff: 0.4 W/m2-K
 Estimated heat loss: 0.633559 MWh
 Cold tank heater set point: 250 °C
 Hot tank heater set point: 365 °C
 Fossil dispatch mode: Minimum backup level

Aux heater outlet set temp: 391
 Tank heater capacity: 25 MWh
 Tank heater efficiency: 0.98
 Hot side HX approach temp: 5 °C
 Cold side HX approach temp: 7 °C
 Heat exchanger derate: 0.877551
 Initial TES fluid temp: 300 °C
 Storage HTF fluid: Solar Salt
 User-defined HTF fluid: Edit...
 Fluid Temperature: 342 °C
 TES fluid density: 1872.49 kg/m3
 TES specific heat: 1.50182 kJ/kg-K

Thermal Storage Dispatch Control

Current dispatch schedule:
 No library match.
 Dispatch schedule library...

Note:
 Schedule libraries do not affect the Storage Dispatch, Turbine Output and Fossil Fill fractions below.

Period	Storage Dispatch		Turb. out.		Fossil fill		Payment Allocation Factor
	w/ solar*	w/o solar*	fraction*	fraction*	fraction*	fraction*	
Period 1:	0	0	1.1	0	0	0	3.28
Period 2:	0	0	1	0	0	0	1.28
Period 3:	0	0	1	0	0	0	0.67
Period 4:	0	0	1	0	0	0	1.02
Period 5:	0	0	1	0	0	0	0.82
Period 6:	0	0	1	0	0	0	0.65
Period 7:	0.1	0.1	1	0	0	0	0.65
Period 8:	0.1	0.1	1	0	0	0	0.65
Period 9:	0.1	0.1	1	0	0	0	0.65

Notes:
 1. Storage dispatch fractions apply to the maximum energy storage.
 2. Turbine output and fossil fill fractions apply to the design turbine thermal input.
 3. Payment Allocation Factors apply to Utility Dispatch and Utility Bid Price Financing only.

Weekday Schedule

	12am	1am	2am	3am	4am	5am	6am	7am	8am	9am	10am	11am	12pm	1pm	2pm	3pm	4pm	5pm	6pm	7pm	8pm	9pm	10pm	11pm
Jan	6	6	6	6	6	6	5	5	4	4	4	4	4	4	4	4	4	4	4	4	4	4	5	5
Feb	6	6	6	6	6	6	5	5	4	4	4	4	4	4	4	4	4	4	4	4	4	4	5	5
Mar	6	6	6	6	6	6	5	5	4	4	4	4	4	4	4	4	4	4	4	4	4	4	5	5
Apr	6	6	6	6	6	5	5	4	4	4	4	4	4	4	4	4	4	4	4	4	4	4	5	5
May	6	6	6	6	6	5	5	4	4	4	4	4	4	4	4	4	4	4	4	4	4	4	5	5
Jun	3	3	3	3	3	3	2	2	2	2	1	1	1	1	1	1	1	2	2	2	2	2	2	3
Jul	3	3	3	3	3	3	2	2	2	2	1	1	1	1	1	1	2	2	2	2	2	2	2	3
Aug	3	3	3	3	3	3	2	2	2	2	1	1	1	1	1	1	2	2	2	2	2	2	2	3
Sep	3	3	3	3	3	3	2	2	2	2	1	1	1	1	1	1	2	2	2	2	2	2	2	3
Oct	6	6	6	6	6	5	5	4	4	4	4	4	4	4	4	4	4	4	4	4	4	4	5	5
Nov	6	6	6	6	6	5	5	4	4	4	4	4	4	4	4	4	4	4	4	4	4	4	5	5
Dec	6	6	6	6	6	5	5	4	4	4	4	4	4	4	4	4	4	4	4	4	4	4	5	5

Weekend Schedule

	12am	1am	2am	3am	4am	5am	6am	7am	8am	9am	10am	11am	12pm	1pm	2pm	3pm	4pm	5pm	6pm	7pm	8pm	9pm	10pm	11pm
Jan	6	6	6	6	6	6	5	5	5	5	5	5	5	5	5	5	5	5	5	5	5	5	5	5
Feb	6	6	6	6	6	6	5	5	5	5	5	5	5	5	5	5	5	5	5	5	5	5	5	5
Mar	6	6	6	6	6	6	5	5	5	5	5	5	5	5	5	5	5	5	5	5	5	5	5	5
Apr	6	6	6	6	6	5	5	5	5	5	5	5	5	5	5	5	5	5	5	5	5	5	5	5
May	6	6	6	6	6	5	5	5	5	5	5	5	5	5	5	5	5	5	5	5	5	5	5	5
Jun	3	3	3	3	3	3	3	3	3	3	3	3	3	3	3	3	3	3	3	3	3	3	3	3
Jul	3	3	3	3	3	3	3	3	3	3	3	3	3	3	3	3	3	3	3	3	3	3	3	3
Aug	3	3	3	3	3	3	3	3	3	3	3	3	3	3	3	3	3	3	3	3	3	3	3	3
Sep	3	3	3	3	3	3	3	3	3	3	3	3	3	3	3	3	3	3	3	3	3	3	3	3
Oct	6	6	6	6	6	5	5	5	5	5	5	5	5	5	5	5	5	5	5	5	5	5	5	5
Nov	6	6	6	6	6	5	5	5	5	5	5	5	5	5	5	5	5	5	5	5	5	5	5	5
Dec	6	6	6	6	6	5	5	5	5	5	5	5	5	5	5	5	5	5	5	5	5	5	5	5

File Case Results Simulations Developer Help

100 MW Phys Trough - NREL Ref Wet Plant | 100 MW Phys Trough - NREL Ref Dry Plant | 64MW w 0hrs TES - Nevada in 2005 | 250MW w 6hrs TES - Arizona

Select Technology and Market... [CSP Trough Physical, Independent Power Producer]

System Summary

Climate
 Location: BLYTHE RIVERSIDE CO ARPT, CA
 Lat: 33.6 Long: -114.7 Elev: 119.0 m

Financing
 Analysis: 30 years

Tax Credit Incentives

Payment Incentives

Annual Performance
 Degradation: 0 % per year
 Availability: 96 %

Trough System Costs
 Total Installed: \$ 899,146,082
 Est. per Capacity (\$/kW): \$ 9,082

Solar Field
 Solar Multiple: 2.30332
 Number of Loops: 262
 Aperture Area: 985749

Collectors (SCAs)

Receivers (HCEs)

Power Cycle
 Nameplate: 99 MWe
 Rated efficiency: 0.3774

Thermal Storage
 Storage Hours: 6
 Fluid Volume: 26032

Parasitics

User Variables

Parasitics

			Design Point Totals			
Piping thermal loss coefficient	0.45	W/m2-K				
Tracking power	125	W/sca	Tracking	262000	W	
Required pumping power for HTF through power block	0.55	kJ/kg				
Required pumping power for HTF through storage	0.15	kJ/kg				
Fraction of rated gross power consumed at all times	0.0055		Fixed	0.605	MWe	
			Factor	Coeff 0	Coeff 1	Coeff 2
Balance of plant parasitic	0.02467	MWe/MWcap	1	0.483	0.517	0
Aux heater, boiler parasitic	0.02273	MWe/MWcap	1	0.483	0.517	0
			BOP	2.7137	MWe	
			Aux	2.5003	MWe	

File Case Results Simulations Developer Help

100 MW Phys Trough - NREL Ref Wet Plant | 100 MW Phys Trough - NREL Ref Dry Plant | 64MW w 0hrs TES - Nevada in 2005 | 250MW w 6hrs TES - Arizona

Select Technology and Market... [CSP Trough Physical, Independent Power Producer]

System Summary

Climate
Location: BLYTHE RIVERSIDE CO ARPT, CA
Lat: 33.6 Long: -114.7 Elev: 119.0 m

Financing
Analysis: 30 years

Tax Credit Incentives

Payment Incentives

Annual Performance
Degradation: 0 % per year
Availability: 96 %

Trough System Costs
Total Installed: \$ 899,146,082
Est. per Capacity (\$/kW): \$ 9,082

Solar Field
Solar Multiple: 2.30332
Number of Loops: 262
Aperture Area: 985749

Collectors (SCAs)

Receivers (HCEs)

Power Cycle
Nameplate: 99 MWe
Rated efficiency: 0.3774

Thermal Storage
Storage Hours: 6
Fluid Volume: 26032

Parasitics

User Variables

General Purpose User Variables

These variables can be used as additional inputs to data exchange setups. Like normal SAM input variables, they can be used in parametric and sensitivity simulations.

	Value:	Name and units:
INPUT Cost reference year	2009	INPUT Cost reference year
Annual utility costs (\$/yr) for Variable O&M by Gen check	908090	Annual utility costs (\$/yr) for Variable O&M by Gen check
Estimated O&M labor force	47	Estimated O&M labor force
Labor multiplier (1=AZ, 1.26=US avg, 1.89=CA-union)	1	INPUT Labor multiplier (1=AZ, 1.26=US avg, 1.89=CA-union)
Powerblock cost multiplier (1=wet cooled)	1	Powerblock cost multiplier (1=wet cooled)
User Variable 6	0	
User Variable 7	0	
User Variable 8	0	
User Variable 9	0	
User Variable 10	0	

TRNSYS System Simulation Input User Variables

These variables are similar to the ones above, except that they are written to the TRNSYS simulator input file for use with customized system input decks. Changing the value of one of these variables will cause the TRNSYS simulation to be rerun.

	Value:	Name and units:
System Variable 1	0	
System Variable 2	0	
System Variable 3	0	
System Variable 4	0	
System Variable 5	0	
System Variable 6	0	
System Variable 7	0	
System Variable 8	0	
System Variable 9	0	
System Variable 10	0	